TECHNISCHE UNIVERSITÄT MÜNCHEN

FAKULTÄT FÜR MEDIZIN

INSTITUT FÜR HUMANGENETIK

EXPERIMENTELLE MEDIZIN

Functional validation of mitochondrial disease genes

Ing. Mgr. Eliška Koňaříková

Vollständiger Abdruck der von der Fakultät für Medizin der Technischen Universität München zur Erlangung des akademischen Grades eines

Doktors der Naturwissenschaften (Dr. rer. nat.)

genehmigten Dissertation.

Vorsitzender: Prof. Dr. Carsten Schmidt-Weber

Prüfer der Dissertation:
1. Prof. Dr. Thomas Meitinger
2. Prof. Dr. Hans Rudolf Fries
3. Prof. Dr. Martin Zenker

Die Dissertation wurde am 01. 03. 2019 bei der Technischen Universität München eingereicht und durch die Fakultät für Medizin am 14. 07. 2020 angenommen.

For Michal, Marek and the others.

Abstract

The diagnosis of mitochondrial disorders underwent a tremendeous change towards the Next generation sequencing (NGS) methods in recent years. Decreasing cost of rapid sequencing methods make them available for increasing number of patients. The NGS techniques free the patients from the biopsy testing unless absolutely necessary. Yet, unfortunately, half of the cases still remains undiagnosed. The mitochondrial research provides opportunity to cover this unmet need. Future development lays in improvements of NGS techniques together with functional validations of genes previously not associated with a disease.

In this thesis, I focused on two crucial aspects of mitochondrial biology. Energy production in mitochondria is ensured by the activity of oxidative phosphorylation system (OXPHOS). Complexes of the OXPHOS are among other functions producing reactive oxygen species (ROS), which gains its importance mainly during stress conditions. However, ROS must be sustained at certain level and that is ensured by enzymes and molecules of ROS defence system. Additionally, the activity of OXPHOS complexes strongly depends on cofactors, among others flavin adenine dinucleotide (FAD). FAD is a part of the catalytically active site of Complex I and II as well as of about a hundred of other enzymes, primarily located in mitochondria. In any case, FAD must be syntesized in humans from its precursor riboflavin (vitamin B2). Based on the crucial function of ROS defence or production of cofactors for mitochondrial and cellular homeostasis, it was unexpected to find any disturbances in either of the systems. Yet, whole exome sequencing analysis at the Institute of Human Genetics found loss-of-function mutations in *TXN2* and *FLAD1*. Neither of the genes have previously been assocciated with a mitochondrial disease based on a proper experimental validation.

My task was to functionally validate the sequencing findings. In the case of variant in *TXN2*, thioredoxin 2 (TXN2) protein is a key enzyme of ROS defence located in mitochondria. In this project, investigations of patient cells showed an absence of TXN2 protein and subsequently a lack of its enzymatic activity, together with increased ROS, and impaired OXPHOS function. Most importantly, lentiviral expression of a wild type *TXN2* copy restored all these parameters and hence validated the mutational cause in disease development in patient. Moreover, because the patient presented with an infantile-onset neurodegenerative disorder with severe cerebellar atrophy, I validated the importance of TXN2 function in neuronal development. Above that, my functional observations led to investigation of antioxidant supplementation that effectively improved cell viability and suppressed cellular ROS levels. Finally, 15 years after the disease onset, I could suggest a rational antioxidant therapy to the patient, which resulted in significant mitigation of clinical symptoms and improved quality of life of the whole family.

In the second case, variants in *FLAD1* were associated with combined respiratory chain deficiency and multiple acyl-CoA dehydrogenase deficiency. Altogether, in six out of seven families, a predicted loss-of-function null-variant in *FLAD1* was found to be located in the first part of the gene, possibly disrupting the resulting protein function. Flavin adenine dinucleotide synthase 1 (FLAD1) is the main and potentially only cellular producer of FAD. However, sufficient amounts of FAD levels were observed in patients. The investigations of the genetics

of *FLAD1* unravelled a novel RNA isoform, which resulted in a discovery of enzymatically active truncated protein. The activity of truncated FLAD1 explained the utility of recommended riboflavin suplementation in patients.

To conclude, the functional validations presented here helped to label both genes as novel mitochondrial disease genes. My investigations led to an explanation of phenotypic-genotypic correlation in both cases. Most importantly, I was able to suggest a rational treatment based on the experimental observations and enzymatic function. Both genes are now connected to a treatable mitochondrial disorders. My observations will help to initiate the therapy early enough in any potential future patients carrying malfunctioning *TXN2* or *FLAD1*.

Abstrakt

Die Diagnostik mitochondrialer Erkrankungen wird in den letzten Jahren immer mehr von Next Generation Sequencing (NGS) -Methoden bestimmt. Sinkende Kosten für schnelle Sequenzierungsmethoden machen sie für eine wachsende Anzahl von Patienten verfügbar. Die NGS-Techniken ersparen den Patienten aufwendige Biopsien, sofern dies nicht unbedingt erforderlich ist. Leider wird dennoch in der Hälfte der Fälle keine Diagnose gefunden. Die Mitochondrienforschung bietet die Möglichkeit, einen Teil davon zu lösen. In Zukunft werden sowohl die NGS-Techniken noch als auch funktionelle Validierungen von Genen, die zuvor nicht mit einer Krankheit assoziiert waren, weiter verbessert werden.

In dieser Arbeit konzentrierte ich mich auf zwei entscheidende Aspekte der Biologie der Mitochondrien. Die Energieproduktion in Mitochondrien wird durch das oxidative Phosphorylierungssystems (OXPHOS) sichergestellt. Die Komplexe des OXPHOS erzeugen, neben anderen Aufgaben, reaktive Sauerstoffspezies (ROS), die vor allem unter Stressbedingungen an Bedeutung gewinnen. ROS müssen jedoch auf einem bestimmten Niveau gehalten werden. Dies wird durch Enzyme und Moleküle des ROS-Abwehrsystems sichergestellt. Darüber hinaus hängt die Aktivität von OXPHOS-Komplexen stark von Cofaktoren ab, darunter Flavinadenindinukleotid (FAD). FAD ist ein Teil des katalytisch aktiven Zentrums von Komplex I und II sowie von etwa hundert anderen Enzymen, die sich hauptsächlich in Mitochondrien befinden. FAD muss beim Menschen aus seinem Vorläufer Riboflavin (Vitamin B2) synthetisiert werden. Gemessen an der wichtigen zentralen Funktion der ROS-Abwehr oder der Produktion von Cofaktoren für die mitochondriale und zelluläre Homöostase, war es daher unerwartet, in einer der beiden Systeme Störungen zu finden. Die Analyse des Whole Exome Sequencing am Institut für Humangenetik ergab jedoch Loss-of-function Mutationen in *TXN2* und *FLAD1*. Keines der Gene wurde zuvor mit einer mitochondrialen Erkrankung assoziiert basierend auf einer ordnungsgemäßen experimentellen Validierung.

Meine Aufgabe bestand darin, die Ergebnisse der Sequenzierung funktional zu überprüfen. Im Falle der Variante in *TXN2* ist das Thioredoxin 2 (TXN2)-Protein ein Schlüsselenzym der ROS-Abwehr in Mitochondrien. In diesem Projekt zeigten Untersuchungen von Patientenzellen ein Fehlen des TXN2-Proteins und dadurch eine fehlende enzymatische Aktivität zusammen mit einer erhöhten ROS-Produktion und einer verminderten OXPHOS-Funktion. Am wichtigsten war jedoch, dass die lentivirale Expression einer Wildtyp-*TXN2*-Kopie alle diese Parameter wiederherstellte und somit die Mutationsursache in der Krankheitsentwicklung beim Patienten bestätigte. Da der Patient eine neurodegenerative Erkrankung mit Beginn im Kleinkindalter und eine schwere Kleinhirnatrophie aufwies, bestätigte ich außerdem die Bedeutung der Funktion von TXN2 in der neuronalen Entwicklung. Darüber hinaus führten meine funktionellen Beobachtungen zur Untersuchung einer antioxidativen Supplementierung, die die Zelllebensfähigkeit effektiv verbesserte und die zellulären ROS-Spiegel verminderte. Schließlich, 15 Jahre nach Beginn der Erkrankung, konnte ich dem Patienten eine rationale antioxidative Therapie vorschlagen, die zu einer deutlichen Abschwächung der klinischen Symptome und einer Verbesserung der Lebensqualität der gesamten Familie führte.

Im zweiten Fall waren die Varianten in *FLAD1* mit einem kombinierten Mangel der Atmungskette und einem mehrfachen Acyl-CoA-Dehydrogenase-Mangel verbunden. Insgesamt wurde in sechs von sieben Familien Loss-of-function Varianten in *FLAD1* gefunden. Alle Varianten wurden im ersten Teil des Gens gefunden, wodurch möglicherweise die resultierende Proteinfunktion gestört wird. Flavin-Adenin-Dinukleotid-Synthase 1 (FLAD1) ist der Haupt- und möglicherweise der einzige zelluläre Produzent von FAD. Bei den Patienten wurden jedoch ausreichende Mengen an FAD gemessen. Die Untersuchungen der Genetik von *FLAD1* enthüllten eine neuartige RNA-Isoform, die zur Entdeckung eines enzymatisch aktiven verkürzten Proteins führte. Die Aktivität des verkürzten FLAD1 erklärte die positive Wirkung der empfohlenen Riboflavinsuplementation bei Patienten.

Zusammenfassend kann gesagt werden, dass die hier vorgestellten funktionalen Validierungen dazu beigetragen haben, beide Gene als neuartige mitochondriale Krankheitsgene zu kennzeichnen. Meine Untersuchungen führten in beiden Fällen zu einer Erklärung der phänotypisch-genotypischen Korrelation. Am wichtigsten war, dass ich aufgrund der experimentellen Beobachtungen und der enzymatischen Funktion eine rationelle Behandlung vorschlagen konnte. Beide Gene sind jetzt mit einer behandelbaren mitochondrialen Erkrankung verbunden. Meine Beobachtungen werden dazu beitragen, die Therapie in Zukunft bei Patienten, die Mutationen in *TXN2* oder *FLAD1* tragen, früh genug zu initiieren.

Table of Contents

List of Abbreviations X
List of Figures XIII
List of Tables XV
List of Peer-Reviewed Publications XVI
1 Introduction 1
1.1 Mitochondria 1
1.1.1 Mitochondrial genetics 2
1.2 Mitochondrial disorders 4
1.2.1 Clinical diagnosis and the phenotypic spectrum of mitochondrial disorders 5
1.2.2 Metabolic diagnosis 7
1.2.3 Biochemical diagnosis 9
1.2.4 Genetic diagnosis of mitochondrial disorders 10
1.3 Treatment of mitochondrial disorders 17
1.4 Introduction to reactive oxygen species (Thioredoxin 2 project) 19
1.4.1 Sites of reactive oxygen species production 20
1.4.2 Principles of reactive oxygen species scavenging and signalization 22
1.4.3 Redox imbalance causes ROS-dependent signalling 24
1.4.4 Impairment of ROS scavenging system 25
1.4.5 Thioredoxin 2 in detail 27
1.4.6 Principles of antioxidant therapies for mitochondrial disorders of the redox system 30
1.4.7 Inhibitors connected to the ROS production and ROS defence system 32
1.5 Introduction to riboflavin metabolism (Flavin adenine dinucleotide synthase 1 project) 34
1.5.1 Acquisition and transport of riboflavin 34
1.5.2 Metabolic conversion of riboflavin into FMN and FAD 36
1.5.3 The domains and isoforms of Flavin Adenine Dinucleotide Synthase 1 37
1.5.4 FMN and FAD transport and delivery to flavoproteins 39
1.5.5 Human flavoproteome 40
1.5.6 Disorders connected to the flavin cofactors 43
1.5.7 Multiple acyl-CoA dehydrogenase deficiency 45
1.5.8 Pathologies associated with FAD synthesis by alterations in RFK and FLAD1 46
2 Aims of the Thesis 47
3 Material and Methods 48
3.1 Material 48
3.1.1 Nucleic acids 48

3.1.2 Cell lines 48
3.1.3 Antibodies and ladder 49
3.1.4 Chemicals and solutions 49
3.2 Methods 49
3.2.1 Cell culture 49
3.2.2 Extraction of DNA and RNA from human fibroblasts 50
3.2.3 Expression of a wild type copy of a gene of interest in human fibroblasts 51
3.2.4 Determination of oxygen consumption rate by Seahorse XF Analyzer 56
3.2.5 Cell viability and antioxidant treatment 56
3.2.6 SDS PAGE and Western blot analysis 58
3.2.7 Statistical analysis 58
3.2.8 Methods done in collaboration 58
4 Case Reports 62
4.1 Thioredoxin 2: Case report 62
4.2 Flavin adenine dinucleotide synthase 1: Case reports 64
5 Results 68
5.1 Results of Thioredoxin 2 project 68
5.1.1 Genetic analysis reveals a premature stop codon in TXN2 68
5.1.2 The observed variant does not allow expression of a functional enzyme 69
5.1.3 The TXN2 protein is undetectable 69
5.1.4 Mitochondrial function is impaired due to an interference with respiratory chain complexes 70
5.1.5 PRDX3 monomers are not restored due to lack of TXN2 function 71
5.1.6 Patient cells are highly sensitive to mitochondrial inhibitors 73
5.1.7 The expression of wild type TXN2 is stable in both cell lines 74
5.1.8 $TXN2^{wt}$ restores mitochondrial respiration 74
5.1.9 PRDX3 dimers are reduced by the reexpressed wild type TXN2 75
5.1.10 Total glutathione levels stay unchanged among cell lines 77
5.1.11 Expression of wild type TXN2 protects the cells against inhibition of ROS defence pathways 78
5.1.12 Antioxidants serve as an effective therapy for patients with defective TXN2 79
5.1.13 Idebenone as a successful rational therapy 79
5.1.14 General antioxidative pathways do not decrease ROS levels 80
5.2 Results of Flavin adenine dinucleotide synthase 1 project 82
5.2.1 Genetic analysis of the first family reveals a frameshift in FLAD1 82
5.2.2 The variant causes a reduction of the cytosolic FLAD1 protein 82

5.2.3 Cells show decreased multiplication rate 83
5.2.4 HPLC quantification revealed a sufficient concentration of FAD in blood derived from both patients 84
5.2.5 A collaborative effort exposed genotypic and phenotypic similarities in families with defective FLAD1 85
5.2.6 The particular variant types present with an unequal distribution along the gene 89
5.2.7 Truncated FLAD1 isoforms are stably expressed 90
5.2.8 A 26-kDa isoform was proved to contain FLAD1 specific peptides 91
5.2.9 Several alternative start codons can secure a functional FLAD1 isoform while avoiding the mutation hot-spot region 92
5.2.10 Real time PCR confirms the presence of the newly identified isoform 6 95
5.2.11 Patient RNA is sufficiently expressed, however does not reveal the exact mechanism of FAD production 96
6 Discussion 97
6.1 Current shift in the diagnosis of mitochondrial disorders 97
6.2 Functional validation of novel mitochondrial disease genes 98
6.2.1 ROS defence is a crucial mechanism, therefore any disruptions are improbable 98
6.2.2 Lack of TXN2 activity affects mitochondrial homeostasis 99
6.2.3 Expression of wild type TXN2 validates the causality of the gene and helps to find the treatment strategy 100
6.2.4 A system with malfunctioning TXN2 presents a valuable experimental model of ROS defence pathways 100
6.2.5 Further experimental potential lays in a study of the affected tissue as well as in investigations of any future patient 101
6.2.6 FAD cofactor affects the stability and activity of about 100 enzymes, hence lack of FAD is highly unexpected 101
6.2.7 Cells with affected FAD production are highly sensitive towards lack of riboflavin; however, FAD production was confirmed in patient blood samples 102
6.2.8 Fusion of FLAD1 domains was repeated during evolution 103
6.2.9 The mutation load acknowledges the role of both FLAD1 domains 103
6.2.10 Residual production of FAD led to the identification of novel isoforms and final explanation of the observed phenotype 104
6.2.11 Information burden of public databases 105
6.2.12 All predicted loss-of-function variant must be carefully inspected 106
6.3 Unravelling of a rational therapy for both novel mitochondrial disease genes 107
6.3.1 Functional validation helped to provide a cure to the patient with defective ROS defence 107
6.3.2 Riboflavin supplementation mitigated possible adverse outcomes in the following cases 108

6.3.3 Early implementation of riboflavin therapy is highly recommended 109
6.4 Future outlook 109
6.4.1 Towards the omics era and personalized medicine 109
6.4.2 Further development of treatment strategies 110
7 References 111

List of Abbreviations

A	adenine
ACAD9	acyl-CoA dehydrogenase 9
ADP	adenosindiphosphate
AIF	apoptosis inducing factor
ALS	amyotropic lateral sclerosis
AO	alternative oxidase
AoO	age of onset
ANT	adenine nucleotide translocator
ARE	antioxidant response element
ASK1	apoptosis stress kinase-1
ATP	adenosintriphosphate
α-KGDH	α-ketoglutharate dehydrogenases
bp	base pair
BSO	buthionine sulfoximine
BVVLS	Brown-Vialetto-Van Laere syndrome
CACT	carnitine-acylcarnitine translocase
cDNA	complementary deoxyribonucleic acid
CK	creatine kinase
CoA	coenzyme A
CoQ	coenzyme Q
COX	cytochrome *c* oxidase
CPEO	chronic progressive external ophthalmoplegia
CPT2	carnitine O-palmitoyl transferase 2
CRISPR	clustered regularly interspaced short palindromic repeats
CS	citrate synthase
Cu/ZnSOD	copper-zinc superoxide dismutase
cyt	cytochrome
D loop	displacement loop
DH	dehydrogenase
DHODH	dihydroorotate dehydrogenase
DMEM	Dulbecco's modified Eagle medium
DMSO	dimethyl sulfoxide
DNA	deoxyribonucleic acid
DNCB	2,4-dinitrochlorobenzene
dNTP	deoxynucleotide
e.g.	exempli gratia – *for example*
ECL	enhanced chemiluminescence
EDTA	ethylene diamine tetra acetic acid
EM	electron microscopy
ER	endoplasmic reticulum
et al.	et alii – *and others*
ETF	electron transfer flavoprotein
ETF-QO	ETF ubiquinone oxidoreductase
ETFDH	ETF-dehydrogenase
ExAC	The Exome Aggregation Consortium
F	forward primer
FAD	flavin adenine dinucleotide
FADS	FAD synthase domain

FGF-21	fibroblast growth factor 21
FLAD1	flavin adenine dinucleotide synthase 1
FMN	flavin mononucleotide
G	guanine
GDF-15	growth differentiation factor 15
GLRX	glutaredoxin
gnomAD	genome aggregation database
GPx	glutathione peroxidase
GRXCR2	glutaredoxin domain-containing cysteine-rich protein 2
GSH	glutathione monomers
GSR	glutathione reductase
GSSG	glutathione homodimers
GST	glutathione S-transferase
HEK	human embryonic kidney
HO-1	heme oxygenase-1
HPLC	high-performance liquid chromatography
hRFT	human riboflavin transporter
HRP	horseradish peroxidase
Hsp60	heat shock protein 60
i.e.	id est – *that is*
IGV	Integrative Genomics Viewer
IMM	inner mitochondrial membrane
Keap1	Kelch-like ECH-associated protein 1
KO	knockout
LCFA	long chain fatty acid
LHON	Leber's hereditary optic neuropathy
MADD	multiple acyl-CoA dehydrogenase deficiency
Maf	musculoaponeurotic fibrosarcoma
MAO	monoamine oxidase
MELAS	mitochondrial encephalopathy lactic acidosis and stroke-like episodes
MERRF	myoclonic epilepsy with ragged-red fibers
mGPDH	mitochondrial glycerophosphate dehydrogenase
MIM	mitochondrial inner membrane
MnSOD	manganese superoxide dismutase
MPTb	molybdopterin binding domain
MR	magnetic resonance
MRI	magnetic resonance imaging
mRNA	messenger RNA
MRS	magnetic resonance spectroscopy
mtDNA	mitochondrial DNA
MTS	mitochondrial targeting sequence
NADH	nicotinamide adenine dinucleotide
NADPH	nicotinamide adenine dinucleotide phosphate
NARP	neuropathy, ataxia and retinitis pigmentosa
NGS	Next generation sequencing
NHDF	normal human dermal fibroblasts
NHDFneo	neonatal normal human dermal fibroblasts
NOS	nitric oxide synthase
NQO-1	NAD(P)H quinone oxidoreductase-1
Nrf2	nuclear factor erythroid 2-related factor 2

OCR	oxygen consumption rate
OMIM	Online Mendelian Inheritance in Man
OMM	outer mitochondrial membrane
OXPHOS	oxidative phosphorylation system
PAO	phenylarsine oxide
PAPS	3'-phosphoadenosine-5'-phosphosulfate
PBS	phosphate buffered saline
PCR	polymerase chain reaction
PDH	pyruvate dehydrogenase
PRDX3	peroxiredoxin 3
PVDF	polyvinylidene difluoride
R	purine / reverse primer
RFK	riboflavin kinase
RFT	riboflavin transporter
RNA	ribonucleic acid
ROS	reactive oxygen species
RR-MADD	riboflavin responsive MADD
rRNA	ribosomal RNA
SDH	succinate dehydrogenase
SDHA	succinate dehydrogenase, subunit A
SFN	sulphoraphane
TALEN	transcription activator-like effector nucleases
TBS	tris buffered saline
Tris	tris(hydroxymethyl)aminomethane
tRNA	transfer RNA
TXN2	thioredoxin 2
TXNRD2	thioredoxin reductase 2
WES	whole exome sequencing
WGS	whole genome sequencing
wt	wild type
ZFNs	zinc finger endonucleases

List of Figures

Figure 1: Structure of the human mitochondrial DNA molecule (from Gorman et al. 2016) ...2
Figure 2: Different levels of heteroplasmy, threshold effect, and a disease manifestation (from https://clinicalgate.com/mitochondrial-encephalopathies/) ...3
Figure 3: Phenotypic spectrum of mitochondrial diseases (from Koene & Smeitink 2011) ...7
Figure 4: Overview of Next generation sequencing technology (from Illumina 2016) ...12
Figure 5: Sequencing strategies in human genetics ...14
Figure 6: Overview of analysis workflow ...15
Figure 7: Sites of ROS production (modified from Holzerova and Prokisch 2015) ...21
Figure 8: Molecular mechanisms of reactive oxygen species scavenging mechanism (modified from Holzerova and Prokisch 2015) ...22
Figure 9: Reactive oxygen species scavenging pathways (modified from Holzerova and Prokisch 2015) ...23
Figure 10: Nrf2-Keap1 antioxidant pathway (from Lee et al. 2011) ...25
Figure 11: Crystal structure of human TXN2 protein (modified from Smeets et al. 2005) ...28
Figure 12: Chemical structure glutamyl-L-cysteinyl-glycine, glutathione in short ...30
Figure 13: Chemical structure of the α-tocopherol form of vitamin E ...31
Figure 14: Chemical structure of Trolox (6-hydroxy-2,5,7,8-tetramethylchroman-2-carboxylic acid) ...31
Figure 15: Chemical structure of coenzyme Q ...31
Figure 16: Chemical structure of MitoQ ...32
Figure 17: Chemical structure of Idebenone ...32
Figure 18: Schematic representation of OXPHOS, enzymes of the ROS defence system and their inhibitors (modified from Holzerova et al. 2016) ...33
Figure 19: The path of riboflavin in human metabolism (from Haack, Makowski, et al. 2012) ...35
Figure 20: Structure of flavins ...36
Figure 21: Schematic presentation of FLAD1 gene and protein isoforms ...38
Figure 22: Riboflavin, FMN and FAD transport cycle in mitochondria (modified from Barile et al. 2000) ...40
Figure 23: Chromosomal map of genes encoding flavoproteins (from Lienhart et al. 2013) ...41
Figure 24: The human flavoproteome (based on Lienhart et al. 2013, Schiff et al. 2016 and Mayr JA personal communication) ...42
Figure 25: Schematic presentation of the cloning vector and its insert (Gene of Interest) ...52
Figure 26: Brain imaging (from Holzerova et al. 2016) ...63
Figure 27: Sanger sequencing analysis showing the variant on the DNA level (modified from Holzerova et al. 2016) ...68
Figure 28: Schematic interpretation of thioredoxin 2 gene (NC_000022.11) and protein (CAG30487; modified from Holzerova et al. 2016) ...69
Figure 29: Loss of TXN2 protein ...70
Figure 30: Oxygen consumption rate assessed by the Seahorse XF Analyzer ...71
Figure 31: Cycling of PRDX3 in the oxidative environment (modified from Holzerova et al. 2016) ...72
Figure 32: Cell sensitivity test of mitochondrial inhibitors ...73

Figure 33: Immunoblot analysis of cell lines (modified from Holzerova et al. 2016) ...74
Figure 34: Oxygen consumption rate assessed by the Seahorse instrument ...75
Figure 35: Immunoblot analysis of PRDX3 dimers (modified from Holzerova et al. 2016) ...76
Figure 36: Concentrations of total glutathione in studied cell lines ...77
Figure 37: Cell sensitivity test in cell lines (modified from Holzerova et al. 2016) ...78
Figure 38: ROS production in the cells and effect of antioxidants (from Holzerova et al. 2016) ...79
Figure 39: Effect of Idebenone in cells treated with DNCB (modified from Holzerova et al. 2016) ...80
Figure 40: Sulphoraphane treatment ...81
Figure 41: Pedigree of the Turkish family from Vienna and Sanger sequencing of FLAD1 (modified from Olsen et al. 2016) ...82
Figure 42: Immunoblot analysis of FLAD1 protein (modified from Olsen et al. 2016) ...83
Figure 43: Fibroblasts growth curves ...84
Figure 44: HPLC quantification of riboflavin FMN and FAD in (A) blood plasma and (B) erythrocytes (modified from Olsen et al. 2016) ...85
Figure 45: Pedigrees of investigated families and localization of studied variants (modified from Olsen et al. 2016) ...86
Figure 46: The expression of different FLAD1 isoform detected by immunoblotting ...90
Figure 47: Immunoblot detection of FLAD1 protein and its truncated variants (modified from Olsen et al. 2016) ...91
Figure 48: Schematic representation of Sashimi plots ...92
Figure 49: FLAD1 transcript isoforms and their predicted products (modified from Olsen et al. 2016) ...94
Figure 50: Quantitative real time PCR of FLAD1 (modified from Olsen et al. 2016) ...95
Figure 51: RNA sequencing of the fibroblast sample derived from the younger sister from the Turkish family ...96

List of Tables

Table 1: Concentration of the working solution of DNCB ...57
Table 2: Genetic, clinical and biochemical findings in individuals with FLAD1 mutations (modified from Olsen et al. 2016) ...88

List of Peer-Reviewed Publications

Yépez VA, Kremer LS, Iuso A, Gusic M, Kopajtich R, **Koňaříková E**, Nadel A, Wachutka L, Prokisch H, Gagneur J. ***OCR-Stats: Robust estimation and statistical testing of mitochondrial respiration activities using Seahorse XF Analyzer***. PLoS One, 2018 Jul 11;13(7):e0199938. doi: 10.1371/journal.pone.0199938. eCollection 2018.

Piekutowska-Abramczuk D, Assouline Z, Mataković L, Feichtinger RG, **Koňaříková E**, Jurkiewicz E, Stawiński P, Gusic M, Koller A, Pollak A, Gasperowicz P, Trubicka J, Ciara E, Iwanicka-Pronicka K, Rokicki D, Hanein S, Wortmann SB, Sperl W, Rötig A, Prokisch H, Pronicka E, Płoski R, Barcia G, Mayr JA. ***NDUFB8 Mutations Cause Mitochondrial Complex I Deficiency in Individuals with Leigh-like Encephalomyopathy***. American Journal of Human Genetics, 2018 Mar 1;102(3):460-467. doi: 10.1016/j.ajhg.2018.01.008. Epub 2018 Feb 8.

Kremer LS, Bader DM, Mertes C, Kopajtich R, Pichler G, Iuso A, Haack TB, Graf E, Schwarzmayr T, Terrile C, **Koňaříková E**, Repp B, Kastenmüller G, Adamski J, Lichtner P, Leonhardt C, Funalot B, Donati A, Tiranti V, Lombes A, Jardel C, Gläser D, Taylor RW, Ghezzi D, Mayr JA, Rötig A, Freisinger P, Distelmaier F, Strom TM, Meitinger T, Gagneur J, Prokisch H. ***Genetic diagnosis of Mendelian disorders via RNA sequencing***. Nature Communication, 2017 Jun 12;8:15824. doi: 10.1038/ncomms15824.

Olsen RKJ*****, **Koňaříková E**[*], Giancaspero TA*****, Mosegaard S*****, Boczonadi V*****, Mataković L*****, Veauville-Merllié A, Terrile C, Schwarzmayr T, Haack TB, Auranen M, Leone P, Galluccio M, Imbard A, Gutierrez-Rios P, Palmfeldt J, Graf E, Vianey-Saban C, Oppenheim M, Schiff M, Pichard S, Rigal O, Pyle A, Chinnery PF, Konstantopoulou V, Möslinger D, Feichtinger RG, Talim B, Topaloglu H, Coskun T, Gucer S, Botta A, Pegoraro E, Malena A, Vergani L, Mazzà D, Zollino M, Ghezzi D, Acquaviva C, Tyni T, Boneh A, Meitinger T, Strom TM, Gregersen N, Mayr JA, Horvath R, Barile M, Prokisch H. ***Riboflavin-Responsive and -Non-responsive Mutations in FAD Synthase Cause Multiple Acyl-CoA Dehydrogenase and Combined Respiratory-Chain Deficiency***. American Journal of Human Genetics, 2016 Jun 2;98(6):1130-1145. doi: 10.1016/j.ajhg.2016.04.006.

[*] These authors contributed equally to this work

Holzerová E, Danhauser K, Haack TB, Kremer LS, Melcher M, Ingold I, Kobayashi S, Terrile C, Wolf P, Schaper J, Mayatepek E, Baertling F, Friedmann Angeli JP, Conrad M, Strom TM, Meitinger T, Prokisch H, Distelmaier F. ***Human thioredoxin 2 deficiency impairs mitochondrial redox homeostasis and causes early-onset neurodegeneration***. Brain, 2016 Feb;139(Pt 2):346-54. doi: 10.1093/brain/awv350. Epub 2015 Dec 1.

Holzerová E, Prokisch H. ***Mitochondria: Much ado about nothing? How dangerous is reactive oxygen species production?*** International Journal of Biochemistry & Cell Biology, 2015 Jun;63:16-20. doi: 10.1016/j.biocel.2015.01.021. Epub 2015 Feb 7.

Haghighi A, Haack TB, Atiq M, Mottaghi H, Haghighi-Kakhki H, Bashir RA, Ahting U, Feichtinger RG, Mayr JA, Rötig A, Lebre AS, Klopstock T, Dworschak A, Pulido N, Saeed MA, Saleh-Gohari N, **Holzerová E**, Chinnery PF, Taylor RW, Prokisch H. ***Sengers syndrome: six novel AGK mutations in seven new families and review of the phenotypic and mutational spectrum of 29 patients***. Orphanet Journal of Rare Diseases, 2014 Aug 20;9:119. doi: 10.1186/s13023-014-0119-3.

1 Introduction

Inherited mitochondrial diseases affect at least 20 individuals per 100.000 people (Gorman et al. 2016). Mitochondrial disorders possess genetic and clinical heterogenity as they appear at any age, present with various phenotypes affecting any organ and are caused by any mode of inheritance. What mitochondrial diseases have in common characteristically, is impairment of respiratory chain activity, which is responsible for more than 90% of energy production within cells. With the introduction of Next generation sequencing techniques in patients with respiratory chain deficiencies, it has become possible to screen all genes in one step and to identify pathogenic variants in genes which are predicted to play a role in mitochondrial homeostasis, but are not yet associated with a disease.

The core of a proper mitochondrial function lays in the respiratory chain. The correct enzymatic activity of complexes of the respiratory chain is secured by cofactor availability, among others. Furthermore, one of the products of such enzymatic reactions is the production of reactive oxygen species. Both of these aspects are reflected in my work, described in results section (chapter 5) and evaluated in the discussion (chapter 6). Therefore, the basics of mitochondrial disorders and their diagnosis, followed by introductions to reactive oxygen species and cofactor metabolism will be reviewed.

1.1 Mitochondria

Mitochondria are ancient organelles fundamental for normal physiology and health (Henze and Martin 2003). They typically form a network, which occupies a substantial part of the cytosol (*e.g.* about 20% of the cell volume in human liver cells; Alberts et al. 1994). According to the endosymbiotic theory, these organelles developed from proteobacteria by absorption into a eukaryotic cell (Margulis 1975). Consequently, they present with very specific attributes such as having their own circular genome, double membranes, a different type of ribosome, and presence of cardiolipin.

Mitochondria are responsible for various functions essential for cellular metabolism. The respiratory chain, localized to the inner mitochondrial membrane, generates approximately 90% of cellular energetic currency, adenosine triphosphate (ATP), via oxidative phosphorylation (OXPHOS; Rich 2003). The OXPHOS system is constituted from five membrane complexes and two mobile electron carriers (coenzyme Q and cytochrome *c*), whereby some of these complexes can form higher molecular assemblies called supercomplexes (Wittig et al. 2006b).

In addition to the respiratory chain and ATP production itself, mitochondria host additional functions such as the tricarboxylic acid cycle (*i.e.* Krebs cycle), the urea cycle, gluconeogenesis and ketogenesis, enzymes of calcium signalling, adaptive thermogenesis, ion homeostasis, fatty acid oxidation, amino acid metabolism, lipid metabolism, proteins involved in the biosynthesis

of steroids, haem and iron–sulfur clusters, in a programmed cell death and others (Voet et al. 2013).

1.1.1 Mitochondrial genetics

Mitochondrial structure and function are under the control of two genomes, the nuclear and mitochondrial. The mitochondrial DNA (mtDNA, Figure 1), is 16.569 base pairs long in humans. Unlike the nuclear genome, mtDNA exists in up to several thousand copies per cell, depending on the cell type (Sciacco et al. 1994; Taylor and Turnbull 2005). Most of the mtDNA sequence is coding and lacks an intron–exon structure, with the majority of the genes located on the one strand of the DNA molecule. This strand is also known as the heavy strand due to the higher proportion of heavier nucleotides - adenine and guanine (Gorman et al. 2016). However, several genes are coded by the other DNA strand, conversely known as the light strand. Two of the genes are even overlapping. In addition, replication, transcription and translation of mtDNA are all controlled by a single non-coding region, known as the displacement loop ('D loop' in short; Gorman et al. 2016). As shown in Figure 1, mtDNA encodes 13 mitochondrial proteins, two ribosomal RNAs (rRNAs), and 22 transfer RNAs (tRNAs). Due to the fact that most of the mtDNA is RNA coding, mutations in the majority of the sequence can give rise to mitochondrial genetic disorders. A comprehensive collection of data on human mitochondrial DNA variations are being summarized by MITOMAP, which currently reports polymorphisms and mutations from more than 47.000 human mtDNA sequences (http://www.mitomap.org/ [January 25th, 2019]).

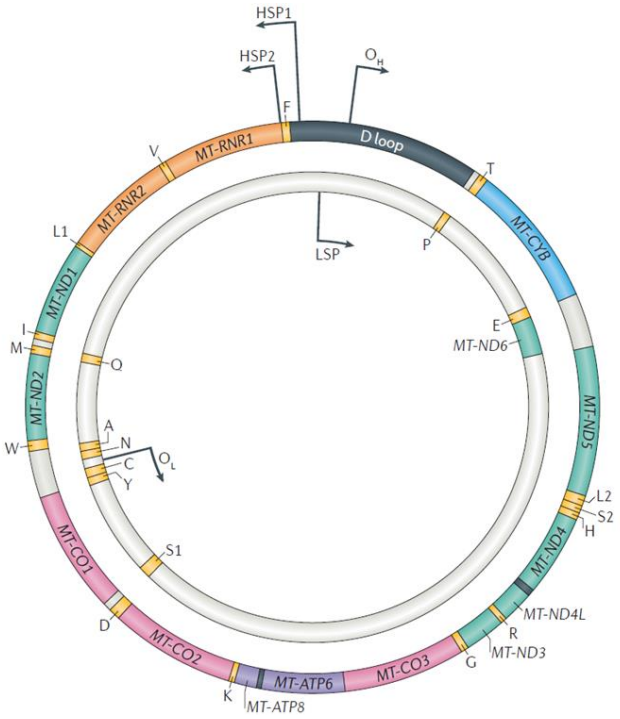

Figure 1: Structure of the human mitochondrial DNA molecule (from Gorman et al. 2016). MtDNA consists of two strands with different loads of coding genes. Altogether mtDNA encodes 13 proteins of the OXPHOS, two ribosomal RNAs, and 22 transfer RNAs. The D loop in the upper part is responsible for the regulation of replication, transcription and translation.

The available evidence indicates that mtDNA is constantly undergoing mutagenesis, for example point mutations, deletions, rearrangements and copy number variations. Because these acquired mutations occur at random, they are often present at a very low level and therefore might not be detected (Taylor and Turnbull 2005). Hence, it is considered that most people have only one type of mtDNA. Generally, this condition is called homoplasmy. However, in case of clonal expansion of a single mutation with one of the many copies of mtDNA existing per mitochondria and per cell, the variant itself will occur in a higher proportion (> 10%) of the mtDNA molecules. This effect is known as heteroplasmy (Gorman et al. 2016).

If the percentage of heteroplasmy surpasses a certain level, called a threshold, a mitochondrial disorder can manifest. For some common mitochondrial diseases the threshold level is known. Typically, a high proportion of mutated mtDNA (> 60%) is a prerequisite of cellular defects (Koene and Smeitink 2011). For example, the phenotypic threshold level for mtDNA deletions is around 60% (Grady et al. 2014). For point mutations observed in cases with defective $tRNA^{Lys}$, 90% heteroplasmy is required (Shoffner et al. 1990). In other cases of disease caused by mitochondrial tRNA mutations, almost 100% of mutant mtDNA is required, as the cell is able to compensate the defect by supporting the expression of the healthy tRNAs (Chomyn et al. 2000). Typically, the various clinical presentations of mutations in mitochondrial DNA manifest as a direct consequence of the heteroplasmy level in the specific tissue (Stewart and Chinnery 2015). A schematic representation of levels of heteroplasmy is shown in Figure 2.

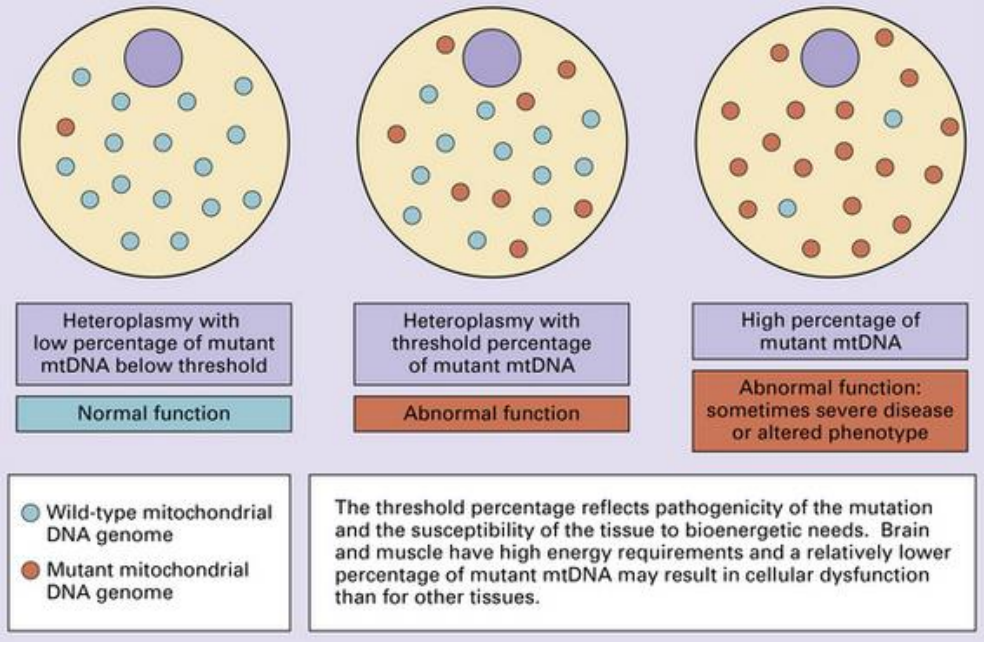

Figure 2: Different levels of heteroplasmy, threshold effect, and a disease manifestation (from https://clinicalgate.com/mitochondrial-encephalopathies/). Very low levels of heteroplasmy (on the left) result in normal mitochondrial function. Heteroplasmy on such a level is not usually detected. The heteroplasmy in the middle and on the right typically results in a disorder, depending on the type and severity of the variant.

MtDNA codes for only 13 proteins in total. Proper mitochondrial function is therefore dependent on the nuclear genes, responsible for about 99% of the mitochondrial proteome (Chacinska et al. 2009). Due to the bi-genomic control of mitochondrial function, all modes of inheritance are seen in mitochondrial diseases. MtDNA is inherited exclusively in humans from the mother (Giles et al. 1980). In the case of nuclear encoded variants, the disease can be monogenic or polygenic. In the case of monogenic disorders, the mode of inheritance is either dominant or recessive. Additionally, X-linked mitochondrial disease genes are also known. Defects in *PDHA1*, coding for a subunit of pyruvate dehydrogenase complex, is the most frequent example of an X-linked mitochondrial disorder (Sperl et al. 2015). These disease causing variants are not all necessarily inherited, some may also appear *de novo*.

1.2 Mitochondrial disorders

Mitochondrial disorders present the most heterogeneous group of metabolic diseases and are among the most common forms of inborn errors of metabolism and inherited neurological disorders (Smeitink 2003; Thorburn 2004; Mayr et al. 2015; Gorman et al. 2016). It is estimated that mitochondrial disorders manifest in five to 15 children out of 100.000. The pediatric cases are most often caused by a mutation with a recessive mode of inheritance, typically presenting with a severe and progressive phenotype (Scaglia et al. 2004). The adult-onset mitochondrial diseases are typically caused by a variant in the mtDNA and affects ten in 100.000 individuals, or three out of 100.000 in the case of nuclear genes (Skladal et al. 2003; Thorburn 2004; Gorman et al. 2016). To date, variants in more than 300 nuclear genes have been reported as disease causing (Stenton and Prokisch 2018). The analysis of monogenic mitochondrial diseases has considerably enhanced general knowledge of the cellular pathophysiology of mitochondrial (dys)function.

The first mitochondrial patient was described in 1959. The uncoupling of respiratory chain and ATP production was causing a severe hypermetabolism, weakness, increased perspiration and reduced body weight despite polyphagia (Ernster et al. 1959; Luft et al. 1962). Traditionally, mitochondrial disorders have been associated with an impaired OXPHOS system. Surprisingly, most patients do not possess variants within the limited number of OXPHOS genes. In addition to defects in the OXPHOS subunits and their assembly factors, impairments can be found in substrate generation upstream of the OXPHOS, hence the Krebs cycle, pyruvate dehydrogenase complex or the import of substrates. Similarly, in defective cofactor biosynthesis and malfunctioning mitochondrial DNA, RNA and protein synthesis. Finally, defects in mitochondrial maintenance such as biogenesis, fusion and fission, protein import and processing of lipids may all be responsible for the disorder (Mayr et al. 2015).

With regards to the OXPHOS complexes themselves, defects are most frequently found in Complex I (Lazarou et al. 2009). In about half of the cases (49%), a further defect of more than one of the other respiratory complexes manifests. These combined defects of Complexes I, III, IV and V are usually caused by defects in mitochondrial replication, transcription or translation, as the core subunits are encoded by the mtDNA (Mayr et al. 2015; Ghezzi and Zeviani 2018).

1.2.1 Clinical diagnosis and the phenotypic spectrum of mitochondrial disorders

The diagnosis of mitochondrial diseases is challenging due to the large number of genes involved. Additionally, the phenotypic presentation is highly heterogeneous. As an example, a common disease-causing mtDNA mutation m.3243A>G in *MTTL1* coding for $tRNA^{Leu}$ (1 in 400 cases) is associated with mitochondrial encephalopathy, lactic acidosis and stroke-like episodes (MELAS; OMIM #540000). However, the mutation is also responsible for maternally inherited deafness and diabetes, progressive external ophthalmoplegia either isolated or in any combination of phenotypes. Moreover, about a third of patients with *MTTL1* variants present with clinical manifestations that are currently not recognised as a classical mitochondrial disease and 9% of the mutation carriers are asymptomatic (Nesbitt et al. 2013).

Similarly, mutations in the nuclear DNA in *POLG*, coding for the mitochondrial DNA polymerase gamma, are responsible for mitochondrial disease in about one fourth of adult patients. Different mutations in *POLG* are associated with a variety of phenotypes. The most commons falls under the phenotypic decription of Alpers syndrome (OMIM #203700), characterized by seizures, liver degeneration, and psychomotoric deterioration. The seizures can rapidly progress and the hepatopathy often results in liver failure (Saneto et al. 2013). Mutations in *POLG* can, however, also result in myopathy, ataxia, ptosis, deafness, ophthalmoplegia, parkinsonism, premature ovarian failure, hypogonadism, and/or gastrointestinal dysmotility (Tchikviladze et al. 2015).

Hence, in some genes the mutations give rise to many common clinical syndromes. Unfortunately, the reverse is also true. Consequently, some of the mitochondrial disease syndromes can have a very multifarious genetic background. As an example, Leigh syndrome (OMIM #256000) has been reported to be caused by mutations in 75 genes located across the mitochondrial and nuclear genomes (Lake et al. 2016). Leigh syndrome is a severe neurological disorder with typical onset during the first year of life, characterized by a progressive mental retardation and a psychomotor regression. The magnetic resonance imaging of patients reveals symmetrical lesions in the brainstem or basal ganglia. The first symptoms include vomiting, diarrhea and dysphagia resulting in failure to thrive. Associated manifestations are hypotonia, dystonia, ataxia and peripheral neuropathy. In many individuals the symptoms include degeneration of the optic nerve (*i.e.* optic atrophy) together with nystagmus or ophthalmoparesis. Some patients develop a hypertrophic cardiomyopathy or suffer from lactic acidosis. Very often the symptoms worsen in the following years and result in death due to acute respiratory failure (Baertling et al. 2014).

Despite the above mentioned difficulties in diagnosis, there are several recognizable clinical manifestations established for the diagnosis of a mitochondrial disease. Examples of adult-onset disorders include chronic progressive external ophthalmoplegia (CPEO; OMIM #609286 and #157640), Kearns-Sayre syndrome (a clinical subtype of CPEO and/or pigmentary retinopathy with cerebellar ataxia, cardiomyopathy, dementia, deafness, short stature, and endocrine abnormalities; OMIM #530000; Shemesh & Margolin 2018) and Leber's hereditary optic neuropathy (LHON syndrome; OMIM #535000), a common mitochondrial disease, characterized by a bilateral visual loss. This vision loss is more frequent in males and begins in one eye, with the second affected within the following weeks to months (Dimitriadis et al.

2014). Additionally, MERRF syndrome (myoclonic epilepsy with ragged-red fibers; OMIM #545000) is caused by a point mutation m.8344A>G coding for $tRNA^{Lys}$ in about 90% of cases. MERRF phenotypes include involuntary twitching of a muscle (*i.e.* myoclonus), epilepsy, ataxia and the presence of ragged red fibers on muscle biopsy (Lorenzoni et al. 2014). Last but not least, the NARP syndrome (neuropathy, ataxia and retinitis pigmentosa; OMIM #551500) is associated with neurogenic muscle weakness and sensory neuropathy with ataxia and pigmentary retinopathy. Onset of NARP is mostly during childhood causing learning difficulties (Thorburn et al. 1993).

The most commonly and severely affected tissues in mitochondriopathies are the high energy demanding tissues, such as the brain, retina, kidney, liver and skeletal or cardiac muscle. Hence, patients present with neurodegenerations, in many cases in combination with muscle weakness, cardiomyopathy, optic athrophy, or liver failure. This frequently makes mitochondriopathy a multisystemic disorder. Although, most mitochondrial disorders are progressive, there are many which manifest with a more stable course over decades, or even see amelioration of their symptomes (Koene and Smeitink 2011). Moreover, mitochondrial impairment is often observed in association with common disease, very often Parkinson's, Alzheimer's and Huntington's disease (Hadrava Vanova et al. 2020).

Figure 3 summarizes the frequent symptoms. When at least three of the organs are affected, the diagnosis of a mitochondrial disorder is very likely (Koene and Smeitink 2011). The observation that the phenotypic spectrum of mitochondrial disorders is extremely broad and that the clinical symptoms can affect any single tissue or organ or their combination at any age of onset was summarized by Munnich and Rustin. They postulated that mitochondriopathies appear with '*any symptom, in any organ or tissue, at any age, with any mode of inheritance'* (Munnich and Rustin 2001).

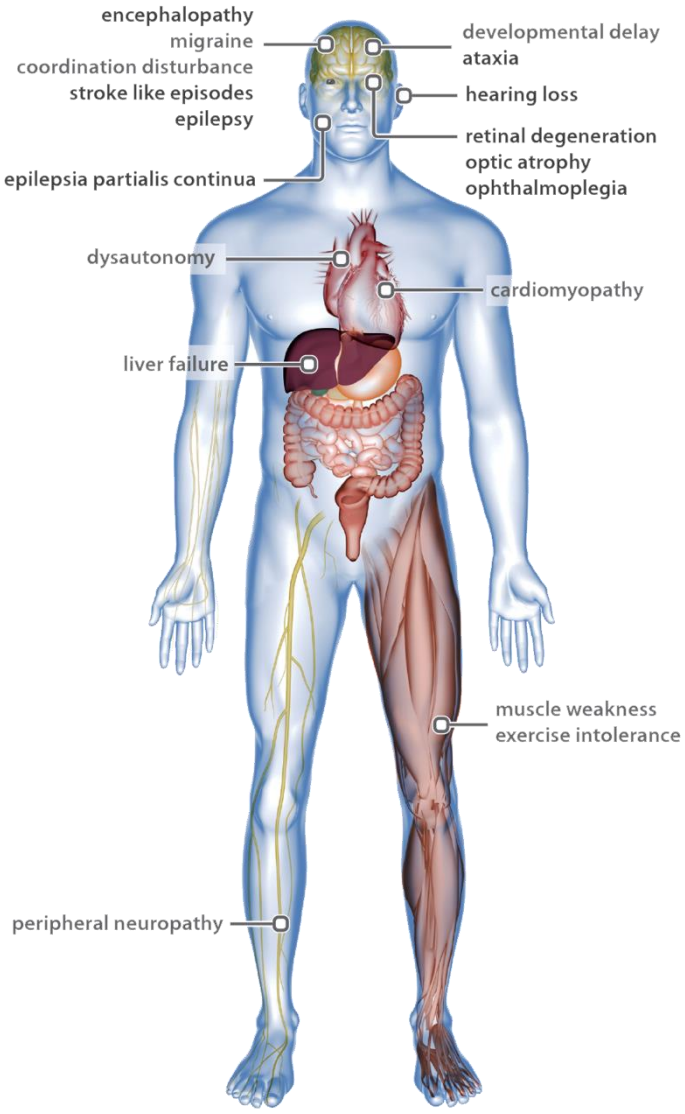

Figure 3: Phenotypic spectrum of mitochondrial diseases (from Koene and Smeitink 2011). Mitochondrial disorders affect various organ systems of the human body. If at least three of the phenotypes highlighted in bold are involved, mitochondrial impairment is highly suspected.

1.2.2 Metabolic diagnosis

Mitochondrial disorders are traditionally associated with a malfunctioning OXPHOS system. To overcome the energetic debt, the cells boost glycolysis to increase ATP production (Haas et al. 2008). In normal conditions the glycolytic pathway converts one molecule of glucose into two molecules of pyruvate in order to produce two molecules of ATP and two molecules of NADH. Resulting pyruvate is then transformed by a complex reaction of pyruvate dehydrogenase into acetyl coenzyme A (CoA) whose energy is subsequently used in reactions of Krebs cycle and the respiratory chain. In case of blockage of the acetyl-CoA utilization, pyruvate is increasingly reduced to lactate to recycle NAD^+. Therefore, lactic acidosis or hyperlactatemia has become the most apparent and common biomarker for mitochondrial dysfunction (Stacpoole 1997). Lactate level is therefore often measured when a

mitochondriopathy is suspected. Some patients may, however, show increased lactate levels only when undergoing a metabolic crisis or directly after a physical exercise (Debray et al. 2007). Nevertheless, lactic acidosis may occur with other phenotypes such as systemic and metabolic disorders and a variety of other conditions (infection of central nervous system, stroke, inflammation, malignancy, and seizures) and is therefore non-specific in nature. This, it is recommended to measure lactate repeatedly (Chow et al. 2005).

Mitochondrial disorders often result in alternated levels of various products of metabolism. As an example, a mitochondrial disease may be reflected by change in the levels of amino acids. Typically, elevation of alanine, but also proline, glycine, and sarcosine has been reported as well as elevated tyrosine in newborn screening studies (Wolf and Smeitink 2002; Phoenix et al. 2006; Shatla et al. 2014). Similarly, investigation of organic acids levels gives valuable information about the proper functioning of metabolism. Organic acids are produced as a result of catabolism of proteins, carbohydrates and fatty acids. High levels of excreted organic acids directly indicate an inborn error of metabolism. Specifically, ethylmalonic acid or 3-methyl glutaconic as products of Krebs cycle; or C6-C10 dicarboxylic acids (*i.e.* adipic-suberic-sebacic) from fatty acids oxidation were connected to mitochondrial disorders (Divry et al. 1983; Gibson et al. 1991; Barshop 2004). Additionally, a strong correlation between levels of specific analytes, mainly fumarate and malate, and mitochondrial metabolic disorder have been found (Barshop 2004).

Furthermore, Krebs cycle arrest may result in elevated levels of ketone bodies, hence acetoacetate, β-hydroxybutyrate, acetone and their breakdown products. Upon disease conditions, ketone bodies are produced in the liver from acetyl-CoA and are excreted into the blood stream. However, ketone bodies also arrise in healthy individuals during periods of starvation (Smeitink et al. 2006; Shatla et al. 2014). The advantage of the above mentioned investigations is their very low invasivity. The levels of lactate, amino and organic acids or ketone bodies can be analyzed from a blood and/or urine sample. The handling and storage of the samples is crucial, as it may result in false positive or false negative results (Haas et al. 2008).

In order to detect inborn errors of metabolism, of which mitochondriopathies present a significant part, a newborn screening of carnitines and acylcarnitines from blood droplets was established (Jones et al. 2010). Carnitines and acylcarnitines are essential compounds for the β-oxidation of fatty acids, which is typically highly active in heart or muscle tissue. Carnitine deficiency has also been connected to primary OXPHOS disorders. Screening of these compounds is able to identify many affected individuals before the onset of the first symptoms (Kompare and Rizzo 2008).

Imaging also plays an important role in mitochondrial disease diagnosis. Wong *et alii* showed that investigation of the brain with magnetic resonance imaging (MRI) of the mitochondrial patient, is able to assess disease severity, monitor disease progression, and measure effects of provided treatment (Wong et al. 2017). Evaluation of brain anatomy is an established approach in neurometabolic disorders. However, when considering mitochondrial disorders, MRI features may change over time (Barkovich et al. 1993; van der Knaap et al. 1996; Valanne et al. 1998). Thus, a new neuroimaging technique called proton magnetic resonance spectroscopy

(MRS) has been developed. MRS is able to capture the behavior of small chemical compounds, such as lactate, N-acetyl-L-aspartate, succinate, creatine, choline, and myo-inositol. Therefore, MRS possesses the posibility to visualize metabolic changes, especially in the areas that otherwise appear normal. It also helps to non-invasively track metabolites in neurometabolic disorders (Bianchi et al. 2003; Dinopoulos et al. 2005).

In the course of the search for a biomarker in human mitochondrial disorders, an evaluation of fibroblast growth factor 21 (FGF-21) has been assessed. FGF-21 functions as a metabolic regulator, influencing glucose homeostasis and lipid metabolism (Choi et al. 2018). Dr. Anu Suomalainen and her co-workers aimed to reduce the need of muscle biopsy in the cases of suspected mitochondrial diseases affecting skeletal muscle. Evaluation of patients with confirmed respiratory chain deficiencies revealed elevated FGF-21 with a sensitivity of 92,3%, therefore suggesting FGF-21 as a strong biomarker (Suomalainen et al. 2011). Unfortunately, recent publications have conversly identified FGF-21 as a weak biomarker for mitochondrial inborn errors of metabolism (Finsterer and Zarrouk-Mahjoub 2018).

Similarly, growth differentiation factor 15 (GDF-15) has been reported to be significantly elevated in the serum of patients with mitochondrial disorders. When compared with other biomarkers (FGF-21, lactate, pyruvate, or creatine kinase), GDF-15 showed highest sensitivity (98%) and specificity (86%; Yatsuga *et al.*, 2015). Both FGF-21 and GDF-15 showed high yield in the specific cases of mitochondrial respiratory chain deficiencies. However, it must always be kept in mind that mitochondrial disorders consist of a large number of other deficiencies and can therefore not all be addressed with a single investigation.

1.2.3 Biochemical diagnosis

As mentioned, about half of the known mitochondrial disorders are caused by genetic defects in the OXPHOS complexes, whereof isolated or combined deficiency of Complex I in muscle is the most frequent biochemical finding (Mayr et al. 2015). In mitochondrial disorders, muscle tissue (*i.e.* skeletal or cardiac muscle) is typically affected due to the high energy demand (Larsson and Oldfors 2001). Measuring the enzymatic activities of individual or coupled complexes in samples from muscle biopsy became a gold standard for mitochondrial diagnosis in the era before massive usage of genetical testing (Wortmann et al. 2017).

The first systematic biochemical and morphological testing was set in 1970s and led to a description of a number of new metabolic defects, including deficiencies of pyruvate dehydrogenase complex, palmitoylcarnitine transferase, carnitine, as well as defects of Complexes III and IV (DiMauro and Garone 2010). Taken together, they highlight the very heterogeneous cause of mitochondrial disorders. Therefore, especially in the pre-genetic era, biochemical and morphological investigations of muscle biopsies were essential for disease diagnosis. In particular, certain other neuromuscular diseases can be omitted by investigations of a muscle biopsy (Parikh et al. 2015).

In early days, the OXPHOS function was analyzed polarographically. This method measures oxygen consumption and allows to study coupling between electron transport through

Complexes I to IV as well as the ATP synthesis in a sample of freshly isolated mitochondria (Rustin et al. 1991). Later, this technique further developed and expanded as the Oroboros Oxygraph Instrument by the group of Erich Gnaiger (Haller et al. 1994) or as Seahorse XF Analyzer (Rogers et al. 2011).

Histochemical staining of the enzymatic activity of Complexes II and IV and/or V in muscle fibres has also proven to be a valuable method in the diagnosis of mostly paediatric cases with mitochondrial myopathy (Oldfors et al. 1991). Alternatively, a double staining of Complex II and IV activities stains the ragged muscle fibres blue, whereas the healthy fibres appear brown. If this double staining of a muscle reveals a mixed picture in a sample from one patient, mtDNA mutations can be assumed. This is a direct consequence of a heteroplasmic pattern in the muscle cells (Sciacco et al. 1994).

Additionally, immunohistochemical studies are able to detect decreased content of respiratory chain complexes. Also, enzymatic activities can be measured by in-gel functional assays (Wittig et al. 2007) and electron microscopy may reveal abnormalities in mitochondrial ultrastructure pointing to a cause of the myopathy (Oldfors et al. 1991; Larsson and Oldfors 2001).

1.2.4 Genetic diagnosis of mitochondrial disorders

1.2.4.1 Single gene diagnostics

The importance of genetic testing in mitochondrial disease diagnosis has been growing over time. In the late years, sequencing techniques have become the state of the art tool to diagnose mitochondrial disorders. The era *'from function to gene'* supported the approach of biochemical investigation first, followed by a targeted Sanger sequencing of candidate genes (Wortmann et al. 2017). Sanger sequencing is a technique developed in 1977 by Frederick Sanger and his co-workers. It is based on a chain termination protocol during *in vitro* DNA polymerization, where labeled dideoxynucleotides are incorporated (Sanger et al. 1977). Nowadays, instead of the original radioactive labelling, each of the four nucleotide is labeled by a different fluorescent dye, subsequently visualized as peaks for sequence determination.

Sanger sequencing is at the present time used in laboratory practice to confirm findings from the Next generation sequencing (NGS). This method has the advantage of obtaining results within hours to days and is easy and reliable to interpret. Moreover, in the setting of strong suspicion for a variant in a limited number or even in a single gene, for example due to family history, Sanger sequencing is still a beneficial first-tier apporach. As an example, LHON is caused by only three distinct mtDNA point mutations in more than 95% of cases (Yu-Wai-Man et al. 2002). Next, MELAS was reported to be caused by a variant in *MTTL1* coding for $tRNA^{Leu}$ in about 80% of the patients (Goto et al. 1990), or the Sengers syndrome which is genetically associated with variants in *AGK* (Haghighi et al. 2014). Each of which is a good candidate for Sanger sequencing before more holistic apporaches such as NGS.

Based on the nature of Sanger sequencing utilization, requiring selection of candidate genes, this method is unable to unravel new disease causing genes. Sanger sequencing was reported to reach a diagnostic yield of only 11% for mitochondrial diseases (Neveling et al. 2013). Other

disadvantages become striking with the incorporation of NGS techniques. As shown, the phenotypic-genotypic correlation is rather weak in the case of mitochondrial disorders (Haack et al. 2012b). Moreover, an incorrect interpretation of previous biochemical findings, can mislead the choice of candidate genes (Taylor et al. 2014). Subsequent sequencing of series of genes is laborious, time-consuming, not to mention expensive. Above that, many patients with clinically suspected mitochondrial disease are carrying mutations in genes not yet associated with a mitochondriopathy (Stenton and Prokisch 2018).

1.2.4.2 Methods based on Next generation sequencing

In case of searching for the genetic cause of a disease without a previously suspected gene, Sanger sequencing methods have been replaced by NGS approaches. The rapid development of high-throughput NGS techniques deems them the method of choice in the diagnosis of mitochondrial disorders (Wortmann et al. 2017). One striking advantage is the rapidly reducing cost of NGS, which has dropped to approximately 700€ per whole exome sequencing and about 2.000€ per whole genome sequencing at the Institute of Human Genetics (Dr. Riccardo Berutti, personal communication). Not to mention the overall advantage of a wider information burden.

To briefly introduce the principle of NGS, these methods are based on massive parallel sequencing of short reads coming from a fragmented target DNA. In the case of Illumina sequencing-by-synthesis method (Figure 4), individual DNA fragments are provided with specific adapters, immobilized on a flow cell matrix and clonally amplified. Sequencing cycles include incorporation of fluorescently labelled nucleotides, which are detected by a digital imaging system. The results are two, generally non-overlapping reads. Short reads are aligned to a reference genome. The defined length of the reads and the adapter sequence with a known insert size serves as an internal control measure (Illumina 2016). Different companies have developed different sequencing approaches, however the market is dominated by Illumina (van Dijk et al. 2018). Other main representatives include 454 pyrosequencing based on luciferase by Roche, SOLiD sequencing by ligation owned now by Life Technologies or single-molecule real-time sequencing approach used by Pacific Biosciences.

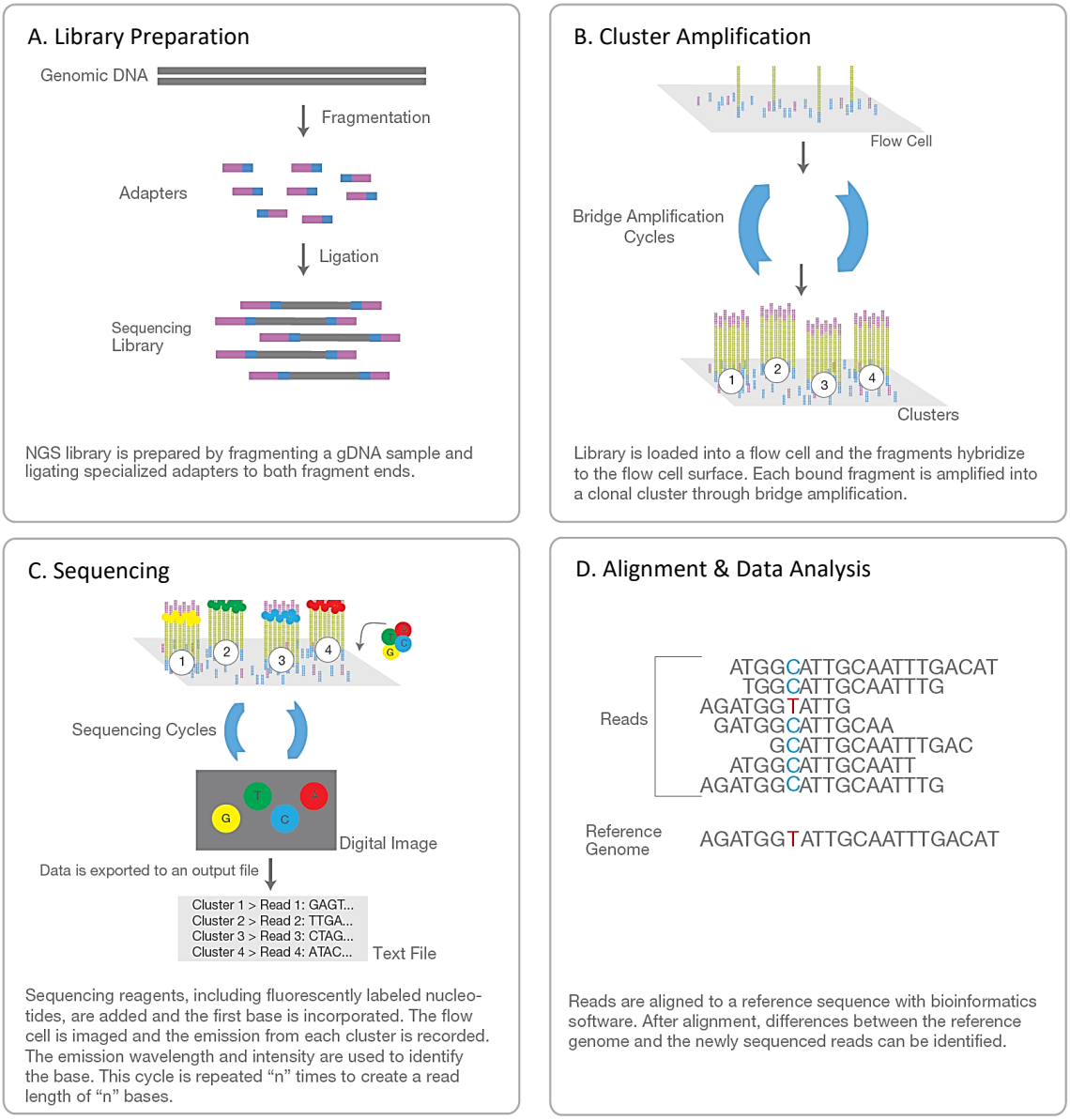

Figure 4: Overview of Next generation sequencing technology (from Illumina 2016). The DNA fragments (A) are ligated with adapters, (B) bound to the flow cell and locally amplified to create clonal clusters of identical fragments. (C) For every sequencing cycle, fluorescently labelled nucleotides are incorporated and detected by an imaging software. (D) Fragment sequences are aligned to the reference genome.

NGS gene panels

Current NGS approaches may be divided into targeted (panels, MitoExome and whole exome sequencing) and non-targeted (whole genome sequencing) sequencing. Targeting is usually fast and cost-effective in obtaining results, but due to the pre-defined gene set, the so called 'panel', novel disease causing genes will be missed. For nuclear genes coding for mitochondrial proteins a comprehensive inventory of 1.158 human proteins, i.e. MitoCarta2.0, was compiled by the group of Vamsi Mootha (Calvo et al. 2016). Based on their list with the addition of other genes

causing diseases similar to mitochondriopathies, a panel called MitoExome was created. It is a combination of sequencing mtDNA together with approximately 1.600 nuclear genes to unravel disease causing genes in patients with suspected mitochondrial disorders (Lieber et al. 2013).

However, the panel sequencing used for patients with suspected mitochondrial disorders was unable to achieve a high diagnostic yield. The rates of correct identification of a causative mutation were only 8,8% when using a 447-gene panel (DaRe et al. 2013) or 15,2% with 132 genes (Legati et al. 2016). However, both groups analyzed only about 130 previously undiagnosed patients. The application of MitoExome could identify an already known disease gene in 24% of the cases and a new potential disease causing gene in 31% of the patients (Calvo et al. 2012). In the meantime, fifteen new disease causing genes associated with a mitochondrial disorder, that are currently not included in the MitoExome list, have been discovered (Stenton and Prokisch 2018).

WES

The principle of the whole exome sequencing (WES) approach is to capture and sequence the exonic regions, encompassing about 1,6% of total human DNA length (Carroll et al. 2014). It is estimated that 85% of disease causing variants are located in such exonic coding regions (Lindor et al. 2017). Soon after the implementation of WES in 2009 (Choi et al. 2009), the very first gene connected to a mitochondrial disorder was reported. Dr. Tobias Haack and co-workers identified variants in *ACAD9* as the cause of Complex I deficiency in three unrelated families by using the WES technique (Haack et al. 2010). Later, WES became clinically available and has become increasingly used diagnostic tool for patients with suspected mitochondrial disease (Falk et al. 2012; Wong 2013). Since then, NGS techniques as a part of molecular diagnostics was involved in an identification of about 300 new disease causing genes (Ohtake et al. 2014; Taylor et al. 2014; Wortmann et al. 2017). Moreover, it was accredited as a routine diagnostic tool for mitochondrial disorders in The Netherlands (Wortmann et al. 2015).

The diagnostic yield of Sanger sequencing has been easily overtaken by WES. As an example, a study of 113 paediatric patients reported up to 59,3% of the likely causative mutations including variants in mitochondrial and nuclear genome. Half of the identified variants were novel and 18 genes were newly connected to a mitochondrial disorder (Pronicka et al. 2016). Another large scale study provided a firm genetic diagnosis in 34,5% of patients with the discovery of 37 novel mutations, three novel causative genes and three chromosomal aberrations in the cohort (Kohda et al. 2016). Similarly, a study comparing WES and a panel with 238 genes for mitochondrial disorders revealed a diagnostic yield of 38,5%, which would be only half of it in the case of the panel. In this study, when taken additional clinical, histochemical, biochemical, and neuroradiological findings, a diagnosis for 57% of the patient was reached (Wortmann et al. 2015).

Despite the fact that the implementation of WES significantly increased the diagnostic yield, a large cohort of patients still remain undiagnosed. Either the variant can be misidentified as a variant of unknown significance, or it is located in the 98,4% of non-sequenced DNA (Stenton and Prokisch 2018).

WGS

Whole genome sequencing (WGS), is an untargeted approach which aims to obtain the full genomic sequence information. It possesses the potential to disclose all genetic variants hidden in the human genome, including structural variants and breakpoints. This is mainly possible due to new techniques sequencing (ultra-)long reads (Jain et al. 2018). A diagnostic application of WGS has the potential to facilitate the identification of copy number variations and deep intronic mutations missed by exome capture (Lightowlers et al. 2015). Nevertheless, especially in long repetitive elements or complex regions, the coverage remains incomplete (Dewey et al. 2014; Goodwin et al. 2016).

The 1000 Genomes Project Consortium claims that a typical genome differs from the reference human genome at 4,1 million to 5,0 million sites (Auton et al. 2015), whereas WES starts on about 70.000 variants in an individual in comparison to a reference genome. The amount of variants together with incomplete annotations present a challege in variant prioritization (Biesecker and Green 2014)

Both WES and WGS approaches provide a full coverage of the mtDNA. This comes at very high coverage in WGS experiments (typically hundred to thousand times as many as the genomic coverage) and at a good coverage in WES (typically half of the exomic coverage) as an unspecific off-target product of the capture, due to the high copy number of mtDNA (Picardi and Pesole 2012). The range of different sequencing strategies is schematically depicted in Figure 5.

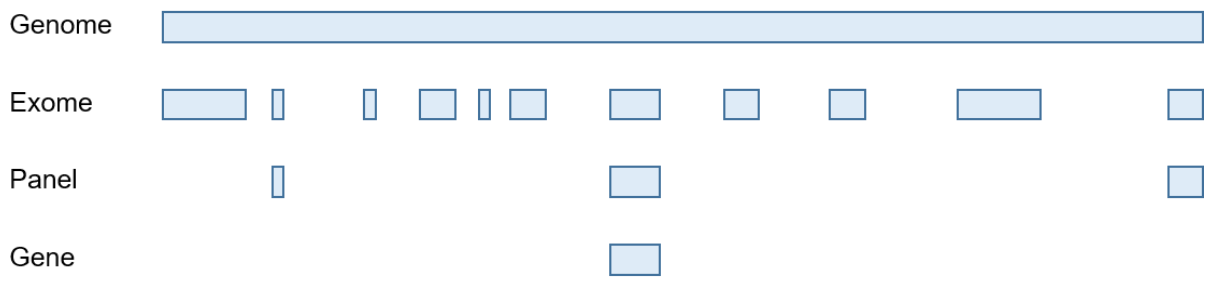

Figure 5: Sequencing strategies in human genetics. Sequencing of gene, panel, exome or genome covers different range of sequenced genomic DNA and therefore results in a different amount of data.

1.2.4.3 Variant prioritization

Variant filtering for whole exome sequencing has been developed to unravel the causal variant(s) (Haack et al. 2010). As seen in Figure 6, comparing a patient sequence with the reference genome, several thousands (~85.000) single nucleotide variants are typically found in the whole exome sequencing of an individual. By filtering for only rare variants (minor allele frequency < 0,01) with predicted impact on protein function, this large number of variants can be reduced to about two hundreds (~200). The following filtering steps focus on a recessive

type of inheritance because of a severe and early-onset presentation of a suspected rare genetic mitochondrial disorder. This is typically requiring two hits in a gene – compound heterozygous or homozygous variants – which leads to only a few candidates (~5-20). For the final selection four main points can be considered: whether the gene is coding for a mitochondria-related protein; whether the variant is predicted to impair the function; the lack of variants in a control population; and phenotypic-genotypic correlation.

In order not to miss or overestimate causal variants, several points must be kept in mind. Genes differ markedly in their tolerance to variation (Bustamante et al. 2005) and rare variants predicted to be damaging in disease-associated genes are often observed even in population controls (MacArthur et al. 2012). Furthermore, about half of healthy individuals carry at least one *de novo* protein-altering mutation (Veltman and Brunner 2012). In many cases, strong evolutionary sequence conservation helps to indicate relevant protein-coding and non-coding variations (Cooper and Shendure 2011).

Specifically, many mitochondrial gene and/or protein sequences are highly conserved. In the case of a known animal model, observed phenotypes can be compared and validated. Next, statistical support must be always considered. The larger the cohort of patients sharing the same phenotype and genotype, the more accurate the variant identification becomes. Publicly available datasets and databases provide useful aggregated information to increase filtering power and evaluate variants, both with predictions and statistical information (*e.g.* on predicted vs. observed frequency of loss-of-function variants on each gene like Exome Aggregation Consortium – ExAC or genome aggregation database – gnomAD).

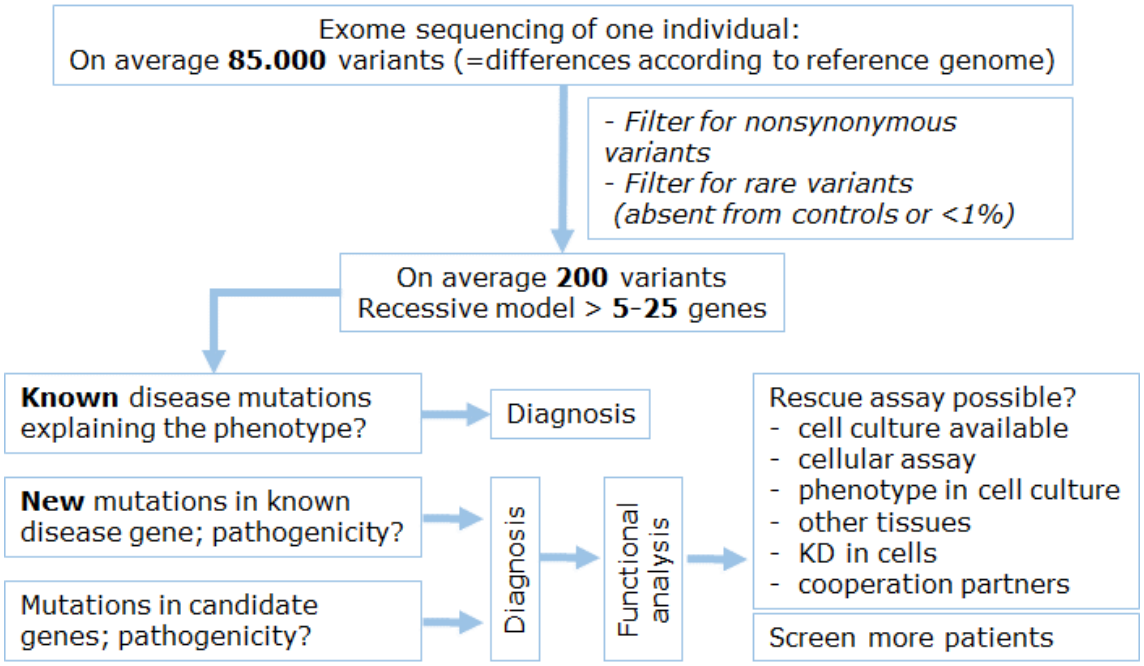

Figure 6: Overview of analysis workflow. Several filtration steps typically lead to a manageable number of potential gene candidates. By comparison to the phenotype, a known disease gene can emerge. In the case of a novel variant or a suspicion in a completely new disease gene, further analysis is required.

1.2.4.4 Functional studies to validate the WES/WGS findings

The molecular findings obtained by whole exome sequencing need to be validated. Firstly, Sanger sequencing of the identified variant is required to confirm the WES finding and to avoid sequencing errors or sample mixing (Haack et al. 2010). Segregation analysis done by a targeted sequencing of the affected allele(s) should follow Mendel's Law of segregation. The segregation itself does not prove the variant causality. However, if variants segregate with the disease within a family, then such variants are highly likely to be disease causing. At the same time, if the variants do not segregate, they can be inmediatelly excluded (Sosnay and Cutting 2014).

Based on the variant itself, a prediction of the effect on the protein function can be sought. For example, a stop codon producing variant either results in a truncated protein or complete loss of the protein. A variant in the functional domain can dramatically alter the enzymatic activity. These assumptions must however be confirmed in a functional assay (Haack et al. 2010). To study the transcript or protein stability, experiments such as real time PCR, RNA sequencing or Western blot analysis can be utilised. Quantitative proteomics presents a further possible solution.

In the case of mitochondrial disorders, measurements of the enzymatic activity of the individual or coupled respiratory chain complexes are available (Spinazzi et al. 2012). To monitor the overall function of the respiratory chain it is feasible to quantify the oxygen consumption rate. In this case, Oroboros Oxygraph Instrument and Seahorse XF Analyzer replaced the original Clark-type oxygen electrode developed to measure the mitochondrial respiration (Brand and Nicholls 2011; Yepez et al. 2018). Staining of Complex II and IV visualizes their stability and the mitochondrial content (Sciacco and Bonilla 1996). Moreover, an advanced method developed specifically to study mitochondrial disorders is a blue-native electrophoresis giving the information about functional composition of respiratory chain complexes (Wittig et al. 2006a).

All functional assays require biological material. A tissue biopsy, typically muscle, is the established gold standard for mitochondrial diagnosis and to observe alteration in respiratory chain enzymes activities (Wortmann et al. 2017). As a side product of a muscle biopsy, a culture of skin fibroblasts may be established. These cells represent a valuable tool for numerous standard biochemical and histological assays (*e.g.* mitochondrial morphology, reactive oxygen species and calcium levels, ATP handling, etc.). Moreover, the defect of OXPHOS found in skeletal muscle is frequently reflected in the fibroblasts, representing a valuable resource in connecting pathogenicity to new mutations (Koopman et al. 2012; Gorman et al. 2016). The fibroblast cells can also be used for genetic complementation experiments. The wild-type DNA copy of the candidate gene is introduced into those patient-derived cells by lentiviral delivery. If the proper mitochondrial function is sufficiently restored, the pathogenicity of the variant is demonstrated (Danhauser et al. 2011).

1.3 Treatment of mitochondrial disorders

Unfortunately, the increased success of diagnosis has not been reflected by the increased success in treatment of mitochondrial diseases. The number of drugs and therapies suitable for the majority of mitochondrial diseases is still very restricted (Lightowlers et al. 2015). Moreover, the variety of mitochondrial disease connected phenotypes complicates the situation. The first choice in suspected mitochondrial disorders, for instance, is a cocktail of nutritional supplements and vitamins, typically provided to any patient for a limited period of time (Chinnery and Turnbull 2001; Koene and Smeitink 2011; Pfeffer et al. 2012). The exact composition varies among clinicians and is based on the specific patient's needs. Most commonly the cocktail includes L-arginine (for metabolic strokes), coenzyme Q10 (in the form of ubiquinol or ubiquinone), creatine (to facilitate recycling of ATP), and L-carnitine (as an antioxidant and energy source; Enns 2014).

As an example, a rational therapy is currently available for coenzyme Q10 (CoQ) biosynthesis defects. The CoQ biosynthetic pathway consists of ten consecutive enzymatic reactions, where each of them can be dysfunctional. The supplementation of CoQ may overcome the insufficient natural production (Hargreaves 2014; Awad et al. 2018). Next, thiamine, vitamin B1, is beneficial in patients with a defective cerebral thiamine transporter, where it was reported to prevent further neurological deterioration (Haack et al. 2014). Thiamine supplementation also helps to correct some metabolic disorders, such as maple syrup urine disease and Leigh syndrome (Jauhari et al. 2017). The derivatives of thiamine play a role in several metabolic pathways, above all in the enzymatic reactions of sugar and amino acids catabolism or alcoholic fermentation.

Another member of vitamin B family is riboflavin, vitamin B2. It is recommended to modulate mitochondrial electron transfer flux for patients with impaired flavoproteome. Riboflavin itself or its derivatives take part in more than 100 enzymatic reactions, including function of Complexes I and II of the respiratory chain and their assembly factors (Lienhart et al. 2013). As an example, the riboflavin therapy was effective and mitigated symptoms in a deficiency of flavin adenine dinucleotide-containing acyl-CoA dehydrogenase 9 (ACAD9). This enzyme is involved in β-oxidation as well as in assembling of Complex I (Haack et al. 2010; Schiff et al. 2015; Repp et al. 2018).

The last example here of a supplement from the vitamin B family is nicotinamide riboside, a form of vitamin B3. Nicotinamide riboside is a nicotinamide adenine dinucleotide (NAD^+) precursor. NAD^+ (or NADH if reduced) acts as a coenzyme in redox reactions or as a donor of ADP-ribose (Billington et al. 2006). Additionaly, mitochondria and especially the OXPHOS require organic and inorganic cofactors for their proper function. Therefore, vitamins such as biotin, niacin, riboflavin or thiamine or non-vitamin cofactors CoQ or heme can be administrated. Also, several metal inorganic cofactors may be beneficial in some cases, for example copper, iron, magnesium, molybdenum, and zinc. These cofactors are not connected to any harmful side effects (Distelmaier et al. 2017).

Mitochondrial disorders are often associated with increased levels of reactive oxygen species (ROS). A defective respiratory chain is prone to leak a superoxide; or the natural removal of

ROS is malfunctioning, both leading to an increase of oxidative stress. To restore the balance between their production and removal, various antioxidants exist. Due to their nature, it is 'any substance that delays, prevents, or removes oxidative damage to a target molecule' (Halliwell and Gutteridge 2015). The naturally-derived antioxidants include vitamin C (ascorbic acid) and E (tocopherol), glutathione or CoQ (Marshall 2014). Based on their properties, artificial antioxidants have been produced, *e.g.* Trolox (analogue of vit. E), Idebenone and MitoQ (analogues of CoQ). Also, compounds such as N-acetylcysteine and α-lipoic acid are able to boost the glutathione biosynthesis (Magalhaes et al. 2016). The group of antioxidant drugs also includes L-carnitine, resveratrol, vitamin K1, or commercially produced EPI-743 (a para-benzoquinone analogue), Bendavia™ (a peptide binding to cardiolipin; Enns 2014) or the currently tested KH176 (derivative of Trolox; de Haas et al. 2017; Koene et al. 2017).

Another treatment example is that of endurance exercise, demonstrated to have an advantage in mitochondrial myopathies. In principal, endurance exercise training delays deconditioning and progressive deterioration and has been shown to improve exercise capacity over time. It was reported that endurance training improved mitochondrial function in muscle biopsies by an increase in total mitochondria content and by their increased activity visualized by staining of the COX activity. Consequently, it facilitated improvement in maximal oxygen uptake, peripheral muscle strength, not to mention the overall improvement of clinical symptoms (Taivassalo et al. 2006; Safdar et al. 2016).

The next option is a ketogenic diet, which is mainly suitable for patients suffering from epileptic seizures or pyruvate dehydrogenase defect. The principle lays in carbohydrate fasting replaced by a high-fat diet. The lack of carbohydrates, hence glucose, leads to an increased liver utilization of fats, and production of fatty acids and ketone bodies. Biochemically, the function of PDH is bypassed by energy production coming from β-oxidation. Patients with mitochondrial neurodegeneration characterized by seizures as well as other neurodegenerative disorders such as Amyotrophic Lateral Sclerosis, Parkinson's, Alzheimer's and Huntington's disease, may benefit from the ketogenic diet, because the alternative energy source forces brain tissue to utilize other metabolic pathways. The ketogenic diet was described to prevent formation of abnormal mitochondrial ultrastructures, to induce mitochondrial biogenesis via activation of AMPK and PGC1α and to decrease oxidative stress (Paoli et al. 2014; Koppel and Swerdlow 2018) in mouse models (Ahola-Erkkila et al. 2010; Sperl et al. 2015) as well as in children with various respiratory complex defects (Kang et al. 2007; Kossoff et al. 2014; Vidali et al. 2015).

A completely different approach is realized by gene therapy. There are several principles, suitable for different types of disorders. Gene replacement is effective in monogenic disorders; gene addition may help in complex disorders such as heart failure and cancer or infectious diseases; gene expression alteration by RNA interference resulting in a removal of a target malfunctioning RNA; or genome editing via zinc finger endonucleases (ZFNs), TALENs (transcription activator-like effectors nucleases), or CRISPR (clustered regularly interspaced palindromic repeat)/Cas9 systems (Baker 2012; Hsu et al. 2014; Wang and Gao 2014). In the case of mitochondrial disorders, specifically in LHON syndrome, a gene therapy approach is being investigated in an ongoing clinical trial, currently in phase 3. Patients are injected with a

wild type ND4 protein into the healthy eye. As reported, their visual acuity improved and visual field was enlarged (Wan et al. 2016). Furthermore, the CRISPR/Cas9 editing system was reported in a model of CoQ deficiency, where it succesfully corrected a mutation in the gene coding for an enzyme COQ4 (Romero-Moya et al. 2017).

Genome editing systems are being used in manipulation of mtDNA heteroplasmy. Briefly, the mutated mtDNA is targeted for removal, and is hence kept under the threshold level. As an example, restriction endonuclase *SmaI* reduced levels of mtDNA carrying m.8399T>G mutation that resulted in an increased ATP production (Tanaka et al. 2002a). Next, ZFNs and TALENS have been manipulated for mitochondrial localization. MtZFNs *in vivo* succesfully reduced pathogenic mtDNA with m.8993T>G and m.5024C>T point mutations or with a large "common deletion" (Gammage et al. 2014; Gammage et al. 2018). The MitoTALENs were able to target mtDNAs with various point mutations and deletions in patient cells (Bacman et al. 2013). The current limitation of this approach for clinical usage lays in the theoretical danger of rapid depletion of mtDNA (Hirano et al. 2018).

Recently in 2015, a mitochondrial donation, whereby mtDNA is obtained from a donor mother, has been permitted in the United Kingdom (Lightowlers et al. 2015; Gorman et al. 2016). If a mother is at risk of transmitting mutated mtDNA to her offsprings, she can take the advantage of mitochondrial donation techniques. Either a maternal spindle transfer or pronuclear transfer is used, differing in the timing of the transfer, whether it is perfomed pre- or post-fertilization. In principle, the nuclear material (*i.e.* spindle or pronuclei) is removed from a mother's oocyte and transferred into a donor denucleated oocyte, where the healthy mitochondria are already located in cytoplasm (Rai et al. 2018).

1.4 Introduction to reactive oxygen species (Thioredoxin 2 project)

Thioredoxin 2 (TXN2) is one of the enzymes removing reactive oxygen species, the production of which is an important by-product of the mitochondrial respiratory chain. For a long time, ROS have been seen only as dangerous agents that attack proteins, lipids and nucleic acids. However, in the last two decades, the importance of ROS in several signalling pathways has been described. Among others, homeostatic levels of ROS were shown to be required for correct differentiation during embryonic expansion of stem cells (Bigarella et al. 2014).

The first intensive debate about ROS started after the Denham Harman's publication *Aging: a theory based on free radical and radiation chemistry* (Harman 1956). In this work it was shown that about 2% of the oxygen being transferred through the respiratory chain in mitochondria may leak. Such free oxygen molecules can, in the environment of the respiratory chain, rapidly consume a single electron in order to create a highly reactive superoxide radicalanion $O_2^{\bullet -}$. Therefore, it is supposed that most of the reactive oxygen species production is coming from the electron transport chain in mitochondria, in addition to some ROS produced in the cell cytosol. A number of enzymes within the cell were described to produce ROS. However, the precise proportion of ROS originating from all of the different sites remains not yet fully determined. ROS production also depends on the cell type, microenvironment, and fitness.

1.4.1 Sites of reactive oxygen species production

Energy production in mitochondria is part of aerobic cellular metabolism. The superoxide or hydrogen peroxide production is in most cases a result of imperfect oxidation of oxygen to water in the mitochondrial respiratory chain. Among the ROS producing sites (Fig. 7), respiratory chain complexes are believed to be the central producers. Two out of eight iron-sulphur clusters and a flavin mononucleotide (FMN) site in Complex I are prone to leak an electron, and hence produce ROS (Genova et al. 2001; Kushnareva et al. 2002; Kussmaul and Hirst 2006; Esterhazy et al. 2008; Koopman et al. 2010). Also, several subunits of Complex III have a tendency to leak electrons, but their role in the respiratory chain is based on reaction cycles with coenzyme Q (Boveris et al. 1976; Turrens et al. 1985; Raha et al. 2000). Complex II is not a classical ROS producer, however a mutated protein (Guo and Lemire 2003; Slane et al. 2006) or low substrate conditions (Quinlan et al. 2012) can change this behaviour. There are also other minor ROS producers within mitochondria, for example electron transfer flavoprotein (ETF) and ETF ubiquinone oxidoreductase (Ruzicka and Beinert 1977), glycerolphosphate dehydrogenase (Drahota et al. 2002), a multisubunit pyruvate dehydrogenase complex (Starkov et al. 2004) or α-ketoglutarate dehydrogenase (Starkov et al. 2004), or aconitase (Vasquez-Vivar et al. 2000) and potentially also Complex IV (Koopman et al. 2010).

Several ROS producing sites are also described in the cytoplasm (Fig. 7). First of all, the family of NADPH oxidases, proteins able due to an increased ROS production to kill unwanted microorganisms during phagocytosis (Hampton et al. 1998). Stress conditions cause an increase in the production of ROS in other organelles: the unfolded protein response in the endoplasmic reticulum and in peroxisomes as a part of the long-chain fatty acid oxidation (Holmstrom and Finkel 2014). Additional ROS producers are located in the cytoplasm, such as cyclooxygenase, cytochrome P450 monoxygenase, D-amino acid oxidase as well as lipoxygenase or xanthine oxidase (Holmstrom and Finkel 2014). Similarly, reactive nitrogen species are a product of nitric oxide synthase (Koopman et al. 2010).

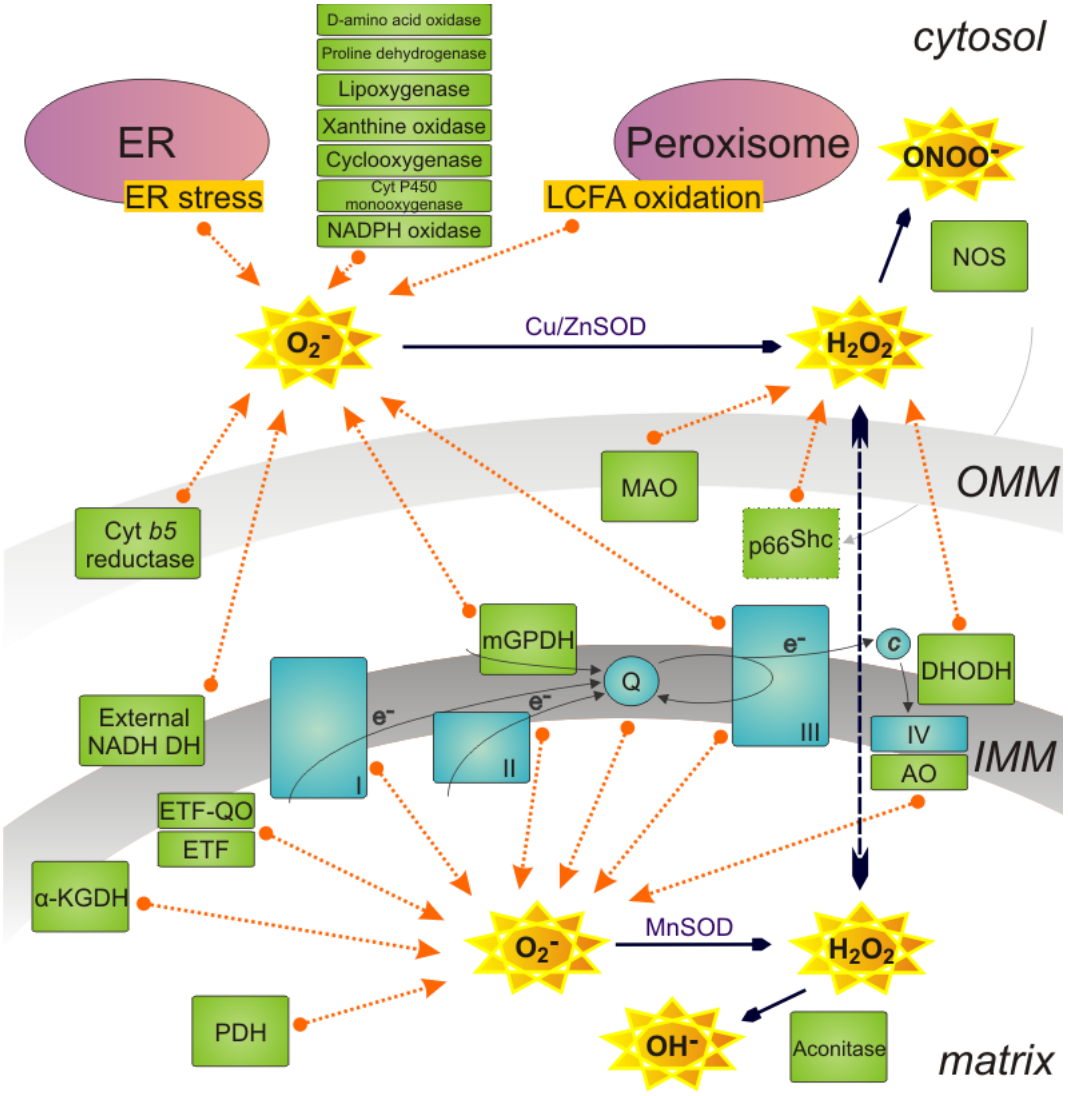

Figure 7: Sites of ROS production (modified from Holzerova and Prokisch 2015). Most of the enzymes responsible for ROS production are located in mitochondria: Complex I (I), Complex II (II), Complex III (III), Complex IV (IV); α-ketoglutharate dehydrogenases (α-KGDH), aconitase, alternative oxidase (AO), cytochrome (cyt) b5 reductase, dihydroorotate dehydrogenase (DHODH), electron transfer flavoprotein (ETF) and ETF ubiquinone oxidoreductase (ETF-QO), external NADH dehydrogenase (NADH DH), mitochondrial glycerophosphate dehydrogenase (mGPDH), monoamine oxidase (MAO), protein p66Shc, and pyruvate dehydrogenase (PDH). Additional ROS producers are located in cell cytosol, including nitric oxide synthase (NOS), a producer of reactive nitrogen species ($ONOO^-$) by reaction with H_2O_2. Respiratory chain complexes are depicted in blue, other ROS contributors in green, organelles in violet. Reactive oxygen or nitrogen species are portrayed as yellow stars. Enzymes produce typically either superoxide anion $O_2^{\bullet-}$ or hydrogen peroxide. Their transformation is ensured by superoxide dismutases, manganese (MnSOD) in mitochondria or copper-zinc (Cu/ZnSOD) in inner membrane space and cytosol. ER – endoplasmic reticulum, IMM – inner mitochondrial membrane, LCFA – long chain fatty acid, OMM – outer mitochondrial membrane.

1.4.2 Principles of reactive oxygen species scavenging and signalization

Redox-sensitive proteins contain thiol groups, which are able to scavenge the presence of ROS that they can use also for an active signalling. The redox changes mostly affect cysteine residues of the thiol groups, in particular cysteines with low pKa and a thiolate anion (S^-) at a physiological pH. However, methionines, tryptophans and tyrosines are also sensitive to redox imbalance. Likewise, enzymes with iron–sulphur clusters, such an aconitase, typically provide the sulphur from their cysteine residues (Holzerova and Prokisch 2015).

The active thiol group in cysteines can undergo a peroxide attack, resulting in a formation of reversible sulphenic acid (-SOH). This highly reactive group forms a disulphide bridge if another -SOH is present. Likewise, a sulphonamide (-SN-) is created as a result of reaction with an amine, *e.g.* at the end of an amino acid (Fig. 8). Both changes are reversible redox modifications, which can be restored by molecules or proteins of the ROS scavenging systems (Fig. 9). However, continuing exposure to hydrogen peroxide in the redox environment will further oxidize the sulphenic groups, and irreversible sulphinic ($-SO_2H$) or sulphonic ($-SO_3H$) acids will be created (Kiley and Storz 2004). Irreversibly produced proteins are potentially dangerous, if their removal is malfunctioning.

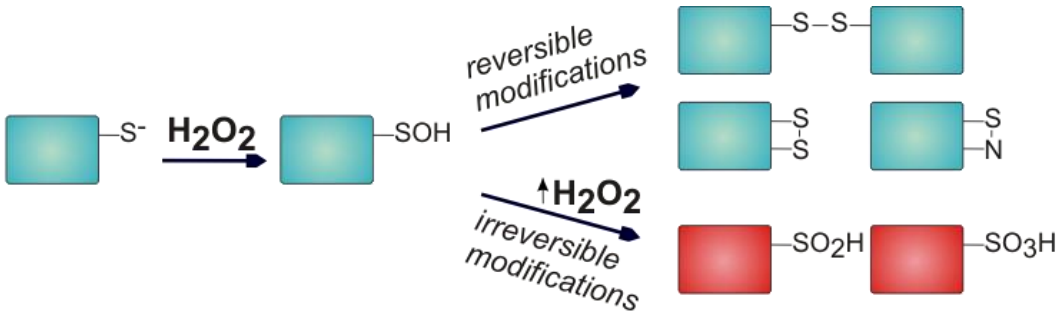

Figure 8: Molecular mechanisms of reactive oxygen species scavenging mechanism (modified from Holzerova and Prokisch 2015). Redox environment produces either reversible or irreversible changes in redox sensitive proteins. The available sulphur in cysteines undergoes oxidation in the presence of hydrogen peroxide. Reversible modifications are restored by enzymes and molecules displayed in Figure 9. Ongoing oxidative environment depicted by ↑H_2O_2 results in production of end products with sulphinic ($-SO_2H$) or sulphonic ($-SO_3H$) acids.

As most of ROS production occurs in mitochondria, a complex defence system has developed therein. There are two main groups of enzymes, so called glutathione or thioredoxin (including TXN2) pathways. Both groups cooperate in a way to keep ROS at a manageable level. Peroxiredoxin and glutathione peroxidase in mitochondria directly react with hydrogen peroxide in order to decompose it into molecules of water (Fig. 9). The enzymes are oxidized as a result of the reaction. Proteins of the peroxiredoxin family (mostly PRDX3) form homodimers in the redox environment via disulphide bridges, which are subsequently oxidized by thioredoxins (TXN2 in mitochondria). Cells with peroxiredoxin monomers are sufficiently ready to fight ROS. Oxidized thioredoxin molecules are later on reduced by the reaction of

thioredoxin reductase (TXNRD2 in mitochondria) with the reduction equivalents provided by NADPH.

Likewise, oxidized glutathione peroxidase (GPx) is reduced by molecules of glutathione, a tripeptide antioxidant with high cellular concentration of 1-10 mM (Gilbert 1990; Schafer and Buettner 2001). In the redox environment, glutathione forms homodimers (GSSG) or is attached to another protein via a disulphide bridge. Restoration of glutathione monomers (GSH) is then ensured by glutathione reductase (GSR). GPx can also be reduced by glutaredoxin (GLRX). GLRX is responsible for crosstalk with the thioredoxin pathway, while it can reduce the PRDX3 dimers (Gladyshev et al. 2001; Lundberg et al. 2001; Hanschmann et al. 2010). Likewise, TXNRD2 is able to directly reduce peroxiredoxin dimers. Moreover, GLRX or glutathione can reduce TXN2 (Casagrande et al. 2002).

Glutathione or thioredoxin form the main molecules of the ROS scavenging mechanism. The whole machinery is mostly active in mitochondria, but the same or analogous enzymes exist in the cytosol. For instance, thioredoxin 1 or thioredoxin reductase 1. In particular, peroxisomes produce ROS to maintain their function, hence they also developed a complex defence system. Catalase is also an enzyme responsible of disassembly of hydrogen peroxide into oxygen and water; however, it is primarily found and active in peroxisomes (Kirkman and Gaetani 1984).

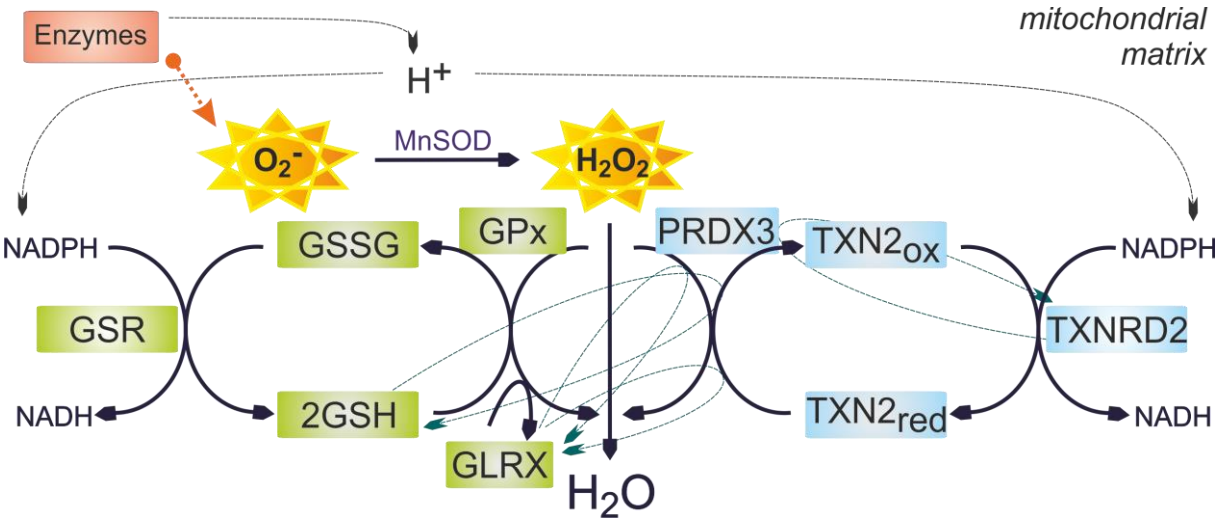

Figure 9: Reactive oxygen species scavenging pathways (modified from Holzerova and Prokisch 2015). ROS, thus superoxide radicalanion ($O_2^{\bullet -}$) or hydrogen peroxide (H_2O_2) are produced by enzymatic activities of respiratory chain complexes as well as other enzymes. In mitochondria is superoxide converted to hydrogen peroxide either spontaneously or by the reaction of manganese superoxide dismutase (MnSOD). ROS scavenging systems are displayed as molecules of the thioredoxin (on the right part in blue) and glutathione (on the left part in green) systems. Within mitochondria, hydrogen peroxide is reduced by enzymatic reaction of peroxiredoxin 3 (PRDX3) and oxidation of PRDX3 is reduced by thioredoxin 2 (TXN2), thioredoxin reductase 2 (TXNRD2) and NADPH. In the glutathione pathway, glutathione peroxidase (GPx) reduces H_2O_2 into water and it is reduced by glutathione (GSH) molecule, which forms dimers (GSSG). Glutathione reductase (GSR) reduces dimers of GSH by using reducing equivalents of NADPH. Similarly, GPx can be reduced by a molecule of glutaredoxin

(GLRX). The crosstalk of the pathways and the minor reactions are depicted by light blue arrows.

1.4.3 Redox imbalance causes ROS-dependent signalling

In the case of supposedly malfunctioning TXN2, part of the defence system, imbalance of ROS levels and following signalling pathways was suspected. In theory, redox environment causes an oxidation of thiol groups in proteins, which inactivates several enzymes that actively block particular signalling pathways. Such indirect inhibition is then responsible for activation of ROS signalling. Protein phosphatases are an example of a group of enzymes, which are inactivated by H_2O_2. As a result, the level of phosphorylated proteins in the cell increases (Meng et al. 2002). Likewise, protein tyrosine phosphatases are reversibly inactivated in redox environment (Denu and Tanner 1998). Also, a receptor tyrosine kinase is directly approached by ROS, hence the kinase signalling is affected (Truong and Carroll 2013). A burst of ROS generation is then responsible for a stimulation by a growth factor, followed by an increased tyrosine phosphorylation, leading to a signal transduction (Sundaresan et al. 1995; Bae et al. 1997).

Reactive oxygen species, among others, attack DNA, but the redox signalling affects transcription factors, such as bacterial OxyR. OxyR is a redox sensitive protein with the ability to promote the antioxidant stress response. Oxidation of cytosine residues in OxyR creates an intra-molecular disulphide bond that locks the transcription factor in its active form (Xanthoudakis and Curran 1992; Lee et al. 2004).

An antioxidant pathway of a nuclear factor erythroid 2-related factor 2 (Nrf2) and Kelch-like ECH-associated protein 1 (Keap1) is an example of a general ROS defence (Fig. 10). This pathway is activated in a presence of oxidative or electrophilic environment as well as nutrition or artificial drugs. Upon normal conditions, Nrf2 is found in cytosol and bound to Keap1. However, activating stimuli cause Nrf2 release and its translocation to the nucleus. Therein, Nrf2 forms a heterodimer with musculoaponeurotic fibrosarcoma (Maf) that together mount to antioxidant response element (ARE) in DNA. This stimulates transcription of antioxidant enzymes such as catalase, glutathione peroxidase or glutathione *S*-transferase (Lee et al. 2011).

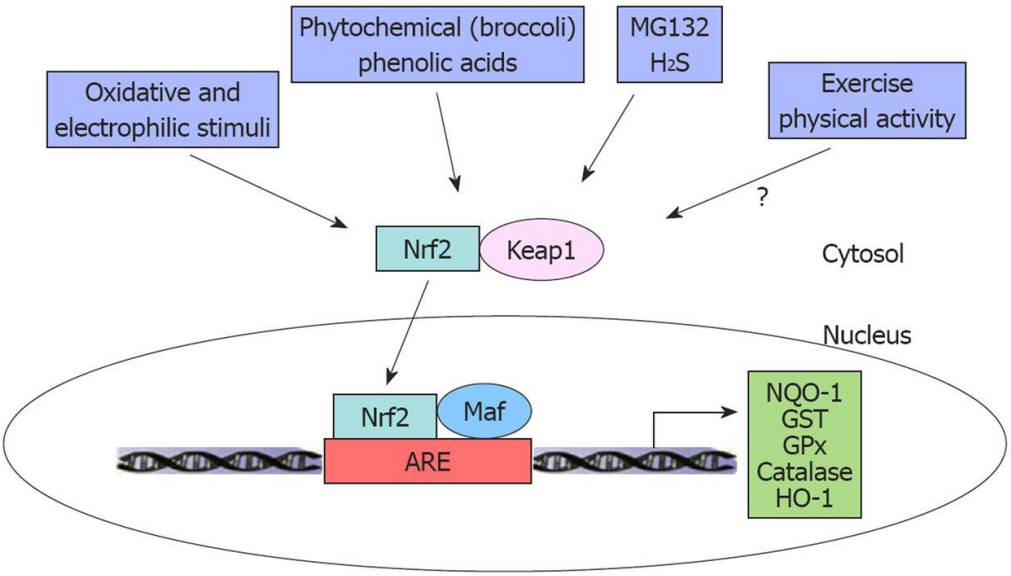

Figure 10: Nrf2-Keap1 antioxidant pathway (from Lee et al. 2011). Several different, typically redox stress stimuli (in blue boxes) affect the complex of nuclear factor erythroid 2-related factor 2 (Nrf2) and Kelch-like ECH-associated protein 1 (Keap1). Once the Nrf2 is released, immediately translocates to cell nucleus, where it forms dimer with musculoaponeurotic fibrosarcoma (Maf). This dimer is then effectively bound to DNA in a position of antioxidant response element (ARE) that starts transcription of antioxidant genes, e.g. catalase, heme oxygenase-1 (HO-1), NAD(P)H quinone oxidoreductase-1 (NQO-1), glutathione peroxidase (GPx), or glutathione S-transferase (GST).

Numerous other pathways and proteins are connected to ROS production. Such as actin polymerization, DNA binding of transcription factors activator protein 1, activity of the calcium/calmodulin-dependent kinase, or forkhead box protein O, and nuclear factor erythroid 2-related factor 2, essential autophagy protein ATG4 (Holmstrom and Finkel 2014). In many scenarios, increased ROS production triggers mitophagy, an effective quality control system.

1.4.4 Impairment of ROS scavenging system

Mitochondrial dysfunction is traditionally linked to an increased ROS production, and *vice versa*. The missing enzymatic reaction of TXN2 can possibly trigger a burst of ROS; however, the evidence in literature is not that concrete. So far, no patient with loss-of-TXN2 has been reported, however variants in cooperating proteins have been found or modelled.

Interestingly, no increased ROS generation was observed in a so called mutator mouse model. This model accumulates mutations in the mtDNA due to an inactivation of proofreading function of mitochondrial DNA polymerase (Trifunovic and Larsson 2008; Bratic and Larsson 2013). Over time the mutator mouse showed a variety of ageing phenotypes, such as osteoporosis, greying of the hair, hair loss, reduction of weight and decreased fertility. However, minor or no increase of oxidative stress has been observed (Trifunovic et al. 2004).

The same conclusion has been reached in a mouse model with dysfunctional Complex I subunit NDUFS4 (Chouchani et al. 2014).

The increase of ROS in mitochondria can happen due to various reasons, some of which might not be known to date. In terms of the defence mechanism, responsible for keeping ROS at a certain level, full or partial inactivity can occur. Accordingly, several disorders in the scavenging mechanism have been described. Recently, a homozygous variant in the mitochondrial selenoprotein thioredoxin reductase (*TXNRD2*; OMIM #617825) has been observed. This mutation was found to be associated with a familial glucocorticoid deficiency in seven individuals from a consanguineous family (Prasad et al. 2014). This was the first observation of a homozygotic variant in enzymes of the thioredoxin ROS defence pathway causing an inherited disorder in living patients.

On the contrary, *Txnrd2* knockout (KO) mouse model presented with an embryonic lethality (Conrad et al. 2004). The mouse embryos died at embryonic day 13 and were significantly smaller, severely anaemic and showed increased apoptosis in the liver. It appeared that Txnrd2 played a key role in haematopoiesis and above all in a correct heart development and function. As reported, heterozygous mutations in *TXNRD2* were observed in patients with dilated cardiomyopathy (OMIM #115200; Sibbing et al. 2011). Both observations suggest that the embryonic lethality is likely a consequence of an inability to restore the Txnrd2 function leading to a cardiac arrest. To study this phenotype, the group of Dr. Marcus Conrad created a mouse model with a cardiac cell-specific inactivation of the *Txnrd2* gene. Accordingly, these mice developed a fatal dilated cardiomyopathy and died shortly after birth. Further investigations unravelled the role of Txnrd2 in the removal of ROS and the maintenance of mitochondrial homeostasis. The *in vitro* experiments showed that the glutathione system is incapable to compensate for the TXNRD2 loss leading to a growth of ROS levels (Conrad et al. 2004).

Similarly, mouse embryos lacking cytosolic thioredoxin reductase (Txnrd1) showed limited cell proliferation resulting in a severe growth retardation and early embryonic lethality (Jakupoglu et al. 2005). Such observations were described as well in thioredoxin 1 (Txn1) knockout mice. Txn1 KO died shortly after implantation because of proliferation defect of their inner mass cells. Txn1 is therefore essential for early morphogenesis and differentiation of the mouse embryo. In opposite, heterozygotes $Txn1^{+/-}$ are viable, fertile, and seem normal (Matsui et al. 1996).

In the glutathione ROS defence pathway, a consanguineous family with a frameshift mutation has been reported. The variant, more specifically a duplication of one thymine at position c.714, was found in glutaredoxin domain-containing cysteine-rich protein 2 (GRXCR2; Imtiaz et al. 2014). It affects the cysteine-rich region of GRXCR2 and results in abnormal extension of the C-terminus. The patients suffer from early onset, bilateral and progressive hearing loss (OMIM #615837). The phenotype can be explained by the localization of the wild type GRXCR2 in the microvilli of sensory hair cells in the inner ear (Odeh et al. 2010), where in contrast the mutated GRXCR2 is unstable and was found predominantly in cytosol (Imtiaz et al. 2014). However, ROS levels were not analysed in this study.

Furthermore, a mouse model with glutathione deficiency was induced by administration of buthionine sulfoximine, a selective inhibitor of gamma-glutamylcysteine synthetase. These mice presented with decreased glutathione levels in cerebral cortex and enlargement and degeneration of mitochondria. The authors suggest that lower GSH levels lead to an increased mitochondrial and cell damage due to higher ROS occurrence (Jain et al. 1991; Martensson et al. 1991). Later, a mouse model lacking the catalytic subunit of glutamate cysteine ligase showed the essentialness of GSH synthesis, as mouse embryos died before birth (Dalton et al. 2000).

The mentioned GSH deficiency model aims to help the study of various defects of human GSH synthesis. The production of glutathione is assured by six enzymes, for which five hereditary deficiencies have been described. Most of the mutations are leaky, hence the enzymes have residual activity. Nevertheless, all are very rare and autosomal recessive. The phenotypes differ from haemolytic anaemia, metabolic acidosis, 5-oxoprolinuria to disorders of the central nervous system and neuromuscular function (OMIM #266130; #230450; #231900; Ristoff & Larsson 2007).

Next, acatalasemia is a state characterized by very low levels of catalase (OMIM #614097). It develops as a result of homozygous mutations in the *CAT* gene, in which 12 mutations have been described to date (Goth and Nagy 2012). Acatalasemia causes increased ROS levels, which play a role in the pathogenesis of several diseases. As an outcome, it increases the risk of developing a disorder, particularly in a combination of an additional impairment (Terlecky et al. 2006).

Last but not least, a general increased ROS production has been described in neurodegenerative disorders, such as Alzheimer's, Parkinson's or Huntington's disease (Manoharan et al. 2016).

1.4.5 Thioredoxin 2 in detail

Thioredoxin 2 is encoded by a nuclear *TXN2* gene located on chromosome 22q12.3. It is a 13-kDa redox protein with an active site Trp-*Cys*-Gly-Pro-*Cys* at positions 89 to 93. Its first 59 amino acids represent a mitochondrial targeting sequence responsible for the subcellular localization (Spyrou et al. 1997). Unlike the TXN1, TXN2 does not create intermolecular dimers, however such polymerization still occurs in the crystal structure mainly as a result of hydrophobic contacts. Moreover, the TXN2 crystal structure reveals possible interaction domains and helps in further studies of the enzymatic activity (Fig. 11; Smeets et al. 2005). Within the redox environment the cysteine residues create an intramolecular disulphide bond that needs to be reduced by thioredoxin reductase and NADPH (Holmgren 1985; Arner and Holmgren 2000).

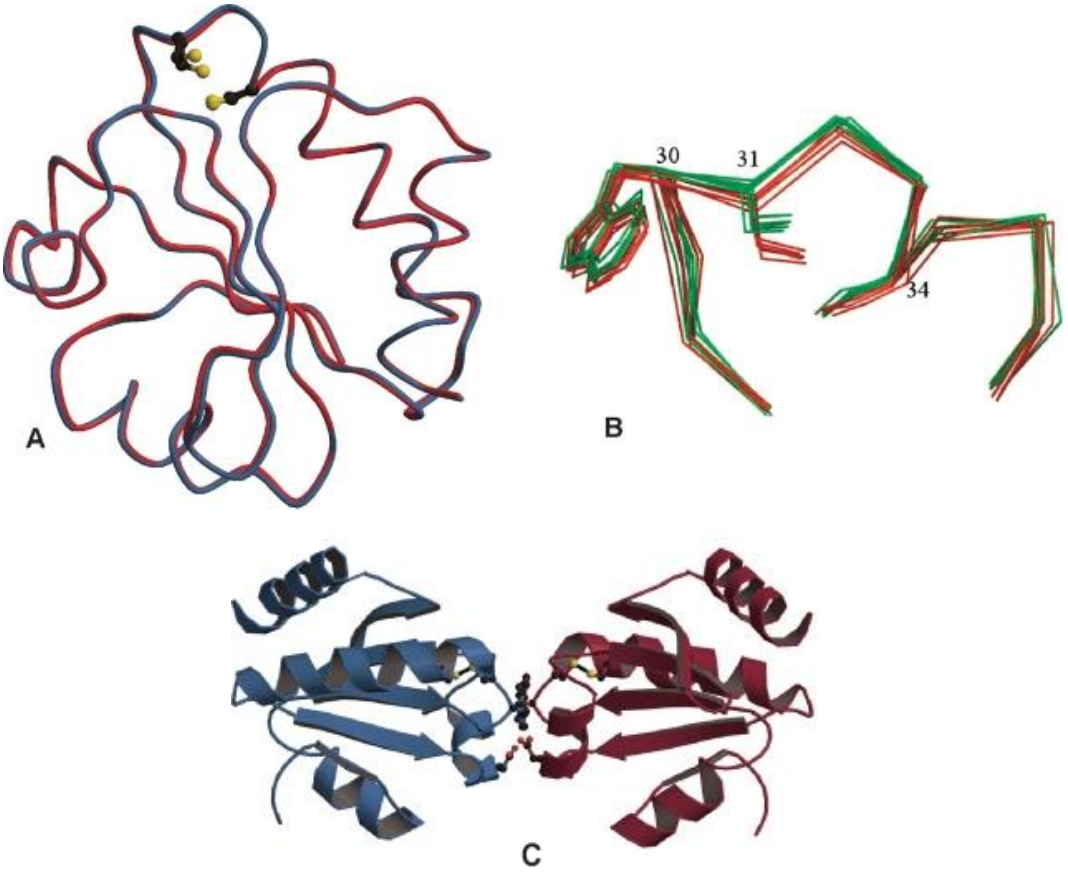

Figure 11: Crystal structure of human TXN2 protein (modified from Smeets et al. 2005). Crystal of reduced and oxidized human thioredoxin 2 were described at 2,0 and 1,8 Å resolution. (A) Superposition of oxidized (red) and reduced (blue) molecules of TXN2. The side chains of redox active cysteines are depicted as yellow balls. (B) The C^a chain of residues 27–38 counted without the mitochondrial targeting sequence, hence in the full-length protein residues 86–97. The side chains of Trp30 (resp. 89), Cys31 (90), and Cys34 (93) are also shown. Red coloured chain presents the oxidized TXN2, green the reduced one, altogether after superposition of 12 molecules. (C) Crystal dimerization of oxidized TXN2 led by hydrophobic interactions. The side chains of following amino acids are also presented: Trp30 (89), Cys31 (90), Cys34 (93), and Asp60 (119).

TXN2 is ubiquitously expressed with high expression primarily in tissues with increased metabolic activity, both in the adults and the foetus. The highest expression levels were observed in the brain tissue and neurons (Rybnikova et al. 2000), but also in others organs with high metabolic demand, including the stomach, testis, ovary, liver, heart, and adrenal glands.

Beyond the maintenance of ROS homeostasis, TXN2 regulates apoptosis induced by the oxidative environment (Damdimopoulos et al. 2002; Tanaka et al. 2002b; Lu and Holmgren 2012). Interestingly, a pharmacological inhibition of the mitochondrial thioredoxin system leads to decreased oxygen consumption together with decreased ATP/ADP ratios, and increased formation of lactate in human endothelial cells (Lowes and Galley 2011). Likewise,

the thioredoxin system was shown to regulate glucose homeostasis, thus subsequently affect mitochondrial bioenergetics. Thioredoxin has hence been exposed as the linkage between antioxidant defence, cell survival, and energy metabolism (Yoshioka and Lee 2014). Additionally, it was observed that enzymes of the Krebs cycle and collaborating mitochondrial pathways harbour thioredoxin binding sites. This points to a potential role in redox regulation by oxidative signalling, specifically the regulation of the Complex II, fumarase and citrate lyase was described (Daloso et al. 2015).

Next, it was reported that TXN2 interacts with thiols of the membrane adenine nucleotide translocator (ANT). Oxidation of cysteine residues in ANT and their crosslinking converts ANT into an open unspecific pore that causes mitochondrial membrane permeabilization (Vieira et al. 2000; Chen et al. 2002; Halestrap et al. 2002). This leads into a release of, among others, cytochrome *c* and a launch of the apoptotic cascade. TXN2 also affects apoptosis by inhibition of apoptosis stress kinase-1 (ASK1). ASK1 is activated upon oxidative stress by its dissociation from a complex with thioredoxin. Subsequently, ASK1 triggers mitochondrial-dependent apoptotic cell death (Zhang et al. 2004; Huang et al. 2015).

A knockout mouse model of the thioredoxin 2 had been created (Nonn et al. 2003), but the $Txn2^{-/-}$ embryos died between embryonic days 10,5 and 12,5. Hence, similarly to Txnrd1, Txn1 and Txnrd2 KO models, Txn2 is crucial for prenatal development, thus for proliferation and protection from apoptosis. The most striking phenotype is an open anterior neural tube together with massively increased apoptosis at the tenth day postcoitus. The anterior neural tube is a precursor for the brain development, which forms itself, once the tube closes. Moreover, exencephaly occurs (Harris and Juriloff 1999). As has been reported, between the tenth and twelfth day of embryogenesis, mitochondria mature rapidly and begin to utilize the OXPHOS and the Krebs cycle (Shepard et al. 1998). Because of the embryonic lethality of Txn2 KO, Nonn and colleagues also studied the $Txn2^{+/-}$ mice. These heterozygous mice appeared normal and were fertile. Only the levels of thioredoxin RNA and protein were decreased (Nonn et al. 2003).

Cardiac-specific Txn2 KO mice were studied as a model for patients with dilated cardiomyopathy resulting from reduced expression levels of TXN2 in the heart. The mice developed dilated cardiomyopathy at one month of age together with several additional cardiac impairments, resulting in death by four months of age. Mitochondria in such hearts lost their ultrastructure, integrity, membrane depolarization and ability to maintain ROS at eligible levels. The morphological alteration was accompanied by reduced protein expression of OXPHOS subunits and increased electron leakage. Additionally, ATP production was reduced and apoptosis occurred more often (Huang et al. 2015).

Studies of the conditionally *Txn2* deficient chicken β-cells observed an accumulation of ROS, which was in contrast with a decrease of the total and mitochondrial GSH levels in such an environment. As a result, these cells more often underwent apoptosis. Hence, Tanaka *et alii* claimed that functioning Txn2 is essential for cell viability (Tanaka et al. 2002b).

On the contrary, overexpression of *Txn2* in human HEK 293 cells was described to increase protection against etoposide-induced toxicity as well as to increase sensitive to rotenone. Also,

a connection between Txn2 and the transmembrane potential has been described. Likewise, thioredoxin 2 interfered with the ATP synthase and played an important role in interaction with specific components of the respiratory chain (Damdimopoulos et al. 2002).

1.4.6 Principles of antioxidant therapies for mitochondrial disorders of the redox system

Understanding the mechanism of ROS defence and scavenging helps to describe specific impairments and to suggest suitable rational therapies. Utilization of antioxidants seems as a reasonable treatment for disorders with increased ROS levels, as suspected in the patient with variant in *TXN2*. Therefore, several of the available antioxidants are here described in detail:

Glutathione, chemically glutamyl-L-cysteinyl-glycine, is a tripeptide with a gamma peptide linkage (Fig. 12). GSH is a natural antioxidant present in plants, animals, fungi, some bacteria, and archaea. Its main role is to reduce disulfide bonds in proteins by serving as an electron donor and to neutralize ROS. After such reaction, glutathione itself becomes prone to react, in such cases a dimerization is plausible due to the high concentration of glutathione in cells (up to 10 mM; Kaplowitz 1981). In healthy environment, more than 90% of GSH is in the reduced form (Halprin and Ohkawara 1967). The ratio of reduced to oxidized glutathione within cells is used as an indication of cellular oxidative stress (Pastore et al. 2001; Lu 2013). Glutathione can theoretically be obtained as a dietary supplement; however, it is a target of proteases and there are no specific glutathione carriers in cell membranes (Witschi et al. 1992; Allen and Bradley 2011).

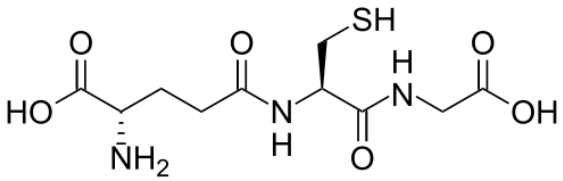

Figure 12: Chemical structure glutamyl-L-cysteinyl-glycine, glutathione in short.

Glutathione is part of the cellular non-enzymatic antioxidant system also containing carotenoids, flavonoids and vitamins C and E (Koopman et al. 2010).

Vitamin E, usually in the form of γ-tocopherol or α-tocopherol is obtained from nourishment (Fig. 13; Reboul et al. 2006). It supresses the propagation of ROS through biological membranes or fats, mostly because vitamin E is lipophilic and incorporates into membranes. The reactive oxygen species or the reactive lipid radicals are made to react with vitamin E to create a tocopheryl radical that is being reduced by a hydrogen donor (Brigelius-Flohe and Traber 1999). No significant benefit of vitamin E administration has been observed in healthy individuals (Bieri 1974).

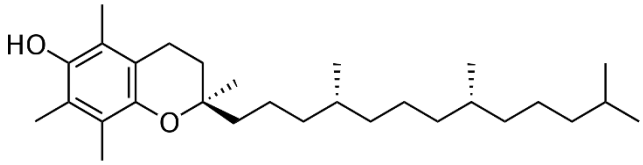

Figure 13: Chemical structure of the α-tocopherol form of vitamin E.

Trolox is a cell-permeable, water-soluble analogue of vitamin E (Fig. 14), also used as an antioxidant to reduce oxidative stress. It was reported that Trolox decreases lipid peroxidation, cytotoxicity, and levels of apoptosis in Hep G2 cells (Chen and Cederbaum 1998). Likewise, Trolox was shown to quench free radicals and inhibit reactive oxygen species generation in rat glial cells (Kaur et al. 2010). It also enhances treatment of lymphoma, while protecting against liver toxicity (Diaz et al. 2007). However, Trolox is mainly used in a method called Trolox equivalent antioxidant capacity that is a standard method of measuring antioxidant capacity, mostly in food and supplements (Cos et al. 2003; Huang et al. 2005; Prior et al. 2005).

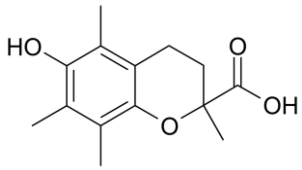

Figure 14: Chemical structure of Trolox (6-hydroxy-2,5,7,8-tetramethylchroman-2-carboxylic acid).

Another group is that of coenzyme Q10 (CoQ10) and its synthetic analogues (Fig. 15). CoQ10 is a coenzyme that is ubiquitously expressed in animals and most bacteria. Its main role is in the transfer of up to two electrons per molecule in the electron transport chain. CoQ10 has not been approved as a drug by the Food and Drug Administration. Nevertheless, it is sold as a food supplement (Garrido-Maraver et al. 2014). Coenzyme Q10 is typically well tolerated (Wyman et al. 2010; Acosta et al. 2016), however it is insoluble in water. Therefore, its hydrophilic analogue with only one isoprene repeat in the tail, CoQ1, is administered to patients or used in *in vitro* experiments. It is estimated that the daily intake of CoQ10 is about 3 to 6 mg per day, mostly from meat (Pravst et al. 2010).

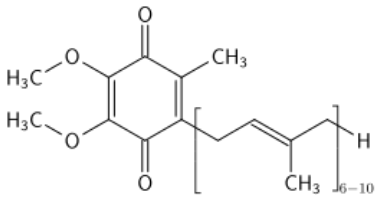

Figure 15: Chemical structure of coenzyme Q. This antioxidant varies in the number of isoprene repeats, e.g. rats contain nine repeats, humans ten.

MitoQ is an artificial mitochondrially targeted CoQ analog, mitoquinone mesylate in the full name (Fig. 16). It mimics the role of CoQ and moreover it aims to augment the antioxidant capacity. MitoQ was developed to cure the Parkinson's disease and liver damage caused by Hepatitis C viral infection (Tauskela 2007). Administration of MitoQ in healthy wild type mice did not alter the mitochondrial function (Rodriguez-Cuenca et al. 2010). However, daily administration of a 100 μM dose to a mouse model of Alzheimer's disease improved their memory, cognitive behaviour and reduced lipid peroxidation (McManus et al. 2011).

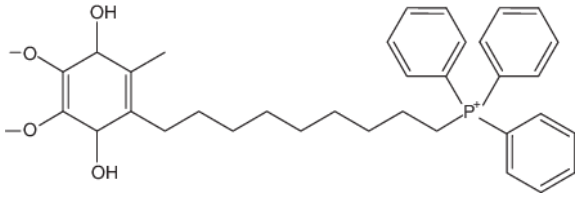

Figure 16: Chemical structure of MitoQ. MitoQ results from a conjugation of coenzyme Q and triphenylalkylphosphonium ion. This ion helps to locate MitoQ into mitochondria due to the gradient of mitochondrial membrane potential.

Last but not least, Idebenone is a drug originally developed to treat Alzheimer's disease and similar cognitive defects (Fig. 17; European Medicines Agency 2008). Later, clinical trials tend to use Idebenone for patients with Friedreich's ataxia and Duchenne muscular dystrophy, however usage in all settings has not been successful or approved (Buyse et al. 2003; Di Prospero et al. 2007; Tonon and Lodi 2008). Despite this, Idebenone was approved as a treatment for Leber's hereditary optic neuropathy in Europe showing a discontinuation of further visual impairment (Klopstock et al. 2011). Idebenone can by-pass malfunctioning Complex I and can feed electrons directly to Complex III. It is also recapturing electrons outside the inner mitochondrial membrane to prevent ROS production. Idebenone can easily be administered with fatty food and it is well absorbed into cells, but less than 1% is able to pass through the liver into circulation.

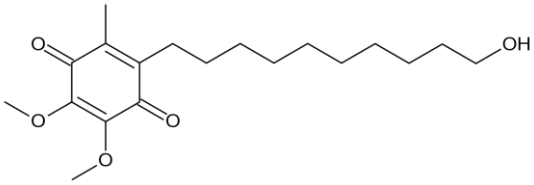

Figure 17: Chemical structure of Idebenone.

1.4.7 Inhibitors connected to the ROS production and ROS defence system

Artificial deficiencies of the ROS defence system can be created by using inhibitors of specific enzymes. This helps in *in vitro* experiments, where models are not available, costly, or results are needed in a limited time frame. Inhibitors of such system further challenge the interconnected enzymes and help to unravel the essence of human disorders of ROS

homeostasis. In our cellular model with loss-of-TXN2, I could take the advantage of available inhibitors to study the ROS system and to validate the effect of a potential antioxidant treatment.

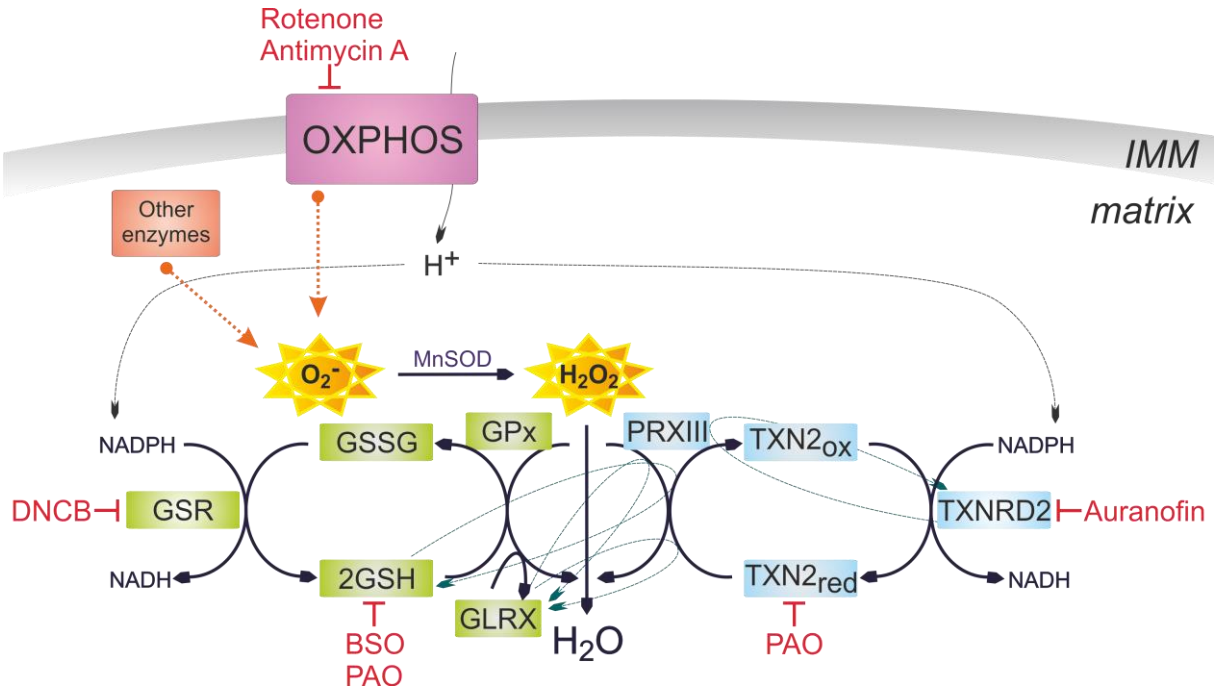

Figure 18: Schematic representation of OXPHOS, enzymes of the ROS defence system and their inhibitors (modified from Holzerova et al. 2016). In red are depicted various inhibitors that block the activity of either OXPHOS or components of the ROS scavenging system. The crosstalk of the pathways and the minor reactions are depicted by light blue arrows. Details about the course of their action are described in text.

First of all, rotenone and Antimycin A are two of many inhibitors of complexes of the respiratory chain. Rotenone is a natural substance that blocks the electron transfer from iron-sulphur clusters in Complex I to coenzyme Q in the membrane. This causes, on one hand, reduced ATP production as a result of limited formation of the proton gradient; on the other hand, impaired electron transfer makes the cell prone to produce ROS (Caboni et al. 2004; Heinz et al. 2017). Similarly, Antimycin A interacts with electrons leaving Complex III at the so called Q_I site. Equally, electrons tend to leak from the membrane microenvironment, and the proton gradient is not being efficiently built (Kim et al. 1999). Both inhibitors are used in experimental conditions to stimulate ROS production in the investigated system.

Secondly, 2,4-dinitrochlorobenzene or DNCB is used as an inhibitor of the GSH defence system. It is used in settings where it is essential to distinguish the contribution of glutathione and thioredoxin ROS defence systems (Aon et al. 2012). It has a GSH depleting effect as well as it inhibits glutathione reductase (Jocelyn and Cronshaw 1985). The inhibition of GSR was described to increase levels of glutathione disulphide, consequently to increase ratios of NADH/NAD^+ and NADPH/$NADP^+$, and to increase the level of protein glutathionylation. However, solely inhibition of GSR does not affect ROS production nor expression of enzymes of the ROS defence pathways (Zhao et al. 2009).

Next, buthionine sulfoximine (BSO) is a selective inhibitor of gamma-glutamylcysteine synthetase, hence the production of GSH (Bailey 1998). This reaction is also the limiting step of GSH biosynthesis. BSO has been tested as an anti-cancer drug that enhances the effect of many cytotoxic agents (O'Dwyer et al. 1996).

Phenylarsine oxide (PAO) is a phosphotyrosine phosphatase inhibitor that cross-links vicinal thiol groups, thereby inactivating phosphatases possessing XCysXXCysX motifs. It forms stable complexes with neighboring cysteine residues, as it possesses high affinity towards sulphur, particularly in organic compounds (Gerhard et al. 2003; Verspohl 2006).

The lastly mentioned inhibitor, auranofin, is a molecule containing a gold atom in its structure. It is established as an antirheumatic agent (Bernhard 1982). Auranofin is an inhibitor of selenocysteine enzymes, hence thioredoxin reductase and glutathione peroxidase. Different concentration can selectively inhibit either the first or both enzyme systems (Venardos et al. 2004a). Due to its targets, auranofin prevents removal of ROS leading to an oxidative stress and increased apoptosis (Rigobello et al. 2005; Venardos et al. 2004b). Also, the inhibition of TXNRD2 leads to increased levels of oxidized thioredoxin 2 that is in such status more accessible for degradation (Chen et al. 2014).

1.5 Introduction to riboflavin metabolism (Flavin adenine dinucleotide synthase 1 project)

1.5.1 Acquisition and transport of riboflavin

Riboflavin, or vitamin B2, is a water-soluble precursor for flavin mononucleotide (FMN) and flavin adenine dinucleotide (FAD), essential cofactors of numerous enzymes involved in cellular metabolism. Riboflavin is synthetized in bacteria, plants and fungi; however, this ability has been lost in higher organisms (Kaiser et al. 2002). It must therefore be obtained from food, mainly seafood, meat, milk, eggs, leaf vegetable and mushrooms (Phillips and Shephard 1993).

Once in the digestive system, riboflavin is released from dietary proteins by their denaturation and from non-covalently bound complexes by the action of phosphatases (Said 2011). Next, riboflavin is absorbed into cells via a specific transporter in the small intestine. In the enterocytes, it is either directly converted into FMN and FAD; or it is transferred across the basolateral membrane into the blood stream (Powers 2003). Therein, riboflavin is bound to albumin or immunoglobulins and subsequently distributed throughout the whole body (Said 2011).

To date, three specific riboflavin translocators have been identified: hRFT1, hRFT2 and hRFT3 (Moriyama 2011), as well as a multidrug transporter ABCG2, primarily expressed in the mammary gland (Vlaming et al. 2009). The three members of the riboflavin transporter (RFT) family differ in their amino acid sequence and transport mechanism, but mainly in their tissue specific expression (Subramanian et al. 2011). hRFT1 is predominantly found in the basolateral membrane of enterocytes, while hRFT2 is primarily found on the apical side; hRFT3 however is present in intracellular vesicles, salivary glands and brain (Fig. 19; Yonezawa & Inui 2013; Haack, Makowski, et al. 2012).

Within cells riboflavin undergoes rapid transformation into its catalytically active cofactors. As riboflavin is soluble in water, hence in cytosol or plasma; and moves across membranes, the conversion mechanism is able to trap required flavins within cells and use it further. There is little or no deposition in the body, so any riboflavin surplus is rapidly derived into its catabolites and excreted in urine (Zempleni et al. 1996).

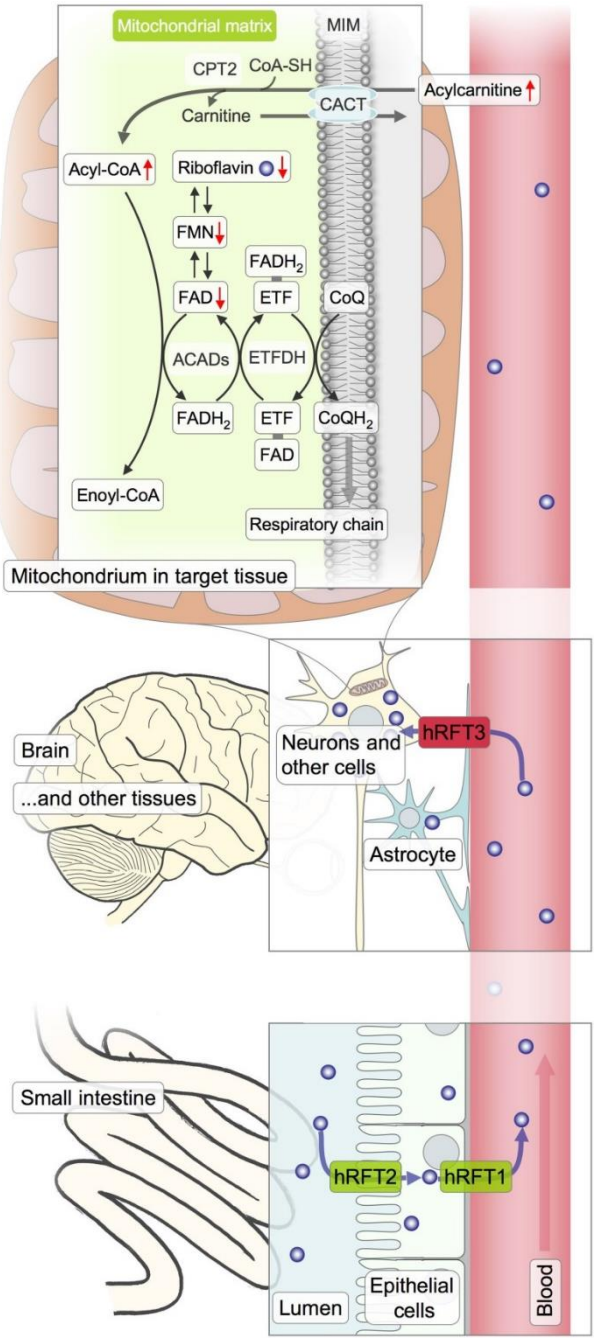

Figure 19: The path of riboflavin in human metabolism (from Haack, Makowski, et al. 2012). Riboflavin is taken up from the diet by human riboflavin transporter 2 (hRFT2) on the intestinal side of epithelial cells. It is released from those cells on the other side by hRFT1 into the blood stream. Uptake into the target cells occurs via passive diffusion or, most likely, yet unknown transporters. hRFT3 is highly expressed in the brain tissue and is responsible for the uptake of riboflavin into neuronal cells, where it is converted into FMN and FAD. The consequences of

riboflavin shortage are depicted on the upper part. Lack of FAD, as the conversion product of riboflavin, causes disturbed acyl-coenzyme A dehydrogenation, leading to increased levels of acylcarnitines. CACT - carnitine-acylcarnitine translocase; CPT2 - carnitine O-palmitoyl transferase 2; ETF - electron transfer flavoprotein; ETFDH - ETF-dehydrogenase; MIM - mitochondrial inner membrane

1.5.2 Metabolic conversion of riboflavin into FMN and FAD

Riboflavin is formed by a tricyclic heterocycle isoalloxazine bound to a ribityl residue. Within cells, riboflavin kinase (RFK) converts riboflavin into FMN. In this reaction, a phosphoryl group originating from ATP is added to the last hydroxyl group of the ribityl residue. Most of the FMN molecules are then adenylated to form FAD by FAD synthase (or FLAD1), also in ATP-dependent manner (Fig. 20; Depeint et al. 2006).

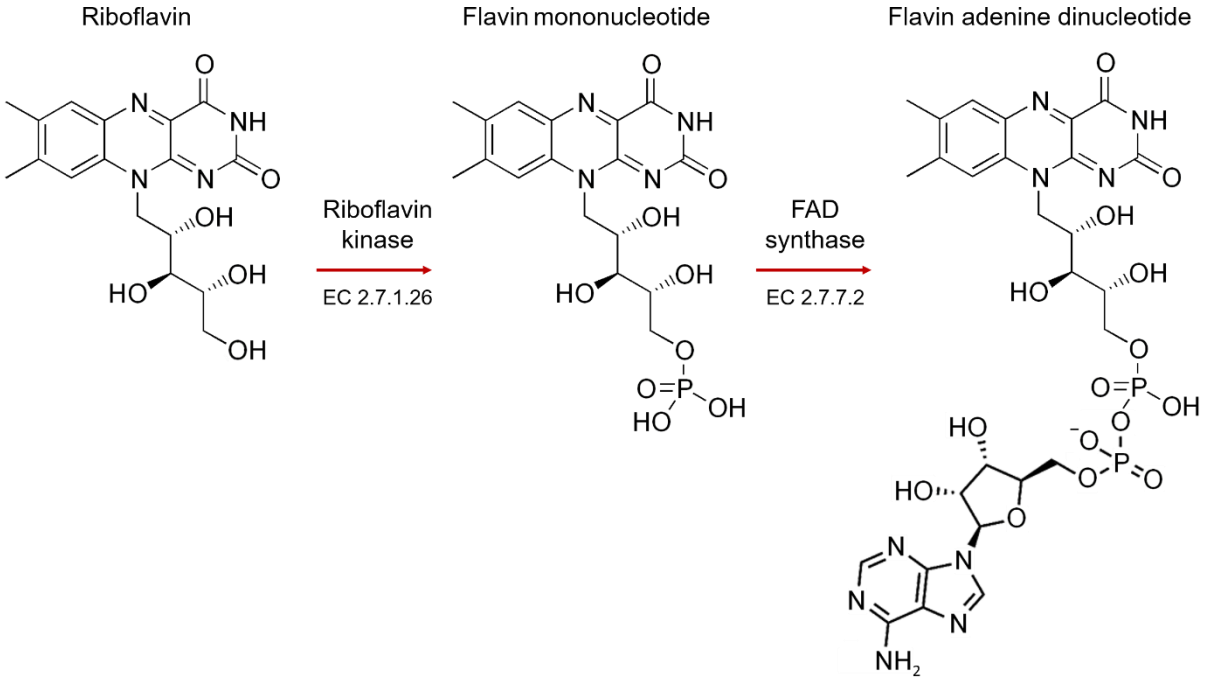

Figure 20: Structure of flavins. Riboflavin serves as a precursor for FMN and FAD. Riboflavin kinase catalyses an ATP-dependent phosphorylation of riboflavin in order to form FMN. FAD synthase, also known as FLAD1, is then responsible for adenylation most of the FMN molecules in order to create FAD.

In bacteria, riboflavin conversion to FAD is catalyzed by a bifunctional protein, such as *RibF* in *Escherichia coli* or *RibC* in *Bacillus subtilis*. In such enzymes, the C-terminal domain catalyzes riboflavin phosphorylation, whereas the N-terminus part is responsible for FMN adenylation. While the RFK activity exists also alone, no observation of an isolated FAD synthase enzyme in bacteria has been reported (Herguedas et al. 2010; Abbas and Sibirny 2011).

In eukaryotes, two families of enzymes with distinct activities developed, hence either RFK or FAD synthase. It was reported that RFK is the rate-limiting step in FAD production, while FAD synthase strictly requires Mg^{2+} for its activity (McCormick et al. 1997; McCormick 2000; Giancaspero et al. 2009). Moreover, FAD and FMN hydrolysis take place to keep flavin cofactors at certain pool homeostasis. The first reaction is catalyzed by FAD pyrophosphatase (EC 3.6.1.18), located in the outer mitochondrial membrane; the second by FMN phosphohydrolase (EC 3.1.3.1) in the intermembrane space (Fig. 22; Vergani et al. 1999; Barile et al. 1997).

1.5.3 The domains and isoforms of Flavin Adenine Dinucleotide Synthase 1

Human FAD synthase enzyme, in short FLAD1 or FADS, is encoded by *FLAD1* located on chromosome 1, position 1q21.3. It was found based on a homology search by using yeast *Fad1p* as a template (Brizio et al. 2006). Unlike the yeast protein, FLAD1 contains two domains: a domain with FAD synthase activity at the C-terminus, and a molybdopterin binding domain at the N-terminal side. These two domains are distinct from the bi-functional prokaryotic enzyme containing RFK and FAD synthase activity on one strand.

The FAD synthase domain is also known as 3'-phosphoadenosine-5'-phosphosulfate (PAPS) reductase domain. As the two FLAD1 domains exist as separate proteins in lower organisms, they were both intensively studied. Human PAPS domain shares similarities with the yeast Fad1p. It has been described that the isolated human FAD synthase domain is sufficient to catalyze FAD synthesis by itself with almost the same K_m as the wild type enzyme (0,24 vs. 0,35 μM for FMN and 6,23 vs. 15,3 μM for ATP). The molybdopterin binding (MPTb) domain is therefore not strictly required for the reaction (Miccolis et al. 2012).

Based on the protein sequence, the MPTb domain, is similar to a plant Cnx1 G domain that binds molybdopterin with high affinity and supports the catalysis of molybdenum insertion (Kuper et al. 2004). Molybdopterin is a complex tricyclic heterocycle that itself does not bind molybdenum. The insertion of molybdenum into the molybdopterin results in a complete ligand called molybdenum cofactor. This is an essential cofactor of the active site of all molybdenum-dependent enzymes (Hover et al. 2015). Until recently, the role of the molybdopterin binding domain in the human FAD synthase was unknown. However, it was shown, that MPTb domain stabilizes the FAD synthase domain and has a positive effect on its activity. Moreover, the MPTb domain was unravelled as a domain with FAD hydrolase activity (Giancaspero et al. 2015).

The FLAD1 transcript covers seven exons. The MPTb domain is coded by exons 1 and 2, whereas PAPS is coded by exons 3 to 7. According to UCSC Genome Browser, *FLAD1* codes for seven distinct RNAs. These RNAs differ in number of exons and in coding of the two functional domains (Fig. 21). Likewise, NCBI Entrez Gene and UniProt databases list four, resp. five FLAD1 RNA and/or protein isoforms. Isoform 1 codes for the longest protein, other variants differ in 5' and 3' ends and use an alternative start codon, some of them also partially use another reading frame. So far, only one experiment was reported to observe a concurrent

presence of isoforms 1, 3 and 4 at transcript level. This experiment used the human colon adenocarcinoma cell line HT29 (Barile et al. 2013).

However, only isoforms 1 and 2 were studied in detail. In the longer isoform, isoform 1, a mitochondrial targeting sequence was described. Based on computer prediction, the first 17 amino acids represent the mitochondrial targeting peptide (Torchetti et al. 2010). Isoform 1 is considered as the canonical full-length RNA. The resulting protein consists of 587 amino acids with a predicted molecular mass of 65,3 kDa. The shorter isoform, isoform 2, starts at methionine at position 98 and has been predicted to localize in the cytosol (Brizio et al. 2006; Galluccio et al. 2007; Torchetti et al. 2011). Thus, isoform 2 contains only 490 amino acids with a weight of 54,2 kDa. Moreover, FAD synthesis and degradation were reported in the cell nucleus. Although the nuclear isoform has not been described yet, the enzyme is responsible for a local flavin cofactor pool (Giancaspero et al. 2013).

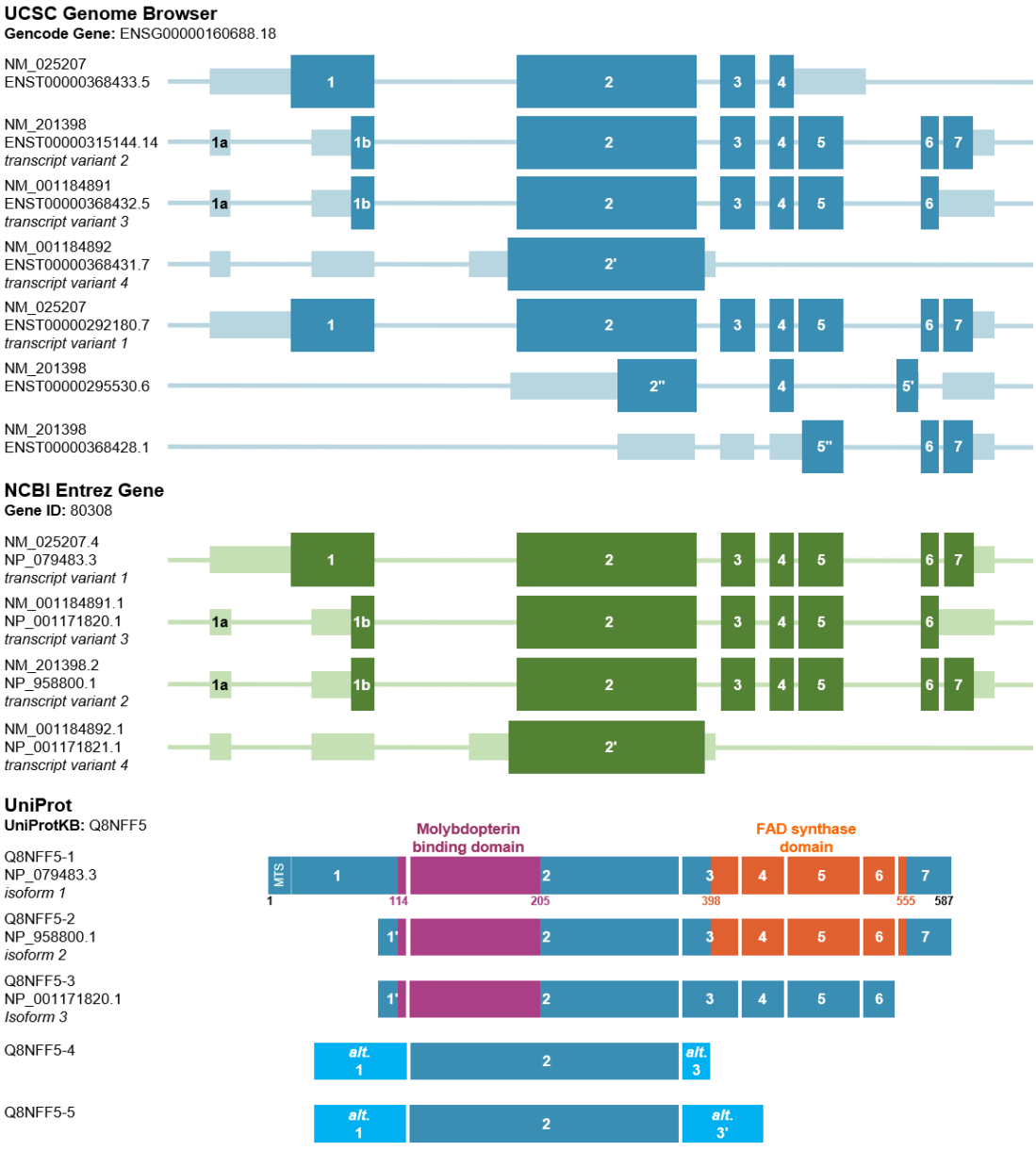

Figure 21: Schematic presentation of FLAD1 gene and protein isoforms. FLAD1 is organized into seven exons that code for several different isoforms. Structures from USCS Genome

Browser and NCBI Entrez Gene represent exons and introns with highlighted translated regions. Translated protein isoforms show data from UniProt server. RNA isoform 1 (NM_025207.4) is coding for the longest protein (NP_079483.3) containing at the N-terminus a mitochondrial targeting sequence (MTS). Other isoforms use alternative start codons and/or alternative open reading frame. Within the first protein sequence, the numbers represent the very first and last position of amino acids as well as position of starts and ends of the highlighted functional domains, molybdopterin binding domain in violet and FAD synthase domain in orange.

1.5.4 FMN and FAD transport and delivery to flavoproteins

Once synthesized, FAD must be delivered to client apo-flavoproteins. Based on observations with other organic cofactors (Padovani and Banerjee 2009), FAD release from FLAD1 requires well-defined states and conditions, among others this includes correct redox state. At the same time, apo-flavoproteins must be protected from premature degradation.

In the case of mitochondrial proteins, the apo-proteins are bound to heat shock protein 60 (Hsp60) chaperones during the import to mitochondria. Already in several examples, FAD was acting as a chaperon-like molecule *per se*, helping Hsp60 to fold and assemble particular enzymes. Flavinylation improves molecular stability and enzymatic activity and prevents proteolytic degradation in several proteins, namely electron transfer flavoprotein and the electron transfer flavoprotein:ubiquinone oxidoreductase (Olsen et al. 2007; Henriques et al. 2009), apoptosis inducing factor (Ghezzi et al. 2010), medium-chain acyl-CoA dehydrogenase (Saijo and Tanaka 1995), short-chain acyl-CoA dehydrogenase or glutaryl-CoA dehydrogenase (Lucas et al. 2011). All of these proteins bind flavin non-covalently into a site that is created after protein folding. This is true for the vast majority of flavoenzymes (about 90%). Some flavoproteins bind FAD covalently. Typical covalent bond is created between one methyl group of the isoalloxazine ring and, in most cases, a histidine residue, but also tyrosine or cysteine (Mewies et al. 1998).

FAD and FMN are synthesized in the cell cytosol as well as in the mitochondrial matrix. However, to retain the flavin cofactors homeostasis and presence in all cell compartments, targeted transport must occur. For example, a human multi-cofactor peroxisomal carrier (*SLC25A17*) has been found (Agrimi et al. 2012). As most flavoproteins play a role in mitochondria, the transport in and out has been studied in detail. A riboflavin importer was described by the group of Dr. Maria Barile, but export remained questionable. Also, they observed only mitochondrial FAD export (Barile et al. 2000). Just recently, a human mitochondrial FAD importer coded by *SLC25A32*, located at the inner mitochondrial membrane was found (Schiff et al. 2016). Figure 22 summarizes the flavin cofactors cycle occurring between mitochondrial matrix, intermembrane space and cytosol.

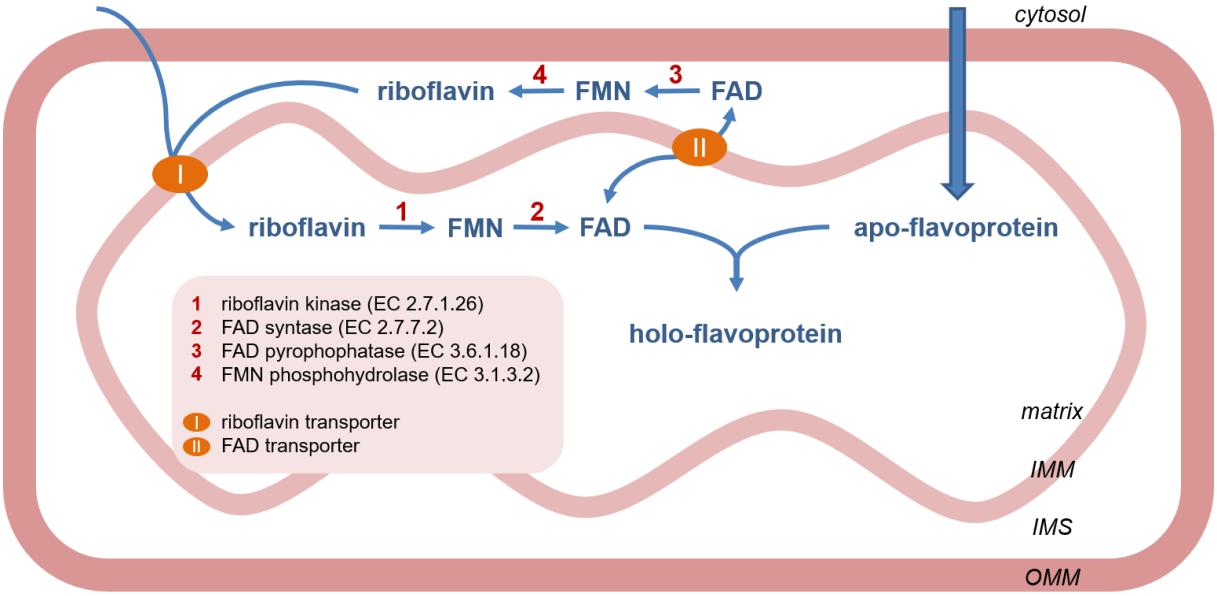

Figure 22: Riboflavin, FMN and FAD transport cycle in mitochondria (modified from Barile et al. 2000). Riboflavin is transported into mitochondria via a specific carrier (I). Therein, it is converted into flavin cofactors FMN and FAD by action of RFK (1) and FLAD1 (2). Client apo-proteins are meanwhile transported into mitochondrial matrix by post-translational transport based on mitochondrial targeting sequence. Apo-flavoproteins together with FAD form a functional holo-flavoprotein. To sustain a flavin cofactor homeostasis, FAD can by degraded into FMN or to riboflavin by enzymatic activity of FAD pyrophosphatase (3) and FMN phosphohydrolase (4). Membrane transporter marked I and II ensure the riboflavin and FAD transport across the membrane. IMM – inner mitochondrial membrane, IMS – intermembrane space, OMM – outer mitochondrial membrane

1.5.5 Human flavoproteome

The human flavoproteome contains altogether around a hundred enzymes described so far, showing the importance of riboflavin conversion products in cellular maintenance. In the case of human enzymes, 84% necessitate FAD cofactor and 16% FMN, only a very small minority has a requirement for both. Except for chromosomes 13, 18, 21 and Y, the flavoprotein coding genes are uniformly distributed over the genome (Fig. 23; Lienhart et al. 2013). Deep study of 374 flavin-dependent enzymes from 22 archaeal, eubacterial, protozoan and eukaryotic genomes confirmed that even among different species, more than 90% of those proteins are oxidoreductases. The principle of such reactions is based on the fact that the isoalloxazine ring is able to reversibly accommodate one or two electrons at the two available nitrogen atoms. The acceptance of electrons is reflected in optical properties of flavins or flavoproteins, respectively. While oxidized cofactors are yellow, and fully reduced colorless, the semi-reduced form is blue or red depending on pH (Gibson et al. 1962).

Interestingly, overall non-covalent binding is preferred (about 90%). While the vast majority of FAD-dependent protein binds the cofactor into a Rossman fold protein structure, FMN-containing enzymes prefer a $(\beta\alpha)_8$-(TIM)-barrel-like or flavodoxin-like fold. Only six enzymes

have been described to bind FAD covalently (Lienhart et al. 2013). However, quite a variety of structures appears in flavoproteins, because very specialized biological reactions mostly tend to call for unusual folds. Interestingly, when compared to other species, the number of human genes coding for flavin-dependent protein is around the average. That is because some organisms developed a very flavin-dependent life style, based of oxidoreductases. However, when compared within a particular genome, flavoprotein-coding genes present less than 0,3% (Macheroux et al. 2011).

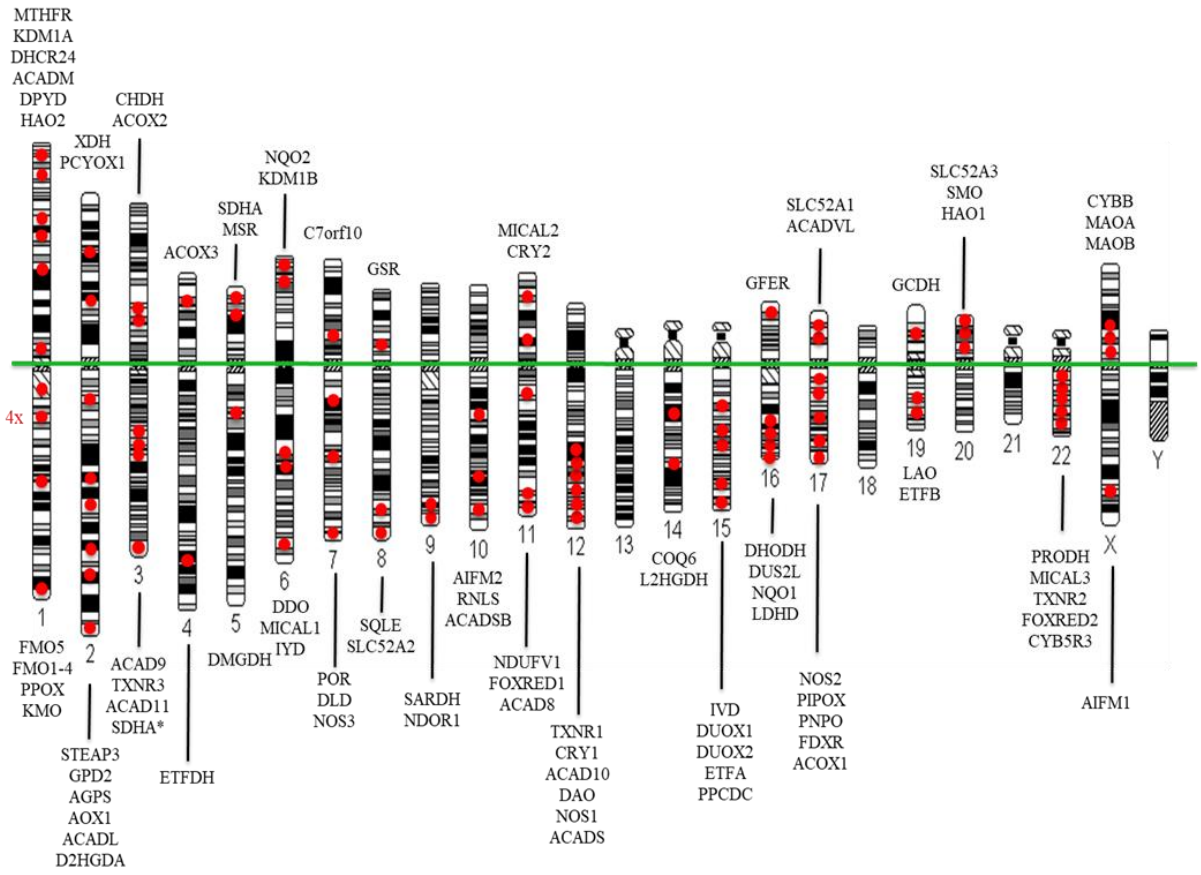

Figure 23: Chromosomal map of genes encoding flavoproteins (from Lienhart et al. 2013). Genes encoding the human flavoproteome are distributed among 19 autosomes (apart from 13, 18 and 21) and the sex chromosome X.

The redox reactions of flavins are often coupled with electron transfer to iron-sulphur clusters within complex enzymes. Accordingly, that is used typically in complexes of the mitochondrial respiratory chain, namely Complex I and II as well as in associated enzymes like electron transferring flavoprotein or mitochondrial glycerophosphate dehydrogenase. The reactions of flavoenzymes play a role also in other cellular pathways, such as the citric acid cycle, β-oxidation, ROS defence, iron-sulphur cluster biosynthesis and delivery or degradation of amino acids. They are also found in biosynthesis of other essential cofactors and hormones such as coenzyme A, coenzyme Q, heme, pyridoxal 5'-phosphate, steroids and thyroxine or regulation of folate metabolites (De Colibus and Mattevi 2006; Joosten and van Berkel 2007). All known

flavoenzymes, their localization and some of the pathways are schematically depicted in Figure 24.

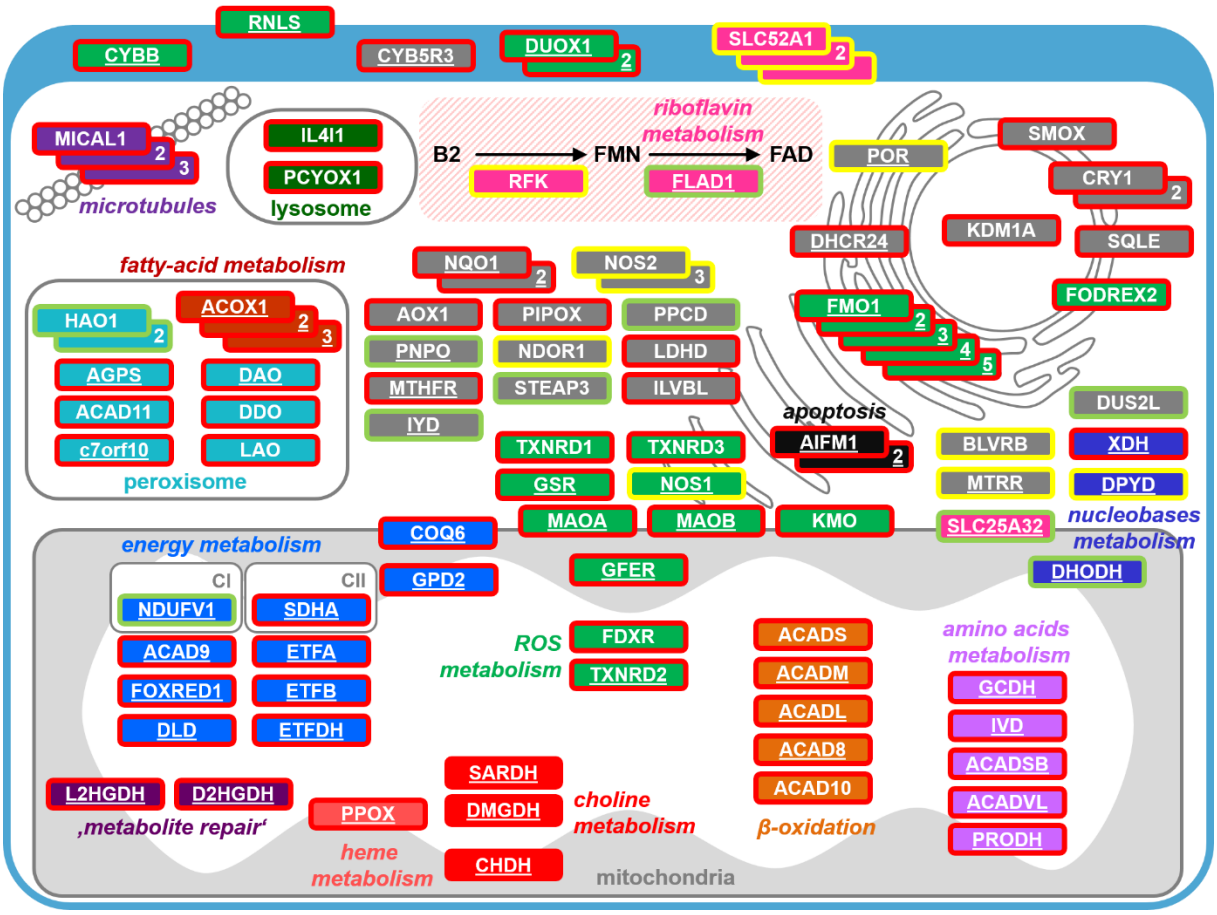

Figure 24: The human flavoproteome (based on Lienhart et al. 2013, Schiff et al. 2016 and Mayr JA personal communication). 99 different depicted enzymes create a various human flavoproteome. The central pathway of FMN and FAD production is depicted only in cytosol for space reasons, but simultaneously occurs also in mitochondria. The localization and function of flavoenzymes is displayed schematically. The inner field color code represents their affiliation to different pathways or organelles, where particular enzymes play their role; see the descriptions within Figure. Grey color stands for other or not yet clear function. Colours of the field borders represent the needed cofactor – red is for FAD, green for FMN, and yellow for combinations FAD and/or FMN and/or riboflavin. The underlined enzyme abbreviations have been described to be connected to a human disorder.

ACAD8-11 - acyl-CoA dehydrogenase isoforms 8-11; ACADS - short-chain acyl-CoA dehydrogenase; ACADSB - 2-methylbutyryl-CoA dehydrogenase; ACADL - long-chain acyl-CoA dehydrogenase; ACADM - medium-chain acyl-CoA dehydrogenase; ACADVL - very long-chain acyl-CoA dehydrogenase; ACOX1-3 - acyl-CoA oxidase1-3; AGPS - alkyldihydroxyacetone phosphate synthase; AIFM1, 2 - apoptosis inducing factor mitochondria associated 1, 2; AOX1 - aldehyde oxidase; BLVRB - biliverdin reductase B; c7orf10 - glutaryl-CoA oxidase; CHDH - choline dehydrogenase; COQ6 - coenzyme Q6 monooxygenase; CRY1, 2 - cryptochrome circadian regulator 1, 2; CYB5R3 - cytochrome-b5 reductase; CYBB - cytochrome b-245, beta chain; D2HGDH - L-2-hydroxyglutarate dehydrogenase; DAO - D-

amino acid oxidase; DDO - D-aspartate oxidase; DHODH - dihydroorotate dehydrogenase; DLD - dihydrolipoyl dehydrogenase; DMGDH - dimethylglycine dehydrogenase; DPYD - dihydropyrimidine dehydrogenase; DUOX1, 2 - dual oxidase 1, 2; DUS2L - dihydrouridine synthase 2; ETFA, B - electron transferring flavoprotein subunit A, B; ETFDH - electron-transferring flavoprotein ubiquinone oxidoreductase; FDXR - ferredoxin-NADP$^+$ reductase; FLAD1 - FAD synthase; FMO1-5 - flavincontaining monooxygenase isoforms 1-5; FOXRED1, 2 - FAD-dependent oxidoreductase 1, 2; GCDH - glutaryl-CoA dehydrogenase; GFER - growth factor, augmenter of liver regeneration; GPD2 - glycerol 3-phosphate dehydrogenase; GSR - glutathione-disulfide reductase; HAO1, 2 - (S)-2-hydroxy-acid oxidase; IL4I1 - interleukin 4 induced 1; IVD - isovaleryl-CoA dehydrogenase; IYD - iodotyrosine deiodinase; KDM1A - lysine-specific histone demethylase 1A; KMO - kynurenine 3-monooxygenase; L2HGDH - L-2-hydroxyglutarate dehydrogenase; LAO - L-amino acid oxidase; LDHD - D-lactate dehydrogenase; MAOA, B - monoamine oxidase isozyme A, B; MICAL1-3 - microtubule associated monooxygenase, calponin and LIM domain containing 1-3; MTHFR - N-5,10-methylenetetrahydrofolate reductase; MTRR - methionine synthase reductase; NDOR1 - NADPH-dependent diflavin oxidoreductase 1; NDUFV1 - NADH-ubiquinone oxidoreductase of Complex I, subunit UQOR1; NOS1-3 - nitric-oxide synthase 1-3; NQO1, 2 - NAD(P):quinone oxidoreductase 1, 2; PCYOX1 - prenylcysteine oxidase; PIPOX - L-pipecolate oxidase; PNPO - pyridoxal 5'-phosphate oxidase; POR - P450 oxidoreductase; PPCD - 4'-phosphopantothenoylcysteine decarboxylase; PPOX - protoporphyrinogen IX oxidase; PRODH - proline dehydrogenase; RFK - riboflavin kinase; RNLS - renalase, FAD dependent amine oxidase; SARDH - sarcosine dehydrogenase; SDHA - succinate dehydrogenase subunit A; SLC25A32 - solute carrier family 25 member 32; SLC52A1-3 - riboflavin transporter 1-3; SMOX - spermine oxidase; SQLE - squalene monooxygenase; STEAP3 - ferrireductase (biliverdin IX beta reductase); TXNRD1-3 - thioredoxin reductase 1-3; XDH - xanthine dehydrogenase

1.5.6 Disorders connected to the flavin cofactors

Generally, riboflavin shortage causes biochemical defects on the molecular level, which is reflected by a phenotypic spectrum. The most common symptoms in humans are various dermatitis conditions, mostly affecting the mouth, tongue, face, sides of the nose or scalp, together with lens opacity or cataracts. Long-lasting avitaminosis results in more severe conditions, *e.g.* abnormal fetal development. Also, inadequate intake has been observed to be connected to anaemia, cancer, neurodegeneration, cardiovascular disease and migraine (Powers 2003).

The obvious results of riboflavin deficit are decreased levels of FMN and FAD. Interestingly, in such conditions, special changes arise in the cellular distribution of the flavin cofactors, resulting in a specific hierarchical response to this deficiency. Some of the cellular pathways are supported and preserved, such as the OXPHOS system, and contrarily others are diminished (Ross and Hansen 1992). Riboflavin depletion in Caco-2 and HepG2 cells *in vitro* increased the expression of riboflavin uptake and metabolism enzymes. Moreover, it resulted in cell cycle arrest and halted proliferation. FAD-dependent production of glutathione was also stopped

leading into DNA oxidative damage (Said and Ma 1994; Werner et al. 2005; Manthey et al. 2006). Next to riboflavin deficiency, in over 60 flavoenzymes, an allelic variant affecting the function has been described. As any excess of riboflavin is excreted in the urine, a number of such disorders is treated by riboflavin intake and early variant identification helps to start the necessary treatment (Horvath 2012).

The riboflavin-related defects of respiratory chain complexes include mainly deficiencies of Complex I and II. Both complexes consist of several subunits and a number of flavin-dependent assembly factors is required, they also both use flavin cofactor in their electron transferring path. Moreover, in the case of Complex I, two different genomes are involved. An example, one for all, a deficiency in ACAD9 (acyl-CoA dehydrogenase 9; OMIM #611126) has been described already in 70 patients (Repp et al. 2018). ACAD9 is involved in β-oxidation, but more importantly, it is a FAD-containing assembly factor for Complex I (Haack et al. 2010; Schiff et al. 2015). In this example as well as in several others, riboflavin therapy was effective and mitigated symptoms. Increased FAD availability improved protein folding and stability (Bernsen et al. 1993; Gerards et al. 2011). Complex II deficiencies are rare, causing progressive motor and mental deterioration. However, riboflavin supplementation moderately improved the neurological conditions. *In vitro* studies reported 2-fold increase of Complex II activity in patient cells (Bugiani et al. 2006). The inefficient enzyme activities of respiratory chain complexes can cause Leigh syndrome (OMIM #256000) or other related deficiencies.

Historically, riboflavin treatment was connected to Brown-Vialetto-Van Laere syndrome (BVVLS; OMIM #211530). BVVLS is a rare autosomal recessive disorder characterized by hearing loss and a variety of cranial nerve palsies. The typical onset of the disease is within the first two years of life or during the teenage years. By studying a large consanguineous family with many affected individuals, it was shown that BVVLS is caused by mutations in the *SLC52A3* gene coding for riboflavin intestinal transporter hRFT2 (Green et al. 2010). High-dose riboflavin treatment in some patients rapidly improved observed clinical symptoms (Bosch et al. 2011; Anand et al. 2012), yet in one patient had no effect (Koy et al. 2012). Likewise, BVVL syndrome was found in a patient with compound heterozygous mutations in the *SLC52A2* gene coding for riboflavin transporter 3. Also here, riboflavin treatment was effective (Haack et al. 2012b). The third known riboflavin transporter (*SLC52A2* and hRFT1) was also connected to BVVLS, also presenting with symptoms of multiple acyl-CoA dehydrogenase deficiency. The newborn patient fully recovered after riboflavin supplementation (Chiong et al. 2007; Ho et al. 2011). To note, BVVLS is phenotypically very similar to Fazio-Londe disease (OMIM #211500), apart from the hearing loss. Fazio-Londe disease was also described to be caused by a homozygous mutation in the *SLC52A3* gene and to be riboflavin responsive (Dipti et al. 2005; Bosch et al. 2011; Bosch et al. 2012).

Consequently, other riboflavin responsive pathologies connected to shortage of flavin cofactors must be considered. X-linked mitochondrial encephalomyopathy (OMIM #300614) is caused by a deletion in a gene coding for apoptosis inducing factor (AIF). Upon apoptogenic stimuli, AIF is released by proteolytic cleavage and translocates from the mitochondria into the nucleus, stimulating DNA fragmentation. The positive response to riboflavin treatment probably reflects the protein stabilization after FAD binding (Ghezzi et al. 2010).

Next, two riboflavin responsive neuro-metabolic acyl-CoA dehydrogenase deficiencies were connected to variants in L-2-hydroxyglutaric dehydrogenase (OMIM #236792; Yilmaz 2009) and short acyl-CoA dehydrogenase (OMIM #201470; Kmoch et al. 1995). Both enzymes require FAD for their function and deficiency causes glutaric aciduria or epilepsy.

Likewise, Friedreich ataxia (OMIM #229300), a neurodegenerative disorder caused by decreased expression of frataxin, has been linked to lack of riboflavin. Frataxin is involved in the biogenesis of iron-sulphur clusters, therefore assuring proper mitochondrial function. It physically interacts with the FAD-dependent subunit of Complex II. The *in vitro* experiments with frataxin knock-down seemed to respond to FAD supplementation (Gonzalez-Cabo et al. 2010).

The variety of flavoproteome is reflected in the vast genotypic-phenotypic spectrum. Allelic variants were found, for example, in genes for *FOXRED1* (OMIM #252010; Fassone et al. 2010), *DMGDH* (OMIM #605850; Moolenaar et al. 1999), *FMO3* (OMIM #602079; Treacy et al. 1998), *SARDH* (OMIM #268900), *MTHFR* (OMIM #607093; Frosst et al. 1995), *PPOX* (OMIM #176200; Sassa 2006), *PNPO* (OMIM #603287; Mills et al. 2005), *COQ6* (OMIM #614647; Heeringa et al. 2011), *DUOX2* (OMIM #606759; Moreno et al. 2002), and *IYD* (OMIM #612025; Afink et al. 2008; Moreno et al. 2008).

1.5.7 Multiple acyl-CoA dehydrogenase deficiency

Multiple acyl-CoA dehydrogenase deficiency (MADD; OMIM #231680), or glutaric aciduria type 2, is a clinically and biochemically heterogeneous disorder of cellular metabolism with disturbed fatty-acid oxidation, amino acid and choline metabolism, combined respiratory chain deficiency, increased production of reactive oxygen species, and a complex neuromuscular phenotype. MADD can be mild or severe and has both neonatal and adult onset of the disease. Patients typically present with muscular lipid storage, muscle weakness and most importantly high plasmatic and urinary levels of acylcarnitine and organic acids. Both sets of compounds are ordinarily investigated within newborn screening (Barile et al. 2013; Olsen et al. 2016). The very first patient was described by Niels Gregerson and coworkers. A 3-years old boy presented with severe hypoglycemia, metabolic acidosis and unexplained attacks of lethargy and hypotonia (Gregersen et al. 1982).

In most cases, MADD is caused by a mutation in one of two genes coding for electron transferring flavoprotein *ETFA* or *ETFB* or in the gene for electron-transferring flavoprotein ubiquinone oxidoreductase *ETF:QO* (or *ETFDH*; Olsen et al. 2007; Olsen et al. 2016; Cornelius et al. 2014; Horvath 2012). ETF and ETFDH are central players in mitochondrial metabolism, collecting superfluous electrons from other flavoproteins to restore their enzymatic activity. Moreover, MADD was connected to dysfunctions of the riboflavin transporter genes *SLC52A1*, *SLC52A2*, and *SLC52A3* (Bosch et al. 2011; Ho et al. 2011; Foley et al. 2014; Mosegaard et al. 2017) or the mitochondrial FAD transporter gene *SLC25A32* (Schiff et al. 2016) as well as with alteration in FAD pyrophosphatase activity (Vergani et al. 1999).

To note, some MADD patients respond well to riboflavin supplementation. Such a responsive condition is then called RR-MADD, read: riboflavin-responsive. RR-MADD can be explained on the molecular level as a chaperone-like role of the FAD cofactor. Its increased availability supports the folding, function and stability of various flavoproteins, hence restoring the mitochondrial and cellular homeostasis (Gianazza et al. 2006; Cornelius et al. 2014).

1.5.8 Pathologies associated with FAD synthesis by alterations in RFK and FLAD1

So far, RFK, the first enzyme of FAD synthesis, has not been connected to any pathogenic variant in humans. The enzyme activity of RFK seems to be too essential for normal development, to an extent that complete loss of function would not be compatible with life. And indeed, the only study describing RFK deficiency in higher organisms demonstrated that complete loss of RFK resulted in an embryonic lethality in mice (Yazdanpanah et al. 2009).

Already in 1985, changes in flavin cofactor levels in rats were induced by thyroid hormone quantity. In hyperthyroid animal, activities of RFK and FLAD1 were increased, and in hypothyroid decreased (Lee and McCormick 1985). These observations were utilized in the treatment of six hypothyroid human adults, where thyroxine therapy resulted in normal flavin levels (Cimino et al. 1987). Similarly, phenobarbital administration led to increased activity of RFK as well as FLAD1, therefore inducing FAD synthesis in rats (Hamajima et al. 1979).

Reduced FLAD1 expression level was also connected to two broad human pathologies: amyotropic lateral sclerosis (ALS; OMIM #105400) and cancer. ALS is a neurodegenerative disease connected on the molecular level to oxidative stress, mitochondrial dysfunction, altered RNA processing or neuroinflammation. The study of *FLAD1* mRNA unravelled simultaneous decreased expression of *RFK*, *CYC1* (cytochrome *c1*), and *SDHB* (succinate dehydrogenase complex subunit B; Lin et al. 2009). It is however not clear whether decreased RNA levels are the cause of the disease, or a secondary consequence. Nevertheless, the result of impaired flavoproteome was described as diminishing patients' fitness and causing their motoneurons to be vulnerable to degenerate. Also, a connection to cancer has been described in several cases; however, none of them with a clear explanation (Powers 2003; Nakano et al. 2011; Barile et al. 2013).

The only animal model presenting with non-functioning FAD synthesis, was prepared by silencing of the FAD synthase gene R53.1 in *C. elegans*. It is a classical model of neurogenerative disease, aiming to obtain more information about ALS and flavin homeostasis/flavoenzyme biogenesis. Impaired locomotion and flavoprotein levels were described, together with increased oxidative stress (Liuzzi et al. 2012).

2 Aims of the Thesis

The main aim of this thesis is to provide convincing evidence in order to be able to label a gene as a new disease gene. Variants in *TXN2* and *FLAD1* were found to be likely pathogenic by analysis of whole exome sequencing at the Institute of Human Genetics, but have not yet been associated with a mitochondrial disease. These genes were selected based on their clinical picture of a mitochondrial disorder and were highly ranked to be disease causing. I aim to validate these two potential novel mitochondrial disease genes by carrying out functional validation.

My task is to prove that *TXN2* and *FLAD1* are the causal genes in both cases and to investigate if there is phenotypic-genotypic correlation. Since mitochondrial disorders often display rather weak association between phenotype and genotype, validation and collection of evidence for the candidate genes constitutes the core part of this thesis. Multiple classes of functional approach will help to explain the pathogenicity at the level of both the gene and the protein, and include genetic, informatic and experimental data.

Another crucial task is to suggest a rational treatment based on the experimental observations and enzymatic function. The search for rational therapy in the presented cases expands the utilization of this work for future patients carrying the same or similar variants.

- Thioredoxin 2 protein is part of the reactive oxygen species defence within mitochondria. To determine the outcome of predicted loss-of-function mutation, I aim to assess TXN2 availability and (a lack of) enzymatic activity. To better understand the observed mitochondrial dysfunction, it is necessary to investigate the connection between TXN2, OXPHOS and the ROS defence pathway in detail. Furthermore, I have to analyse imbalance in the ROS levels and to explore efficacy of potential antioxidant treatment *in vitro* and in the best case *in vivo*.

- Flavin adenine dinucleotide synthase 1 is the main and potentially only producer of cellular cofactor FAD in humans. Predicted loss-of-function mutation is possibly responsible for lack of FAD, a cofactor needed in about 100 enzymes, primarily located in mitochondria. To ensure their enzymatic reactions, I aim to look for feasible manners of FAD production. In order to investigate any residual FLAD1 activity, I will further inspect the two functional domains of FLAD1. Furthermore, as riboflavin (vit. B2) is a FAD precursor; I plan to investigate its therapeutic potential.

3 Material and Methods

3.1 Material

3.1.1 Nucleic acids

3.1.1.1 DNA

The investigated DNA of controls and patients with suspected mitochondrial disorders are part of the DNA collection of the Institute of Human Genetics. For all samples, informed consent was obtained.

3.1.1.2 cDNA

TXN2 cDNA (catalog number: HSH006764-31-LvnU6) was purchased from GeneCopoeia (Rockville, MD, USA). *FLAD1* cDNA (plasmid ID HsCD00039838) was obtained from DNASU Plasmid Repository (Tempe, AZ, USA). The cDNAs for truncated *FLAD1* isoforms were cloned from the DNASU plasmid containing wild type *FLAD1* by using self-designed primers.

3.1.1.3 Oligonucleotides

The oligonucleotides were synthesized by Metabion (Planegg, DE).

FLAD1 M98 forward	5'-CGCCATGACATCTAGGGCCT-3'
FLAD1 M268 forward	5'-CGCCATGAAGGGACTATTCC-3'
FLAD1 M355 forward	5'-CGCCATGCCCAACGCTGTGG-3'
FLAD1 M355org forward	5'-CCCCTACATGCCCAACGCTGTGG-3'
FLAD1 reverse	5'-TCATGTGCGGGAGTTCCGCT-3'
FLAD1 variant seq forward	5'-AGGGACACACTCAGGACACC-3'
FLAD1 variant seq reverse	5'-AGTCAGGGTAGGAACCCAGG-3'
TXN2 forward	5'-CGCCATGGCTCAGCGACTTCTTCTGAGG-3'
TXN2 reverse	5'-TCAGCCAATCAGCTTCTTCAGGAAGGCC-3'
TXN2 variant seq forward	5'-CTGAGCCCTGAGTACTCCCC-3'
TXN2 variant seq reverse	5'-TGAGCAGCATAGAACATGGC-3'
CMV	5'-CGCAAATGGGCGGTAGGCGTG-3'
V5	5'-ACCGAGGAGAGGGTTAGGGAT-3'

3.1.2 Cell lines

Following cell lines were used for the experiments:

NHDFneo	normal human dermal fibroblasts derived from neonatal foreskin – used as a control cell line (Lonza) – referred as NHDF or control

HEK 293 FT	clonal isolate derived from human embryonal kidney cells transformed with the SV40 large T antigen to facilitate lentiviral experiments (Life Technology) – also referred as HEK 293
Patient cell lines	fibroblasts derived from a skin biopsy, in many cases the culture was started by colleagues at the Institute of Human Genetics

3.1.3 Antibodies and ladder

The primary antibodies were used as follows: anti-TXN2 (HPA000994, rabbit polyclonal, Sigma-Aldrich), anti-FLAD1 antibody (HPA028563, rabbit polyclonal, Sigma-Aldrich), anti-β-actin (A5441, mouse monoclonal, Sigma-Aldrich), anti-SDHA (ab14715, mouse monoclonal, Abcam) and a previously described self-made anti-peroxiredoxin-3 antibody (Godoy et al. 2011) as a kind gift from Dr. Marcus Conrad.

The secondary antibodies were purchased from Jackson Immuno Research Laboratories (West Grove, PA, USA). Both antibodies – anti-rabbit (111-036-045) and anti-mouse (115-036-062) are conjugated with horseradish peroxidase (HRP) for visualization.

PageRuler™ Plus Prestained Protein Ladder 10 to 250 kDa (catalog number: 26619) was obtained from Thermo Scientific.

3.1.4 Chemicals and solutions

The standard laboratory chemicals or solutions were purchased from Sigma-Aldrich (St. Louis, MO, USA) or Merck (Darmstadt, Germany). Most of the chemicals for cell culture were obtained from Gibco or Invitrogen, both parts of Thermo Fisher Scientific (Waltham, MA, USA). Other providers are stated in the particular method description.

3.2 Methods

All methods as described below were performed by myself if not stated otherwise.

3.2.1 Cell culture

3.2.1.1 Media and chemicals

Dulbecco's modified Eagle medium (High Glucose; 4.500 mg/l) was supplemented with 10% Fetal Bovine Serum, 1% Penicillin-Streptomycin (100 X; 5.000 U/ml) and 200 μM Uridine – referred as $DMEM^{+}$. All obtained fibroblast cell lines were tested for mycoplasma contamination by using the MycoAlert Mycoplasma detection kit (Lonza, Basel, Switzerland). For the test, 2 ml samples of medium in which the cell lines had been growing for at least two days were taken and then the manufacturer's protocol was followed.

3.2.1.2 Cell stock deposition

To keep aliquots of cells of a low passage number, freezing in 10% dimethyl sulfoxide (DMSO) in DMEM$^+$ was applied. 1,5 ml of cell suspension was transferred into cryo vials and stored in -20 °C for at least 2 hours, then in -80 °C for at least 24 hours and finally transferred into liquid nitrogen for a long-term storage.

For further work, cell aliquots were slowly warmed up. After thawing the cell suspension, cells were transferred into 75 cm^2 flask with 15 ml of DMEM$^+$. The culturing medium was changed the following day to wash out DMSO, which is used as a cryo preservant.

3.2.1.3 Cell maintenance

Cells were kept in 75 cm^2 or 175 cm^2 culturing bottles suitable for adherent cells. The medium was exchanged every second or third day. If necessary, cells were split by washing once with PBS and detached by Trypsin-EDTA solution (2,5 ml for 75 cm^2 flask, 3,5 ml for 175 cm^2). When all detached, cells were transferred by excess of DMEM$^+$ into 15 ml Falcon tube and centrifuged for 3,5 min at 500 rpm. The supernatant was discarded, and cell pellet was dissolved in DMEM$^+$ and one third or one fourth of the cell suspension was transferred back into the culturing flask. The rest was either divided into additional bottles or used for other experiments.

Optionally, cell pellets were used for further experiments. In this case cells were washed in 1 ml PBS and centrifuged once more.

3.2.1.4 Determination of a cell number

For several experiments it was important to determine the cell number. It was also a principle of the growth curve experiment. To do this, the cell pellet was then dissolved in 5 ml of DMEM$^+$. To determine the cell concentration, the cell suspension was dissolved 1:10 in PBS to a total volume of 200 µl in a 1,5 ml Eppendorf tube. This was analyzed by Scepter™ Handheld Cell Counter with 60 µm Scepter™ Sensors by following instruction on the instrument. The cell number was typically measured in duplicates.

3.2.2 Extraction of DNA and RNA from human fibroblasts

Cell pellet was washed once in PBS, subsequently dissolved and lysed in RLT buffer and froze at -20 °C. Cell homogenate was further disrupted by using a QIAshredder column. DNA and RNA were extracted from the lysate by using AllPrep DNA / RNA mini kit from Qiagen. The isolation was done according to the manufacturer's protocol. The purity and concentration and of resulting DNA and RNA were determined by using the ND-1000 UV-Vis Spectrophotometer NanoDrop (Thermo Scientific). DNA was then stored at 4 °C, RNA at -80 °C.

3.2.3 Expression of a wild type copy of a gene of interest in human fibroblasts

3.2.3.1 Primer design

To amplify a wild-type copy of a cDNA, specific primers were designed. To secure the expression Kozak consensus sequence (CGCC, alternatively CACC) was added at the beginning of the forward primer directly before the start ATG codon. The reverse primer was designed by starting at the stop codon (eg. TGA in *TXN2*). Specificity of the primers was verified by UCSC In-Silico PCR (https://genome.ucsc.edu/cgi-bin/hgPcr), melting temperature was determined by NEB Tm calculator (http://tmcalculator.neb.com/). The melting temperatures of both primers should be different by maximum of 5 °C. From the lower melting temperature of both primers, the annealing temperature was calculated (Ta = Tm_lower + 3 °C).

3.2.3.2 PCR amplification of the gene of interest

Purchased cDNA copies were used for amplification of a wild-type copy of a gene of interest in peqSTAR Thermocycler.

PCR reaction

10x High Fidelity PCR Buffer	1 µl	(final concentration: 1x)
2 mM dNTP mix	1 µl	(0,2 mM each)
50 mM $MgSO_4$	0,4 µl	(2 mM)
10 µM forward primer	0,2 µl	(0,2 µM)
10 µM reverse primer	0,2 µl	(0,2 µM)
cDNA	0,2 µl	(<5 ng)
Platinum® Taq DNA Polymerase High Fidelity (5 U/µL)	0,04 µl	(0,2 U)
Ultrapure H_2O	to 10 µl	

PCR program

Heat lid		110 °C				
Denature		95 °C	2 min			
30x cycles:	Denature	95 °C	30 s			
	Anneal	64,4 °C	30 s	or	65,6 °C	30 s
	Extend	68 °C	45 s			
Extend		68 °C	10 min			
Store		8 °C	forever			

The PCR products were checked for the correct size on an agar gel. To add A-end to the products, 0,2 µl of Taq polymerase was added to the samples and kept for 10 min at 72 °C. A-ends are essential for correct insertion into vector by a TOPO cloning procedure.

3.2.3.3 TOPO cloning

This procedure was followed as suggested in User Manual for pLenti6.3/V5-TOPO® TA Cloning Kit (Invitrogen #K531520).

Fresh PCR product	0,5 µl or 1 µl
Salt solution	1 µl
pLenti 6.3/V5 TOPO® vector	1 µl
Sterile water	to 5 µl

This mixture was kept for 5 min at room temperature. 3 µl of the mixture was transferred into a vial of One Shot® Stbl3™ chemically competent *E. coli* cells and mix gently followed by an incubation on ice for 30 min. Next, heat-shock of the cells was performed for 30 s at 42 °C in a pre-warmed water bath. Another incubation on ice for 2 min. Next, 225 µl S.O.C. medium (kept at room temperature) was added to the cell vial. Then, *E. coli* with S.O.C. were shaken horizontally at 37 °C, 45% shaking in Heiz Thermomixer HTML 133 for at least 1 hour. 50 µl and 100 µl of the cell suspension were spread on a pre-warmed LB Ampicillin agar plates and incubated overnight at 37 °C. The remaining transformation mixture was kept at 4 °C for plating additional cells if necessary.

3.2.3.4 Colony PCR

Distinct colonies were selected and transferred into 20 µl of HPLC water and spread on a new agar plate for further usage with a proper labelling. 1 µl of the HPLC water mixture with *E. coli* colony was used for a colony PCR reaction to determine clones with correct size and orientation of the insert. Typically, 20-50 colonies were picked up.

The amplified copy of the gene of interest can be inserted in both directions, the TOPO cloning is not specific in this step; or the amplified PCR product can be shortened or disrupted. The pLenti 6.3/V5 TOPO vector contains two strong primer binding sites – CMV before the site of insertion and V5 after.

Therefore, to ensure the size and orientation, specific combination of primers was used: CMV primer with gene specific reverse primer; and gene specific forward primer with V5. Schematic presentation is shown in Fig 25.

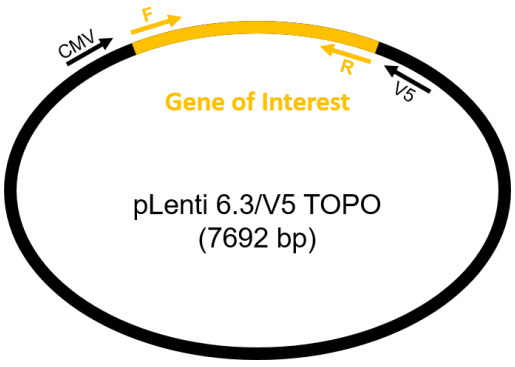

Figure 25: Schematic presentation of the cloning vector and its insert (Gene of Interest). CMV and V5 as well as F (forward) and R (reverse) are two pair of primers used in the insertion and sequencing strategies.

PCR reaction (x n+1 amount of colonies)

10x PCR Buffer	1 µl	(final concentration: 1x)	
2 mM dNTP mix	1 µl	(0,2 mM each)	
10 µM forward primer	0,2 µl	(0,2 µM)	CMV F-*TXN2*
10 µM reverse primer	0,2 µl	(0,2 µM)	R-*TXN2* V5
colony	1 µl		
Taq DNA Polymerase	0,04 µl	(0,2 U)	
Ultrapure H_2O	to 10 µl		

PCR program

Heat lid		110 °C	
Denature		95 °C	2 min
30x cycles:	Denature	95 °C	30 s
	Anneal	65 °C	30 s
	Extend	72 °C	1 min
Extend		72 °C	10 min
Store		8 °C	forever

The length of the PCR products was analyzed on a 1,5% agarose gel.

Expected size (analogously for *FLAD1*):

CMV – TXN2 cDNA reverse = 162 bp + 505 bp = 667 bp
TXN2 cDNA forward – V5 = 505 bp + 96 bp = 601 bp

Positive clones (up to 10) were selected for further amplification. For that, the rest of HPLC water with the clone mixtures were transferred into 5 ml of LB medium with Ampicillin and cultured overnight at 37 °C while being shaken.

3.2.3.5 Extraction of DNA from 5 ml *E. coli* colonies

Overnight cultures of the *E. coli* clones were pelleted by centrifugation at >8.000 rpm for 3 min at room temperature.

The plasmids were purified exactly as described in QIAprep® Miniprep Handbook (Qiagen #27104 or #27106).

The plasmid DNA was eluted by 50 µl of Buffer EB (10 mM TrisCl, pH 8,5). DNA concentration was subsequently measured in 1 µl samples by NanoDrop ND-1000 Spectrophotometer.

3.2.3.6 Sanger sequencing

Sequence of the purified plasmid DNA was assessed by a standard Sanger sequencing.

For the sequencing PCR reaction 10 ng / 100 bp was needed:

pLenti6.3/V5 TOPO vector + insert (*TXN2*) = 7.692 bp + 505 bp = 8.197 bp

→ cca 800 ng/1 ul is necessary, but typically 80 – 400 ng/µl were obtained

For the sequencing reaction, the BigDye® v3.1 Terminator Sequencing Kit from Applied Biosystems was used. All samples are sequenced twice – either from the forward or from the reverse primer.

PCR reaction

Purified plasmid DNA	4 µl (up to 200 ng/µl) or 1 µl (800 ng/µl)
10 µM CMV primer OR 10 µM V5 primer	2 µl (final concentration: 2 µM)
Big Dye Terminator v.3.1 Ready Reaction mix	1 µl
Big Dye Terminator 5x Sequencing Buffer	3 µl
Ultrapure H_2O	to 10 µl

PCR program - sequencing

Heat lid		110 °C	
Denature		96 °C	2 min
25x cycles:	Denature	96 °C	10 s
	Anneal	50 °C	5 s
	Extend	60 °C	4 min
Extend		60 °C	10 min
Store		8 °C	forever

PCR product was further cleaned before sent for sequencing. The products were transferred into a new 96-well plate with 25 µl of 100% EtOH per well and left for 15-30 min at room temperature without any light access. Next, the plate was centrifuged at 3.000 rpm for 30 min at 10 °C. The EtOH supernatant was removed and exchanged by 125 µl of a fresh 75% EtOH and centrifuged again at 2.000 rpm for 30 min at 10 °C. Ethanol was again removed and shortly spinned for the last time. The plate was left at a dark place for at least 10 min to let the residual ethanol evaporate. Lastly, the samples were dissolved in 40 µl H_2O and the plate was sealed by an adhesive foil.

3.2.3.7 Midi prep

After identification of clones with correct insert without mutations, *E. coli* were amplified in a 100 ml overnight culture with 1% ampicillin. Next day, they were pelleted by centrifugation at 6.000 rpm at 4 °C for 10 min. The purification of the plasmid was assess as described in QIAprep® Midiprep Handbook. After the last centrifugation step, DNA pellets were dried out under the cell culture hood to avoid any contamination coming from air. DNA concentration was determined by NanoDrop ND-1000 Spectrophotometer.

3.2.3.8 Transduction and transfection

The following media were filtered through a 0,22 μm filter using a SteriCup® and SteriTop® from Millipore.

Medium 1: DMEM, 10% (vol/vol) FBS
Medium 2: DMEM, 10% (vol/vol) FBS, 1% (vol/vol) penicillin-streptomycin and 200 μM Uridine
Medium 3: DMEM
Medium 4: DMEM, 2% (vol/vol) FBS
Medium 5: normal fibroblast cell culture medium (nonfiltered) – $DMEM^+$

HEK 293 FT cells were thawed and kept in medium 1. The next day HEK 293 were placed on a 10 cm dish with approximately 8 ml of medium 1. One dish of HEK 293 is sufficient for the transduction of two cell lines (typically patient and control). The cells should be 70-80% confluent in the evening on the following day. Too confluent HEK 293 cells form a monolayer that easily detaches from surface.

The transfection procedure itself is carried out on the following day. Before, medium 1 and 3 are warmed up and Packaging Mix is thawed on ice. The required amount of vector in μl equals 3.000 ng / plasmid concentration measured in ng/μl. In 15 ml Falcon tube 1,5 ml of medium 3 with 36 μl of Lipofectamine are mixed and incubated at room temperature for 5 min. Meanwhile, 1,5 ml of medium 3 is enriched by 9 μl of Packaging Mix and 3 μg of pLenti vector (as calculated previously). This mixture is dropwise added to the solution with Lipofectamine and gently mixed by inverting the tube. Next, it is incubated for 20 min at room temperature. The whole procedure leads to an enclosing of the vector DNA into small packages that can be transferred in the target cells by lipofection, thus making small holes in the lipid layer of the cell.

In the meantime, the medium of HEK cells prepared the previous day is aspirated and provided with 5 ml of fresh medium 1. After the 20 min incubation, the solution with the vector is dropwise added to the HEK 293 cells. All steps are carried out carefully to avoid the detachment of the cells. HEKs are then incubated overnight at 37 °C. From this moment, HEK 293 are a biosafety level 2.

On the next day, the patient and control cells are prepared to be 70-80% confluent in two or three days. For each cell line a 10 cm dish with 8 ml of medium 2 is required. The medium of transfected HEK cells is carefully replaced by 7 ml of medium 4, then incubated for 72 hours.

In two or three days, the procedure continues. First, the centrifuge must be cooled down to 4 °C and medium 2 warmed up. The supernatant from HEK cells is transferred into 15 ml Falcon tubes and centrifuged supernatant at 2.000*g* for 15 minutes at 4 °C. 3-4 ml of medium 2 are prepared in a 50 ml Falcon tube. After centrifugation, supernatant is filtered through a 45 μm filter into the 50 ml Falcon tube and then mixed gently with medium 2. The medium from fibroblasts is aspirated and interchanged with the of viral supernatant. The excess of viral supernatant can be stored in cryotubes at -80 °C.

On the following day the medium is replaced by medium 5. In two days, the selection is started by addition of blasticidine in a final concentration of 5 μg/ml. The cells are typically virus free in 2 weeks.

3.2.4 Determination of oxygen consumption rate by Seahorse XF Analyzer

The seahorse medium (SH medium; vial of sodium bicarbonate free DMEM powder dissolved in 900 ml ultrapure H_2O, with 10 mM sodium pyruvate and 22,5 ml 20% glucose; pH = 7,2; filled up to 1 l with H_2O) is stored as 50 ml aliquots at -20 °C. One aliquot per one cell plate is thawed up directly before the experiment.

For accessing the cell respiration by Seahorse instrument, cells were collected and 20.000 cells per well in 80 μl $DMEM^+$ were plated onto the XF96 Cell Culture Microplate. The corner wells (A1, A12, H1, H12) were filled with $DMEM^+$ only and the plate was incubated at 37 °C and 5% CO_2 overnight.

A calibration of the XF96 utility plate was done for every plate to be measured at least one day before the measurement. 200 μl of XF calibrant solution per well was prepared and the utility plate was incubated at 37 °C overnight.

On the day of the experiment, the cells on the XF96 Cell Culture Microplate were inspected under the microscope to ensure they formed a monolayer in each well. Then, 60 μl of the media was aspirated from each well, 150 μl of the Seahorse media was added and removed again, and 160 μl were added to end up with 180 μl in each well before the measurement. This procedure was done very carefully to avoid scratching off the cells from the surface.

The oxygen consumption rate (OCR) was then measured by using a XF96 Extracellular Flux Analyzer (Seahorse Biosciences). OCR was determined without supplements (basal), after addition of oligomycin (1 mM), after addition of carbonyl cyanide-4-(trifluoromethoxy)phenylhydrazone (FCCP, 0,4 mM), and after addition of rotenone (2 mM). The data were assessed and analysed by the software provided by Seahorse Biosciences.

3.2.4.1 Determination of cell number by CyQuant assay

The cells attach with a different strength and multiplicate with a different grow rate, therefore the cell number must be again determined after finishing the Seahorse assay. For the determination by CyQuant assay, the cells were washed in PBS and frozen at -20 °C to disrupt the cell membrane directly after the OCR determination. The cell number quantification by the CyQuant Cell Proliferation Kit (Thermo Fisher Scientific, Waltham, MA, USA) was done according to the manufacturer's protocol.

3.2.5 Cell viability and antioxidant treatment

3.000 cells per well in 100 μl $DMEM^+$ were seeded on a 96-well plate, typically 3 rows per cell line, one control cell line and three different patient cell lines. Then, cell attached over night at

37 °C, 5% CO_2. After overnight culture, cells were ready for a 72 hours drug exposure (*e.g.* 2,4-dinitrochlorobenzene (DNCB), inhibitor of glutathione reductase). 100 µl $DMEM^+$ were added to the first row to see the basal condition. Next, solution with the highest needed concentration was prepared (row 8 in Table 1, 'new stock solution'). As an example, 100 mM stock solution (in DMSO) is diluted to obtain the highest needed concentration (40 µM), which was further mixed in with the fresh $DMEM^+$ according to the table. Several dilutions of drug solutions were prepared for each well. As there were already 100 µl of $DMEM^+$ from the previous day, it was necessary to calculate the two-fold concentration, indicated as 'Needed concentration' in the Table 1.

Row	Desired concentration [µM]	Needed concentration [µM]	Volume per plate [µl]	Volume of new stock solution [µl]	$DMEM^+$ [µl]
1	0	0	1.300	0	1.300
2	1	2	1.300	65	1.235
3	2	4	1.300	130	1.170
4	4	8	1.300	260	1.040
5	6	12	1.300	390	910
6	8	16	1.300	520	780
7	10	20	1.300	650	650
8	20	40	1.300	1.300	0

Table 1: Concentration of the working solution of DNCB.

Final solutions of DNCB in DMEM are prepared in the increasing concentration by mixing $DMEM^+$ and a 'new stock solution' with the highest needed concentration. 100 µl of the drug dilutions were added to each well. Cells were then kept at 37 °C, 5% CO_2 for 72 hours.

After 72 hours after treatment, cell viability is assessed using Aquabluer Kit as an indicator of viable cells according to the manufacturer's recommendations (MultiTarget Pharmaceuticals LLC, available at http://www.aquaplasmid.com/).

First, a working Aquabluer solution as 1:100 dilution in pre-warmed $DMEM^+$ was prepared. Aquabluer is light-sensitive, therefore it is necessary to work without direct exposure to light and to decrease the light access to minimum. Next, medium from cells was removed and 100 µl of Aquabluer-$DMEM^+$ solution was added to each well and then kept for at least 3 hours at 37 °C, 5% CO_2. The survival rate was determined by measuring the changes in colour in a plate reader. Excitation 540 nm, emission 590 nm. To analyse the results, values were compared within each cell line with the first line, where no drug was added.

According to the design of the experiments, different drugs or antioxidants were added to the medium (rotenone, phenylarsine oxide, auranofin, Idebenone). The concentrations are indicated in the result section.

3.2.6 SDS PAGE and Western blot analysis

Cell pellets were resuspended in 100 µL RIPA buffer (50 mM Tris-HCl pH 7,4, 150 mM NaCl, 1% (v/v) NP-40, 0,1% (w/v) SDS, 0,5% (w/v) Deoxycolate) supplemented with 1:100 Protease Inhibitor Cocktail Set III, Animal-free (Calbiochem, an affiliated of Merck, Darmstadt, Germany). All samples were then incubated on a rotating wheel for 1h at 4 °C to be disrupted chemically. Optionally, the lysates were homogenized by 10 strokes with a 0,30 x 8 mm syringe.

The samples were centrifuged for 10 min at 15.000 g at 4 °C to remove the unbroken cells. In the supernatant the whole protein amount was quantified by using the Bradford assay. Subsequently, samples were adjusted to 1,5 µg protein/µL in 1x Laemmli buffer (5% (w/v) SDS, 250 mM Tris-HCl pH 6,8, 50% (v/v) glycerol, 500 mM ß-mercaptoethanol, 0,025% (w/v) bromphenol blue) and heated for 10 min at 50 °C. Designated protein amounts were loaded on precast gels (Lonza, Basel, Switzerland). Electrophoresis was running in 1x ProSieve EX Running buffer (Lonza, Basel, Switzerland) at 40 V for 30 min in the beginning. After the samples slowly and completely entered into the gel, the electrophoresis was continued at 120 V for 60 min. The separated protein samples were subsequently transferred by semi-dry method to PVDF membranes (GE Healthcare Life Sciences, Chalfont St. Giles, UK) using 1x ProSieve EX Western Blot Transfer buffer (Lonza, Basel, Switzerland) at a constant voltage of 25 V for 10 min. The membranes were blocked in 5% non-fat milk (Bio Rad) in TBS-T (150 mM NaCl, 30 mM Tris base, pH 7,4, 0,1% Tween 20) for at least 1 h and immunoblotted by using primary antibodies. Their binding was visualized by incubation with HRP-conjugated goat anti-rabbit and goat anti-mouse secondary antibodies and by using ECL Plus Western Blotting Detection System (GE Healthcare Life Sciences, Chalfont St. Giles, UK) on the Vilberscan Fusion FX7. Alternatively, Ponceau or Trihalo staining were used as loading controls. These stainings unspecifically color proteins transferred to the PVDF membrane.

3.2.7 Statistical analysis

Where the statistics is indicated, to determine the statistical significance the two-tailed two-sample Student's t-test was followed, assuming a normal distribution. Indicated error bars show standard deviation and standard error of mean. A p value of $< 0,05$ was considered statistically significant ($*p < 0,05$; $**p < 0,01$; $***p < 0,001$).

3.2.8 Methods done in collaboration

3.2.8.1 Exome sequencing

The techniques of the NGS are a standard at the Institute of Human Genetics. A whole department led by Dr. Tim-Matthias Strom is responsible for the sample collection, preparation, handling, sequencing and the data processing. In brief, DNA samples were enriched by using the SureSelect Human All Exon kit from Agilent (Agilent Technologies, Santa Clara, CA, USA) and sequenced as 100 bp paired-end runs on Illumina HiSeq2000 and Illumina HiSeq2500 (AG_50MB_v4 and AG_50MB_v5 exome kit samples) or as 76 bp paired-end runs

on the Illumina GAIIx (AG_38MB_v1 and AG_50MB_v3 exome kit samples; Illumina, San Diego, CA, USA). Resulting reads were aligned to the human reference genome (UCSC Genome Browser build hg19) using Burrows-Wheeler Aligner. Single nucleotide variants or small insertions and deletions were detected with SAMtools.

3.2.8.2 RNA sequencing and transcriptome analysis

Similarly, RNA sequencing was performed as 100 bp paired-end runs on an Illumina HiSeq2500 platform. RNA-seq reads were mapped to the hg19 genome assembly. Fragments per kilobase of transcript per million mapped reads were calculated as previously described (Mortazavi et al. 2008) by using Perseus. The algorithms allowing a systematic analysis were optimized by the group of Prof. Dr. Julien Gagneur (Department of Informatics, Technical University of Munich), as described (Kremer et al. 2017). The visualization via Sashimi plots and the quantitative imagining of splice junctions of the alignments was assessed in the Integrative Genomics Viewer (Robinson et al. 2011).

3.2.8.3 Determination of total glutathione

Together with Dr. Sho Kobayashi (Institute of Developmental Genetics, Helmholtz Zentrum München), total glutathione levels were analysed as he previously described (Kobayashi et al. 2015). In brief, cells were seeded on a 6-well plate in $DMEM^+$ and cultured for 24 hours at 37 °C, 5% CO_2. Next, cells were washed three times with ice-cold PBS, extracted with 5% trichloroacetic acid. The samples were then treated with ether to eliminate trichloroacetic acid. The total glutathione levels were assessed in the aqueous layer. The final analysis is based on an enzymatic method of the catalytic action of glutathione in the reduction of 5,5′-dithiobis(2-nitrobenzoic acid) by the glutathione reductase system (Tietze 1969).

3.2.8.4 Determination of ROS levels

Measurement and analysis of the ROS production was mainly prepared in the collaboration with Dr. Katharina Danhauser and Dr. med. Felix Distelmaier (Department of General Paediatrics, Neonatology and Paediatric Cardiology, University Children's Hospital, Heinrich-Heine-University Düsseldorf). Cells were seeded on a 96-well plate in DMEM with low glucose and no phenol red for 24 hours at 37 °C, 5% CO_2. Next, cells were washed with PBS and incubated in 5-(and-6)-chloromethyl-20,70-dichlorodihydrofluorescein diacetate (CM-H_2DCFDA; 10 mM for 20 min) in HEPES-Tris medium (132 mM NaCl, 4,2 mM KCl, 1mM $MgCl_2$, 5,5 mM D-glucose, 10 mM HEPES, 1 mM $CaCl_2$, pH 7,4). The fluorescence measurements were achieved within 10 min (Tecan Infinite M200 Multiplate reader; excitation 485 nm, emission 520 nm). The normalization was done by CyQuant as described above.

3.2.8.5 HPLC quantification of riboflavin, FAD and FMN

The sample preparation and quantification of riboflavin, FAD and FMN was done in the group of Dr. Johannes A. Mayr by Dr. Lavinija Mataković (Department of Paediatrics, Paracelsus Medical University Salzburg). For the analysis, EDTA blood from subjects was separated into plasma, mononuclear cells, and enriched erythrocytes purified by Ficoll gradient centrifugation. 50 ml of each sample was mixed with 375 ml of 10% trichloroacetic acid and 75 ml of water and incubated on ice for 5 min. Next, after centrifugation at 13.000 *g* for 5 min, the supernatant was extracted with equal amounts of diethyl ether twice, and 100 ml was applied to HPLC separation on a reversed-phase column (Agilent, Eclipse Plus C18, 5 mm, 4,6 x 150 mm) for measuring riboflavin, FMN, and FAD.

3.2.8.6 qRT PCR

Also, the real-time PCR experiment was assessed in a collaboration with Dr. Johannes A. Mayr and Dr. Lavinija Mataković (Department of Paediatrics, Paracelsus Medical University Salzburg). RNA sample for the qRT-PCR analysis (iQ SYBR Green Supermix, iCycler, Bio-Rad) was prepared as described above. To analyse *FLAD1*, primers covering all coding regions were designed. Threshold cycles (Ct) were normalized (ΔCt) to housekeeping genes *HPRT* and *RPL27*. The PCR products expression was then compared to corresponding samples of control fibroblasts (ΔΔCt).

3.2.8.7 Mass spectrometry

The samples for the mass spectrometry and the analysis of results was done in collaboration with Signe Mosegaard, Dr. Rikke K.J. Olsen and Dr. Niels Gregersen (Research Unit for Molecular Medicine, Department of Clinical Medicine, Aarhus University). 80 mg of protein samples and SDS-PAGE separation were done as described above. The bands of ~60, 50, 37, 32, and 27 kDa were cut out and processed by an in-gel trypsin-digestion protocol as described previously (Hansen et al. 2011). The selection of peptides, development method and analysis of data were obtained with a Skyline software (MacLean et al. 2010). Five peptides were analyzed by liquid chromatography coupled with the TSQ Vantage Triple Quadrupole Mass Spectrometer (Thermo Fisher Scientific). Four or more transitions were detected for each peptide, and synthetic isotopically labelled tryptic peptides (SpikeTide from JPT Peptide Technologies) were added to each sample for quality assurance.

3.2.8.9 FACS and determination of response to sulphoraphane treatment

Together with Dr. José Pedro Friedmann Angeli (Institute of Developmental Genetics, Helmholtz Zentrum München), we analysed a treatment with sulphoraphane and its influence on ROS production. ROS measurements were performed according to manufacturer‘s instructions for MitoSOX Red using flow cytometry analysis (FACSCanto II, BD Biosciences) after an overnight treatment with 10 μM sulphoraphane. A representative experiment is done

for 10.000 analysed cells per cell line (excitation 488 / emission 617). The experiment was performed as described previously (Mandal et al. 2010).

4 Case Reports

Both projects arise from collaborations with clinicians, who are seeing the patients. Their detailed descriptions of symptoms and measurements observed in muscle biopsy or brain imaging are typically a starting point for my functional validations and further biochemical investigations. Our cooperations also tend to suggest correct treatment options.

4.1 Thioredoxin 2: Case report

The following case report was prepared by Prof. Dr. Felix Distelmaier (University Children's Hospital, Heinrich-Heine-University Düsseldorf). The report and Figure 26 were published as a part of publication *Human thioredoxin 2 deficiency impairs mitochondrial redox homeostasis and causes early-onset neurodegeneration* by Holzerova E. *et alii* printed in Brain, 2016; doi: 10.1093/brain/awv350.

The boy is the first child of healthy, non-consanguineous German parents. Prenatal ultrasound at 16 weeks gestation revealed bilateral subependymal cysts and brachycephaly but was otherwise normal. The child was born at term without complications. Apart from primary microcephaly, no specific dysmorphic features or anomalies were seen. However, the parents noted that the child appeared relatively quiet and less active.

At the age of 6 months, the child was severely microcephalic (head circumference 4 cm below 3rd percentile) and showed a reduced spontaneous movement pattern. Brain magnetic resonance imaging detected an abnormally increased T2 signal intensity of the cerebellum and indicated global brain atrophy. In addition, abnormal hippocampal shape and bilateral subependymal cysts were seen (Fig. 26). Lumbar puncture and analysis of cerebrospinal fluid revealed elevated lactate (4,6 mmol/L, norm <2,8 mmol/L) and protein (67 mg/dl; norm <50 mg/dl) levels. In addition, blood lactate was repeatedly increased (up to 3,1 mmol/L, norm <1,6 mmol/L).

Follow-up at the age of 14 months revealed impaired psychomotor development characterized by markedly disturbed muscle tone and movement coordination. Brain MRI demonstrated a rapid progression of cerebellar atrophy and indicated delayed myelination. At the age of 22 months, a muscle biopsy with biochemical analysis of the oxidative phosphorylation system revealed reduced activities of mitochondrial Complex I (56 mU/U CS, norm 70-250) and Complex III (1.500 mU/ UCs, norm 2.500-6.610) and a reduced global ATP production rate (9 mmol ATP/mU CS; norm 42-81), confirming a mitochondrial disorder.

The further clinical course was characterized by severely disturbed global development with a spastic-dystonic movement disorder. Starting from the age of 4 years, the boy developed severe, drug-resistant epilepsy. Feeding difficulties required placement of a percutaneous endoscopic gastrostomy. The patient developed a gastrointestinal motility disturbance most likely due to

autonomic neuropathy. Clinical follow-up at the age of 12 years revealed severe optic neuropathy and retinopathy. Nerve conduction studies demonstrated peripheral neuropathy with axonal degeneration (Fig. 26). MR-spectroscopy was without pathological findings.

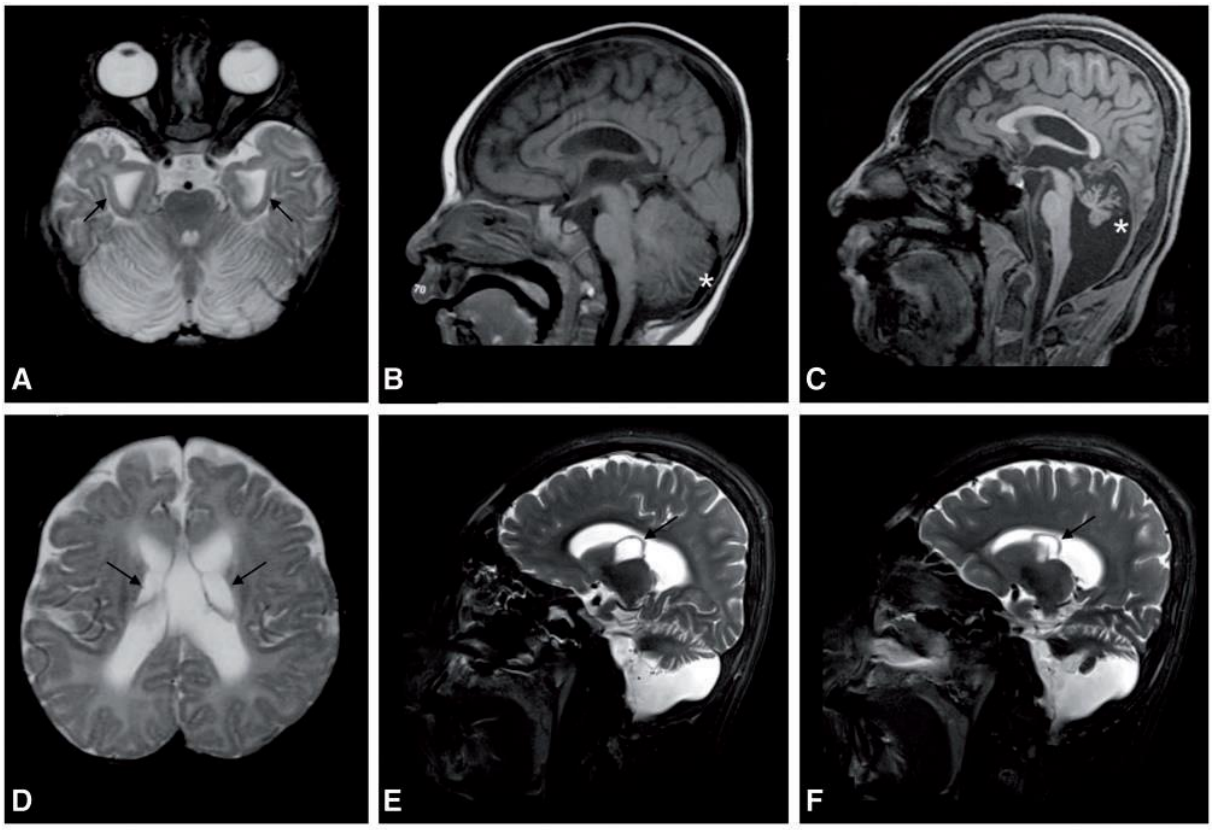

Figure 26: Brain imaging (from Holzerova et al. 2016). (A) Brain MRI, T2-weighted image, axial view at the age of 6 months demonstrating bilateral abnormal hippocampal shape (black arrows). Moreover, an abnormally increased T2 signal intensity of the cerebellum is observed. (B and C) T1-weighted images, sagittal view at the age of 6 months (B) and 12 years (C) showing the development of severe cerebellar atrophy (cerebellum is marked by asterisks). (D) T2-weighted image, axial view at the age of 6 months demonstrating large bilateral subependymal cysts (black arrows). (E and F) T2-weighted images, right (E) and left (F) parasagittal view at the age of 12 years, also depicting the bilateral subependymal cysts.

4.2 Flavin adenine dinucleotide synthase 1: Case reports

The following case reports were published as a part of Supplemental Data in publication *Riboflavin-Responsive and -Non-responsive Mutations in FAD Synthase Cause Multiple Acyl-CoA Dehydrogenase and Combined Respiratory-Chain Deficiency* by Olsen RK, Koňaříková E *et alii* printed in American Journal of Human Genetics, 2016; doi: 10.1016/j.ajhg.2016.04.006.

Altogether, nine cases from seven unrelated families derived from metabolic centers in seven countries were described. The affected individuals presented with muscle symptoms and multiple-respiratory-chain deficiency, some responded well to riboflavin treatment. Personally, in the beginning I was performing experiments on a cell line coming from an Austrian patient of a Turkish origin (Family 4). She and her sister were recruited by collaborators Dr. Vassiliki Konstantopoulou and Dr. Dorothea Möslinger from Vienna and Dr. Johannes A. Mayr from Salzburg as potential mitochondrial patients. However, later I was performing experiments with samples coming from other families, as well. Pedigrees of the families and a schematic presentation of variants is depicted in Figure 45.

Family 1 (F1) described by Dr. Avihu Boneh, Murdoch Children's Research Institute and University of Melbourne, Australia. Subject S1a, a boy of Turkish consanguineous parents presented with cardiorespiratory collapse at 32 hours of life and died 3 days later. A metabolic post-mortem analysis, done immediately after his death, showed elevated C5-, C8-, C14-carnitines and slightly elevated C5-DC/glutaryl-carnitine in blood spots. Urine organic acids revealed markedly elevated ethylmalonic acid and adipic acid, elevated suberic and dehydro-sebacic acids and slightly elevated hexanoylglycine levels. ETF and ETFDH activities in cultured fibroblasts were within control range. Muscle and liver respiratory chain complexes activities were within control range. Family history revealed an older sister (individual S1b), who had been treated for cardiomyopathy in the first year of her life. Screening of this girl showed elevated C4-carnitine on a blood acylcarnitine profile, and urine organic acids showed elevation of ethylmalonic acid and trace methylsuccinic acid. After treatment with riboflavin all metabolites normalized. Compliance with treatment was variable; in periods without treatment high urinary ethylmalonic acid was found, accompanied by episodes of supraventricular tachycardia. She was treated with riboflavin again and urinary metabolites decreased to control range. She is currently 22 years old and doing well with a pacing/defibrillator device. There were four miscarriages between individual S1a and his sister, S1b.

Family 2 (F2) described by Dr. Mari Auranen, Clinical Neurosciences, Neurology, University of Helsinki and Helsinki University Hospital, Finland and Dr. Tiina Tyni, Department of Pediatric Neurology, Helsinki University Central Hospital, Finland. Subject S2's developmental milestones were normal. During childhood she was able to run but was slower than her peers and experienced symptoms of illness during long-lasting exercise. First evident muscle weakness was observed at age 20 years as she carried heavy bags. Thereafter, she experienced muscle discomfort and weakness during physical activity, and after strenuous

exercise she had occasional muscle pain, vomiting and loss of weight. She had tachycardia and used beta blocking medication. During her pregnancy at age 30, one month before the delivery, her muscle weakness drastically deteriorated with a raise in creatine kinase (CK) activities ranging between 5.000-6.612 U/l (control range 35-210 U/l). It was difficult for her to control her head. She had swallowing and speech difficulties and a prominent scoliosis. No hearing or visual impairments were found. She was advised to follow a high carbohydrate, moderate protein and low-fat diet (dietary fat max. 20 g/day), which ameliorated her symptoms. Blood analysis revealed increases in C8- and C10-acylcarnitine species, and urine analysis showed increased amount of lactate, mildly increased ethylmalonic acid, an increased 2-hydroxyglutarate combined with a low/normal 2-ketoglutarate excretion that was consistent with MADD. Fibroblast fatty acid oxidation flux studies and Western blot analysis of ETF and EFTDH protein were found to be within control range. Multiple respiratory chain deficiency with lipid storage myopathy was detected in a muscle biopsy. Riboflavin therapy (100 mg daily) was introduced, and she continued the dietary therapy. This resulted in drastic amelioration of muscle symptoms and increase in muscle strength.

Family 3 (F3) described by Dr. Lodovica Vergani, Neuromuscular Center, Department of Neurosciences, University of Padova. Subject S3 is a 56-year-old woman, who was born at term after an uneventful pregnancy from non-consanguineous Italian parents. Early psychomotor development was normal. In the teens a mild scoliosis was diagnosed that did not require surgical or medical correction. At 45 years the affected individual presented with exercise intolerance, gait difficulties, weakness in both arms and muscle hypotrophy prevalent in the shoulder girdle. Her symptoms progressed since then and prompted neurological evaluation at age 46. Neurological examination revealed a mild waddling gait with bilateral foot drop. Standing or walking on heels was impossible. Scapular winging with hypotrophy of upper limbs, calf pseudohypertrophy and scoliosis were noticed. She was not able to lift her arms to the horizontal level, but was able to rise from the floor with Gowers maneuver. Lower limb weakness, graded using the medical research council (MRC) scale, involved iliopsoas and tibialis anterior muscles (4/5 MRC). In the upper limb, deltoid and teres muscles were the weakest (3+/5 MRC), while biceps and triceps were mildly affected (4+/5 MRC). A mild weakness in the orbicularis oris was observed. A needle EMG showed mild myopathic changes in the proximal muscles. CK was mildly elevated at 380 U/L (control range <170 U/L). Acylcarnitine profile showed increased C5-, C8-, C10-, C10:1-, and C14-carnitines in blood and glutaryl-carnitine in urine. Urine organic acid revealed elevated ethylmalonic acid and presence of tiglylglycine. A muscle biopsy showed a vacuolar myopathy with fiber size variation. No muscle fiber necrosis or regeneration was observed. Oil Red O staining showed lipid storage myopathy. Several cytochrome c oxidase (COX) negative fibers were also observed. Fatty acid oxidation analysis in a fresh muscle biopsy showed a reduced oxidation of C8 and C16 but not of C4. Activity of CI+CIII and CII+CIII Complexes were reduced compared to control, whereas citrate synthase activity was augmented. Heart and respiratory evaluations were normal. Lipid storage myopathy was diagnosed and supplementation with riboflavin (100 mg/day) and carnitine (2 g/day) was initiated. At follow up evaluation, 7 months later, the affected individual reported a complete resolution of exercise intolerance and improvement of muscle strength. She was able to walk on her heels, to lift her arm above the horizontal level,

and to rise from the floor with minimal support of one hand. Muscle weakness was limited to deltoid, teres, and iliopsoas muscles and graded 4+/5 MRC. Muscle hypotrophy and scapular winging did not improve. An acylcarnitine/free carnitine ratio within control range, and normal respiratory chain and citrate synthase activities were found in a post-treatment muscle biopsy, but with reduced total carnitine (7,6 nM/mg protein; control range: 10,5-29,5 nM/mg protein). Currently, 10 years after initial diagnosis, she is stable and still on riboflavin and carnitine supplementation.

Family 4 (F4) described by Dr. Johannes A. Mayr, Department of Paediatrics, Paracelsus Medical University Salzburg, Austria. S4a, a girl of consanguineous Turkish parents, presented after term delivery and uneventful neonatal period with increasing muscle hypotonia within the first months of life. Metabolic work up showed moderate elevation of acylcarnitines from C4 - C18:2 without the full pattern of MADD. Urine organic acids revealed variable ketosis and excretion of adipic and suberic acids in early age and moderate ethylmalonic acid and methylsuccinic acid excretion later. Activities of muscle respiratory chain enzymes were reduced, mainly for Complexes I, II. Pyruvate dehydrogenase was also reduced. Family history revealed an older sister (affected individual S4b), who also suffered from severe muscle hypotonia, which was diagnosed in the first year of life after term delivery and uneventful neonatal period. Metabolic follow-up showed either normal acylcarnitines, but also a measurement with an increase of multiple acylcarnitines (C4-OH, C5, C6, C8, C10, C14:1, C16:1). Variable mild ketosis was seen in organic acid evaluation. Both girls presented with severe muscle hypotonia and weakness, and S4b developed massive scoliosis. Tube feeding was necessary to avoid aspiration. Both sisters had reduced speech capacity. S4b was mentally able to finish elementary school training, whereas her sister S4a attended special school due to global developmental delay. Brain MRIs performed at the age of 6 years (S4a) or 16 years (S4b) revealed no abnormalities. Investigations of nerve conduction velocity (NCV) of peripheral nerves (tibial nerve, median nerve) were normal. No hearing or visual impairments were found; however, eyelid ptosis was observed on both eyes. Riboflavin (3 x 60 mg daily) was introduced in the treatment of S4a, but could not correct biochemical abnormalities such as acylcarnitine profiles. Clinical improvement of hypotonia was however obvious. The riboflavin treatment of the older sister was discontinued due to side effects. Unfortunately, S4b died at the age of 16 years after pneumonia and subsequent septicaemia. The family also had one older son, who died at the age of 4 years with similar symptoms and suspicion of mitochondrial disorder as well, but no detailed clinical or biochemical data are available (S4c). There is also one healthy son in this family, who is heterozygous for the FLAD1 mutation.

Family 5 (F5) described by Dr. Rita Horvath, Wellcome Trust Centre for Mitochondrial Research, Institute of Genetic Medicine, Newcastle University, Newcastle upon Tyne, UK. Subject S5 is a boy, who was born at 31st week of gestation following a twin pregnancy from Turkish consanguineous parents. He presented with poor sucking and hypotonia in the first few months of life and was hospitalized due to pulmonary infection at age of 6 months. During the hospital course, he developed sudden cardiac arrest few times. Holter monitoring revealed pause and pacemaker was implanted. Multiple respiratory chain deficiency with lipid storage myopathy and faint COX staining was seen in skeletal muscle. Blood analysis revealed increase in C3, C5, C6 and C8:1 acylcarnitine species with a low free carnitine, and urine analysis

showed increased amount of adipic acid. He died of multiorgan failure at 7 months of age. Post-mortem examination showed mild macrovascular steatosis in the liver, acute lung injury, nephrolithiasis and hemorrhagic necrosis of the kidney and spleen. There were no features of cardiomyopathy and COX staining was normal in heart.

Family 6 (F6): described by Dr. Daniele Ghezzi, Molecular Neurogenetics Unit, Foundation IRCCS Neurological Institute C. Besta, Milan, Italy. Subject S6 is a girl born to Italian non-consanguineous parents at 33 weeks after pregnancy complicated with uterine contractions. The mother had a previous miscarriage at 10 weeks. Soon after birth she presented with hypotonia, poor sucking, frequent vomiting episodes, and gastro-esophageal reflux. She was repeatedly hospitalized because of bronchiolitis and severe respiratory insufficiency. Due to persistent hypotonia with no head control, a suspicion of muscle disease was raised at age 5 months, and the girl underwent muscle biopsy. The spectrophotometric determination of respiratory chain complex activities in the muscle biopsy displayed a severe reduction of Complex II and Complex II+III activities, with a marked increase of citrate synthase, suggesting mitochondrial proliferation. She was treated with riboflavin, but with bad compliance and without response. She died aged 9 months due to septic shock following pneumonia.

Family 7 (F7) described by Dr. Cecile Acquaviva, Service Maladies Héréditaires du Métabolisme et Dépistage Néonatal, Centre Hospitalier Universitaire Lyon, France. Subject S7, a girl of Turkish consanguineous parents, presented with severe neonatal hypotonia and muscle weakness with elevated plasma CK activity (717 U/L – control range < 240). When she was 2 months old she was hospitalized for swallowing difficulties, requiring nasogastric feeding. Outcome was severe with a sudden respiratory deterioration at 4 months of age, requiring non-invasive ventilation and leading to death. Acylcarnitine profile in plasma revealed increase in C10-, C12-, C14:1-, C16:1-, C16- and C18:1-carnitines and to a lesser extent in C4-, C6-, C8- and C10:1-carnitines. Urine organic acids revealed markedly elevated ethylmalonic and 2-hydroxyglutaric acid. Muscle biopsy revealed major lipid accumulation and a faint SDH staining with normal COX.

5 Results

5.1 Results of Thioredoxin 2 project

5.1.1 Genetic analysis reveals a premature stop codon in TXN2

Whole exome sequencing of a patient suffering from neurodegeneration at our institute identified a homozygotic variant in the *TXN2* gene. To confirm the variant, I performed a Sanger sequencing analysis. Also, to exclude *de novo* mutations, I used DNA samples from blood of the parents and the patient. The analysis revealed an adenine (A) base at position 71 instead of guanine (G) in the patient's sample and purine (R) in the parents' samples. Hence, both non-consanguineous parents carry the variant. The variant produces a premature stop codon at the mRNA level by changing a tryptophan codon UGG into UAG 'amber' stop codon (Fig. 27).

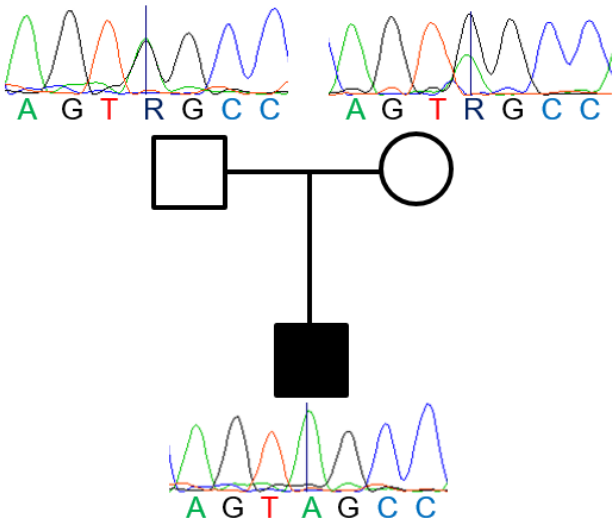

Figure 27: Sanger sequencing analysis showing the variant on the DNA level (modified from Holzerova et al. 2016). Parents are heterozygotic carriers, they have both – guanine and adenine base at the suspected position. The patient carries a homozygotic variant at position 71, leading into a premature stop codon on a protein level.

In about 7.000 exomes (in-house database of the Institute of Human Genetics) only this patient was identified with a homozygous loss-of-function variant. The Exome Aggregation Consortium lists only eight different loss-of-function variants in *TXN2* (three at splice acceptor site, three stop gained variants and two frameshifts), altogether observed in 12 alleles out of 121.412. The Genome Aggregation Database constituting 123.136 exomes and 15.496 genomes covers 16 different loss-of-function variants (six frameshifts, six stop gained variants, three at splice acceptor site and one at\ splice donor) in 225 alleles. However, 204 of them represent a relatively common variant in a non-canonical transcript. None of the rare loss-of-function variants nor any other rare missense variant is reported to be homozygous. The same is true for

the ClinVar database. Only larger heterozygous copy number variants were recorded to include the *TXN2* gene, seven duplications and one deletion.

5.1.2 The observed variant does not allow expression of a functional enzyme

TXN2 is located on chromosome 22 and consists of four exons, the first of which is not translated. As depicted in Figure 28, the observed variant is located in the first half of exon 2. On the protein level, it affects the mitochondrial targeting sequence (MTS), consisting of the first 59 amino acids (uniprot database; Vaca Jacome et al. 2015). On the lower part of Figure 28, a blue star indicates the redox-active site of TXN2 at the beginning of exon 3. This site consists of two cysteine residues at positions 90 and 93, specifically Trp-*Cys*-Gly-Pro-*Cys*. During the enzymatic reaction of TXN2, they form a disulfide bridge, which reduces the reaction target, in this context PRDX3 or PRDX5. Unfortunately, no in-frame start codon is located between the c.71G>A observed variant and the downstream active site, which would allow to produce a truncated active enzyme.

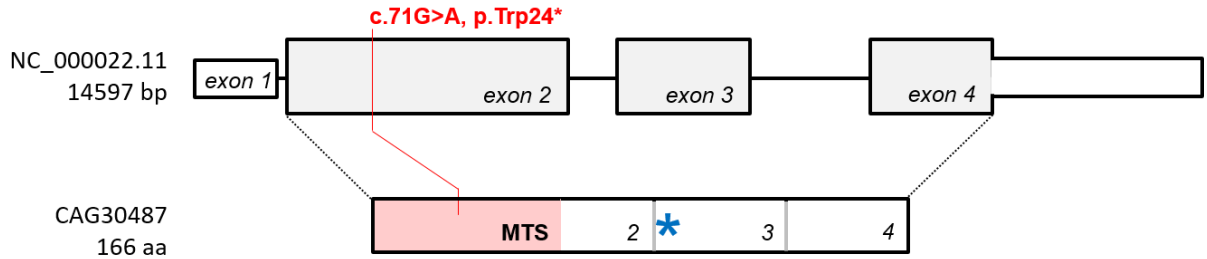

Figure 28: Schematic interpretation of thioredoxin 2 gene (NC_000022.11) and protein (CAG30487; modified from Holzerova et al. 2016). Exon 1 is not translated into a protein. The observed variant is highlighted in red. Protein N-terminus contains mitochondrial targeting sequence (MTS). The TXN2 active site is marked by a blue star at the beginning of exon 3.

5.1.3 The TXN2 protein is undetectable

To validate the predicted loss of protein, I performed an immunoblot analysis. Lysates of patient fibroblast were separated by a gel electrophoresis, transferred to a PVDF membrane and the protein samples were detected by specific antibodies. Anti-TXN2 antibody detected a single protein band at the expected molecular weight of about 13 kDa in the control sample. This polyclonal antibody covers 138 amino acids out of 166, thus most of the protein (83%). As no band was observed in patient samples in several subsequent experiments, the protein is either not present at all or below the detection limit of the antibody. Therefore, the full function of TXN2 is not present in such cells. Subunit A of Complex II (SDHA) and beta-actin were used as mitochondrial and cytosolic loading controls (Fig. 29).

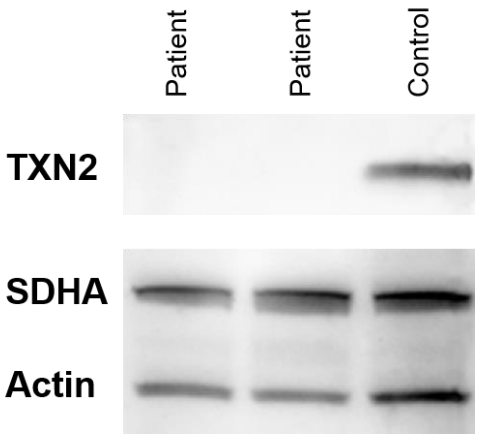

Figure 29: Loss of TXN2 protein. Anti-TXN2 antibody did not detect any TXN2 band in the patient cell line. Anti-SDHA and anti-Actin antibodies were used as loading controls.

5.1.4 Mitochondrial function is impaired due to an interference with respiratory chain complexes

As thioredoxin 2 is active in mitochondria and it was reported that the patient has reduced activities of mitochondrial Complex I and III, I analysed the cell energy metabolism. The fibroblast cell line underwent a cell mitochondrial stress test, which confirmed decreased oxygen consumption rate capacity (Fig. 30A). Several parallel measurements revealed that a basal respiration and a maximal respiration of the patient cells were reduced to 55,1%, resp. 52,5% when compared to the control cell line and after subtraction of non-mitochondrial respiration (Fig. 30B). TXN2 is one of the key enzyme of mitochondrial ROS defence, while Complexes I and III are main ROS producers (Holzerova and Prokisch 2015). The ROS imbalance can therefore have an effect on the activity of both Complexes (Korge et al. 2015).

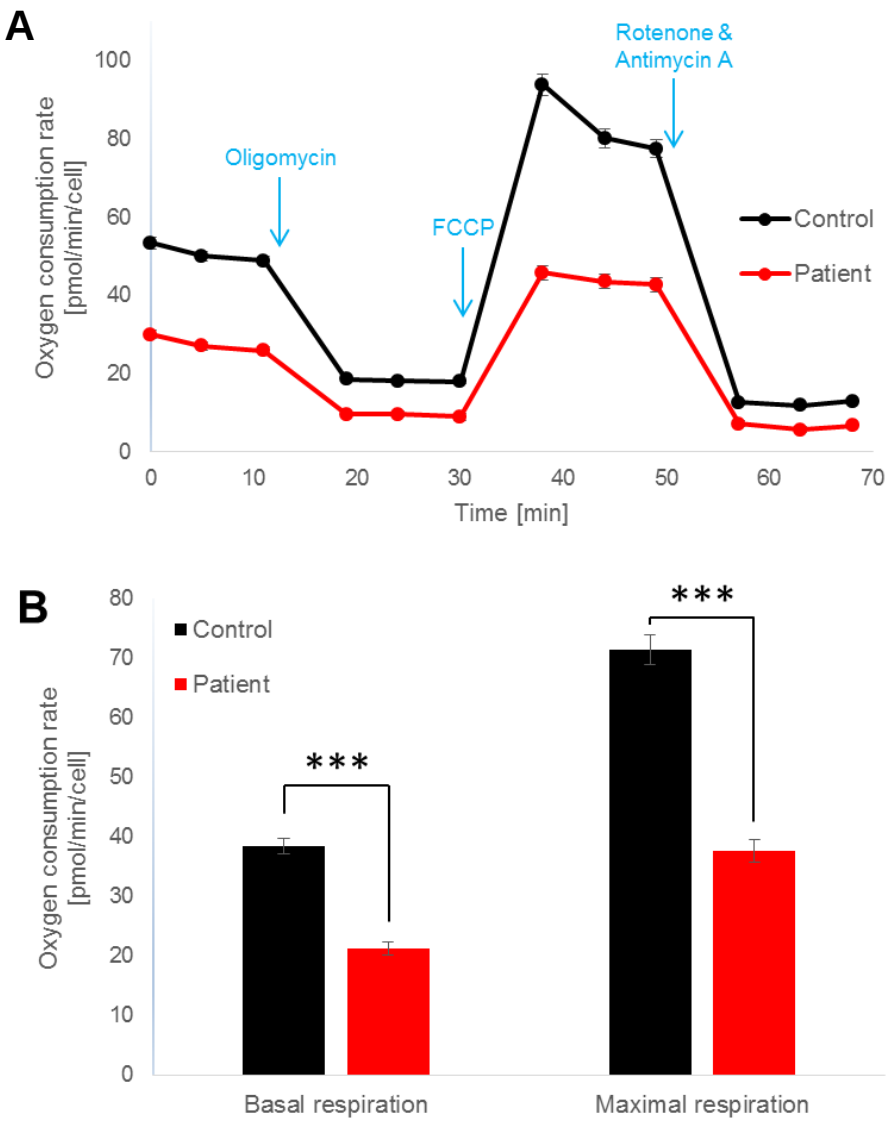

Figure 30: Oxygen consumption rate assessed by the Seahorse XF Analyzer. (A) Cell mitochondrial stress test profile after correction to the cell number showed decreased respiration capacity in the patient cell line. (B) Non-mitochondrial respiration was subtracted from the values for basal and maximal respiration. Both were significantly reduced in the patient cell line (to 55,08%, resp. 52,51%).

5.1.5 PRDX3 monomers are not restored due to lack of TXN2 function

The role of TXN2 in ROS defence lays in the reduction of intermolecular disulphide bridges, which are formed upon oxidation between two molecules of PRDX3. In an oxidative environment, two cystein residues 108 and 229 undergo an attack of the peroxide bond, which leads to the formation of reversible sulphenic acid (-SOH). This is highly reactive and can rapidly create a disulfide bridge. Therefore, in the oxidative environment PRDX3 typically forms intermolecular homodimers (Fig. 31A). Efficient cycling and thus recovery of reduced and active peroxiredoxins is a key step in the ROS defence.

Immunoblot detection of the PRDX3 monomer and dimer signals is therefore a proxy analysis of the TXN2 function. I used this approach to observe if the ROS defence and the collaboration between TXN2 and PRDX3 is impaired. I detected a substantial amount of PRDX3 dimers in the protein samples from the patient cell line, whereas no dimers were observed in the control sample under standard growth conditions (Fig. 31B). TXN2 is mainly responsible for the reduction of PRDX3 dimers. Therefore, the observed PRDX3 dimers are a direct consequence of TXN2 loss on the cellular level. However, to sustain the cellular maintenance in patient cells, the PRDX3 cycling can be partially overtaken by enzymes TXNRD2 or GLRX2 or by the molecule of NADPH (Fig. 9; Hanschmann et al. 2010).

Figure 31: Cycling of PRDX3 in the oxidative environment (modified from Holzerova et al. 2016). (A) Schematic interpretation of PRDX3 reaction. PRDX3 undergoes formation of intermolecular disulphide bridges after reduction of H_2O_2 into water molecules. Mainly TXN2, but also other enzymes or molecules, are responsible for the restoration of PRDX3 monomers. (B) Increased amount of PRDX3 dimers is observed in patient cells with malfunctioning TXN2. Anti-SDHA and anti-Actin antibodies were used as loading controls.

5.1.6 Patient cells are highly sensitive to mitochondrial inhibitors

In order to stimulate the ROS defence system and to further challenge it, the cells underwent treatment with several inhibitors. My idea was to observe the vulnerability of the interconnected pathways with a missing TXN2 piece. The control cells should be less affected by inhibition of individual enzymes.

I left the cells for three days in the toxic conditions and observed their survival rate. In this experiment, cells were treated with DNCB, an inhibitor of glutathione reductase; rotenone, an inhibitor of Complex I and inducer of ROS production; PAO, an inhibitor of glutathione; and auranofin, an inhibitor of thioredoxin reductase (in detail in chapter 4.1.7). All incubations showed higher sensitivity of the patient cell line towards the additional stress. The cell environment and the ROS defence system in the patient cell line are impaired; therefore, further inhibition or extra ROS production leads to increased lethality in such experiments (Fig. 32).

Increased sensitivity towards DNCB and PAO indicates the interconnection between thioredoxin and glutathione ROS defence systems. The cells cannot cope with the additional inhibition on the glutathione part of the pathways. Lethality caused by auranofin supports the idea that TXNRD2 reduces other enzymes than just TXN2 as suggested on ROS defence scheme (Fig. 9). No effect of auranofin would point to a sole enzymatic activity of TXNRD2, hence the reduction of TXN2. Rotenone most likely kills the cells due to additional ROS production, with which the cells cannot cope (Fig. 32).

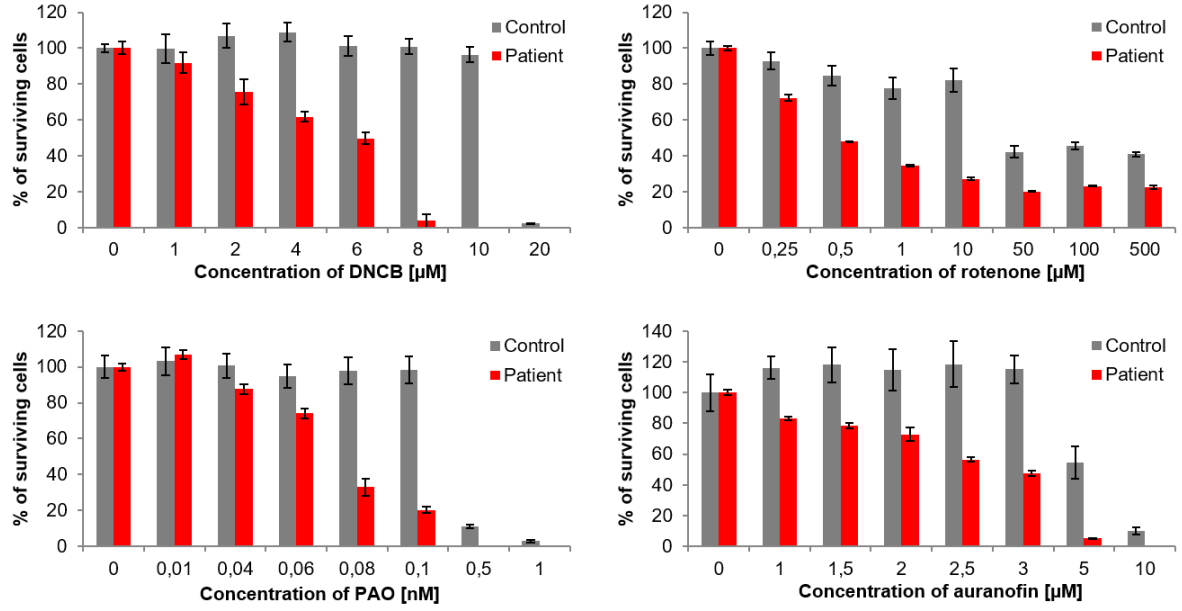

Figure 32: Cell sensitivity test of mitochondrial inhibitors. Cells were incubated for three days in an increasing concentration of various inhibitors, specifically, DNCB, rotenone, PAO, and auranofin. After the treatment, the amount of survived cells was analysed. In general, the patient cells show higher sensitivity towards all tested inhibitors.

5.1.7 The expression of wild type TXN2 is stable in both cell lines

To validate if the loss of TXN2 function is responsible for the observed phenotype and to see if re-expression of *TXN2*^{wt} can restore decreases parameters, I expressed a wild-type cDNA copy of *TXN2* from a cDNA sample obtained from a healthy control cell line. The primers were designed to cover *TXN2* from the start codon till the stop codon, thus exactly 501 base pairs. I added the optimized Kozak sequence CGCC right before the first ATG to ensure better expression. The PCR product of *TXN2*^{wt} was inserted into a vector, sequenced and validated, amplified, cleaned and transfected into the patient and the control cell line.

Stable expression of TXN2 protein was investigated via immunoblot analysis. Strong bands of the *TXN2*^{wt} overexpression of the correct size of 13 kDa were observed in protein samples from patient and control cell lines with *TXN2*^{wt} (Fig. 33).

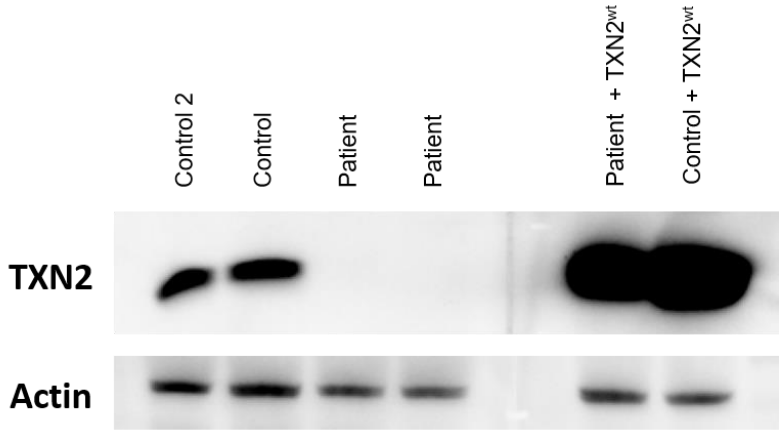

Figure 33: Immunoblot analysis of cell lines (modified from Holzerova et al. 2016). Anti-TXN2 antibody detected a single band in samples from controls and in samples, where TXN2 was expressed artificially. No signal was detected in patient samples. Visualization of actin was used as a loading control.

5.1.8 **TXN2^{wt}** *restores mitochondrial respiration*

First, I analysed if the expressed wild type copy of *TXN2* is active and if the re-expression restores the observed phenotypes. The patient was diagnosed with a mitochondrial disorder, therefore the reestablishment of the activity of mitochondrial respiratory chain after expression of *TXN2*^{wt} confirms the phenotype and correct diagnosis. I measured again the oxygen consumption rate and the values for basal and maximal respiration were restored to the control values upon complementation (Fig. 34). The recovery of the respiratory chain function suggests that the malfunctioning TXN2 is responsible for the observed phenotype, however the exact mechanism is still to be examined.

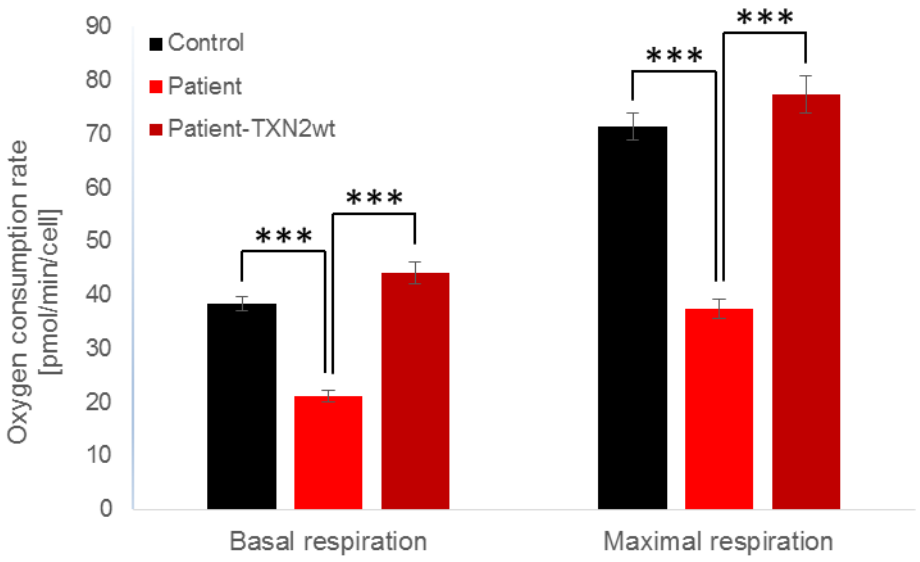

Figure 34: Oxygen consumption rate assessed by the Seahorse instrument. Basal and maximal respiration after correction to the cell number and subtraction of non-mitochondrial respiration showed decreased respiration capacity in the patient cell line and the restoration in cells with expression of TXN2^{wt}.

As a result of decreased mitochondrial respiration and overall cell fitness, my collaborators from Düsseldorf (Dr. Katharina Danhauser and Prof. Dr. Felix Distelmaier) measured lower ATP production in the patient cell line. Likewise, the expression of *TXN2^{wt}* led to normalisation of ATP values (Holzerova et al. 2016). Both above mentioned experiments suggest that a constant control of mitochondrial H_2O_2 levels is necessary for prevention of OXPHOS dysfunction.

5.1.9 PRDX3 dimers are reduced by the reexpressed wild type TXN2

The investigation of the activity of TXN2 via PRDX3 dimers, confirmed the involvement of TXN2^{wt} in the TXN2-PRDX3 cycle (Zhang et al. 2007; Hanschmann et al. 2010). In the cell line with expression of *TXN2^{wt}*, PRDX3 dimers almost disappeared as observed in several parallel experiments. The immunoblot analysis in Figures 33 and 35 shows that the TXN2^{wt} is highly expressed. And moreover, is active in the sense of reducing PRDX3 intermolecular disulphide bridges and hence restoring the PRDX3 monomer pool (Fig. 35).

In the same experiment, I tried to boost the dimer formation by 5 µM H_2O_2 with an increasing incubation time, however this did not have any effect in the setting I chose. The standard SDS-PAGE creates such an environment in which any residual PRDX3 dimers are reduced. Nevertheless, such parallel experiments show repeatedly observed PRDX3 dimers in the samples from patient cell line and lack of their presence in the control samples and samples with TXN2^{wt}.

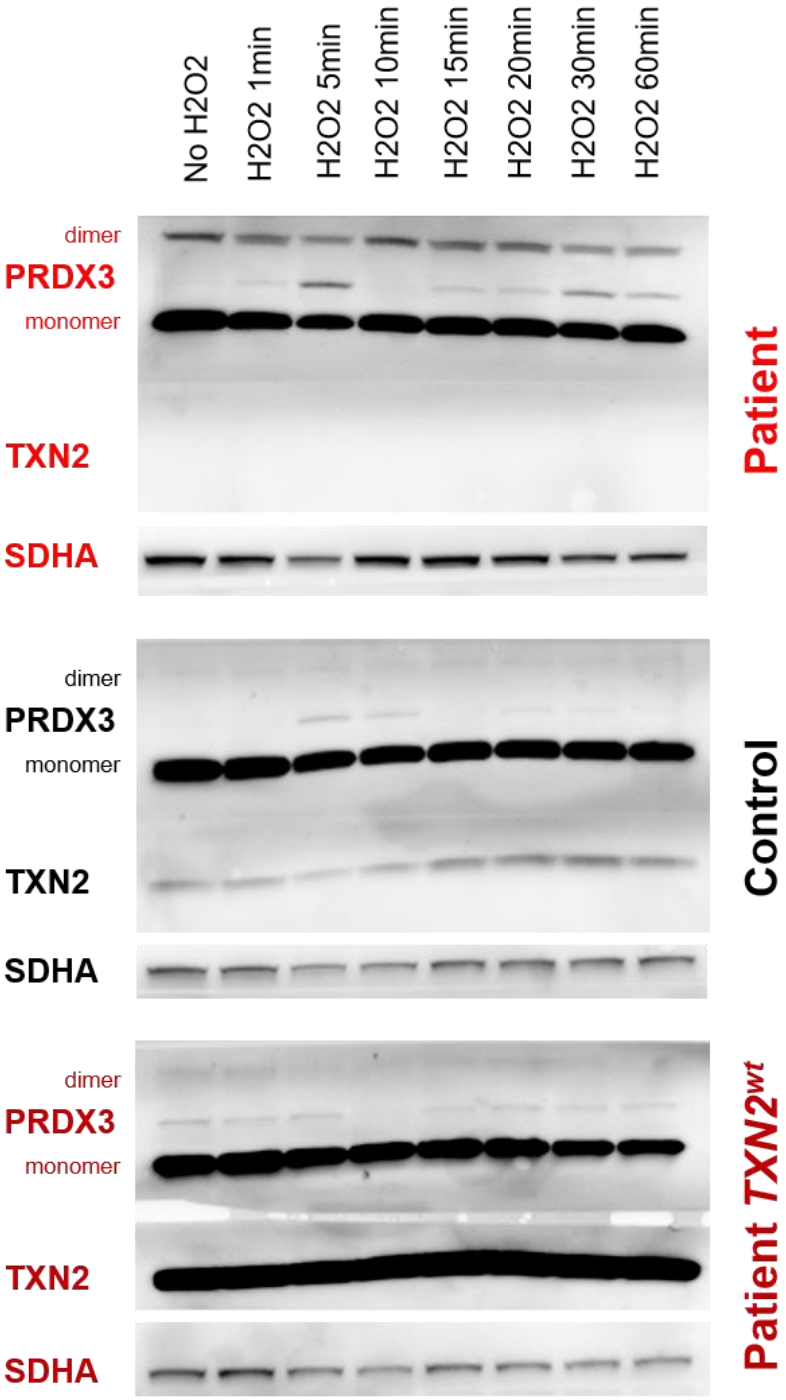

Figure 35: Immunoblot analysis of PRDX3 dimers (modified from Holzerova et al. 2016). Cells were incubated in 5 μM H_2O_2 for an indicated time, then the protein samples were prepared and separated by gel electrophoresis. Anti-PRDX3 antibody detected monomers and dimers of PRDX3. Anti-TXN2 was used as a cell line and a loading control. Anti-SDHA was used as a loading control.

5.1.10 Total glutathione levels stay unchanged among cell lines

Reduction of PRDX3 dimers indicates a direct effect of TXN2 on the thioredoxin part of the pathway. Therefore, I aimed to explore whether there is a compensation by the glutathione part of the pathway.

Glutathione serves as the major redox buffer in the cellular environment (Mailloux and Treberg 2016). It was reported that levels of oxidized (GSSG) and reduced (GSH) glutathione and the GSH/GSSG ratio are important indicators of cellular health (Enns and Cowan 2017). Moreover, while *Saccharomyces cerevisiae* contains the highest amount of glutathione in mitochondria (Zechmann et al. 2011), human-derived cells show equal distribution in all of the cellular compartments (Ault and Lawrence 2003). Nevertheless, these human cells showed a glutathione depletion in an oxidative environment.

Therefore, together with Dr. Sho Kobayashi (Institute of Developmental Genetics, Helmholtz Zentrum München), I measured the glutathione levels directly in the investigated cell lines. I expected either increased level of GSH in the patient cell line as a result of a compensatory effect or decreased level as a consequence of overall inhibition of the ROS defence system or unduly oxidative conditions. Surprisingly, the levels of total glutathione were equal in all analysed cell line (Fig. 36). To further investigate glutathione levels, a mitochondrial isolation would be necessary as well as the analysis of isolated GSH and GSSG.

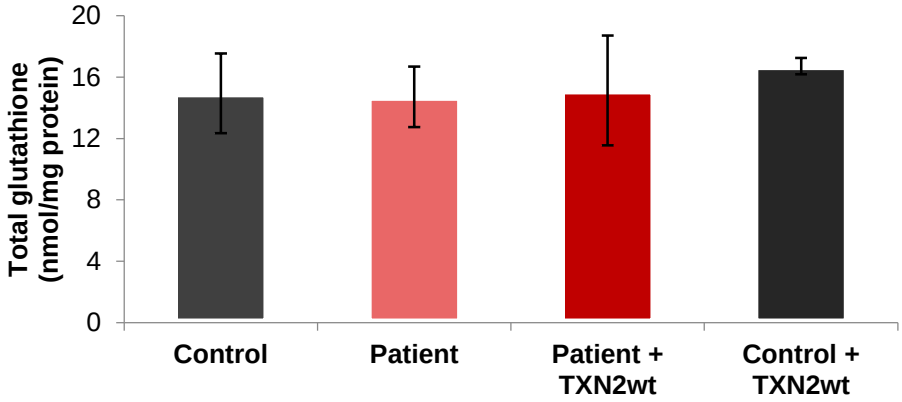

Figure 36: Concentrations of total glutathione in studied cell lines. Cells were grown on a small dish and subsequently the total glutathione was isolated. The levels show that glutathione is intact towards the TXN2 insufficiency.

Similarly, I tried to analyse proteome and transcriptome of the patient cell line in order to observe any compensatory mechanism or impairment caused by the mutation on the RNA and protein level. However, no striking results in the known component of ROS defence system were observed.

5.1.11 Expression of wild type TXN2 *protects the cells against inhibition of ROS defence pathways*

Next, I re-analysed the cell survival rate. It was important to validate that the increased death rate of the patient cell line is not due to a generally decreased fitness of the patient cell line, but specifically caused by the mutation in *TXN2*. I treated the cells for three days with DNCB, auranofin, and PAO, and afterwards I determined the number of living cells (Fig. 37). Fully active wild type copy of *TXN2* led in the patient cells to a higher survival rate. As the cells with re-expressed *TXN2*^{wt} were able to cope with all the toxic conditions similarly as the control cells, the increased sensitivity in patient is due to an impairment in TXN2 activity. Unfortunately, I was not able to repeat the experiment with rotenone.

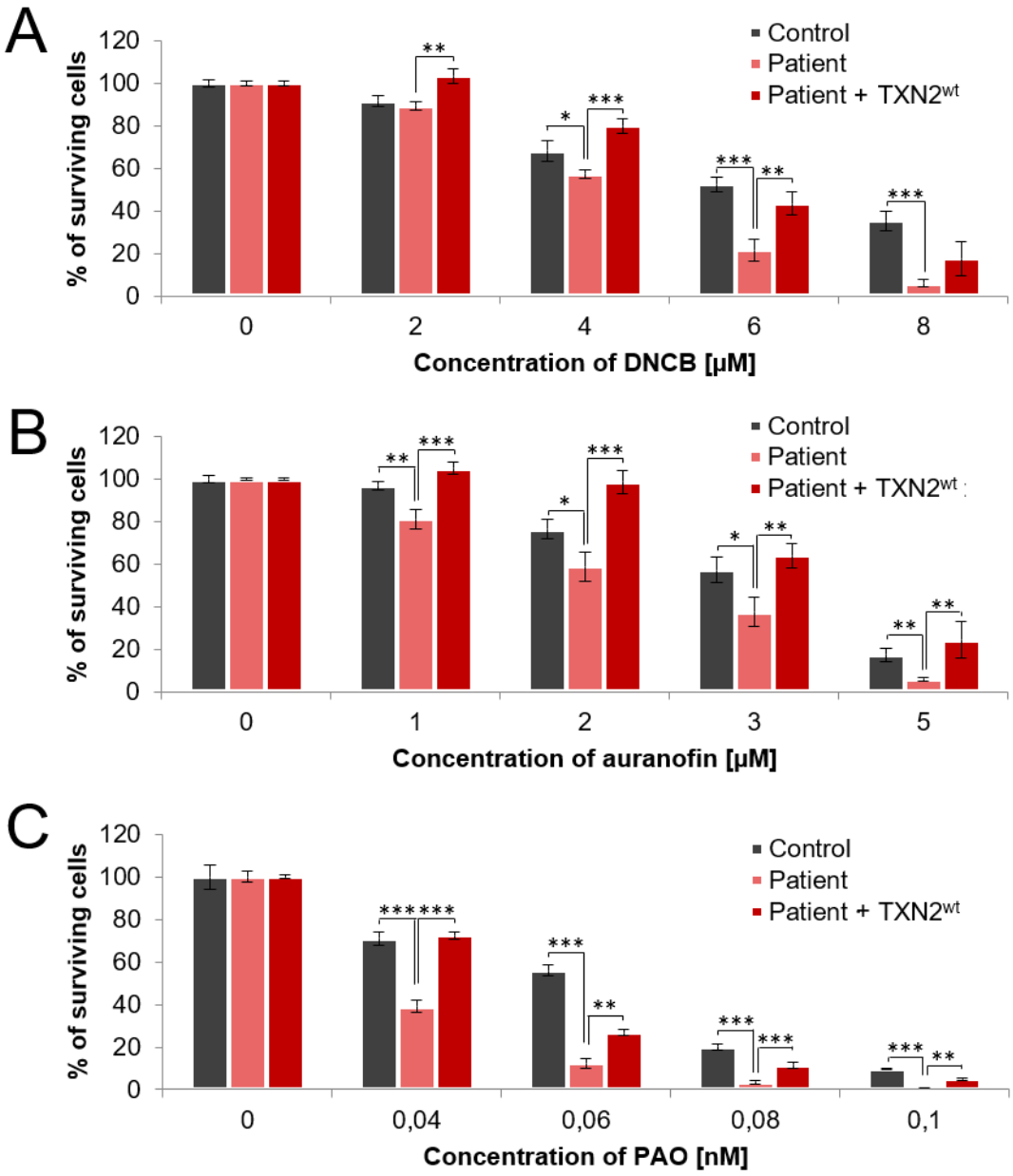

Figure 37: Cell sensitivity test in cell lines (modified from Holzerova et al. 2016). Inhibitors of mitochondrial ROS defence components were administered for three days to the cells. The

patient cell line showed a higher lethal level than control and especially than the cell line with TXN2^{wt}. *Increasing concentrations of all drugs, (A) DNCB, (B) auranofin, (C) PAO, were used.*

5.1.12 Antioxidants serve as an effective therapy for patients with defective TXN2

The previously described experiments suggested that the cause of the mitochondrial disorder was the lack of TXN2 activity, and subsequent insufficient ROS defence. Increased amount of ROS over years most likely caused the neurodegeneration observed in the patient. Therefore, finding an effective treatment is important in such cases. Luckily, several antioxidants are available on the market.

Together with collaborators in Düsseldorf (Dr. Katharina Danhauser and Prof. Dr. Felix Distelmaier), we tested MitoQ, Idebenone and Trolox and their effect on ROS production in the cell environment. Basal measurement of ROS levels confirmed previous observations; hence the relative concentration of ROS is increased in the patient cell line in comparison with the control cell line and the patient cell line transduced with *TXN2^{wt}*. As depicted in Figure 38, treatment with the antioxidants significantly decreased in all cases the amount of detected reactive oxygen species in the patient cell line.

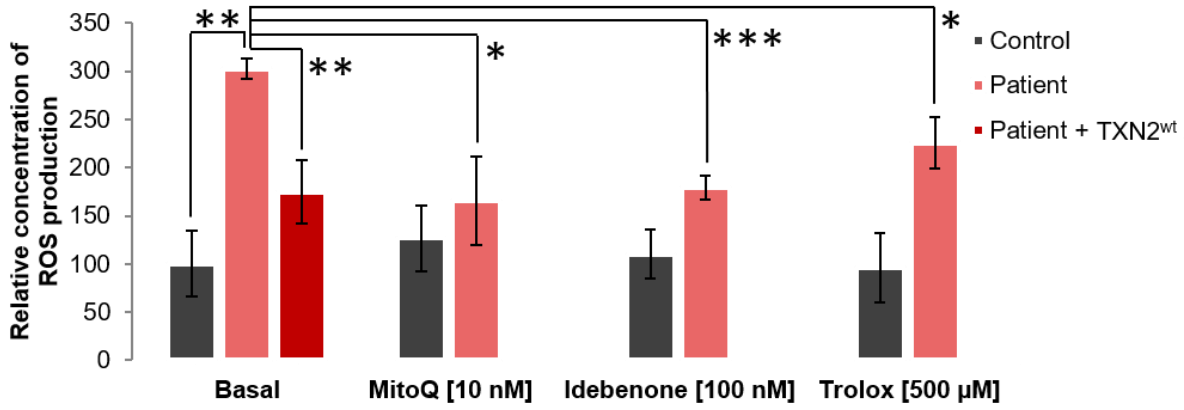

Figure 38: ROS production in the cells and effect of antioxidants (from Holzerova et al. 2016). The amount of ROS was detected with 5-(and-6)-chloromethyl-20,70-dichlorodihydrofluorescein diacetate (CM-H$_2$DCFDA). Treatment with indicated antioxidants (MitoQ, Idebenone, Trolox) significantly decreased observed levels of ROS in patient cell line.

5.1.13 Idebenone as a successful rational therapy

Together with Prof. Dr. Felix Distelmaier and Dr. Holger Prokisch we decided to further evaluate the therapeutic potential of Idebenone only, since it is clinically available and approved for the treatment of patients. Therefore, I tested cell sensitivity towards DNCB with and without the addition of Idebenone. In the experimental conditions, I observed significantly increased cell viability when cells were treated both with DNCB and Idebenone at the same time (Fig. 39) when compared to exclusive DNCB inhibition. This indicates that additional inhibition of GSR can be reverted by using of antioxidants. Such result corresponds to the effect of TXN2^{wt},

with antioxidant administration as the rational treatment strategy accessible rather than a gene therapy.

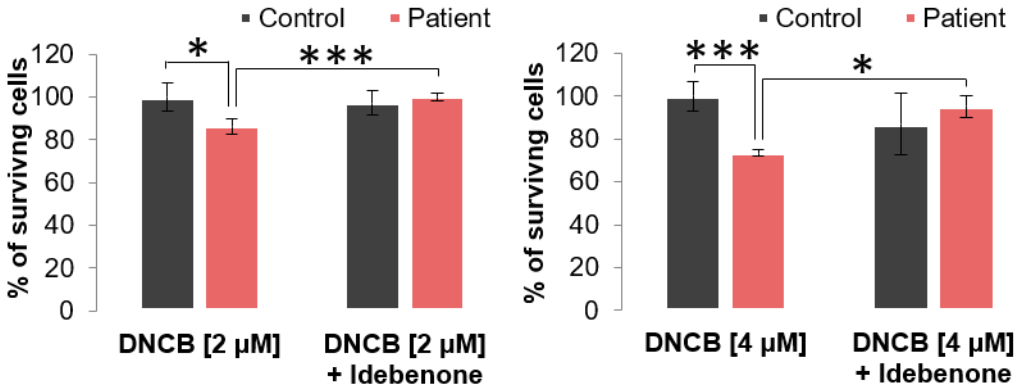

Figure 39: Effect of Idebenone in cells treated with DNCB (modified from Holzerova et al. 2016). 2 and 4 µM was added to a medium with or without 200 nM Idebenone and incubated for three days. Afterwards, the cell amount was determined showing better survival rate of patient cells upon Idebenone treatment.

The positive effect of Idebenone in cell culture motivated Prof. Dr. Felix Distelmaier to start a rational therapy with Idebenone, specifically 900 mg/day in a compassionate use setting. After a relatively short time of administration, several improvements were observed. After ten months of drug supplementation, the parents reported improved feeding behaviour (less tube feeding required). He gained weight from 39,5 kg (BMI < 3rd percentile) to 47 kg at 16 years of age. Simultaneously a sustained improvement in physical capability together with significantly reduced frequency of respiratory infections was observed.

5.1.14 General antioxidative pathways do not decrease ROS levels

Additionally, I was interested if a stimulation of general antioxidative pathways will affect the ROS levels in our experimental model. Together with Dr. José Pedro Friedmann Angeli Institute of Developmental Genetics, Helmholtz Zentrum München), I followed a complementary approach by applying an overnight treatment with sulphoraphane (SFN). SFN is used as a small molecule able to induce the cellular antioxidant response (Holland and Fishbein 2010).

SFN is a potent natural antioxidant response element (ARE) activator that functions by modifying Kelch-like ECH-associated protein 1 (Keap1) cysteine residues, which releases it from its complex with Nuclear factor (erythroid-derived 2)-like 2 (Nrf2) and allows the translocation of Nrf2 to nucleus thus activating genes with an ARE binding site. Among the early responsive genes to Nrf2 induction are SLC7a11, heme-oxygenase 1, γ-glutamyl cysteine ligase and members of the glutathione peroxidase family.

I first established non-toxic SFN treatment conditions (10 µM for 24 hours) which did not impair survival of the cells but increased cellular antioxidant response. As a control experiment,

I measured the release of thiols into the medium, which was increased by 25-44% in all cell lines. Detection of free thiols indicates an increased oxidative environment in the cell cytosol. However, the measurements did not reveal any relevant effects on mitochondrial ROS levels in patient cells, which is in contrast to the treatment by mitochondrial targeted ROS scavengers (Fig. 40).

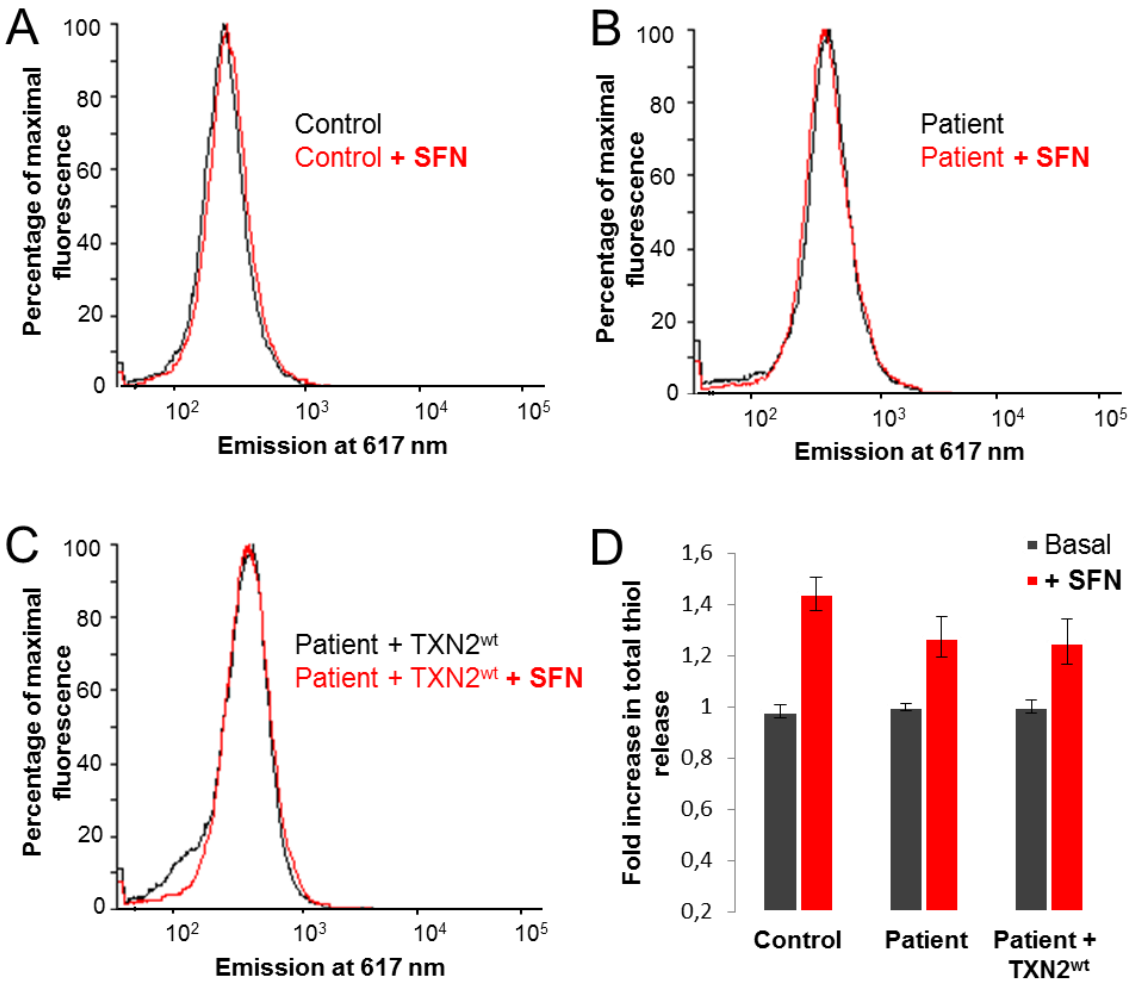

Figure 40: Sulphoraphane treatment. (A-C) Reactive oxygen species were analysed by MitoSOX Red using flow cytometry analysis after an overnight treatment with 10 µM SFN. 10.000 cells per cell line were analyzed. (D) Increased extracellular thiols observed after SFN treatment (10 µM) confirmed overexpression of anti-oxidant pathways; however, the ROS levels stayed intact.

5.2 Results of Flavin adenine dinucleotide synthase 1 project

5.2.1 Genetic analysis of the first family reveals a frameshift in FLAD1

Consanguineous Turkish parents with two daughters suffering from a severe muscle hypotonia within the first months of life have been seen at the Medical University of Vienna (detailed case report as Family 4 in chapter 4.2). In the beginning of the FLAD1 project, I obtained information and samples only from this family.

Genetic analysis via whole exome sequencing revealed a deletion of 12 base pairs in exon 2 in positions 526 till 537 combined with an insertion of 'CA' when compared to isoform 1 of *FLAD1*. This variant causes a frameshift resulting in a premature stop codon occurring eight amino acids after the beginning of the variant. Both parents were identified as heterozygotic carriers and both sisters were homozygotes. One healthy older brother carries only one copy of this mutation. Unfortunately, no sample was available for the oldest deceased sibling to analyse. Figure 41B shows confirmation of this variant by a Sanger sequencing analysis.

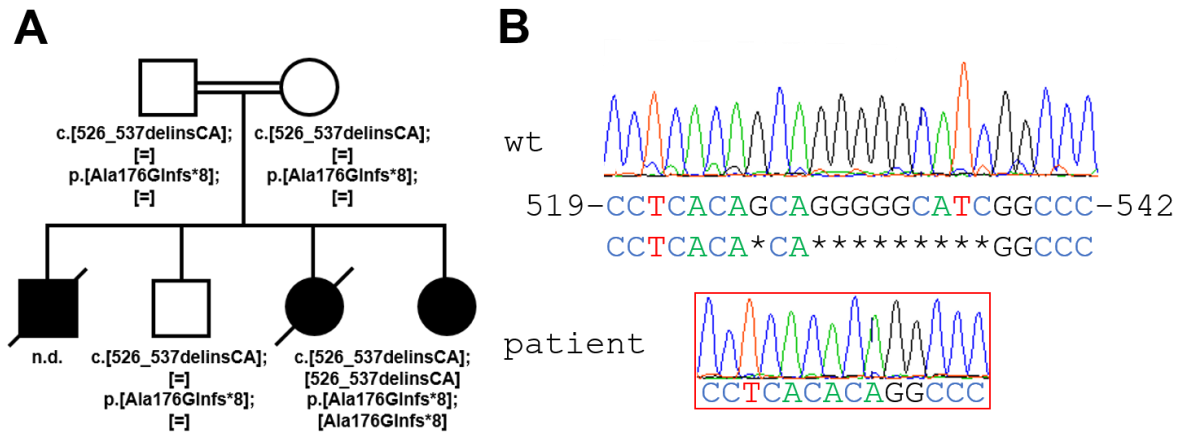

*Figure 41: Pedigree of the Turkish family from Vienna and Sanger sequencing of FLAD1 (modified from Olsen et al. 2016). (A) The consanguineous parents are heterozygotes for the same mutation c.[526_537delinsCA], presenting on the protein level as p.[Ala176Glnfs*8]. Both sisters carry the homozygous variant, the older brother is a heterozygotic carrier. The sequence for the oldest son was not determined (n.d.). (B) Sanger sequencing confirmed a deletion in positions 526 to 537 with an insertion of nucleotides C and A therein.*

5.2.2 The variant causes a reduction of the cytosolic FLAD1 protein

By using the cell line derived from skin of the younger daughter, I could perform several studies and further explore this new genotype. First of all, an immunoblot detection of FLAD1 was performed to validate the effect of the variant on a protein level (Fig. 42). A clear reduction of the 54 kDa band was observed. This corresponds to the shorter cytosolic version of FLAD1 protein, also called isoform 2. Several other bands were additionally detected by the C-terminus antibody and studied in detail in following experiments. Most of them were observed in the patient as well as in the control sample, suggesting either unspecific staining or expression of

alternative isoforms. I tried to confront the observation by using a N-terminal antibody, but unfortunately that antibody provided only unspecific staining (not shown).

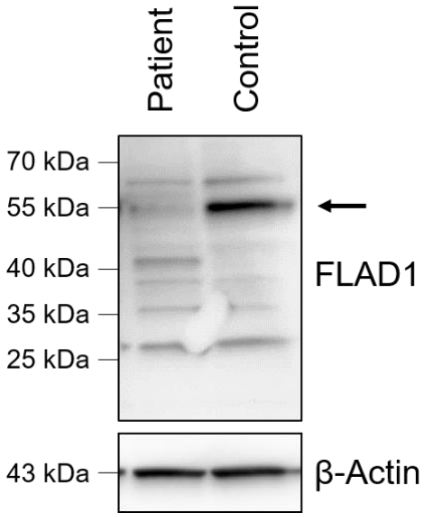

Figure 42: Immunoblot analysis of FLAD1 protein (modified from Olsen et al. 2016). Western blot with the C-terminus anti-FLAD1 antibody revealed a clear reduction of a 54 kDa band corresponding to a cytosolic variant of the FLAD1 protein (marked with an arrow). Other detected bands correspond either to other isoforms or are unspecific. Anti-β-actin antibody was used as a loading marker.

5.2.3 Cells show decreased multiplication rate

Secondly, to study cell viability, I performed a growth curve experiment. The idea was to analyse the fitness of the cell line and to observe response to riboflavin supplementation. Alteration of the growth rate upon addition of riboflavin would point to a leaky mutation, expression of a truncated variant, or presence of an alternative FAD production pathway. However, it must be considered that the cells may be adapted to restricted FAD availability or the reduced growth rate may reflect artefacts of the cell line establishment.

Typical growth curve results are shown in Figure 43. 40.000 of cells were plated and measured after two days at approximately the same time for five following days (Day 4-8) plus a subsequent Monday (Day 11). The patient cell line had reduced basal growth rate when compared to the control one. I tried to boost growing by addition of riboflavin into the culture media. Firstly, I added riboflavin on the Day 1 together with cells (indicated as 'DMEM + riboflavin'). However, the measurement of cell amount, did not reveal any improvement in the cell growth. As seen in Figure 43, cells reached plateau after 6 days of growing independently of the addition of riboflavin or in the course of basal conditions.

Therefore, I proposed that riboflavin could be used up by the exponentially growing cells and experimented with the addition of riboflavin both on Day 1 and 6. This experiment did not increase cell growth. In fact, it appeared that the patient cell line was different from the control cell line and could not grow to such density. While the control cells multiplied more than 17 times, patient cells only reached a fivefold change. Regardless of cell line, both growth rates

were reduced upon riboflavin depletion. The patient cell line did not outreach a treble of the original amount (maximum 2,99 times higher). Moreover, repetitions of the experiment showed a toxic effect of the riboflavin depletion on both cell lines.

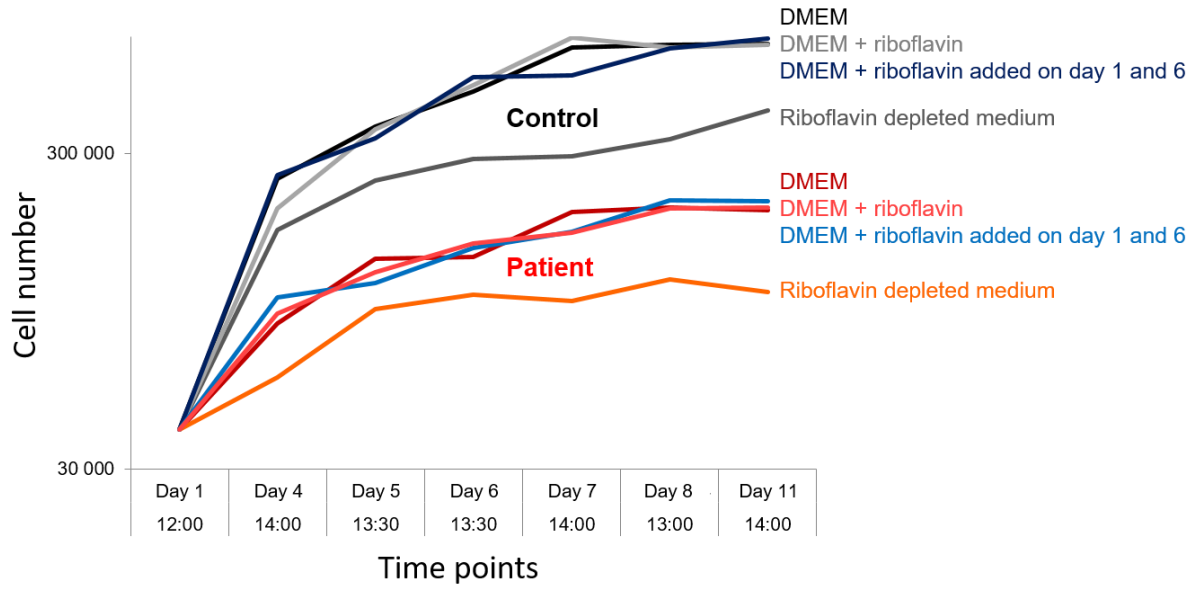

Figure 43: Fibroblasts growth curves. An 11-days growth experiment detected slower multiplication of the patient cell line. Supplementation of riboflavin did not alter the growth rate, in contrast with the riboflavin depletion. Cell amounts were detected for several following days at approximately same time.

5.2.4 HPLC quantification revealed a sufficient concentration of FAD in blood derived from both patients

To directly observe the results of FLAD1 enzymatic activity, FAD levels can be investigated in blood samples. Despite the observed loss-of-function mutation and a clear reduction of both FLAD1 protein and the cell viability, our collaborators in Salzburg (Dr. Lavinija Mataković and Dr. Johannes A. Mayr) were able to detect significant amounts of FAD compound in blood derived from both patients (Figure 44). Surprisingly, FAD levels of both sisters were similar to control levels in blood plasma or in enriched erythrocytes. The younger sister was supplemented with riboflavin (3 x 60 mg daily), seen as a peak in Figure 44A. The administration of riboflavin to the older sister was discontinued due to side effects.

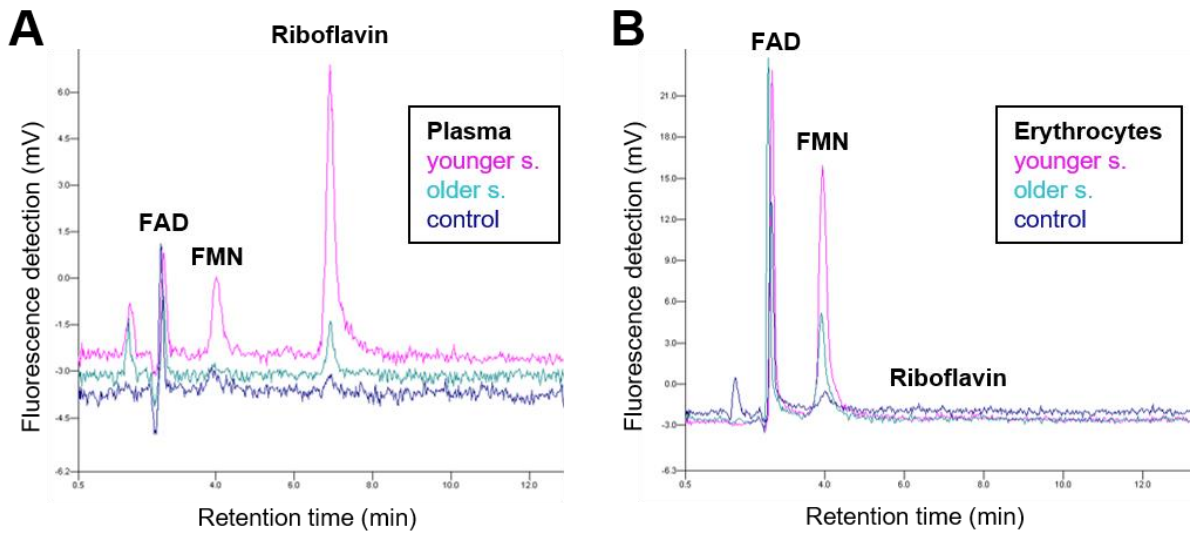

Figure 44: HPLC quantification of riboflavin, FMN and FAD in (A) blood plasma and (B) erythrocytes (modified from Olsen et al. 2016). Samples of EDTA blood were derived from a control, the younger sister under riboflavin treatment and the older sister.

5.2.5 A collaborative effort exposed genotypic and phenotypic similarities in families with defective FLAD1

Continuing investigation led us to start collaborations with medical centres located in Austria, Australia, Finland, France, Italy, and Turkey, and in the end, six other affected families were collected. All pedigrees and variants are depicted in Figure 45.

The collection of affected families allowed us to compare phenotypes and genotypes. Families carrying variants in the FAD synthase domain presented with milder phenotypes. Typically suffering from exercise intolerance and muscle weakness, mainly during physical activity and scoliosis. All were successfully supplemented with riboflavin that ameliorated the symptoms. They also reached adulthood and furthermore the patient from Family 2 went on to have healthy children (full report found in chapter 4.2). With regards to the genetics, the variant was either an in-frame deletion (Ser495del, Family 1), or a missense mutation (Arg530Cys, Family 2 and 3). Family 2 and 3 were, however, also carrying a frame-shift variant in exon 2. This is presumably compensated by the functioning protein with the missense mutation.

On the other hand, individuals from the four other families were severely affected. Most of the patients presented with multiorgan dysfunction, had an early age of onset, were hospitalized several times and were deceased in the early years of life (detailed case reports in chapter 4.2). The variants found in these families were all frameshift mutations located in exons 1 or 2, leading to a premature stop codon. The Turkish family, previously mentioned here in detail, is Family 4 (marked red).

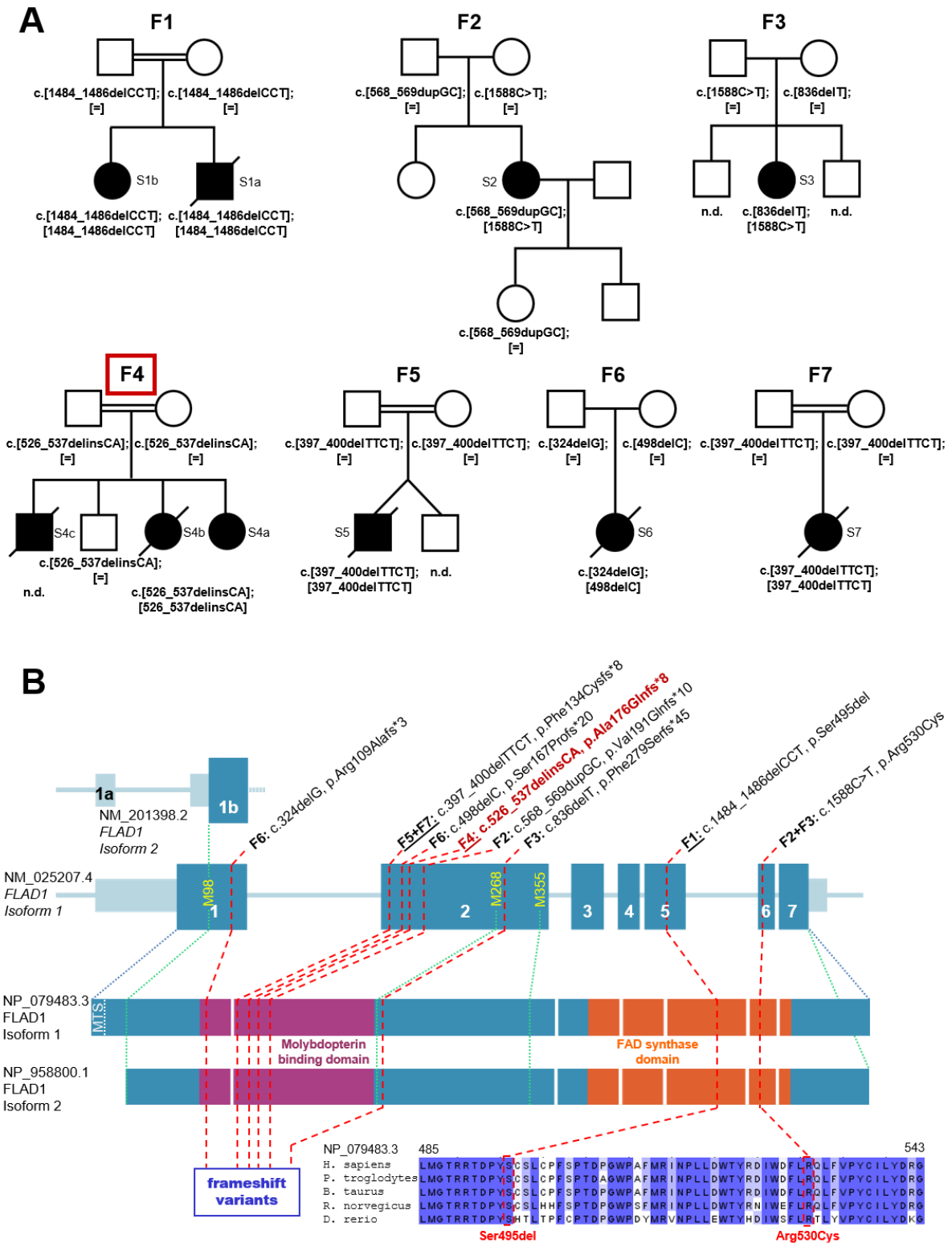

Figure 45: Pedigrees of investigated families and localization of studied variants (modified from Olsen et al. 2016). (A) Overall, seven unrelated families were collected. The investigation showed two groups of phenotypes – mildly (Families 1-3) and severely (Families 4-7) affected individuals. (B) Schematic interpretation of FLAD1 isoforms and localization of specific mutations, where homozygous variants are underlined. Variants affecting exons 1 and 2 cause

frameshift mutations resulting into premature stop codons. All of them are localized within or close to the molybdopterin binding domain in violet. Mutations affecting FAD synthase domain (in orange) are an in-frame deletion or a missense mutation, both in a highly conserved region among eukaryotic species. Methionine residues at positions M98, M268 and M355 are highlighted in yellow. In my functional studies, I mostly focused on family F4, marked red in both (A) and (B).

5.2.5.1 Newborn screening can give warning of patients with defective FLAD1

In addition to the various phenotypes, this group of patients revealed similarities in biochemical screenings, carried out as standard practice in many countries, such as during a newborn screening. In all eight patients, where data were available, increased plasma acylcarnitines were observed. Typically, octanoylcarnitine, decanoylcarnitine or tetradecanoylcarnitine were increased. Similarly, several organic acids in urine had elevated levels. For example, in six cases ethylmalonic acid was observed, adipic in three, often also suberic, dehydrosebacic, methylsuccinic, glutaric acids, hexanoylglycine, and lactate. These patterns usually indicate MADD or associated disorders. However, decreased activities of respiratory chain complexes in five cases and faint SDH and COX staining together in four suggested a mitochondrial defect. Additionally, lipid storage myopathy was found in six cases out of seven. Altogether, these combinations of biochemical findings can help to find the correct diagnosis and provide treatment in the future. The full collection of data is summarized in Table 2.

Table 2 was published in publication *Riboflavin-Responsive and -Non-responsive Mutations in FAD Synthase Cause Multiple Acyl-CoA Dehydrogenase and Combined Respiratory-Chain Deficiency* by Olsen RK, Koňaříková E *et alii* printed in American Journal of Human Genetics, 2016; doi: 10.1016/j.ajhg.2016.04.006.

ID Family	Sex/ Consang.	FLAD1 mutations cDNA (NM_025207.4) protein (NP_079483.3)	Affected domain	AoO	Status	Riboflavin responsive	Increased plasma acylcarnitines	Elevated organic acids in urine	Respiratory chain activities in muscle	Other mitochondrial enzymes	Muscle histology
S1a F1	♂/Yes	c.[1484_1486delCCT]; [1484_1486delCCT] p.[Ser495del];[Ser495del]	FADS	32 h	Dead 3 d	NA	C5, C8, C14, C5-DC, glutaryl carnitine	Ethylmalonic, adipic, suberic, dehydrosebacic, hexanoylglycine	normal	NA	Vacuoles in muscle fibres (EM not done)
S1b F1	♀/Yes	c.[1484_1486delCCT]; [1484_1486delCCT] p.[Ser495del];[Ser495del]	FADS	3 m	Alive 22 y	Yes	C4	Ethylmalonic and methylsuccinic acid	NA	NA	NA
S2 F2	♀/No	c.[568_569dupGC]; [1588C>T] p.[Val191Glnfs*10]; [Arg530Cys]	MPTb (fs), FADS	20 y	Alive 44 y	Yes	C8, C10, C10:1, C12:1, C16:1	Ethylmalonic and 2-hydroxyglutaric acid, lactate	CII↓, CIII↓, CIV↓	CS↑	Lipid storage myopathy; faint COX staining
S3 F3	♀/No	c.[836delT]; [1588C>T] p.[Phe279Serfs*45]; [Arg530Cys]	MPTb (fs), FADS	44 y	Alive 56 y	Yes	C5, C8, C10, C10:1, C14	Ethylmalonic acid and tiglylglycine	CI+III↓, CII+III↓ normal uder treatment	CS↑ ß-oxidation of C8 and C16	Lipid storage myopathy, muscle beta oxidation C4: 132%; C8: 15%; C16: 56%
S4a F4	♀/Yes	c.[526_537delinsCA]; [526_537delinsCA] p.[Ala176Glnfs*8]; [Ala176Glnfs*8]	MPTb (fs)	4 m	Alive 8 y	Yes	C4, C6, C8, C10, C14, C14:1, C14:2, C16:1, C18, C18:1, C18:2	Adipic, suberic, and ethylmalonic acid and methylsuccinate, ketosis	CI↓, CII↓	PDH↓	Lipid storage myopathy
S4b F4	♀/Yes	c.[526_537delinsCA]; [526_537delinsCA] p.[Ala176Glnfs*8]; [Ala176Glnfs*8]	MPTb (fs)	8 m	Dead 16 y	Discon-tinued (side efects)	Normal or C4-OH, C5, C6, C8, C10, C14:1, C16:1	NA	NA	NA	NA
S5 F5	♂/Yes	c.[397_400delTTCT]; [397_400delTTCT] p.[Phe134Cysfs*8]; [Phe134Cysfs*8]	MPTb (fs)	6 m	Dead 6 m	NA	C3, C5, C6, C8:1	Adipic acid	CI↓, CII+III↓	CS↑	Lipid storage myopathy, faint COX staining
S6 F6	♀/No	c.[324delG]; [498delC] p.[Arg109Alafs*3]; [Ser167Profs*20]	MPTb (fs)	birth	Dead 9 m	No	NA	NA	CI↓, CII+III↓	CS↑	Lipid storage myopathy; absent SDH staining; Several NADH and COX-negative fibers
S7 F7	♀/Yes	c.[397_400delTTCT]; [397_400delTTCT] p.[Phe134Cysfs*8]; [Phe134Cysfs*8]	MPTb (fs)	2 m	Dead 4 m	NA	C4, C6, C8, C10, C10:1, C12, C14:1, C16, C16:1, C18:1	Ethylmalonic and 2-hydroxyglutaric acid	NA	NA	Lipid storage myopathy, faint SDH staining, normal COX staining

Table 2: Genetic, clinical and biochemical findings in individuals with FLAD1 mutations (modified from Olsen et al. 2016).

Abbreviations for Table 2: ↓ - decrease; ↑ - increase; ♀ - female; ♂ - male; AoO - age of onset; C4 - butyrylcarnitine; C4-OH - OH-butyrylcarnitine; C5 - isovalerylcarnitine; C5-DC - glutarylcarnitine; C6 - hexanoylcarnitine; C8 - octanoylcarnitine; C10 - decanoylcarnitine; C10:1 - decenoylcarnitine; C12 - dodecanoylcarnitine; C14 - tetradecanoylcarnitine; C14:1 - tetradecenoylcarnitine; C14:2 - tetradecadienoylcarnitine; C16 - hexadecanoylcarnitine; C16:1 - hexadecenoylcarnitine; C18 - octadecanoylcarnitine; C18:1 - octadecenoylcarnitine; C18:2 - octadecdienoylcarnitine; CI–CIV, respiratory chain complexes I–IV; COX - cytochrome c oxidase; CS - citrate synthase; EM - electron microscopy; F - female; FADS - FAD synthase domain; fs - frameshift; h - hours; m - months; M - male; MPTb - molybdopterin binding domain; NA - not available; PDH - pyruvate dehydrogenase; SDH - succinate dehydrogenase; y -years

5.2.6 The particular variant types present with an unequal distribution along the gene

The unequal distribution of different types of variants, led me to further study this phenomenon. Six out of eight variants were located in exons 1 and 2 and all were predicted to cause a frameshift. The other two variants targeted the FAD synthase domain in exons 5 and 6 and only caused a minor change in the resulting protein, despite affecting a very conserved region. None of the predicted loss-of-function frameshift variants was present in our in-house database of about 7.000 distinct WES records and also not in more than 120.000 alleles in the Exome Aggregation Consortium (ExAC) server. Furthermore, no other predicted loss-of-function variant was found to be homozygous. At the date of the study, the c.1588C>T (p.Arg530Cys) variant was listed three times and the c.508T>C (p.Phe170Leu) variant was recorded twice in a heterozygote state in all 121.408 alleles studied by ExAC Browser.

To investigate the mutation load of FLAD1, I separated the FLAD1 gene in two parts. The first part covers exon 1 and 2 coding for the molybdopterin binding domain with a length of 1.117 bp. The second part covers exons 3 to 7 that code for the FAD synthase domain and consists of 647 bp. ExAC Browser registers an equal distribution of missense and synonymous variants among the first (0,178 variants/bp) and the second part of the gene (0,156 variants/bp). It also records 47 alleles with predicted loss-of-function variants affecting exon 1 or 2; however, only two loss-of-function variants were found to have an effect on exons 3 to 7. This examination revealed a significant accumulation of loss-of-function mutations in exon 2, respectively in the first part of the protein, which points to an evolutionary tendency to suppress loss-of-function mutations within the FAD synthase domain. My observation is consistent with the concept of independent function of the FAD synthase domain (Miccolis et al. 2012). The existence of a truncated protein would also explain the residual FAD production observed in the Turkish family. These speculations led to experiments expressing functional proteins translated by using the downstream ATGs, producing proteins starting at M98, M268 and M355.

5.2.7 Truncated FLAD1 isoforms are stably expressed

In order to verify the pathogenicity of identified variants in the *FLAD1* gene and to study possible truncated products, I performed rescue experiments. First of all, by using lentiviral transduction experiments, I expressed the wild type copy of the cytosolic *FLAD1* isoform in a patient (subject S4a) and a control cell line. Following this, as I suspected a potential role of truncated copies starting from ATGs before the FAD synthase domain, I expressed proteins starting from methionines at positions 298 and 355 (numbering according to the long mitochondrial isoform 1 of the FLAD1 protein, NP_079483.3). Directly before every construct I added an artificial Kozak sequence. The consensus 'CGCC' may however vary and the specific sequence before the first ATG only affects the strength of recognition and binding of the ribosome, indicating the translational start site. For this reason, I prepared a construct, supposed to produce a protein starting at M355 without artificial Kozak sequence, but with original wild type sequence right before the ATG (marked as M355org in Figure 46). This sequence 'CCCCTAC' is cytosine-rich, a nucleotide often found in the Kozak sequence.

Subsequently, I verified the expression of long (wt) and all shorter forms in cells by an immunoblot detection (Figure 46). The expression of shorter variants was performed only in the control cells (M268 even in two control cell lines) due to faster duplication and better fitness of such a cell line. All constructed proteins were stably produced. The M355org construct presented with a very faint signal when compared to constructs with the strongest known Kozak sequence. But when compared to the signal of wild type FLAD1 expression, which can be observed as a weak band at 54 kDa in all control samples on the left side of Figure 46, M355org appears to be produced at the same level or even more highly. Previously observed 'unspecific' bands are below the detection limit of this image. Appropriately, no FLAD1 signal was observed in the sample derived from patient cells.

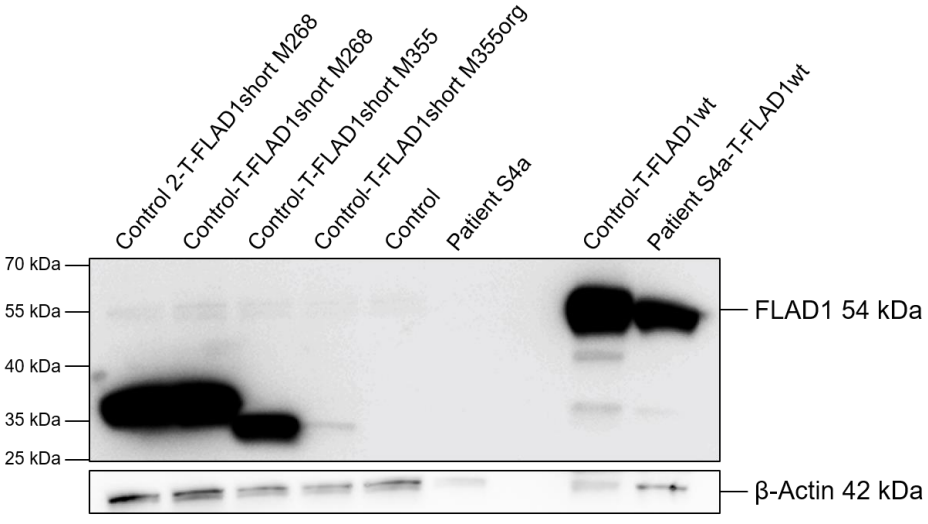

Figure 46: The expression of different FLAD1 isoform detected by immunoblotting. The constructs carrying different FLAD1 isoforms were cloned, transferred and expressed in control and patient fibroblasts. Protein isoforms starting at methionines M98 (wt), M268, M355 and M355org without an artificial Kozak sequence were all stably expressed and detected by anti-FLAD1 antibody. The wild type cytosolic variant presented with correct size of 54 kDa. The strong band on the right size of the picture corresponds to a weak band of a standard

expression in all control samples on the left. M268 construct has predicted size of 36 kDa and the M355 of 26 kDa. Anti-β-actin antibody was used as a loading marker.

5.2.8 A 26-kDa isoform was proved to contain FLAD1 specific peptides

In the course of the search for a truncated FLAD1 protein, our collaborators in Aarhus (Dr. Rikke K.J. Olsen, Signe Mosegaard and Prof. Dr. Niels Gregersen) carried out a mass spectrometry experiment. The gel bands marked with an asterisk in Figure 47A together with the FLAD1 band were analysed and compared to specific synthetic peptides coming from the FLAD1 sequence as schematically marked in Figure 47B. The presence of all peptides was confirmed in the FLAD1 band. On top of this, they detected peptides P3 and P4 in the ’26 kDa FLAD1’ band, which points to a truncated protein. However, peptide P5 was considered as a nonsignificant hint because it was identified at the detection border in all analysed gel bands.

On the right section of Figure 47A, the artificially expressed FLAD1 proteins starting at methionines M98, M268 and M355 run next to the control sample. The concentrations of these samples were reduced to obtain similar intensities of all bands, especially when compared to the control and patient samples. However, the truncated isoforms M268 and M355 did not correspond to any of the studied gel bands. Computer predictions estimated 35,92 kDa for the protein starting at M268 and 26,31 kDa for M355 one, respectively. The actual weight difference between the M268 or M355 protein and the ’26 kDa FLAD1’ lies most likely in a post-translational modification of the specific protein. Of note, as measured in Olsen et al. 2016, the expression of the M268 isoform resulted in an increase of FAD production.

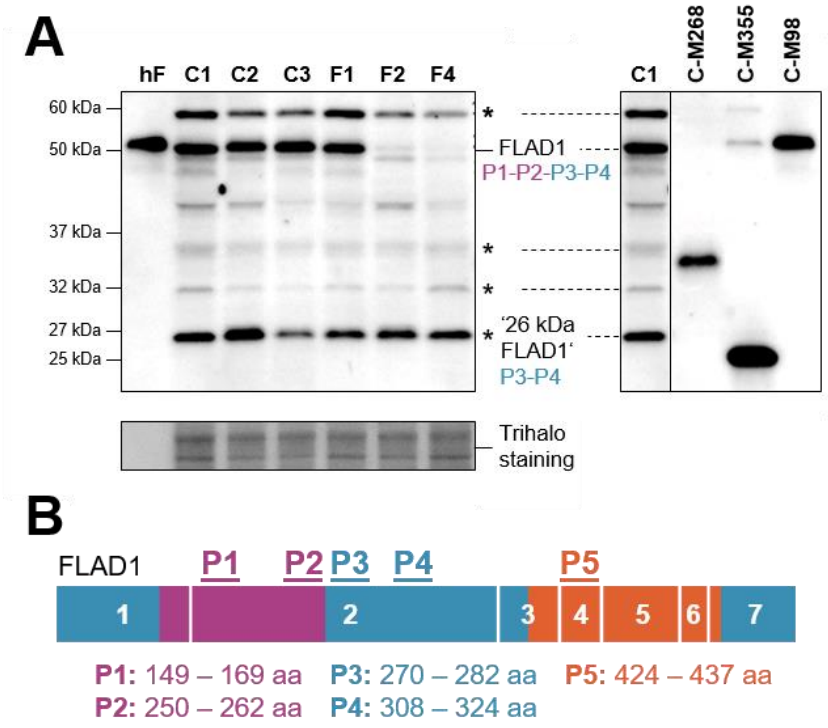

Figure 47: Immunoblot detection of FLAD1 protein and its truncated variants (modified from Olsen et al. 2016). (A) Control (C1-C3) and patient (from families F1, F2 and F4) samples were analyzed. In family F1, the in-frame deletion allows expression of FLAD1. Several bands

were detected with the anti-FLAD1 antibody. Band marked as FLAD1 corresponds to the cytosolic 54 kDa protein. It is of the same size as a wild type copy expressed as M98 protein or the purified human FLAD1 indicated by 'hF'. All labelled gel bands ('' plus 'FLAD1' band) were analyzed by mass spectrometry. (B) Schematic locatization of peptides (P1-P5) for comparison of specificity. Exons of FLAD1 described by numbers, molybdopterin binding domain in violet, FAD synthase domain in orange.*

5.2.9 Several alternative start codons can secure a functional FLAD1 isoform while avoiding the mutation hot-spot region

Since I was able to prepare artificial truncated FLAD1 proteins and the '26 kDa FLAD1' was confirmed by mass spectrometry, it was necessary to investigate *FLAD1* on the mRNA level. In accordance with the UCSC Genome Browser, NCBI Entrez Gene and UniProt, *FLAD1* produces several different isoforms by using alternative start codons (Fig. 21). Some of the transcripts, however, use an intronic ATG or even another open reading frame. Nevertheless, I searched for an in-frame isoform able to transcribe an intact FAD synthase domain.

For that reason, I analysed RNA sequencing data from controls to study *FLAD1* mRNAs represented as Sashimi plots (Figure 48 and 49). In brief, mRNA molecules are cut into short chains, sequenced and aligned back to the genome (represented as mRNA reads in the lower part of Figure 48). Due to mRNA properties, the intronic sequence is missing. The reads starting at one exon and continuing on the next exon are called 'split-reads'. They carry information about the continuity of exons. In the simplest case, the mRNA follows the 'text-book' splicing and the full mRNA results in: 'exon 1-exon 2-exon 3' (as in the upper part of Figure 48). However, several split-reads can skip one of the exons producing an alternatively spliced mRNA. In the end, the number of events is counted and reported in the resulting Sashimi plots. A simplified scheme is presented in Figure 48.

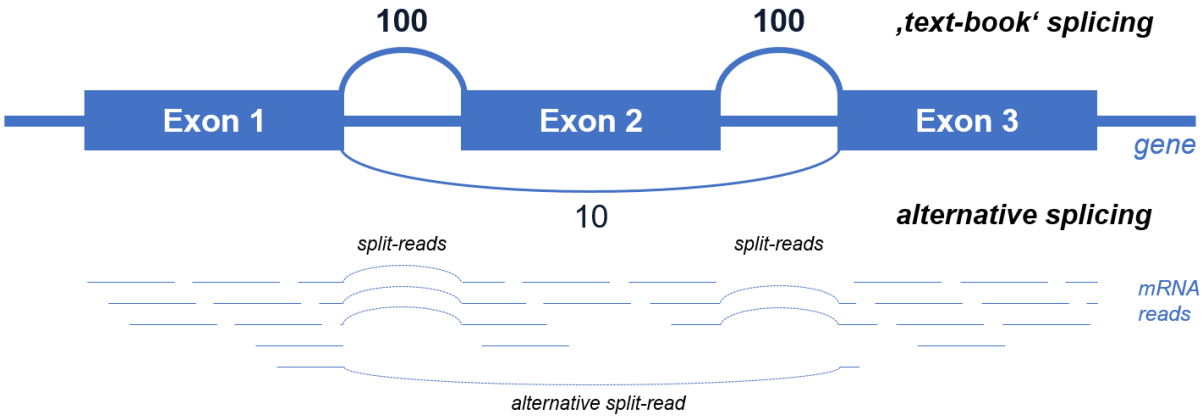

Figure 48: Schematic representation of Sashimi plots. Distinct mRNA parts are sequenced and aligned back to the reference genome. The split-reads that are skipping the intronic areas, represent the occurring splicing events (see the lower part). The number of such events is counted and displayed as shown in the upper part of the picture.

I was looking therefore, for a split-read among the *FLAD1* mRNAs, skipping the area harbouring all of the frameshift variants (exon 1 and 2) with the potential to produce an active protein. Interestingly, the majority of mRNAs resulted in a transcript coding for the cytosolic FLAD1 isoform (isoform 2; Fig. 21, 45 and 49). On the transcript level, isoform 2 contains a non-translated region of exon 1, labelled as '1a'. Typical example presents C1 control fibroblast cell line. However, many other possible transcripts were identified as well, as seen in Figure 49, including several novel *FLAD1* transcripts in control fibroblast and blood samples, confirming the expression of the truncated isoforms.

In control C2 fibroblasts I identified an isoform, named isoform 5, utilizing the '1a' part of exon 1. The split-reads are skipping exons 1b and 2 and continue directly on to exon 3. They represent about 2% of all the split-reads at a given location (marked red in the green sample in Fig. 49B). Since the first downstream in-frame ATG is located in exon 5 at position 460, deep in the FAD synthase domain, I suggested usage of an upstream start codon. In Figure 49A the resulting methionine residue is marked as M-X. I choose to label the methionine 'M-X' as it lies out-frame in respect to the isoform 1. More precisely, it lies 212,3 amino acids upstream of M1, which makes it 637 bases in total. The coding and protein sequences are displayed in Figure 49C, as based on the UCSC Genome Browser. The exon 1a produces 16 amino acids in-frame with exon 3. Importantly, no stop codon is located therein (Fig. 49C). Such a protein codes an intact FAD synthase domain starting within exon 3 and with an approximate predicted size of 26,11 kDa.

Next, similarly to isoform 5, in control C3 blood sample I identified isoform 6 that allows production of a truncated functional protein. About 10% of detected split-reads in control C3 connect exon 1a directly with exon 2 (marked red in the blue sample in Fig. 49B). In this case, I assume the utilization of downstream methionine M268. Starting at M268 or even M355 allows the production of an active FAD synthase domain. This transcript can also use the methionine M-X, however in such cases, translation is blocked in all of the frameshift mutations. Moreover, as tested *in vivo*, the sequence right before M355 can serve as the Kozak sequence and produces a stable protein. As reported above, this protein without posttranslational modification would have approximately 36 kDa (M268), or 26 kDa (M355) respectively.

As a result of these observations, together with Dr. Holger Prokisch we suggested the existence of two new isoforms 5 and 6. Isoforms 3 and 4 were already established in databases. Isoforms 3 and 4 as reported in UCSC Genome Browser, NCBI Entrez Gene and UniProt do not possess the FAD synthase domain and so I did not consider them as transcripts responsible for the functioning enzyme. Overall, the '26 kDa FLAD1' band is most likely based on isoform 5 and/or a proteolytically processed isoform 6. Nevertheless, exact identification requires further experiments.

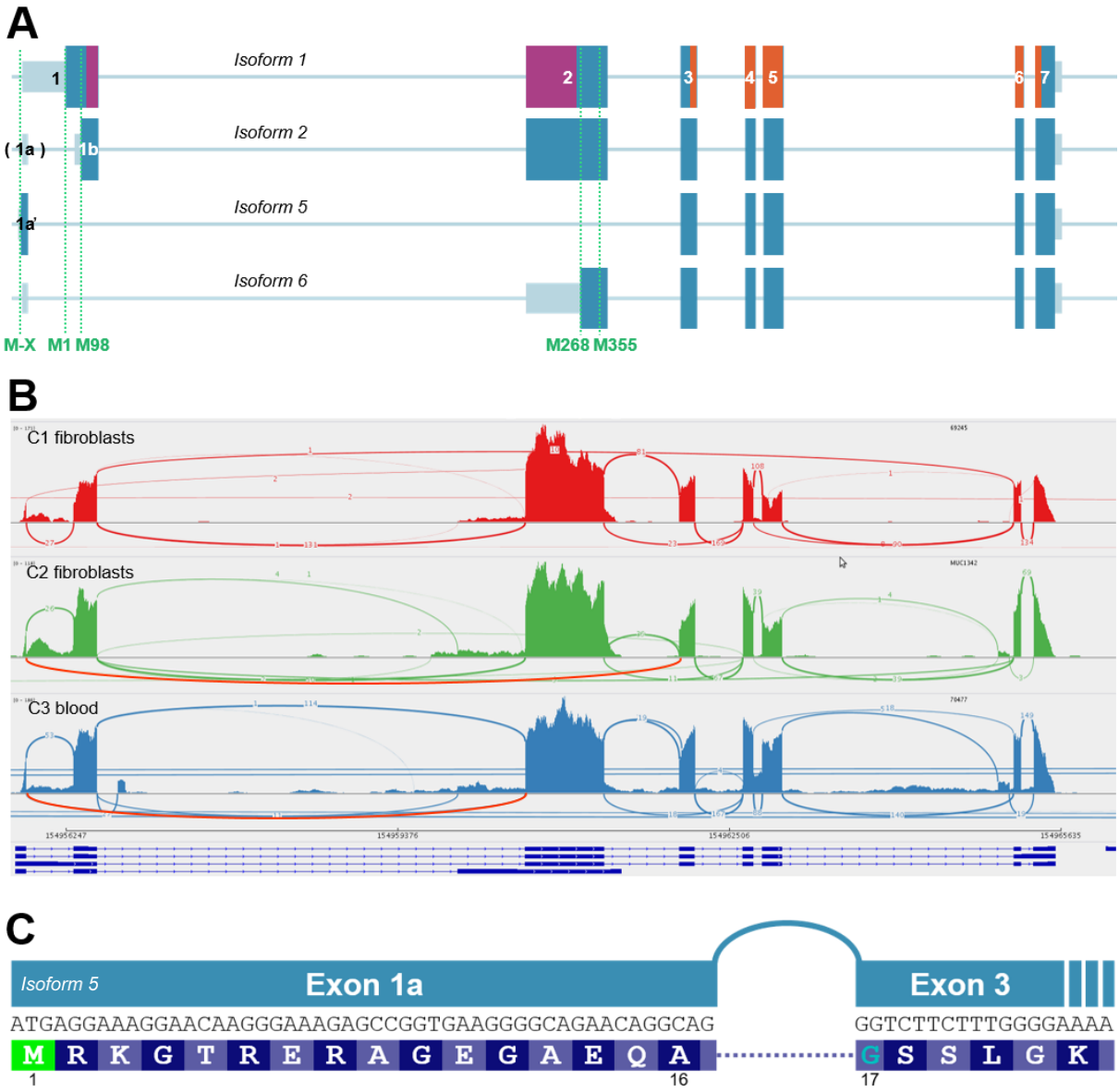

Figure 49: FLAD1 transcript isoforms and their predicted products (modified from Olsen et al. 2016). (A) Two known (1 and 2) and two newly predicted (5 and 6) isoforms of FLAD1 transcript. The numbers represent the FLAD1 exons, in violet is the molybdopterin binding domain, in orange the FAD synthase domain, in green positions of individual methionines. (B) RNA sequencing of FLAD1 depicted as Sashimi plots. RNA is cut into pieces and sequenced and each transcript is plotted. The height of the plot reflects the abundance of each sequence. Connecting lines represent split-reads, where one part of the RNA is in one exon and continues in the next exon. The exonic order is depicted in the lower part, also the Sashimi plots correspond to the schematic gene image in the upper (A) part. Two control fibroblast and one blood sample posses the evidence of alternative splicing occurring in FLAD1. (C) Beginning of the sequence of a suspected isoform 5. Protein starting at methionine M-X continues in-frame directly at exon 3 (based on UCSC Genome Browser).

5.2.10 Real time PCR confirms the presence of the newly identified isoform 6

To confirm the presence of the specific isoforms *in vivo*, our collaborators in Salzburg (Dr. Lavinija Mataković and Dr. Johannes A. Mayr) performed a quantitative real time PCR experiment. As seen in Figure 50A, primers were designed to cover the whole of *FLAD1*. qPCR analysis (Fig 50B) revealed stable FLAD1 transcription with reduction of about 50% when compared to the control sample. The RNA is therefore not degraded by a nonsense mediated decay. By using the same pairs of primers, the resulting qRT-PCR products were amplified, loaded on an agarose gel, separated and visualized. The highlighted primer pair 2 can amplify either the cytosolic isoform 2 with 307 bp, or the newly observed isoform 6 with 82 bp. Both the control and patient sample contained substantial amount of both isoforms *in vivo* (Fig. 50C, all details in Olsen et al. 2016).

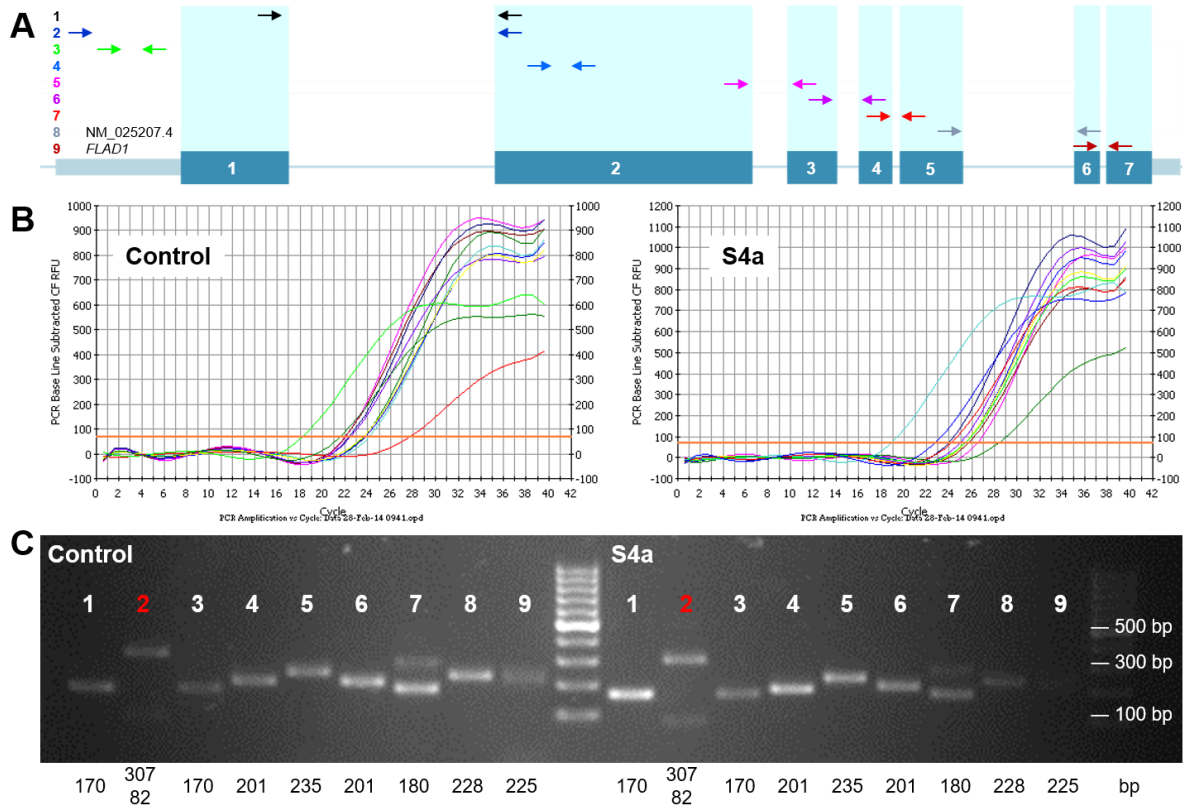

Figure 50: Quantitative real time PCR of FLAD1 (modified from Olsen et al. 2016). (A) Schematic visualization of primer pairs binding. All nine primer pairs cover the whole FLAD1. (B) qRT-PCR analysis revealed stable transcription in both samples. Patient RNA is reduced by about 50% when compared to the control sample and two housekeeping genes (RPL27 and HPRT). (C) qRT-PCR products visualized on an agarose gel. Primer pair 2 amplifies two distinct products, corresponding to isoforms 2 (307 bp) and 6 (82 bp). This experiment was conducted with a help of Dr. Lavinija Mataković and Dr. Johannes A. Mayr.

5.2.11 Patient RNA is sufficiently expressed, however does not reveal the exact mechanism of FAD production

Because Figure 49 only shows control samples, I was interested to see the result of RNA sequencing of the younger sister (S4a) from family F4. Furthermore, I intended to compare it to the qRT-PCR results from Salzburg (Fig. 50). In Figure 51 a Sashimi plot of RNA sequencing from the patient fibroblast cell line is shown. A black arrow marks a clear deletion, which was also seen in WES. As already seen by qRT-PCR, the RNA is stable, hence not completely degraded by a nonsense mediated decay. Therefore, the expression of FLAD1 protein is possible and most likely the '26 kDa FLAD1' is responsible for the residual activity. Unfortunately, I could not identify clear evidence for the existence of the truncated isoform 5 in the RNA sequencing from the patient. However, as reported above, the patient fibroblasts produce substantial amounts of FLAD1 isoforms 2 and 6.

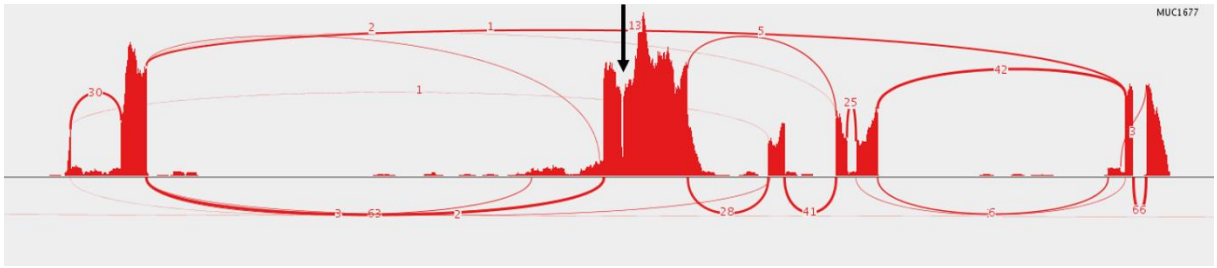

Figure 51: RNA sequencing of the fibroblast sample derived from the younger sister (S4a) from the Turkish family (Family 4). RNA was found stable, not degraded by a nonsense mediated decay. A clear homozygotic deletion c.[526_537delinsCA] is marked by a black arrow.

6 Discussion

6.1 Current shift in the diagnosis of mitochondrial disorders

Mitochondria are complex dynamic organelles whose maintenance requires collaboration of proteins encoded by two genomes. Disruptions in any of these proteins can have a direct effect on mitochondrial homeostasis and overall cellular maintenance. In this thesis, I focused on two crucial aspects of mitochondrial biology, ROS production and cofactor metabolism. Two genes from these two pathways have been for the first time diagnosed and validated as disease causing.

Methods for the diagnosis of mitochondrial disorders have undergone a tremendous shift in the recent years. Traditionally, mitochondrial disorders are defined by a malfunctioning OXPHOS and hence impaired energy production. They have therefore been conventionally diagnosed by analysis of enzymatic activies of respiratory chain complexes, characteristically in samples from muscle biopsy (Larsson and Oldfors 2001; DiMauro and Garone 2010). Additionaly, biomarkes such as lactate, amino and organic acids or carnitines have been usually analyzed in blood or urine samples (Stacpoole 1997; Barshop 2004; Jones et al. 2010; Shatla et al. 2014). However, mitochondrial disorders represent an extremely diverse group of inborn errors of metabolism presenting with clinical, biochemical, and genetic heterogeneity and can manifest at any age.

Since the implementation of Next generation sequencing techniques, such as whole exome sequencing in 2009 (Choi et al. 2009), diagnosis by a molecular-genetic approach is now preferred. This fundamental change in approach not only frees the patients from muscle biopsy testing unless absolutely necessary, but offers a diagnosis with much low invasivity. Consequently, genetic testing allows rapid initiation of a rational therapy and further also genetic counseling or prenatal testing (Wortmann et al. 2017). Whole exome sequencing has been demonstrated as an effective tool allowing diagnosis of about 50% of patients with suspected mitochondrial disorders. However, this means that half of the patients remains undiagnosed, leaving room for an improvement. WES-based analysis faces technical and analytical limitations. Some might be overcome by introduction of WGS, such as detection of indels and copy-number variations as well as the detection of non-coding variants. Given the reducing costs of NGS techniques, WGS will soon replace WES. However, the search deep within the non-coding regions will still remain challenging.

With the acceleration of the discovery of novel variants in known disease genes as well as potential new disease causing genes, comes the neccessity of comprehensive experimental validation (Haack et al. 2010; Wortmann et al. 2017). It is estimated that there are about 1.600 genes involved in the proper mitochondrial function (Lieber et al. 2013). Counting together both involved genomes, mutations in already 360 genes have been reported to date to cause a mitochondrial disease (Mayr et al. 2015; Rahman and Rahman 2018; Stenton and Prokisch 2018). There are therefore many potential novel disease gene discoveries awaiting validation.

The work presented here has made a small, but important contribution to the expansion of knowledge of disease assocciated genes.

6.2 Functional validation of novel mitochondrial disease genes

Functional validation of variants in novel disease genes represents the core of this thesis. Disruption in the ROS defence system caused by a variant in *TXN2* has been investigated. Likewise, mitochondrial biology strongly depends on cofactors; however, potential loss-of-function in *FLAD1* results in lack of FAD that affects about 100 enzymes. The consequences of *FLAD1* variants were studied in this work. *TXN2* was associated with a mitochondriopathy for the first time, *FLAD1* has already been reported as potentially pathogenic, however this report lacked validation of any kind (Taylor et al. 2014). WES analysis found clear hints in *TXN2* and *FLAD1*, which immediately delineated the investigation path corresponding to observed phenotypes.

6.2.1 ROS defence is a crucial mechanism, therefore any disruptions are improbable

Despite the knowledge of reactive oxygen species existence for about 60 years, their exact purpose has not yet been completely unravelled. Indeed, their increased levels harm proteins, lipids or nucleic acids. However, the potential importance of ROS lays in redox signalization as well as *e.g.* organismal protection via ROS production by NAPDH oxidases. The rapid and reversible or non-reversible changes of redox sensitive proteins contribute to spreading of oxidative stress signal. This results in enhanced transcription to fight additional ROS increase or even the preparation of cells for autophagy (Holzerova and Prokisch 2015). The remaining questions ask how we benefit from ROS and how can we influence their levels? Redox biology is a broad field awaiting further research.

Thioredoxin 2 is one of the key players in the reactive oxygen species defence. Its role is to restore PRDX3 or PRDX5 monomers that actively remove H_2O_2 from the mitochondrial environment. The ROS defence system consists of highly interconnected enzymatic activities (in detail in chapter 1.4). According to the study provided by Nonn *et alii*, it was considered that TXN2 function is crucial for organismal development and that absence of TXN2 was improbable. The $Txn2^{-/-}$ knockout mouse model was embryonic lethal. The embryos were found nonviable with an open anterior neural tube and eminently increased apoptosis at the tenth day post-coitus (Nonn et al. 2003). This is also the period of mitochondrial maturation (Shepard et al. 1998). Additionally, a huge difference between the outcomes of variants in *TXNRD2* vs. in *TXN2* was observed, pointing to a very thin line between variants in genes responsible for the same pathway. Malfunctioning TXNRD2 causes a mild phenotype (Prasad et al. 2014), while the TXN2 patient suffers from severe brain deterioration.

Yet, WES analysis at our institute found the very first patient carrying a homozygous loss-of-function variant in *TXN2*. The main observed phenotype was an early-onset neurodegeneration together with rapid progression of cerebellar atrophy and delayed myelination (detailed case report in chapter 4.1). Based on the high expression of TXN2 in the brain (Rybnikova et al.

2000), it seems that thioredoxin-based antioxidation is predominant therein. Moreover, brain tissue uses up about 20% of total basal oxygen to assure its activity (Cobley et al. 2018). Therefore, together with the faulty ROS defence system, the observed progressive neurodegeneration is probably caused by long-term ROS exposure.

Although, one may speculate, that men and mice differ in many biological aspects, rodents have been proposed as a suitable model to study brain development (Semple et al. 2013). In general, animal models are enormously useful in translational research, nevertheless no one should overestimate the outcomes.

6.2.2 Lack of TXN2 activity affects mitochondrial homeostasis

In the first step, I confirmed the variant by Sanger sequencing with both nonconsanguineous parents being heterozygotic carriers. The patient was the very first in our database to carry a bi-allelic variant. Likewise, no homozygous subject had been reported in public databases. The clear homozygotic variant in *TXN2* was – based on the database search – marked as likely pathogenic due to the production of a stop codon in the first translated exon of *TXN2*. Based on my search, no alternative truncated transcript has been observed. However, its product would lack enzymatic function, because the first possible in-frame transcription side lies downstream from the cysteine active side. This isolated information, however, does not prove the variant causality. Nevertheless, the resulting premature stop codon was reflected in the absence of protein as seen by an immunoblot analysis. The anti-TXN2 antibody covers 83% of amino acids, hence any truncated in-frame protein would be most likely detected.

TXN2 interferes with the respiratory chain complexes and affects overall mitochondrial bioenergetics. So far, all studies have described the connection between the thioredoxin system and OXPHOS rather vaguely. Inhibition of the thioredoxin system led to decreased oxygen consumption and ATP/ADP ratios (Lowes and Galley 2011); the thioredoxin system was shown to affect glucose homeostasis, and hence the energy production (Yoshioka and Lee 2014); and a connection between TXN2 and Complex II, fumarase and citrate lyase has been reported (Daloso et al. 2015). The case report in chapter 4.1 lists the reduced activities of respiratory chain Complexes I, III and V together with repeatedly increased blood lactate. Consequently, mitochondrial involvement was suspected. This observation was reproduced in fibroblasts by decreased basal and maximal oxygen consumption rate as well as decreased ATP production.

The exact interconnection between OXPHOS and ROS defence enzymes is however still not sufficiently understood. It was described that adequate ATP production, hence OXPHOS function, is important for correct anatomic development of the cerebellum during pregnancy (Baertling et al. 2016). Therefore, our experimental material provides a valuable resource for further investigations.

6.2.3 Expression of wild type **TXN2** *validates the causality of the gene and helps to find the treatment strategy*

Additional experimental validation was facilitated by the successful establishment of a patient cell line with a wild type copy of *TXN2*. The function of TXN2 can be vicariously assessed by immunoblot analysis of PRDX3 dimers. In the healthy environment the vast majority of PRDX3 dimers is reduced into monomers. However, in the patient's mitochondria I observed increased levels of dimers indicating TXN2 malfunction and hence reduced ROS defence capacity. More importantly, the reduction to monomers was re-established by the $TXN2^{wt}$. In line with this, the oxygen consumption rate, reflecting the OXPHOS function, was restored to control levels in the cells expressing $TXN2^{wt}$.

Significant results were also obtained by the drug sensitivity assay. Overall cell fitness was challenged by several mitochondrial inhibitors. In the diseased cell line, increased ROS (by inhibition of Complex I through rotenone) or inhibition of TXNRD2 (by auranofin), glutathione (by PAO) or GSR (by DNCB) caused lower survival rate when compared to the control cell line. These experiments confirmed the existence of crosstalk between ROS defence pathways by affecting the overall system. Most interestingly, the inhibition of TXNRD2 showed the interconnection of the reductase with the rest of the system, even though the connecting piece TXN2 is malfunctioning. Also, the additional interference by PAO and DNCB demonstrated the cell vulnerability. Accordingly, when the glutathione pathway was inhibited, the cells could not cope with such stress any further. The cell fitness was improved by $TXN2^{wt}$. Most outstandingly, the cell survival rate improved significantly with administering of Idebenone into the cell medium. Idebenone was subsequently suggested as a rational therapy for the patient.

6.2.4 A system with malfunctioning TXN2 presents a valuable experimental model of ROS defence pathways

Altogether, I was able to provide a variety of evidence to further confirm the underlying cause of the suspected mitochondrial disorder. Above that, I was provided by a unique experimental material of malfunctioning ROS defence system. Based on the interplay between glutathione and thioredoxin pathways (Zhang et al. 2007; Hanschmann et al. 2010), I expected increased levels of cellular glutathione. However, this was not proven. To further address this question, it would be necessary to distinguish between mitochondrial and cytosolic glutathione. And particularly in isolated mitochondria in order to separate the oxidized and reduced glutathione pool and/or to determine the GSH:GSSG ratio. This ratio when measured in blood serum was proven to be a valuable biomarker of oxidative stress (Zitka et al. 2012). Interestingly, analysis of conditionally *Txn2* deficient chicken β-cells, revealed decreased total and mitochondrial GSH levels, but increased ROS production (Tanaka et al. 2002b).

The analysis of PRDX3 dimers, indeed, confirmed the insufficient and subsequently restored enzymatic activity of TXN2. Immunoblot detection after the H_2O_2 incubation, however, did not reveal any influence of the additional treatment. This is most likely due to the experimental set up. Western blot samples were prepared through a denaturation step as for any other sample for

SDS electrophoresis. It is probable that the cells contain even higher concentrations or exclusively the PRDX3 dimers and their reduction is only an artefact of sample preparation. Here, further experimental evidence, including *e.g.* non-reducing conditions, would be necessary.

Inactivation of further enzymes of the ROS defence system in this natural experimental model, could provide a deeper insight into the interconnections between both pathways. I assumed that the non-lethal loss-of-TXN2 function was due to this high linkage. In particular, the reduction of PRDX3 dimers is probably preserved by the action of TXNRD2 or GLRX2, or by the molecule of NADPH (Conrad et al. 2004; Zhang et al. 2007). Therefore, switching off additional players *e.g.* by gene-editing techniques, could unravel novel connections or redundancies of the ROS defence pathways.

6.2.5 Further experimental potential lays in a study of the affected tissue as well as in investigations of any future patient

The additional experimental evidence of the whole system could be carried out by studying the most affected tissue, hence the brain. TXN2 is highly expressed in the brain, which also points to the importance of ROS scavenging therein (Rybnikova et al. 2000). However, obtaining neuronal cells from our living patient is not possible due to obvious reasons. Nevertheless, it is well established that patient-derived primary human skin fibroblasts represent valid model system for studying mitochondrial (patho)physiology and they are ideally suited for a broad range of live cell assays (*e.g.* mitochondrial morphology, ROS, calcium/ATP handling, etc.; summarized in *e.g.* Koopman et al. 2012). Therefore, I tried to establish an efficient knock-down model in SH-SY5Y neuroblastoma cell line (Berger et al. 2004). Unfortunately, I was not able to obtain an effective knock-down.

The main limitation of this project is coming from a single-patient based observations, as collection of multiple cases provides further evidence for pathogenicity. The crucial validation of the variant causality was however carried out by expression of the wild type gene in the patient cell line and subsequent restoration of all measured values. This is, in general, a recommended standard approach in cases of rare diseases (Gorman et al. 2016).

6.2.6 FAD cofactor affects the stability and activity of about 100 enzymes, hence lack of FAD is highly unexpected

In higher organisms, riboflavin (vitamin B2) must be obtained from the diet (Kaiser et al. 2002). Its conversion products FMN and FAD present cofactors of more than a hundred of proteins forming various enzymatic pathways of the complex cellular metabolism. FAD is found in about 84% of all flavoproteins (Lienhart et al. 2013). It was shown, that a number of flavoproteins undergo a fast degradation under depletion of riboflavin or flavin cofactors (Wu et al. 1995; Efimov et al. 1998; Solovieva et al. 2003; Henriques et al. 2010).

Riboflavin avitaminosis or inefficient turnover of riboflavin, FMN and FAD, is potentially harmful for a number of enzymes and subsequently the cellular homeostasis. Hence, the correct

function of riboflavin kinase and FAD synthase, an enzyme coded by *FLAD1*, is crucial for cell maintenance. I was among the first to identify a potential loss-of-function variant in the gene coding for this key protein. The first identification of a variant in *FLAD1* as potentially disease causing in patients from Vienna (Family 4) came shortly before the publication from Dr. Robert Taylor and his colleagues (Taylor et al. 2014). However, it took us some time to collect additional patients and most importantly to provide enough experimental validation. The patient presented in publication from Dr. Taylor is the same person as patient from Family 5 presented in this thesis (Taylor et al. 2014; Olsen et al. 2016).

The insertion deletion variant found in *FLAD1* at our institute was predicted to cause a frameshift resulting in a premature stop codon. Based on the essence of FAD necessity, the observed loss-of-function variant was highly unexpected. The variant manifested as a reduction of FLAD1 protein detected by immunoblotting, where the cytosolic protein was absent in contrast to the control sample. The antibody repeatedly showed several additional bands of different sizes, both in patient and control samples. Unfortunately, this result could not be confronted by another antibody, since it gave a very unspecific signal. I could not detect a clear signal of the mitochondrial isoforms from either of the samples. This might be, however, fibroblast specific. The whole matter of several FLAD1 isoforms requires extensive further research involving different tissue samples, especially the affected muscle tissue.

6.2.7 Cells with affected FAD production are highly sensitive towards lack of riboflavin; however, FAD production was confirmed in patient blood samples

Cell fitness was analysed by a growth curve experiment. The patient cells showed a slower multiplication rate in comparison to the control cell line. I may hypothesize that the patient cells are adapted to a slower growth condition. To properly address this question, a broad range of controls would be necessary. The control cell line I used tends towards rapid and extensive growth. It covers the surface as prolongated cells closely attached to one another. The patient cell line also covered the whole surface; however, lower cell numbers were detected. This may be due to a different inner morphology, for example various mitochondrial structures have been observed upon different (patho)physiological conditions (Yoon et al. 2011; Galloway et al. 2012; Picard et al. 2013). The main purpose was to observe the result of riboflavin supplementation and depletion. While addition of riboflavin, even repeatedly, did not alter the growth rate, most likely due to the saturation of the presumed riboflavin conversion pathway; the depletion essentially halted cell growth. This shows the crucial role of riboflavin for cellular maintenance.

Despite clear genetic variant and immunoblot observations, the HPLC detection of riboflavin and its conversion products revealed high levels of all compounds. With my collaborators in Salzburg Dr. Lavinija Mataković and Dr. Johannes A. Mayr, I observed a sufficient concentration of FAD in blood plasma or in enriched erythrocytes derived from two of the patients. This result shows existence of the FAD synthase enzymatic activity. Also, the FMN peak was not significantly increased, which would point to a reduction in FAD synthase

activity. The height of the FMN peak only reflected the administration of riboflavin to the patient.

6.2.8 Fusion of FLAD1 domains was repeated during evolution

The riboflavin conversion to FAD is in prokaryotes catalyzed by a bifunctional protein (Herguedas et al. 2010; Abbas and Sibirny 2011). However, in higher mammals such as humans, rats or mice, the FAD synthase domain is fused to MPTb. *Drosophila melanogaster*, *Caenorhabditis elegans* or *Saccharomyces cerevisiae* for example, do not possess the N-terminal part, only the FAD synthase domain (Krupa et al. 2003). Similarly, plant flavin adenine dinucleotide synthetases in chloroplasts contain highly conserved N-terminal FAD synthase domain. Though the C-termini of these enzymes among plant species differ, they still contain a putative catalytic activity distinct from the prokaryotes. According to Yruela *et alii*, this function is either FMN hydrolase or FAD pyrophosphatase or the plant C-terminus has a nonenzymatic regulatory role or is an evolutionary relic (Sandoval et al. 2008; Yruela et al. 2010). Altogether, fusion of the FAD synthase domain to another is not essential, yet it developed simultaneously more times in evolution with not exactly known function.

In general, eukaryotic FADS are unrelated to prokaryotic ones (Brizio et al. 2006; Huerta et al. 2009; Torchetti et al. 2010) and if fused to another domain, these domains presumably present a regulatory element (Giancaspero *et al.*, 2015). Overall gene and protein fusion is a major contributor to protein evolution, it expands the functional repertoire of an organism and contributes to increase complexity (Koonin et al. 2002; Bornberg-Bauer et al. 2005; Pasek et al. 2006).

6.2.9 The mutation load acknowledges the role of both FLAD1 domains

As I was unable to find any alternative human riboflavin conversion pathway in the literature, I started to further study *FLAD1*. The mRNA consists of seven exons and the resulting protein has two distinct domains. Specifically, the first two exons code for molybdopterin binding domain, exons 3 to 7 code for the FAD synthase domain. Previous observations confirmed that the isolated human FAD synthase domain can sufficiently synthesize FAD by itself (Miccolis et al. 2012). The role of MPTb is in stabilizing the enzyme and it potentially has FAD hydrolase activity (Giancaspero et al. 2015) or is needed for optimal FAD transfer into apoproteins (Torchetti et al. 2011). According to the sequence, expression of the fully active FAD synthase domain is possible with in-frame start codons at protein positions M98 (also the start of the cytosolic protein), M268 and M355.

During the course of this project, additional patients with variants in *FLAD1* have been identified. The collaborative effort collected seven families with ten affected individuals in total. I noticed a broad range of phenotypes, from exercise intolerance and muscle weakness to multiorgan lapse resulting in death in early years of life. The phenotypic spectrum was reflected by the type of the mutation and its position. While the mildly affected patients carried an in-frame deletion (Family 1) or a missense mutation (Family 2 and 3) in the FAD synthase domain;

the severely affected patients with an early-onset all carried frameshift mutations (Families 4 to 7) located in the exons 1 or 2, leading to a premature stop codon.

The projection of observed variants on the gene structure, unravelled a significant accumulation of frameshift variants in the exon 1 or 2, hence in the MPTb domain. The other observed variants were located in exons 5 and 6 in the FAD synthase domain and caused only minor changes in the resulting protein. It is an in-frame deletion of 3 bases, hence serine 495 and a missense mutation changing arginine 530 to cysteine, an amino acid with a shorter side chain. The database search showed accumulation of loss-of-function variants in the exon 1 and 2 in respect to the rest of the gene (47 vs 2). This is underlining an evolutionary suppression of the loss-of-function variants in the FAD synthase domain.

6.2.10 Residual production of FAD led to the identification of novel isoforms and final explanation of the observed phenotype

Based on the observed variant distribution and enzymatic independency of the FAD synthase domain (Miccolis et al. 2012), I expressed functional proteins translated by using the downstream ATGs, producing proteins starting at M98, M268 and M355. Mainly the M268 and the M355 truncated isoforms can overgo the frameshift variants and produce the fully active FAD synthase domain. All of the isoforms were stably expressed and detected by anti-FLAD1 antibody. This included the M355org isoform, before which I did not add a Kozak sequence that is typically attached to ensure the expression.

The further study of additional bands observed by immunoblotting confirmed presence of a truncated ’26 kDa FLAD1’ isoform containing an intact FAD synthase domain. This isoform was present in all available samples – both in controls and patients. However, the 26 kDa protein does not exactly correspond to shortened versions starting at M268 – 36 kDa and M355 – 26 kDa, even though the predicted sizes are similar. Consequently, I searched for a possible explanation on the RNA level. Newly identified isoforms 5 and 6 would allow expression of proteins that would skip the ‘frameshift area’. Nevertheless, both isoforms lack the MPTb domain, the activity of which is significant for proper function.

In addition to the already predicted M268 and M355 (coming from isoform 6) proteins, a new M-X was found, also resulting in a functional protein of predicted 26 kDa (from isoform 5). Hence, the ’26 kDa FLAD1’ is most likely post-translationally modified (*e.g.* phosphorylation or glycosylation) and/or a proteolytically processed result of alternative isoforms 5, 6 or others not yet identified. Importantly, all truncated proteins did not contain the mitochondrial targeting sequence. This presumably alters the FMN/FAD pool within the cellular environment, specifically in mitochondria, where most of the flavoenzymes are localized. Mitochondria would therefore be dependent on cytosolic FAD production.

The finding of additional isoforms was experimentally validated by PCR experiments confirming the presence of RNA isoform 6 *in vivo* in the control as well as in the patient cell line. Further analysis of RNA sequencing of the patient, however, did not bring any new observation. Interestingly, in this case, the RNA sequencing alone would probably not find the

right gene as the transcript in the patient was not significantly degraded. Therefore, combination of approaches and a proper validation is essential. This result demands further comparison to control samples as well as RNA sequencing of additional tissues, to bring tissue-specific expression of isoforms to light.

My findings were followed by the expression of truncated isoform 6 in a bacterial model (Leone et al. 2018). Leone *et alii* demonstrated that this isoform was sufficiently synthesizing FAD. With respect to the full-length protein, the enzymatic activity of the truncated enzyme was decreased to about 70%. The authors however speculate about the cytosolic localization of such a protein and the import of FAD into mitochondria via a recently identified transporter (Schiff et al., 2016). The relevance lays in the lack of FAD production in mitochondria, a place, where many flavoproteins are localized (Lienhart et al. 2013). Leone and co-workers marked the truncated FLAD1 as an *'emergency protein'*, because its existence, though in small quantity, allowed the survival of patients carrying variants in *FLAD1*. This isoform could even find its usability in gene therapy.

6.2.11 Information burden of public databases

In the course of identification and validation of novel disease genes, databases provide a great amount of information. Publicly available resources prove themself important when no other information is available, especially for the identification of genes not previously associated with a disease. The description of enzymatic function is valuable in the first explanation of genotype-phenotype correlation. However, ongoing research may change predicted data. This has been exemplified by a proteomic based study in which a patient with a variant in *NDUFA4* reassigned this protein as a subunit of Complex IV rather than Complex I (Balsa et al. 2012).

Typically, I was searching for pathogenic variants and additional known transcripts, as well as functional domains of proteins or their structure. As an example, in my work the resulting protein of *FLAD1* is responsible for FAD production, however the observed variant according to my first prediction did not allow enzymatic function. In the case of *FLAD1*, information of possible transcripts reported in databases was insufficient, insomuch as the critical transcript was not annotated. One must keep in mind that loss-of-function variants sometimes affect only specific transcripts of an essential gene. The experiments proved on both the RNA and protein level that a not yet described transcript is responsible for a truncated functional protein. Hence, not all loss-of-function variants lead to a degradation of the transcript by nonsense mediated decay deeming translation of the proteins impossible. My observations were submitted for addition into ClinVar database to make them available for further research.

Additionally, as *TXN2* and *FLAD1* are now established as 'known' disease genes, my observations enriched the Online Mendelian Inheritance in Man database. *TXN2* is now connected to OMIM number #616811, meaning *'Combined oxidative phosphorylation deficiency 29'*. However, due to the limitation of a single-patient based observation, OMIM marked this relationship between the phenotype and gene as provisional and will change it only after publication of reports describing additional patients (Joanna Amberger from OMIM, personal communication). In the case of *FLAD1*, the first note in OMIM was already made after

the first mentioning in the literature (Taylor et al. 2014). However, this publication only mentioned the possible pathogenicity and very briefly described the patient. Only the contribution of my work and experimental validation of my collaborators connected *FLAD1* to #255100: *'Lipid storage myopathy due to flavin adenine dinucleotide synthetase deficiency'* without any doubts.

In general, it is important to support the expansion of public databases and datasets. We consider that mitochondrial disorders affect at least 20 individuals per 100.000 people (Gorman et al. 2016). However, with about 83 million inhabitants in Germany and only about 1.500 patients listed in any mitochondrial registry (mostly in mitoNET - German Network for Mitochondrial Disorders, Dr. Holger Prokisch, personal communication), there is still quite a space for improvement. A collaborative effort proved itself important in the case of explanation of *FLAD1* variants. The collection of several families guided me towards the comprehensive analysis of a mutational hot-spot.

6.2.12 All predicted loss-of-function variant must be carefully inspected

The observation of predicted loss-of-function mutations in an essential gene turned into a completely new approach of isoform validation. One must keep in mind that predicted loss-of-function variants sometimes affect only specific isoforms of an essential gene. In general, loss-of-function variants are seen in the context of severe Mendelian disease. Yet, recent large-scale genotyping projects have revealed a large number of such variants in the genomes of healthy individuals. On average, approximately 100 loss-of-function variants per genome were found, including about 30 homozygotic variants (MacArthur and Tyler-Smith 2010; Auton et al. 2015).

The introduction of loss-of-function variants is one of the evolutionary tools. Interestingly, it has proven to be beneficial in several examples. Such as a single nucleotide polymorphism in *CASP12,* increasing survival rate due to the decreased chance of sepsis (Saleh et al. 2004). Or a nonsense variant in *ACTN3* is connected to improved human muscle performance in non-African populations (MacArthur et al. 2007; MacArthur and North 2007). And lastly, a variant in *UGT2B17* causes a complete absence of its transcript. Resulting protein is metabolizing steroid hormones (*e.g.* testosterone) and a vast number of xenobiotics; however, this enzyme tends to be removed in Asian population (Xue et al. 2008).

Such observations are in line with the 'less is more' hypothesis, highlighting evolutionary advantages of transcript reduction (Olson 1999). Maynard V. Olson claims that: "*If, as I suggest, less is often more, where gene function is concerned, adaptive loss of function may occur frequently and may spread rapidly through small populations*." Altogether, next to genetic polymorphisms or sequencing and annotation errors, loss-of-function mutations can be valuable (MacArthur and Tyler-Smith, 2010).

6.3 Unravelling of a rational therapy for both novel mitochondrial disease genes

One of the aims of this thesis was to suggest a rational treatment based on experimental observations and enzymatic functions. The discovery of a molecular defect was crucial to indicate the specific treatment options. The search for a rational therapy in the presented cases expands the utility of this work for future patients carrying the same or similar variant in presented genes.

After publication of both projects, these diagnoses were subsequently marked as '*treatable mitochondrial diseases'*. It was highlighted that the clinical symptoms may be mitigated by a simple action such as antioxidant and vitamin intake. Therefore, the recognition of the target patients, especially when clinically ill, must be accelerated to its maximum to avoid any delay in initiation of treatment (Davison and Rahman 2017; Distelmaier et al. 2017; Udhayabanu et al. 2017).

6.3.1 Functional validation helped to provide a cure to the patient with defective ROS defence

The biggest achievement in the project dealing with defective ROS defence, lays in the genetic identification of disease cause after 15 years from its first evidence. For the patient with variant in *TXN2* an antioxidant supplementation was tested and introduced with beneficial outcome. Daily intake of Idebenone led to improvements in physical capability, slowed down possible further damage due to the course of the disease and generally improved the quality of life of the whole family without reported side effects.

Any other patient with a defective TXN2 or even ROS defence in general might therefore benefit from immediate antioxidant therapy. Distelmaier *et alii* observed that (dys)regulation of reactive oxygen species has critical consequences on mitochondrial function and that oxidative stress may impair the OXPHOS (Distelmaier et al. 2012). The early implementation of antioxidant therapy could decelerate disease progression and minimalize brain damage, mainly cerebellar atrophy and global brain atrophy.

However, no additional patient carrying a variant in *TXN2* has been found, pointing to the developmental importance of such a gene. My study suggests a critical role for thioredoxin 2 in the human neurodevelopment and neuronal maintenance and reactive oxygen species homeostasis, similarly to the one seen in $Txn2^{-/-}$ mouse model (Nonn et al. 2003). The importance of a functional thioredoxin pathway for cerebellar development is as well supported by a mouse model with nervous system-specific deletion of Txnrd1. These mice were significantly smaller and developed a tremor and ataxia together with cerebellar hypoplasia (Soerensen et al. 2008). Potential treatment could therefore include gene therapy in the neuronal tissue, when diagnosed early.

In general, single-patient based observations complicate the feasibility and confidence of clinical trials. Randomized double-blind studies are impossible in these cases (Misra 2012). Nevertheless, based on my results, various authors speculate the possible involvement of

defective TXN2 in many common diseases, such as neurodegeneration with brain iron accumulation (Tello et al. 2018), epilepsy (Kudin et al. 2017) and Alzheimer's disease (Stachowicz et al. 2017). Therefore, early recognition of the disease cause and therapy initiation could mitigate possible detrimental outcomes.

6.3.2 Riboflavin supplementation mitigated possible adverse outcomes in the following cases

Genotype-phenotype correlation was validated in patients with variants in *FLAD1*. Nevertheless, the phenotypic spectrum varied from severe respiratory chain complex disorders to milder multiple acyl-CoA dehydrogenation deficiencies. MADD caused by variants in *FLAD1* is a potentially treatable inborn error of metabolism. Importantly for patients, a clear pattern of abnormality for the disease was observed in standardly assessed newborn screening, namely increased blood acylcarnitines and elevated organic acids. This can in future identify FLAD1 deficiency in the very early days of life and subsequently help to start rational riboflavin supplementation, which was in our hands beneficial in five out of six cases.

No human disorder was directly linked to malfunctioning FLAD1 prior to this project. Likewise, variants in *FLAD1* had not been previously associated with MADD or respiratory chain complex deficiencies. Both were historically connected to a particular flavoprotein (*e.g.* ETF and ETFDH in case of MADD or FMN in Complex I), but not to the synthesis of FAD itself (Olsen et al. 2007). Similarly, the only animal model of FAD synthase deficiency was established in *Caenorhabditis elegans*. Due to the obvious difference between neuronal systems of worms vs. human, silencing of FAD synthase in higher animals would possess new insights into the complexity of flavoproteins. For example, FAD shortage could unravel the hierarchy of preferred pathways. Also, based on our observation, expression of truncated FLAD1 variants in animal models on a FLAD1-null background could help to measure the specific enzyme activities. Or to further investigate the exact function of MPTb domain.

The successful implementation of riboflavin treatment was later followed up by several studies. First of all, Dr. Mari Auranen and coauthors described a significant benefit from long-term riboflavin therapy. For one additional year, they studied the riboflavin effect in the patient from Family 2 carrying compound heterozygous variants in *FLAD1* described here. In this case, disease symptoms ameliorated and the patient did not observe any progression of the disease. This was confirmed also by the normal excretion of metabolites in urine and decreased lipid-storage myopathy (Auranen et al. 2017).

Most importantly, my results led to identification of the causal gene in an additional four patients. First of all, a 7-years-old girl presenting with a similar pattern of urine metabolites and acylcarnitines, carrying two novel loss-of-function mutations in *FLAD1*. One of them in MPTb and the other possibly creating aberrant splicing within FAD synthase domain. Most likely due to the secondly mentioned variant, this patient did not respond to riboflavin, even at higher doses (Garcia-Villoria et al. 2018). Significantly, in two reports the clinicians investigated patients with MADD, with sequencing of *ETFA*, *ETFB* and *ETFDH* not revealing any causal

variant. These genes are more often MADD-associated and correlation with FLAD1 seems rather rare.

The authors in both cases confirm that only after the publication Olsen et alii 2016 they successfully found variants in *FLAD1* (Yildiz et al. 2018; Ryder et al. 2019). Yildiz *et alii* analysed, post-mortem, two siblings carrying compound heterozygous variants and described the same loss-of-function variants as we observed in Families 5 and 7 (Yildiz et al. 2018). Dr. Ryder and her co-workers found a novel riboflavin-responsive variant in *FLAD1* in an 8-years-old boy. This was an additional homozygous loss-of-function variant resulting in stop codon in exon 2. The authors claim that early riboflavin therapy mitigated otherwise severe symptoms (Ryder et al. 2019)

6.3.3 Early implementation of riboflavin therapy is highly recommended

Riboflavin therapy is, in general, beneficial and without side effects. Its surplus is naturally removed from the body; hence no artificial deposits are created. Riboflavin was marked as generally safe for children and adults by the Food and Drug Administration (Electronic Code of Federal Regulations 2018). In six out of already eight cases riboflavin therapy was favorable; however, in one of our patients carrying a loss-of-function mutation in *FLAD1* riboflavin intake was terminated due to side effects.

Taken altogether, it is recommended to sequence *FLAD1* in all cases of MADD as well as to start riboflavin supplementation pre-emptively in case the *FLAD1* variant is confirmed (Olsen et al. 2016; Auranen et al. 2017; Garcia-Villoria et al. 2018; Yildiz et al. 2018; Ryder et al. 2019). Beneficially for any future patient, a clear pattern of the disease can be observed in standardly assessed newborn screening as increased blood acylcarnitines and elevated organic acids. Such accessible biomarkers are rare in mitochondriopathies and therefore treatment may be implemented in the very early days of life. It has even been suggested to initiate the riboflavin treatment while awaiting final diagnostic confirmation (Davison and Rahman 2017).

6.4 Future outlook

Overall, validation of a novel gene for a suspected mitochondrial disease might be delicate. This study highlights the necessity of a broad biochemical procedure in a single-case project. As well as the value of reproduction of the findings in additional independent cases presenting with analogous genotype-phenotype evidence. Both projects have broadened the spectrum of mitochondrial disease genes. Moreover, the published data have already been reflected in almost 70 following publications.

6.4.1 Towards the omics era and personalized medicine

The era of Next generation sequencing continuously brings molecular diagnosis to patients. In combination with the clinical presentation of the patients, this allows for a better estimation of genotype-phenotype correlation. RNA sequencing in combination with quantitative proteomics

and quantitative metabolomics are on the way to accelerate the diagnostic process, initiating the multi-omics era.

During the course of my work, I was also involved in a project aiming to identify novel causal variants by using combination of complementary approaches: RNA sequencing, proteomics and metabolomics (Kremer et al. 2017). The publication by Dr. Laura Kremer *et alii* laid the foundation of RNA sequencing analysis as an alternative approach which provided molecular diagnose for patients with inconclusive WES. Likewise, they used proteomic and metabolomic profiling in order to provide a diagnosis. This new combination of techniques improves the interpretation of variants of unknown significance identified by genotyping. In my thesis, RNA sequencing and proteomic experiments helped to explain the genotypic-phenotypic observations in patients with variants in *FLAD1*.

In general, the omics techniques are widely spread, aiming to fully describe all biological processes and to produce surge of complex data on various levels by combination of high-throughput analytical approaches for every single individual. At the same time, bioinformatic tools need to be improved and accelerated to combine data and obtain results within a relevant time frame. The synthesis of such data will lead towards a personalized medicine in the future. This concept was first proposed in 1990s during the course of the human genome project. As close association between individual genetic features and clinical manifestations has been observed and described for the first time. They brought the basics of studying single nucleotide polymorphisms among individuals (Giacomini et al. 2007). Personalized medicine is, however, the future of medical approach, aiming to provide individually optimized treatment avoiding poor efficacy or serious side effects.

6.4.2 Further development of treatment strategies

The potential for future development lays also in discovery of new therapeutic options. The phenotypic and genotypic range of mitochondrial disorders complicates therapeutic approaches. Evidently, the final decision for a specific treatment must reflect the cause of the disease. Principally, rare mitochondrial disorders demand 'rare' treatment tactics, hence personalized medicine. Luckily, drug development is a rapidly evolving field (*e.g.* KH176; de Haas et al. 2017; Koene et al. 2017). It is unlikely that there will be a drug to address the treatment of a broad range of mitochondrial disorders. Yet, the principles or disease outcomes (such as decelerated glucosis, increased ROS production, lack of a specific vitamin/cofactor) may be similar, revealing potential selective therapeutic directions as well.

Together with novel approaches including gene therapy (Bacman et al. 2013; Gammage et al. 2014; Gammage et al. 2018) or mitochondrial donation (Lightowlers et al. 2015; Gorman et al. 2016), a definitive cure is becoming available for increasing number of patients (Rai et al. 2018). It is therefore important to recognize patients that could profit from any supplementation, such as vitamins or antioxidants, as early as possible, in order to maximize treatment benefits (Distelmaier et al. 2017).

7 References

Abbas, C.A. and Sibirny, A.A. 2011. Genetic control of biosynthesis and transport of riboflavin and flavin nucleotides and construction of robust biotechnological producers. *Microbiology and molecular biology reviews : MMBR* 75(2), pp. 321–360. doi: 10.1128/MMBR.00030-10.

Acosta, M.J. et al. 2016. Coenzyme Q biosynthesis in health and disease. *Biochimica et biophysica acta* 1857(8), pp. 1079–1085. doi: 10.1016/j.bbabio.2016.03.036.

Afink, G. et al. 2008. Molecular characterization of iodotyrosine dehalogenase deficiency in patients with hypothyroidism. *The Journal of clinical endocrinology and metabolism* 93(12), pp. 4894–4901. doi: 10.1210/jc.2008-0865.

Agrimi, G. et al. 2012. The human gene SLC25A17 encodes a peroxisomal transporter of coenzyme A, FAD and NAD+. *The Biochemical journal* 443(1), pp. 241–247. doi: 10.1042/BJ20111420.

Ahola-Erkkila, S. et al. 2010. Ketogenic diet slows down mitochondrial myopathy progression in mice. *Human molecular genetics* 19(10), pp. 1974–1984. doi: 10.1093/hmg/ddq076.

Alberts, B. et al. 1994. *Molecular Biology of the Cell*. New York: Garland Publishing Inc.

Allen, J. and Bradley, R.D. 2011. Effects of oral glutathione supplementation on systemic oxidative stress biomarkers in human volunteers. *Journal of alternative and complementary medicine (New York, N.Y.)* 17(9), pp. 827–833. doi: 10.1089/acm.2010.0716.

Anand, G. et al. 2012. Early use of high-dose riboflavin in a case of Brown-Vialetto-Van Laere syndrome. *Developmental medicine and child neurology* 54(2), pp. 187–189. doi: 10.1111/j.1469-8749.2011.04142.x.

Aon, M.A. et al. 2012. Glutathione/thioredoxin systems modulate mitochondrial H2O2 emission: an experimental-computational study. *The Journal of general physiology* 139(6), pp. 479–491. doi: 10.1085/jgp.201210772.

Arner, E.S. and Holmgren, A. 2000. Physiological functions of thioredoxin and thioredoxin reductase. *European journal of biochemistry* 267(20), pp. 6102–6109.

Ault, J.G. and Lawrence, D.A. 2003. Glutathione distribution in normal and oxidatively stressed cells. *Experimental cell research* 285(1), pp. 9–14.

Auranen, M. et al. 2017. Patient with multiple acyl-CoA dehydrogenation deficiency disease and FLAD1 mutations benefits from riboflavin therapy. *Neuromuscular disorders : NMD* 27(6), pp. 581–584. doi: 10.1016/j.nmd.2017.03.003.

Auton, A. et al. 2015. A global reference for human genetic variation. *Nature* 526(7571), pp. 68–74. doi: 10.1038/nature15393.

Awad, A.M. et al. 2018. Coenzyme Q10 deficiencies: pathways in yeast and humans. *Essays in biochemistry* 62(3), pp. 361–376. doi: 10.1042/EBC20170106.

Bacman, S.R. et al. 2013. Specific elimination of mutant mitochondrial genomes in patient-derived cells by mitoTALENs. *Nature medicine* 19(9), pp. 1111–1113. doi:

10.1038/nm.3261.

Bae, Y.S. et al. 1997. Epidermal growth factor (EGF)-induced generation of hydrogen peroxide. Role in EGF receptor-mediated tyrosine phosphorylation. *The Journal of biological chemistry* 272(1), pp. 217–221.

Baertling, F. et al. 2014. A guide to diagnosis and treatment of Leigh syndrome. *Journal of neurology, neurosurgery, and psychiatry* 85(3), pp. 257–265. doi: 10.1136/jnnp-2012-304426.

Baertling, F. et al. 2016. The many faces of paediatric mitochondrial disease on neuroimaging. *Child's nervous system : ChNS : official journal of the International Society for Pediatric Neurosurgery* 32(11), pp. 2077–2083. doi: 10.1007/s00381-016-3190-3.

Bailey, H.H. 1998. L-S,R-buthionine sulfoximine: historical development and clinical issues. *Chemico-biological interactions* 111–112, pp. 239–254.

Baker, M. 2012. Gene-editing nucleases. *Nature methods* 9(1), pp. 23–26.

Balsa, E. et al. 2012. NDUFA4 is a subunit of complex IV of the mammalian electron transport chain. *Cell metabolism* 16(3), pp. 378–386. doi: 10.1016/j.cmet.2012.07.015.

Barile, M. et al. 1997. Flavin adenine dinucleotide and flavin mononucleotide metabolism in rat liver--the occurrence of FAD pyrophosphatase and FMN phosphohydrolase in isolated mitochondria. *European journal of biochemistry* 249(3), pp. 777–785.

Barile, M. et al. 2000. The riboflavin/FAD cycle in rat liver mitochondria. *European journal of biochemistry* 267(15), pp. 4888–4900.

Barile, M. et al. 2013. Biosynthesis of flavin cofactors in man: implications in health and disease. *Current pharmaceutical design* 19(14), pp. 2649–2675.

Barkovich, A.J. et al. 1993. Mitochondrial disorders: analysis of their clinical and imaging characteristics. *AJNR. American journal of neuroradiology* 14(5), pp. 1119–1137.

Barshop, B.A. 2004. Metabolomic approaches to mitochondrial disease: correlation of urine organic acids. *Mitochondrion* 4(5–6), pp. 521–527. doi: 10.1016/j.mito.2004.07.010.

Berger, A. et al. 2004. Galanin receptor subtype GalR2 mediates apoptosis in SH-SY5Y neuroblastoma cells. *Endocrinology* 145(2), pp. 500–507. doi: 10.1210/en.2003-0649.

Bernhard, G.C. 1982. Auranofin therapy in rheumatoid arthritis. *The Journal of laboratory and clinical medicine* 100(2), pp. 167–177.

Bernsen, P.L. et al. 1993. Treatment of complex I deficiency with riboflavin. *Journal of the neurological sciences* 118(2), pp. 181–187.

Bianchi, M.C. et al. 2003. Proton MR spectroscopy of mitochondrial diseases: analysis of brain metabolic abnormalities and their possible diagnostic relevance. *AJNR. American journal of neuroradiology* 24(10), pp. 1958–1966.

Bieri, J.G. 1974. Fat-soluble vitamins in the eighth revision of the recommended dietary allowances. *Journal of the American Dietetic Association* 64(2), pp. 171–174.

Biesecker, L.G. and Green, R.C. 2014. Diagnostic clinical genome and exome sequencing. *The New England journal of medicine* 370(25), pp. 2418–2425. doi: 10.1056/NEJMra1312543.

Bigarella, C.L. et al. 2014. Stem cells and the impact of ROS signaling. *Development* 141(22):4206-4218. doi:10.1242/dev.107086

Billington, R.A. et al. 2006. Emerging functions of extracellular pyridine nucleotides. *Molecular medicine (Cambridge, Mass.)* 12(11–12), pp. 324–327. doi: 10.2119/2006-00075.Billington.

Bornberg-Bauer, E. et al. 2005. The evolution of domain arrangements in proteins and interaction networks. *Cellular and molecular life sciences : CMLS* 62(4), pp. 435–445. doi: 10.1007/s00018-004-4416-1.

Bosch, A.M. et al. 2011. Brown-Vialetto-Van Laere and Fazio Londe syndrome is associated with a riboflavin transporter defect mimicking mild MADD: a new inborn error of metabolism with potential treatment. *Journal of inherited metabolic disease* 34(1), pp. 159–164. doi: 10.1007/s10545-010-9242-z.

Bosch, A.M. et al. 2012. The Brown-Vialetto-Van Laere and Fazio Londe syndrome revisited: natural history, genetics, treatment and future perspectives. *Orphanet journal of rare diseases* 7, p. 83. doi: 10.1186/1750-1172-7-83.

Boveris, A. et al. 1976. Role of ubiquinone in the mitochondrial generation of hydrogen peroxide. *The Biochemical journal* 156(2), pp. 435–444.

Brand, M.D. and Nicholls, D.G. 2011. Assessing mitochondrial dysfunction in cells. *The Biochemical journal* 435(2), pp. 297–312. doi: 10.1042/BJ20110162.

Bratic, A. and Larsson, N.-G. 2013. The role of mitochondria in aging. *The Journal of clinical investigation* 123(3), pp. 951–957. doi: 10.1172/JCI64125.

Brigelius-Flohe, R. and Traber, M.G. 1999. Vitamin E: function and metabolism. *FASEB journal : official publication of the Federation of American Societies for Experimental Biology* 13(10), pp. 1145–1155.

Brizio, C. et al. 2006. Over-expression in Escherichia coli and characterization of two recombinant isoforms of human FAD synthetase. *Biochemical and biophysical research communications* 344(3), pp. 1008–1016. doi: 10.1016/j.bbrc.2006.04.003.

Bugiani, M. et al. 2006. Effects of riboflavin in children with complex II deficiency. *Brain & development* 28(9), pp. 576–581. doi: 10.1016/j.braindev.2006.04.001.

Bustamante, C.D. et al. 2005. Natural selection on protein-coding genes in the human genome. *Nature* 437(7062), pp. 1153–1157. doi: 10.1038/nature04240.

Buyse, G. et al. 2003. Idebenone treatment in Friedreich's ataxia: neurological, cardiac, and biochemical monitoring. *Neurology* 60(10), pp. 1679–1681.

Caboni, P. et al. 2004. Rotenone, deguelin, their metabolites, and the rat model of Parkinson's disease. *Chemical research in toxicology* 17(11), pp. 1540–1548. doi: 10.1021/tx049867r.

Calvo, S.E. et al. 2012. Molecular diagnosis of infantile mitochondrial disease with targeted next-generation sequencing. *Science translational medicine* 4(118), p. 118ra10. doi: 10.1126/scitranslmed.3003310.

Calvo, S.E. et al. 2016. MitoCarta2.0: an updated inventory of mammalian mitochondrial proteins. *Nucleic acids research* 44(D1), pp. D1251-7. doi: 10.1093/nar/gkv1003.

Carroll, C.J. et al. 2014. Next-generation sequencing for mitochondrial disorders. *British*

journal of pharmacology 171(8), pp. 1837–1853. doi: 10.1111/bph.12469.

Casagrande, S. et al. 2002. Glutathionylation of human thioredoxin: a possible crosstalk between the glutathione and thioredoxin systems. *Proceedings of the National Academy of Sciences of the United States of America* 99(15), pp. 9745–9749. doi: 10.1073/pnas.152168599.

Chacinska, A. et al. 2009. Importing mitochondrial proteins: machineries and mechanisms. *Cell* 138(4), pp. 628–644. doi: 10.1016/j.cell.2009.08.005.

Chen, Q. and Cederbaum, A.I. 1998. Cytotoxicity and apoptosis produced by cytochrome P450 2E1 in Hep G2 cells. *Molecular pharmacology* 53(4), pp. 638–648.

Chen, X. et al. 2014. Novel action and mechanism of auranofin in inhibition of vascular endothelial growth factor receptor-3-dependent lymphangiogenesis. *Anti-cancer agents in medicinal chemistry* 14(7), pp. 946–954.

Chen, Y. et al. 2002. Overexpressed human mitochondrial thioredoxin confers resistance to oxidant-induced apoptosis in human osteosarcoma cells. *The Journal of biological chemistry* 277(36), pp. 33242–33248. doi: 10.1074/jbc.M202026200.

Chinnery, P.F. and Turnbull, D.M. 2001. Epidemiology and treatment of mitochondrial disorders. *American journal of medical genetics* 106(1), pp. 94–101. doi: 10.1002/ajmg.1426.

Chiong, M.A. et al. 2007. Transient multiple acyl-CoA dehydrogenation deficiency in a newborn female caused by maternal riboflavin deficiency. *Molecular genetics and metabolism* 92(1–2), pp. 109–114. doi: 10.1016/j.ymgme.2007.06.017.

Choi, J.R. et al. 2018. Serum Fibroblast Growth Factor 21 and New-Onset Metabolic Syndrome: KoGES-ARIRANG Study. *Yonsei medical journal* 59(2), pp. 287–293. doi: 10.3349/ymj.2018.59.2.287.

Choi, M. et al. 2009. Genetic diagnosis by whole exome capture and massively parallel DNA sequencing. *Proceedings of the National Academy of Sciences of the United States of America* 106(45), pp. 19096–19101. doi: 10.1073/pnas.0910672106.

Chomyn, A. et al. 2000. The mitochondrial myopathy, encephalopathy, lactic acidosis, and stroke-like episode syndrome-associated human mitochondrial tRNALeu(UUR) mutation causes aminoacylation deficiency and concomitant reduced association of mRNA with ribosomes. *The Journal of biological chemistry* 275(25), pp. 19198–19209. doi: 10.1074/jbc.M908734199.

Chouchani, E.T. et al. 2014. Complex I deficiency due to selective loss of Ndufs4 in the mouse heart results in severe hypertrophic cardiomyopathy. *PloS one* 9(4), p. e94157. doi: 10.1371/journal.pone.0094157.

Chow, S.L. et al. 2005. The significance of elevated CSF lactate. *Archives of disease in childhood* 90(11), pp. 1188–1189. doi: 10.1136/adc.2005.075317.

Cimino, J.A. et al. 1987. Riboflavin metabolism in the hypothyroid human adult. *Proceedings of the Society for Experimental Biology and Medicine. Society for Experimental Biology and Medicine (New York, N.Y.)* 184(2), pp. 151–153.

Cobley, J.N. et al. 2018. 13 reasons why the brain is susceptible to oxidative stress. *Redox biology* 15, pp. 490–503. doi: 10.1016/j.redox.2018.01.008.

De Colibus, L. and Mattevi, A. 2006. New frontiers in structural flavoenzymology. *Current*

opinion in structural biology 16(6), pp. 722–728. doi: 10.1016/j.sbi.2006.10.003.

Conrad, M. et al. 2004. Essential role for mitochondrial thioredoxin reductase in hematopoiesis, heart development, and heart function. *Molecular and cellular biology* 24(21), pp. 9414–9423. doi: 10.1128/MCB.24.21.9414-9423.2004.

Cooper, G.M. and Shendure, J. 2011. Needles in stacks of needles: finding disease-causal variants in a wealth of genomic data. *Nature reviews. Genetics* 12(9), pp. 628–640. doi: 10.1038/nrg3046.

Cornelius, N. et al. 2014. Cellular consequences of oxidative stress in riboflavin responsive multiple acyl-CoA dehydrogenation deficiency patient fibroblasts. *Human molecular genetics* 23(16), pp. 4285–4301. doi: 10.1093/hmg/ddu146.

Cos, P. et al. 2003. Comparative study of eight well-known polyphenolic antioxidants. *The Journal of pharmacy and pharmacology* 55(9), pp. 1291–1297. doi: 10.1211/0022357021693.

Daloso, D.M. et al. 2015. Thioredoxin, a master regulator of the tricarboxylic acid cycle in plant mitochondria. *Proceedings of the National Academy of Sciences of the United States of America* 112(11), pp. E1392-400. doi: 10.1073/pnas.1424840112.

Dalton, T.P. et al. 2000. Knockout of the mouse glutamate cysteine ligase catalytic subunit (Gclc) gene: embryonic lethal when homozygous, and proposed model for moderate glutathione deficiency when heterozygous. *Biochemical and biophysical research communications* 279(2), pp. 324–329. doi: 10.1006/bbrc.2000.3930.

Damdimopoulos, A.E. et al. 2002. Human mitochondrial thioredoxin. Involvement in mitochondrial membrane potential and cell death. *The Journal of biological chemistry* 277(36), pp. 33249–33257. doi: 10.1074/jbc.M203036200.

Danhauser, K. et al. 2011. Cellular rescue-assay aids verification of causative DNA-variants in mitochondrial complex I deficiency. *Molecular genetics and metabolism* 103(2), pp. 161–166. doi: 10.1016/j.ymgme.2011.03.004.

DaRe, J.T. et al. 2013. Targeted exome sequencing for mitochondrial disorders reveals high genetic heterogeneity. *BMC medical genetics* 14, p. 118. doi: 10.1186/1471-2350-14-118.

Davison, J.E. and Rahman, S. 2017. Recognition, investigation and management of mitochondrial disease. *Archives of disease in childhood* 102(11), pp. 1082–1090. doi: 10.1136/archdischild-2016-311370.

Debray, F.-G. et al. 2007. Diagnostic accuracy of blood lactate-to-pyruvate molar ratio in the differential diagnosis of congenital lactic acidosis. *Clinical chemistry* 53(5), pp. 916–921. doi: 10.1373/clinchem.2006.081166.

Denu, J.M. and Tanner, K.G. 1998. Specific and reversible inactivation of protein tyrosine phosphatases by hydrogen peroxide: evidence for a sulfenic acid intermediate and implications for redox regulation. *Biochemistry* 37(16), pp. 5633–5642. doi: 10.1021/bi973035t.

Depeint, F. et al. 2006. Mitochondrial function and toxicity: role of B vitamins on the one-carbon transfer pathways. *Chemico-biological interactions* 163(1–2), pp. 113–132. doi: 10.1016/j.cbi.2006.05.010.

Dewey, F.E. et al. 2014. Clinical interpretation and implications of whole-genome sequencing. *JAMA* 311(10), pp. 1035–1045. doi: 10.1001/jama.2014.1717.

Diaz, Z. et al. 2007. Trolox enhances the anti-lymphoma effects of arsenic trioxide, while protecting against liver toxicity. *Leukemia* 21(10), pp. 2117–2127. doi: 10.1038/sj.leu.2404891.

van Dijk, E.L. et al. 2018. The Third Revolution in Sequencing Technology. *Trends in genetics : TIG* . doi: 10.1016/j.tig.2018.05.008.

DiMauro, S. and Garone, C. 2010. Historical perspective on mitochondrial medicine. *Developmental disabilities research reviews* 16(2), pp. 106–113. doi: 10.1002/ddrr.102.

Dimitriadis, K. et al. 2014. Leber's hereditary optic neuropathy with late disease onset: clinical and molecular characteristics of 20 patients. *Orphanet journal of rare diseases* 9, p. 158. doi: 10.1186/s13023-014-0158-9.

Dinopoulos, A. et al. 2005. Brain MRI and proton MRS findings in infants and children with respiratory chain defects. *Neuropediatrics* 36(5), pp. 290–301. doi: 10.1055/s-2005-872807.

Dipti, S. et al. 2005. Brown-Vialetto-Van Laere syndrome; variability in age at onset and disease progression highlighting the phenotypic overlap with Fazio-Londe disease. *Brain & development* 27(6), pp. 443–446. doi: 10.1016/j.braindev.2004.10.003.

Distelmaier, F. et al. 2012. Trolox-sensitive reactive oxygen species regulate mitochondrial morphology, oxidative phosphorylation and cytosolic calcium handling in healthy cells. *Antioxidants & redox signaling* 17(12), pp. 1657–1669. doi: 10.1089/ars.2011.4294.

Distelmaier, F. et al. 2017. Treatable mitochondrial diseases: cofactor metabolism and beyond. *Brain : a journal of neurology* 140(Pt 2), p. e11. doi: 10.1093/brain/aww303.

Divry, P. et al. 1983. Dicarboxylic aciduria due to medium chain acyl CoA dehydrogenase defect. A cause of hypoglycemia in childhood. *Acta paediatrica Scandinavica* 72(6), pp. 943–949.

Drahota, Z. et al. 2002. Glycerophosphate-dependent hydrogen peroxide production by brown adipose tissue mitochondria and its activation by ferricyanide. *Journal of bioenergetics and biomembranes* 34(2), pp. 105–113.

Efimov, I. et al. 1998. Proposed steady-state kinetic mechanism for Corynebacterium ammoniagenes FAD synthetase produced by Escherichia coli. *Biochemistry* 37(27), pp. 9716–9723. doi: 10.1021/bi972817j.

Electronic Code of Federal Regulations 2018. Title 21. Part 182 – Substances Generally Recognized As Safe. Available at: https://www.ecfr.gov/cgi-bin/text-idx?SID=fd7384292a759d3d286c4bdf1a53ea91&mc=true&node=se21.1.73_1450&rgn=div8 [Accessed: 10 January 2019].

Enns, G.M. 2014. Treatment of mitochondrial disorders: antioxidants and beyond. *Journal of child neurology* 29(9), pp. 1235–1240. doi: 10.1177/0883073814538509.

Enns, G.M. and Cowan, T.M. 2017. Glutathione as a Redox Biomarker in Mitochondrial Disease-Implications for Therapy. *Journal of clinical medicine* 6(5). doi: 10.3390/jcm6050050.

Ernster, L. et al. 1959. Enzymic activities of human skeletal muscle mitochondria: a tool in clinical metabolic research. *Nature* 184, pp. 1851–1854.

Esterhazy, D. et al. 2008. Production of reactive oxygen species by complex I (NADH:ubiquinone oxidoreductase) from Escherichia coli and comparison to the enzyme

from mitochondria. *Biochemistry* 47(12), pp. 3964–3971. doi: 10.1021/bi702243b.

European Medicines Agency 2008. *CHMP ASSESSMENT REPORT FOR Sovrima*. London. Available at: http://www.ema.europa.eu/docs/en_GB/document_library/EPAR_-_Public_assessment_report/human/000908/WC500070576.pdf.

Falk, M.J. et al. 2012. Mitochondrial disease genetic diagnostics: optimized whole-exome analysis for all MitoCarta nuclear genes and the mitochondrial genome. *Discovery medicine* 14(79), pp. 389–399.

Fassone, E. et al. 2010. FOXRED1, encoding an FAD-dependent oxidoreductase complex-I-specific molecular chaperone, is mutated in infantile-onset mitochondrial encephalopathy. *Human molecular genetics* 19(24), pp. 4837–4847. doi: 10.1093/hmg/ddq414.

Finsterer, J. and Zarrouk-Mahjoub, S. 2018. Fibroblast growth-factor-21 is currently a weak biomarker for identifying mitochondrial and non-mitochondrial inborn errors of metabolism. *Molecular genetics and metabolism reports* 14, pp. 1–2. doi: 10.1016/j.ymgmr.2017.10.005.

Foley, A.R. et al. 2014. Treatable childhood neuronopathy caused by mutations in riboflavin transporter RFVT2. *Brain : a journal of neurology* 137(Pt 1), pp. 44–56. doi: 10.1093/brain/awt315.

Frosst, P. et al. 1995. A candidate genetic risk factor for vascular disease: a common mutation in methylenetetrahydrofolate reductase. *Nature genetics* 10(1), pp. 111–113. doi: 10.1038/ng0595-111.

Galloway, C.A. et al. 2012. Mitochondrial morphology-emerging role in bioenergetics. *Free radical biology & medicine* 53(12), pp. 2218–2228. doi: 10.1016/j.freeradbiomed.2012.09.035.

Galluccio, M. et al. 2007. Over-expression in Escherichia coli, purification and characterization of isoform 2 of human FAD synthetase. *Protein expression and purification* 52(1), pp. 175–181. doi: 10.1016/j.pep.2006.09.002.

Gammage, P.A. et al. 2014. Mitochondrially targeted ZFNs for selective degradation of pathogenic mitochondrial genomes bearing large-scale deletions or point mutations. *EMBO molecular medicine* 6(4), pp. 458–466. doi: 10.1002/emmm.201303672.

Gammage, P.A. et al. 2018. Genome editing in mitochondria corrects a pathogenic mtDNA mutation in vivo. *Nature medicine* . doi: 10.1038/s41591-018-0165-9.

Garcia-Villoria, J. et al. 2018. FLAD1, encoding FAD synthase, is mutated in a patient with myopathy, scoliosis and cataracts. *Clinical genetics* 94(6), pp. 592–593. doi: 10.1111/cge.13452.

Garrido-Maraver, J. et al. 2014. Coenzyme q10 therapy. *Molecular syndromology* 5(3–4), pp. 187–197. doi: 10.1159/000360101.

Genova, M.L. et al. 2001. The site of production of superoxide radical in mitochondrial Complex I is not a bound ubisemiquinone but presumably iron-sulfur cluster N2. *FEBS letters* 505(3), pp. 364–368.

Gerards, M. et al. 2011. Riboflavin-responsive oxidative phosphorylation complex I deficiency caused by defective ACAD9: new function for an old gene. *Brain : a journal of neurology* 134(Pt 1), pp. 210–219. doi: 10.1093/brain/awq273.

Gerhard, R. et al. 2003. Thiol-modifying phenylarsine oxide inhibits guanine nucleotide

binding of Rho but not of Rac GTPases. *Molecular pharmacology* 63(6), pp. 1349–1355. doi: 10.1124/mol.63.6.1349.

Ghezzi, D. et al. 2010. Severe X-linked mitochondrial encephalomyopathy associated with a mutation in apoptosis-inducing factor. *American journal of human genetics* 86(4), pp. 639–649. doi: 10.1016/j.ajhg.2010.03.002.

Ghezzi, D. and Zeviani, M. 2018. Human diseases associated with defects in assembly of OXPHOS complexes. *Essays in biochemistry* 62(3), pp. 271–286. doi: 10.1042/EBC20170099.

Giacomini, K.M. et al. 2007. When good drugs go bad. *Nature* 446(7139), pp. 975–977. doi: 10.1038/446975a.

Gianazza, E. et al. 2006. Coordinated and reversible reduction of enzymes involved in terminal oxidative metabolism in skeletal muscle mitochondria from a riboflavin-responsive, multiple acyl-CoA dehydrogenase deficiency patient. *Electrophoresis* 27(5–6), pp. 1182–1198. doi: 10.1002/elps.200500687.

Giancaspero, T.A. et al. 2009. The occurrence of riboflavin kinase and FAD synthetase ensures FAD synthesis in tobacco mitochondria and maintenance of cellular redox status. *The FEBS journal* 276(1), pp. 219–231. doi: 10.1111/j.1742-4658.2008.06775.x.

Giancaspero, T.A. et al. 2013. FAD synthesis and degradation in the nucleus create a local flavin cofactor pool. *The Journal of biological chemistry* 288(40), pp. 29069–29080. doi: 10.1074/jbc.M113.500066.

Giancaspero, T.A. et al. 2015. Human FAD synthase is a bi-functional enzyme with a FAD hydrolase activity in the molybdopterin binding domain. *Biochemical and biophysical research communications* 465(3), pp. 443–449. doi: 10.1016/j.bbrc.2015.08.035.

Gibson, K.M. et al. 1991. Phenotypic heterogeneity in the syndromes of 3-methylglutaconic aciduria. *The Journal of pediatrics* 118(6), pp. 885–890.

Gibson, Q.H. et al. 1962. The nature of compounds present in mixtures of oxidized and reduced flavin mononucleotides. *The Biochemical journal* 85, pp. 369–383.

Gilbert, H.F. 1990. Molecular and cellular aspects of thiol-disulfide exchange. *Advances in enzymology and related areas of molecular biology* 63, pp. 69–172.

Giles, R.E. et al. 1980. Maternal inheritance of human mitochondrial DNA. *Proceedings of the National Academy of Sciences of the United States of America* 77(11), pp. 6715–6719.

Gladyshev, V.N. et al. 2001. Identification and characterization of a new mammalian glutaredoxin (thioltransferase), Grx2. *The Journal of biological chemistry* 276(32), pp. 30374–30380. doi: 10.1074/jbc.M100020200.

Godoy, J.R. et al. 2011. Redox atlas of the mouse. Immunohistochemical detection of glutaredoxin-, peroxiredoxin-, and thioredoxin-family proteins in various tissues of the laboratory mouse. *Biochimica et biophysica acta* 1810(1), pp. 2–92. doi: 10.1016/j.bbagen.2010.05.006.

Gonzalez-Cabo, P. et al. 2010. Flavin adenine dinucleotide rescues the phenotype of frataxin deficiency. *PloS one* 5(1), p. e8872. doi: 10.1371/journal.pone.0008872.

Goodwin, S. et al. 2016. Coming of age: ten years of next-generation sequencing technologies. *Nature reviews. Genetics* 17(6), pp. 333–351. doi: 10.1038/nrg.2016.49.

Gorman, G.S. et al. 2016. Mitochondrial diseases. *Nature reviews. Disease primers* 2, p. 16080. doi: 10.1038/nrdp.2016.80.

Goth, L. and Nagy, T. 2012. Acatalasemia and diabetes mellitus. *Archives of biochemistry and biophysics* 525(2), pp. 195–200. doi: 10.1016/j.abb.2012.02.005.

Goto, Y. et al. 1990. A mutation in the tRNA(Leu)(UUR) gene associated with the MELAS subgroup of mitochondrial encephalomyopathies. *Nature* 348(6302), pp. 651–653. doi: 10.1038/348651a0.

Grady, J.P. et al. 2014. Disease progression in patients with single, large-scale mitochondrial DNA deletions. *Brain : a journal of neurology* 137(Pt 2), pp. 323–334. doi: 10.1093/brain/awt321.

Green, P. et al. 2010. Brown-Vialetto-Van Laere syndrome, a ponto-bulbar palsy with deafness, is caused by mutations in c20orf54. *American journal of human genetics* 86(3), pp. 485–489. doi: 10.1016/j.ajhg.2010.02.006.

Gregersen, N. et al. 1982. C6-C10-dicarboxylic aciduria: biochemical considerations in relation to diagnosis of beta-oxidation defects. *Scandinavian journal of clinical and laboratory investigation. Supplementum* 161, pp. 15–27.

Guo, J. and Lemire, B.D. 2003. The ubiquinone-binding site of the Saccharomyces cerevisiae succinate-ubiquinone oxidoreductase is a source of superoxide. *The Journal of biological chemistry* 278(48), pp. 47629–47635. doi: 10.1074/jbc.M306312200.

Haack, T.B. et al. 2010. Exome sequencing identifies ACAD9 mutations as a cause of complex I deficiency. *Nature genetics* 42(12), pp. 1131–1134. doi: 10.1038/ng.706.

Haack, T.B. et al. 2012a. Impaired riboflavin transport due to missense mutations in SLC52A2 causes Brown-Vialetto-Van Laere syndrome. *Journal of inherited metabolic disease* 35(6), pp. 943–948. doi: 10.1007/s10545-012-9513-y.

Haack, T.B. et al. 2012b. Molecular diagnosis in mitochondrial complex I deficiency using exome sequencing. *Journal of medical genetics* 49(4), pp. 277–283. doi: 10.1136/jmedgenet-2012-100846.

Haack, T.B. et al. 2014. Infantile Leigh-like syndrome caused by SLC19A3 mutations is a treatable disease. *Brain : a journal of neurology* 137(Pt 9), p. e295. doi: 10.1093/brain/awu128.

de Haas, R. et al. 2017. Therapeutic effects of the mitochondrial ROS-redox modulator KH176 in a mammalian model of Leigh Disease. *Scientific reports* 7(1), p. 11733. doi: 10.1038/s41598-017-09417-5.

Haas, R.H. et al. 2008. The in-depth evaluation of suspected mitochondrial disease. *Molecular genetics and metabolism* 94(1), pp. 16–37. doi: 10.1016/j.ymgme.2007.11.018.

Hadrava Vanova, K. et al. 2020. Mitochondrial complex II and reactive oxygen species in disease and therapy. *Redox Rep,* 25**,** 26-32.

Haghighi, A. et al. 2014. Sengers syndrome: six novel AGK mutations in seven new families and review of the phenotypic and mutational spectrum of 29 patients. *Orphanet journal of rare diseases* 9, p. 119. doi: 10.1186/s13023-014-0119-3.

Halestrap, A.P. et al. 2002. The permeability transition pore complex: another view. *Biochimie* 84(2–3), pp. 153–166.

Haller, T. et al. 1994. A respirometer for investigating oxidative cell metabolism: toward optimization of respiratory studies. *Analytical biochemistry* 218(2), pp. 338–342. doi: 10.1006/abio.1994.1188.

Halliwell, B. and Gutteridge, J. 2015. *Free radicals in biology and medicine*. 5th ed. Oxford: Oxford University Press.

Halprin, K.M. and Ohkawara, A. 1967. The measurement of glutathione in human epidermis using glutathione reductase. *The Journal of investigative dermatology* 48(2), pp. 149–152.

Hamajima, S. et al. 1979. Induction of the FAD synthetase system in rat liver by phenobarbital administration. *International journal for vitamin and nutrition research. Internationale Zeitschrift fur Vitamin- und Ernahrungsforschung. Journal international de vitaminologie et de nutrition* 49(1), pp. 59–63.

Hampton, M.B. et al. 1998. Inside the neutrophil phagosome: oxidants, myeloperoxidase, and bacterial killing. *Blood* 92(9), pp. 3007–3017.

Hanschmann, E.-M. et al. 2010. Both thioredoxin 2 and glutaredoxin 2 contribute to the reduction of the mitochondrial 2-Cys peroxiredoxin Prx3. *The Journal of biological chemistry* 285(52), pp. 40699–40705. doi: 10.1074/jbc.M110.185827.

Hansen, J. et al. 2011. Quantitative proteomics reveals cellular targets of celastrol. *PloS one* 6(10), p. e26634. doi: 10.1371/journal.pone.0026634.

Hargreaves, I.P. 2014. Coenzyme Q10 as a therapy for mitochondrial disease. *The international journal of biochemistry & cell biology* 49, pp. 105–111. doi: 10.1016/j.biocel.2014.01.020.

Harman, D. 1956. Aging: a theory based on free radical and radiation chemistry. *Journal of gerontology* 11(3), pp. 298–300.

Harris, M.J. and Juriloff, D.M. 1999. Mini-review: toward understanding mechanisms of genetic neural tube defects in mice. *Teratology* 60(5), pp. 292–305. doi: 10.1002/(SICI)1096-9926(199911)60:5<292::AID-TERA10>3.0.CO;2-6.

Heeringa, S.F. et al. 2011. COQ6 mutations in human patients produce nephrotic syndrome with sensorineural deafness. *The Journal of clinical investigation* 121(5), pp. 2013–2024. doi: 10.1172/JCI45693.

Heinz, S. et al. 2017. Mechanistic Investigations of the Mitochondrial Complex I Inhibitor Rotenone in the Context of Pharmacological and Safety Evaluation. *Scientific reports* 7, p. 45465. doi: 10.1038/srep45465.

Henriques, B.J. et al. 2009. Role of flavinylation in a mild variant of multiple acyl-CoA dehydrogenation deficiency: a molecular rationale for the effects of riboflavin supplementation. *The Journal of biological chemistry* 284(7), pp. 4222–4229. doi: 10.1074/jbc.M805719200.

Henriques, B.J. et al. 2010. Emerging roles for riboflavin in functional rescue of mitochondrial beta-oxidation flavoenzymes. *Current medicinal chemistry* 17(32), pp. 3842–3854.

Henze, K. and Martin, W. 2003. Evolutionary biology: essence of mitochondria. *Nature* 426(6963), pp. 127–128. doi: 10.1038/426127a.

Herguedas, B. et al. 2010. Oligomeric state in the crystal structure of modular FAD synthetase

provides insights into its sequential catalysis in prokaryotes. *Journal of molecular biology* 400(2), pp. 218–230. doi: 10.1016/j.jmb.2010.05.018.

Hirano, M. et al. 2018. Emerging therapies for mitochondrial diseases. *Essays in biochemistry* 62(3), pp. 467–481. doi: 10.1042/EBC20170114.

Ho, G. et al. 2011. Maternal riboflavin deficiency, resulting in transient neonatal-onset glutaric aciduria Type 2, is caused by a microdeletion in the riboflavin transporter gene GPR172B. *Human mutation* 32(1), pp. E1976-84. doi: 10.1002/humu.21399.

Holland, R. and Fishbein, J.C. 2010. Chemistry of the cysteine sensors in Kelch-like ECH-associated protein 1. *Antioxidants & redox signaling* 13(11), pp. 1749–1761. doi: 10.1089/ars.2010.3273.

Holmgren, A. 1985. Thioredoxin. *Annual review of biochemistry* 54, pp. 237–271. doi: 10.1146/annurev.bi.54.070185.001321.

Holmstrom, K.M. and Finkel, T. 2014. Cellular mechanisms and physiological consequences of redox-dependent signalling. *Nature reviews. Molecular cell biology* 15(6), pp. 411–421. doi: 10.1038/nrm3801.

Holzerova, E. et al. 2016. Human thioredoxin 2 deficiency impairs mitochondrial redox homeostasis and causes early-onset neurodegeneration. *Brain* 139(2), pp. 346–354.

Holzerova, E. and Prokisch, H. 2015. Mitochondria: Much ado about nothing? How dangerous is reactive oxygen species production? *The international journal of biochemistry & cell biology* 63, pp. 16–20. doi: 10.1016/j.biocel.2015.01.021.

Holzerová, E. and Prokisch, H. 2015. Mitochondria: Much ado about nothing? How dangerous is reactive oxygen species production? *International Journal of Biochemistry and Cell Biology* 63, pp. 16–20. doi: 10.1016/j.biocel.2015.01.021.

Horvath, R. 2012. Update on clinical aspects and treatment of selected vitamin-responsive disorders II (riboflavin and CoQ 10). *Journal of inherited metabolic disease* 35(4), pp. 679–687. doi: 10.1007/s10545-011-9434-1.

Hover, B.M. et al. 2015. Mechanism of pyranopterin ring formation in molybdenum cofactor biosynthesis. *Proceedings of the National Academy of Sciences of the United States of America* 112(20), pp. 6347–6352. doi: 10.1073/pnas.1500697112.

Hsu, P.D. et al. 2014. Development and applications of CRISPR-Cas9 for genome engineering. *Cell* 157(6), pp. 1262–1278. doi: 10.1016/j.cell.2014.05.010.

Huang, D. et al. 2005. The chemistry behind antioxidant capacity assays. *Journal of agricultural and food chemistry* 53(6), pp. 1841–1856. doi: 10.1021/jf030723c.

Huang, Q. et al. 2015. Thioredoxin-2 inhibits mitochondrial reactive oxygen species generation and apoptosis stress kinase-1 activity to maintain cardiac function. *Circulation* 131(12), pp. 1082–1097. doi: 10.1161/CIRCULATIONAHA.114.012725.

Huerta, C. et al. 2009. Structure and mechanism of a eukaryotic FMN adenylyltransferase. *Journal of molecular biology* 389(2), pp. 388–400. doi: 10.1016/j.jmb.2009.04.022.

Illumina 2016. *An Introduction to Next-Generation Sequencing Technology*. Available at: https://www.illumina.com/Documents/products/Illumina_Sequencing_Introduction.pdf.

Imtiaz, A. et al. 2014. A frameshift mutation in GRXCR2 causes recessively inherited hearing

loss. *Human mutation* 35(5), pp. 618–624. doi: 10.1002/humu.22545.

Jain, A. et al. 1991. Glutathione deficiency leads to mitochondrial damage in brain. *Proceedings of the National Academy of Sciences of the United States of America* 88(5), pp. 1913–1917.

Jain, M. et al. 2018. Nanopore sequencing and assembly of a human genome with ultra-long reads. *Nature Biotechnology* 36, p. 338. Available at: http://dx.doi.org/10.1038/nbt.4060.

Jakupoglu, C. et al. 2005. Cytoplasmic thioredoxin reductase is essential for embryogenesis but dispensable for cardiac development. *Molecular and cellular biology* 25(5), pp. 1980–1988. doi: 10.1128/MCB.25.5.1980-1988.2005.

Jauhari, P. et al. 2017. Thiamine Responsive Pyruvate Dehydrogenase Complex Deficiency: A Potentially Treatable Cause of Leigh's Disease. *Journal of pediatric neurosciences* 12(3), pp. 265–267. doi: 10.4103/jpn.JPN_191_16.

Jocelyn, P.C. and Cronshaw, A. 1985. Properties of mitochondria treated with 1-chloro-2,4-dinitrobenzene. *Biochemical pharmacology* 34(9), pp. 1588–1590.

Jones, L.L. et al. 2010. Acylcarnitines: role in brain. *Progress in lipid research* 49(1), pp. 61–75. doi: 10.1016/j.plipres.2009.08.004.

Joosten, V. and van Berkel, W.J.H. 2007. Flavoenzymes. *Current opinion in chemical biology* 11(2), pp. 195–202. doi: 10.1016/j.cbpa.2007.01.010.

Kaiser, J. et al. 2002. Biosynthesis of vitamin B2. *European journal of biochemistry* 269(21), pp. 5264–5270.

Kang, H.-C. et al. 2007. Safe and effective use of the ketogenic diet in children with epilepsy and mitochondrial respiratory chain complex defects. *Epilepsia* 48(1), pp. 82–88. doi: 10.1111/j.1528-1167.2006.00906.x.

Kaplowitz, N. 1981. The importance and regulation of hepatic glutathione. *The Yale journal of biology and medicine* 54(6), pp. 497–502.

Kaur, P. et al. 2010. The in vitro effects of Trolox on methylmercury-induced neurotoxicity. *Toxicology* 276(1), pp. 73–78. doi: 10.1016/j.tox.2010.07.006.

Kiley, P.J. and Storz, G. 2004. Exploiting thiol modifications. *PLoS biology* 2(11), p. e400. doi: 10.1371/journal.pbio.0020400.

Kim, H. et al. 1999. Structure of Antimycin A1, a Specific Electron Transfer Inhibitor of Ubiquinol−Cytochrome c Oxidoreductase. *Journal of the American Chemical Society* 121(20), pp. 4902–4903. Available at: http://pubs.acs.org/doi/abs/10.1021/ja990190h.

Kirkman, H.N. and Gaetani, G.F. 1984. Catalase: a tetrameric enzyme with four tightly bound molecules of NADPH. *Proceedings of the National Academy of Sciences of the United States of America* 81(14), pp. 4343–4347.

Klopstock, T. et al. 2011. A randomized placebo-controlled trial of idebenone in Leber's hereditary optic neuropathy. *Brain : a journal of neurology* 134(Pt 9), pp. 2677–2686. doi: 10.1093/brain/awr170.

Kmoch, S. et al. 1995. Riboflavin-responsive epilepsy in a patient with SER209 variant form of short-chain acyl-CoA dehydrogenase. *Journal of inherited metabolic disease* 18(2), pp. 227–229.

van der Knaap, M.S. et al. 1996. Magnetic resonance imaging in lactic acidosis. *Journal of inherited metabolic disease* 19(4), pp. 535–547.

Kobayashi, S. et al. 2015. Cystathionine Is a Novel Substrate of Cystine/Glutamate Transporter: IMPLICATIONS FOR IMMUNE FUNCTION. *The Journal of Biological Chemistry* 290(14), pp. 8778–8788. doi: 10.1074/jbc.M114.625053.

Koene, S. et al. 2017. KH176 under development for rare mitochondrial disease: a first in man randomized controlled clinical trial in healthy male volunteers. *Orphanet journal of rare diseases* 12(1), p. 163. doi: 10.1186/s13023-017-0715-0.

Koene, S. and Smeitink, J. 2011. *Mitochondrial medicine: a clinical guideline*. First edit. Nijmegen, The Netherlands: Khondrion BV. Available at: khondrion.com.

Kohda, M. et al. 2016. A Comprehensive Genomic Analysis Reveals the Genetic Landscape of Mitochondrial Respiratory Chain Complex Deficiencies. *PLoS genetics* 12(1), p. e1005679. doi: 10.1371/journal.pgen.1005679.

Kompare, M. and Rizzo, W.B. 2008. Mitochondrial fatty-acid oxidation disorders. *Seminars in pediatric neurology* 15(3), pp. 140–149. doi: 10.1016/j.spen.2008.05.008.

Koonin, E. V et al. 2002. The structure of the protein universe and genome evolution. *Nature* 420(6912), pp. 218–223. doi: 10.1038/nature01256.

Koopman, W.J.H. et al. 2010. Mammalian mitochondrial complex I: biogenesis, regulation, and reactive oxygen species generation. *Antioxidants & redox signaling* 12(12), pp. 1431–1470. doi: 10.1089/ars.2009.2743.

Koopman, W.J.H. et al. 2012. Monogenic mitochondrial disorders. *The New England journal of medicine* 366(12), pp. 1132–1141. doi: 10.1056/NEJMra1012478.

Koppel, S.J. and Swerdlow, R.H. 2018. Neuroketotherapeutics: A modern review of a century-old therapy. *Neurochemistry international* 117, pp. 114–125. doi: 10.1016/j.neuint.2017.05.019.

Korge, P. et al. 2015. Increased reactive oxygen species production during reductive stress: The roles of mitochondrial glutathione and thioredoxin reductases. *Biochimica et biophysica acta* 1847(6–7), pp. 514–525. doi: 10.1016/j.bbabio.2015.02.012.

Kossoff, E.H. et al. 2014. Transition for patients with epilepsy due to metabolic and mitochondrial disorders. *Epilepsia* 55 Suppl 3, pp. 37–40. doi: 10.1111/epi.12709.

Koy, A. et al. 2012. Brown-Vialetto-Van Laere syndrome: a riboflavin-unresponsive patient with a novel mutation in the C20orf54 gene. *Pediatric neurology* 46(6), pp. 407–409. doi: 10.1016/j.pediatrneurol.2012.03.008.

Kremer, L.S. et al. 2017. Genetic diagnosis of Mendelian disorders via RNA sequencing. *Nature communications* 8, p. 15824. doi: 10.1038/ncomms15824.

Krupa, A. et al. 2003. A conserved domain in prokaryotic bifunctional FAD synthetases can potentially catalyze nucleotide transfer. *Trends in biochemical sciences* 28(1), pp. 9–12.

Kudin, A.P. et al. 2017. Homozygous mutation in TXNRD1 is associated with genetic generalized epilepsy. *Free radical biology & medicine* 106, pp. 270–277. doi: 10.1016/j.freeradbiomed.2017.02.040.

Kuper, J. et al. 2004. Structure of the molybdopterin-bound Cnx1G domain links

molybdenum and copper metabolism. *Nature* 430(7001), pp. 803–806. doi: 10.1038/nature02681.

Kushnareva, Y. et al. 2002. Complex I-mediated reactive oxygen species generation: modulation by cytochrome c and NAD(P)+ oxidation-reduction state. *The Biochemical journal* 368(Pt 2), pp. 545–553. doi: 10.1042/BJ20021121.

Kussmaul, L. and Hirst, J. 2006. The mechanism of superoxide production by NADH:ubiquinone oxidoreductase (complex I) from bovine heart mitochondria. *Proceedings of the National Academy of Sciences of the United States of America* 103(20), pp. 7607–7612. doi: 10.1073/pnas.0510977103.

Lake, N.J. et al. 2016. Leigh syndrome: One disorder, more than 75 monogenic causes. *Annals of neurology* 79(2), pp. 190–203. doi: 10.1002/ana.24551.

Larsson, N.G. and Oldfors, A. 2001. Mitochondrial myopathies. *Acta physiologica Scandinavica* 171(3), pp. 385–393. doi: 10.1046/j.1365-201x.2001.00842.x.

Lazarou, M. et al. 2009. Assembly of mitochondrial complex I and defects in disease. *Biochimica et biophysica acta* 1793(1), pp. 78–88. doi: 10.1016/j.bbamcr.2008.04.015.

Lee, C. et al. 2004. Redox regulation of OxyR requires specific disulfide bond formation involving a rapid kinetic reaction path. *Nature structural & molecular biology* 11(12), pp. 1179–1185. doi: 10.1038/nsmb856.

Lee, S. et al. 2011. Effects of interventions on oxidative stress and inflammation of cardiovascular diseases. *World journal of cardiology* 3(1), pp. 18–24. doi: 10.4330/wjc.v3.i1.18.

Lee, S.S. and McCormick, D.B. 1985. Thyroid hormone regulation of flavocoenzyme biosynthesis. *Archives of biochemistry and biophysics* 237(1), pp. 197–201.

Legati, A. et al. 2016. New genes and pathomechanisms in mitochondrial disorders unraveled by NGS technologies. *Biochimica et biophysica acta* 1857(8), pp. 1326–1335. doi: 10.1016/j.bbabio.2016.02.022.

Leone, P. et al. 2018. Bacterial Production, Characterization and Protein Modeling of a Novel Monofuctional Isoform of FAD Synthase in Humans: An Emergency Protein? *Molecules (Basel, Switzerland)* 23(1). doi: 10.3390/molecules23010116.

Lieber, D.S. et al. 2013. Targeted exome sequencing of suspected mitochondrial disorders. *Neurology* 80(19), pp. 1762–1770. doi: 10.1212/WNL.0b013e3182918c40.

Lienhart, W.-D. et al. 2013. The human flavoproteome. *Archives of biochemistry and biophysics* 535(2), pp. 150–162. doi: 10.1016/j.abb.2013.02.015.

Lightowlers, R.N. et al. 2015. Mutations causing mitochondrial disease: What is new and what challenges remain? *Science (New York, N.Y.)* 349(6255), pp. 1494–1499. doi: 10.1126/science.aac7516.

Lin, J. et al. 2009. Specific electron transport chain abnormalities in amyotrophic lateral sclerosis. *Journal of neurology* 256(5), pp. 774–782. doi: 10.1007/s00415-009-5015-8.

Liuzzi, V.C. et al. 2012. Silencing of FAD synthase gene in Caenorhabditis elegans upsets protein homeostasis and impacts on complex behavioral patterns. *Biochimica et biophysica acta* 1820(4), pp. 521–531. doi: 10.1016/j.bbagen.2012.01.012.

Lorenzoni, P.J. et al. 2014. When should MERRF (myoclonus epilepsy associated with ragged-red fibers) be the diagnosis? *Arquivos de neuro-psiquiatria* 72(10), pp. 803–811.

Lowes, D.A. and Galley, H.F. 2011. Mitochondrial protection by the thioredoxin-2 and glutathione systems in an in vitro endothelial model of sepsis. *The Biochemical journal* 436(1), pp. 123–132. doi: 10.1042/BJ20102135.

Lu, J. and Holmgren, A. 2012. Thioredoxin system in cell death progression. *Antioxidants & redox signaling* 17(12), pp. 1738–1747. doi: 10.1089/ars.2012.4650.

Lu, S.C. 2013. Glutathione synthesis. *Biochimica et biophysica acta* 1830(5), pp. 3143–3153. doi: 10.1016/j.bbagen.2012.09.008.

Lucas, T.G. et al. 2011. Cofactors and metabolites as potential stabilizers of mitochondrial acyl-CoA dehydrogenases. *Biochimica et biophysica acta* 1812(12), pp. 1658–1663. doi: 10.1016/j.bbadis.2011.09.009.

Luft, R. et al. 1962. A case of severe hypermetabolism of nonthyroid origin with a defect in the maintenance of mitochondrial respiratory control: a correlated clinical, biochemical, and morphological study. *The Journal of clinical investigation* 41, pp. 1776–1804. doi: 10.1172/JCI104637.

Lundberg, M. et al. 2001. Cloning and expression of a novel human glutaredoxin (Grx2) with mitochondrial and nuclear isoforms. *The Journal of biological chemistry* 276(28), pp. 26269–26275. doi: 10.1074/jbc.M011605200.

MacArthur, D.G. et al. 2007. Loss of ACTN3 gene function alters mouse muscle metabolism and shows evidence of positive selection in humans. *Nature genetics* 39(10), pp. 1261–1265. doi: 10.1038/ng2122.

MacArthur, D.G. et al. 2012. A systematic survey of loss-of-function variants in human protein-coding genes. *Science (New York, N.Y.)* 335(6070), pp. 823–828. doi: 10.1126/science.1215040.

MacArthur, D.G. and North, K.N. 2007. ACTN3: A genetic influence on muscle function and athletic performance. *Exercise and sport sciences reviews* 35(1), pp. 30–34. doi: 10.1097/JES.0b013e31802d8874.

MacArthur, D.G. and Tyler-Smith, C. 2010. Loss-of-function variants in the genomes of healthy humans. *Human molecular genetics* 19(R2), pp. R125-30. doi: 10.1093/hmg/ddq365.

Macheroux, P. et al. 2011. Flavogenomics--a genomic and structural view of flavin-dependent proteins. *The FEBS journal* 278(15), pp. 2625–2634. doi: 10.1111/j.1742-4658.2011.08202.x.

MacLean, B. et al. 2010. Skyline: an open source document editor for creating and analyzing targeted proteomics experiments. *Bioinformatics (Oxford, England)* 26(7), pp. 966–968. doi: 10.1093/bioinformatics/btq054.

Magalhaes, P.V.S. et al. 2016. Antioxidant treatments for schizophrenia. *The Cochrane database of systematic reviews* 2, p. CD008919. doi: 10.1002/14651858.CD008919.pub2.

Mailloux, R.J. and Treberg, J.R. 2016. Protein S-glutathionlyation links energy metabolism to redox signaling in mitochondria. *Redox biology* 8, pp. 110–118. doi: 10.1016/j.redox.2015.12.010.

Mandal, P.K. et al. 2010. System x(c)- and thioredoxin reductase 1 cooperatively rescue glutathione deficiency. *The Journal of biological chemistry* 285(29), pp. 22244–22253. doi:

10.1074/jbc.M110.121327.

Manoharan, S. et al. 2016. The Role of Reactive Oxygen Species in the Pathogenesis of Alzheimer's Disease, Parkinson's Disease, and Huntington's Disease: A Mini Review. *Oxidative medicine and cellular longevity* 2016, p. 8590578. doi: 10.1155/2016/8590578.

Manthey, K.C. et al. 2006. Riboflavin deficiency causes protein and DNA damage in HepG2 cells, triggering arrest in G1 phase of the cell cycle. *The Journal of nutritional biochemistry* 17(4), pp. 250–256. doi: 10.1016/j.jnutbio.2005.05.004.

Margulis, L. 1975. Symbiotic theory of the origin of eukaryotic organelles; criteria for proof. *Symposia of the Society for Experimental Biology* (29), pp. 21–38.

Marshall, K.G. 2014. Exploring antioxidants. *The West Indian medical journal* 63(2), pp. 119–120. doi: 10.7727/wimj.2014.301.

Martensson, J. et al. 1991. Inhibition of glutathione synthesis in the newborn rat: a model for endogenously produced oxidative stress. *Proceedings of the National Academy of Sciences of the United States of America* 88(20), pp. 9360–9364.

Matsui, M. et al. 1996. Early embryonic lethality caused by targeted disruption of the mouse thioredoxin gene. *Developmental biology* 178(1), pp. 179–185. doi: 10.1006/dbio.1996.0208.

Mayr, J.A. et al. 2015. Spectrum of combined respiratory chain defects. *Journal of inherited metabolic disease* 38(4), pp. 629–640. doi: 10.1007/s10545-015-9831-y.

McCormick, D.B. et al. 1997. Purification and properties of FAD synthetase from liver. *Methods in enzymology* 280, pp. 407–413.

McCormick, D.B. 2000. A trail of research on cofactors: an odyssey with friends. *The Journal of nutrition* 130(2S Suppl), p. 323S–330S.

McManus, M.J. et al. 2011. The mitochondria-targeted antioxidant MitoQ prevents loss of spatial memory retention and early neuropathology in a transgenic mouse model of Alzheimer's disease. *The Journal of neuroscience : the official journal of the Society for Neuroscience* 31(44), pp. 15703–15715. doi: 10.1523/JNEUROSCI.0552-11.2011.

Meng, T.-C. et al. 2002. Reversible oxidation and inactivation of protein tyrosine phosphatases in vivo. *Molecular cell* 9(2), pp. 387–399.

Mewies, M. et al. 1998. Covalent attachment of flavin adenine dinucleotide (FAD) and flavin mononucleotide (FMN) to enzymes: the current state of affairs. *Protein science : a publication of the Protein Society* 7(1), pp. 7–20. doi: 10.1002/pro.5560070102.

Miccolis, A. et al. 2012. Bacterial over-expression and purification of the 3'phosphoadenosine 5'phosphosulfate (PAPS) reductase domain of human FAD synthase: functional characterization and homology modeling. *International journal of molecular sciences* 13(12), pp. 16880–16898. doi: 10.3390/ijms131216880.

Mills, P.B. et al. 2005. Neonatal epileptic encephalopathy caused by mutations in the PNPO gene encoding pyridox(am)ine 5'-phosphate oxidase. *Human molecular genetics* 14(8), pp. 1077–1086. doi: 10.1093/hmg/ddi120.

Misra, S. 2012. Randomized double blind placebo control studies, the 'Gold Standard' in intervention based studies. *Indian journal of sexually transmitted diseases and AIDS* 33(2), pp. 131–134. doi: 10.4103/0253-7184.102130.

Moolenaar, S.H. et al. 1999. Defect in dimethylglycine dehydrogenase, a new inborn error of metabolism: NMR spectroscopy study. *Clinical chemistry* 45(4), pp. 459–464.

Moreno, J.C. et al. 2002. Inactivating mutations in the gene for thyroid oxidase 2 (THOX2) and congenital hypothyroidism. *The New England journal of medicine* 347(2), pp. 95–102. doi: 10.1056/NEJMoa012752.

Moreno, J.C. et al. 2008. Mutations in the iodotyrosine deiodinase gene and hypothyroidism. *The New England journal of medicine* 358(17), pp. 1811–1818. doi: 10.1056/NEJMoa0706819.

Moriyama, Y. 2011. Riboflavin transporter is finally identified. *Journal of biochemistry* 150(4), pp. 341–343. doi: 10.1093/jb/mvr095.

Mortazavi, A. et al. 2008. Mapping and quantifying mammalian transcriptomes by RNA-Seq. *Nature methods* 5(7), pp. 621–628. doi: 10.1038/nmeth.1226.

Mosegaard, S. et al. 2017. An intronic variation in SLC52A1 causes exon skipping and transient riboflavin-responsive multiple acyl-CoA dehydrogenation deficiency. *Molecular genetics and metabolism* 122(4), pp. 182–188. doi: 10.1016/j.ymgme.2017.10.014.

Munnich, A. and Rustin, P. 2001. Clinical spectrum and diagnosis of mitochondrial disorders. *American journal of medical genetics* 106(1), pp. 4–17. doi: 10.1002/ajmg.1391.

Nakano, E. et al. 2011. Riboflavin depletion impairs cell proliferation in adult human duodenum: identification of potential effectors. *Digestive diseases and sciences* 56(4), pp. 1007–1019. doi: 10.1007/s10620-010-1374-3.

Nesbitt, V. et al. 2013. The UK MRC Mitochondrial Disease Patient Cohort Study: clinical phenotypes associated with the m.3243A>G mutation--implications for diagnosis and management. *Journal of neurology, neurosurgery, and psychiatry* 84(8), pp. 936–938. doi: 10.1136/jnnp-2012-303528.

Neveling, K. et al. 2013. A post-hoc comparison of the utility of sanger sequencing and exome sequencing for the diagnosis of heterogeneous diseases. *Human mutation* 34(12), pp. 1721–1726. doi: 10.1002/humu.22450.

Nonn, L. et al. 2003. The absence of mitochondrial thioredoxin 2 causes massive apoptosis, exencephaly, and early embryonic lethality in homozygous mice. *Molecular and cellular biology* 23(3), pp. 916–922.

O'Dwyer, P.J. et al. 1996. Phase I trial of buthionine sulfoximine in combination with melphalan in patients with cancer. *Journal of clinical oncology : official journal of the American Society of Clinical Oncology* 14(1), pp. 249–256. doi: 10.1200/JCO.1996.14.1.249.

Odeh, H. et al. 2010. Mutations in Grxcr1 are the basis for inner ear dysfunction in the pirouette mouse. *American journal of human genetics* 86(2), pp. 148–160. doi: 10.1016/j.ajhg.2010.01.016.

Ohtake, A. et al. 2014. Diagnosis and molecular basis of mitochondrial respiratory chain disorders: exome sequencing for disease gene identification. *Biochimica et biophysica acta* 1840(4), pp. 1355–1359. doi: 10.1016/j.bbagen.2014.01.025.

Oldfors, A. et al. 1991. The correlation between pathology, biochemistry and molecular genetics in mitochondrial encephalomyopathies. In: *In: Gorrod J.W., Albano O., Ferrari E., Papa S. (eds) Molecular Basis of Neurological Disorders and Their Treatment*. Springer,

Dordrecht, pp. 243–254. doi: https://doi.org/10.1007/978-94-011-3114-8_23.

Olsen, R.K.J. et al. 2007. ETFDH mutations as a major cause of riboflavin-responsive multiple acyl-CoA dehydrogenation deficiency. *Brain : a journal of neurology* 130(Pt 8), pp. 2045–2054. doi: 10.1093/brain/awm135.

Olsen, R.K.J. et al. 2016. Riboflavin-Responsive and -Non-responsive Mutations in FAD Synthase Cause Multiple Acyl-CoA Dehydrogenase and Combined Respiratory-Chain Deficiency. *American Journal of Human Genetics* 98(6), pp. 1130–1145.

Olson, M. V 1999. When less is more: gene loss as an engine of evolutionary change. *American journal of human genetics* 64(1), pp. 18–23. doi: 10.1086/302219.

Padovani, D. and Banerjee, R. 2009. A rotary mechanism for coenzyme B(12) synthesis by adenosyltransferase. *Biochemistry* 48(23), pp. 5350–5357. doi: 10.1021/bi900454s.

Paoli, A. et al. 2014. Ketogenic diet in neuromuscular and neurodegenerative diseases. *BioMed research international* 2014, p. 474296. doi: 10.1155/2014/474296.

Parikh, S. et al. 2015. Diagnosis and management of mitochondrial disease: a consensus statement from the Mitochondrial Medicine Society. *Genetics in medicine : official journal of the American College of Medical Genetics* 17(9), pp. 689–701. doi: 10.1038/gim.2014.177.

Pasek, S. et al. 2006. Gene fusion/fission is a major contributor to evolution of multi-domain bacterial proteins. *Bioinformatics (Oxford, England)* 22(12), pp. 1418–1423. doi: 10.1093/bioinformatics/btl135.

Pastore, A. et al. 2001. Determination of blood total, reduced, and oxidized glutathione in pediatric subjects. *Clinical chemistry* 47(8), pp. 1467–1469.

Pfeffer, G. et al. 2012. Treatment for mitochondrial disorders. *The Cochrane database of systematic reviews* (4), p. CD004426. doi: 10.1002/14651858.CD004426.pub3.

Phillips, I.R. and Shephard, E.A. 1993. Primary Trimethylaminuria. In: Adam, M. P. et al. eds. Seattle (WA)

Phoenix, C. et al. 2006. A scale to monitor progression and treatment of mitochondrial disease in children. *Neuromuscular disorders : NMD* 16(12), pp. 814–820. doi: 10.1016/j.nmd.2006.08.006.

Picard, M. et al. 2013. Mitochondrial morphology transitions and functions: implications for retrograde signaling? *American journal of physiology. Regulatory, integrative and comparative physiology* 304(6), pp. R393-406. doi: 10.1152/ajpregu.00584.2012.

Picardi, E. and Pesole, G. 2012. Mitochondrial genomes gleaned from human whole-exome sequencing. *Nature methods* 9(6), pp. 523–524. doi: 10.1038/nmeth.2029.

Powers, H.J. 2003. Riboflavin (vitamin B-2) and health. *The American journal of clinical nutrition* 77(6), pp. 1352–1360.

Prasad, R. et al. 2014. Thioredoxin Reductase 2 (TXNRD2) mutation associated with familial glucocorticoid deficiency (FGD). *The Journal of clinical endocrinology and metabolism* 99(8), pp. E1556-63. doi: 10.1210/jc.2013-3844.

Pravst, I. et al. 2010. Coenzyme Q10 contents in foods and fortification strategies. *Critical reviews in food science and nutrition* 50(4), pp. 269–280. doi: 10.1080/10408390902773037.

Prior, R.L. et al. 2005. Standardized methods for the determination of antioxidant capacity and phenolics in foods and dietary supplements. *Journal of agricultural and food chemistry* 53(10), pp. 4290–4302. doi: 10.1021/jf0502698.

Pronicka, E. et al. 2016. New perspective in diagnostics of mitochondrial disorders: two years' experience with whole-exome sequencing at a national paediatric centre. *Journal of translational medicine* 14(1), p. 174. doi: 10.1186/s12967-016-0930-9.

Di Prospero, N.A. et al. 2007. Neurological effects of high-dose idebenone in patients with Friedreich's ataxia: a randomised, placebo-controlled trial. *The Lancet. Neurology* 6(10), pp. 878–886. doi: 10.1016/S1474-4422(07)70220-X.

Quinlan, C.L. et al. 2012. Mitochondrial complex II can generate reactive oxygen species at high rates in both the forward and reverse reactions. *The Journal of biological chemistry* 287(32), pp. 27255–27264. doi: 10.1074/jbc.M112.374629.

Raha, S. et al. 2000. Superoxides from mitochondrial complex III: the role of manganese superoxide dismutase. *Free radical biology & medicine* 29(2), pp. 170–180.

Rahman, J. and Rahman, S. 2018. Mitochondrial medicine in the omics era. *Lancet (London, England)* 391(10139), pp. 2560–2574. doi: 10.1016/S0140-6736(18)30727-X.

Rai, P.K. et al. 2018. Advances in methods for reducing mitochondrial DNA disease by replacing or manipulating the mitochondrial genome. *Essays in biochemistry* 62(3), pp. 455–465. doi: 10.1042/EBC20170113.

Reboul, E. et al. 2006. Bioaccessibility of carotenoids and vitamin E from their main dietary sources. *Journal of agricultural and food chemistry* 54(23), pp. 8749–8755. doi: 10.1021/jf061818s.

Repp, B.M. et al. 2018. Clinical, biochemical and genetic spectrum of 70 patients with ACAD9 deficiency: is riboflavin supplementation effective? *Orphanet journal of rare diseases* 13(1), p. 120. doi: 10.1186/s13023-018-0784-8.

Rich, P. 2003. Chemiosmotic coupling: The cost of living. *Nature* 421(6923), p. 583. doi: 10.1038/421583a.

Rigobello, M.P. et al. 2005. Effect of auranofin on the mitochondrial generation of hydrogen peroxide. Role of thioredoxin reductase. *Free radical research* 39(7), pp. 687–695. doi: 10.1080/10715760500135391.

Ristoff, E. and Larsson, A. 2007. Inborn errors in the metabolism of glutathione. *Orphanet journal of rare diseases* 2, p. 16. doi: 10.1186/1750-1172-2-16.

Robinson, J.T. et al. 2011. Integrative genomics viewer. *Nature biotechnology* 29(1), pp. 24–26. doi: 10.1038/nbt.1754.

Rodriguez-Cuenca, S. et al. 2010. Consequences of long-term oral administration of the mitochondria-targeted antioxidant MitoQ to wild-type mice. *Free radical biology & medicine* 48(1), pp. 161–172. doi: 10.1016/j.freeradbiomed.2009.10.039.

Rogers, G.W. et al. 2011. High throughput microplate respiratory measurements using minimal quantities of isolated mitochondria. *PloS one* 6(7), p. e21746. doi: 10.1371/journal.pone.0021746.

Romero-Moya, D. et al. 2017. Generation, genome edition and characterization of iPSC lines from a patient with coenzyme Q10 deficiency harboring a heterozygous mutation in COQ4

gene. *Stem cell research* 24, pp. 144–147. doi: 10.1016/j.scr.2016.09.007.

Ross, N.S. and Hansen, T.P. 1992. Riboflavin deficiency is associated with selective preservation of critical flavoenzyme-dependent metabolic pathways. *BioFactors (Oxford, England)* 3(3), pp. 185–190.

Rustin, P. et al. 1991. Assessment of the mitochondrial respiratory chain. *Lancet (London, England)* 338(8758), p. 60.

Ruzicka, F.J. and Beinert, H. 1977. A new iron-sulfur flavoprotein of the respiratory chain. A component of the fatty acid beta oxidation pathway. *The Journal of biological chemistry* 252(23), pp. 8440–8445.

Rybnikova, E. et al. 2000. Expression of novel antioxidant thioredoxin-2 in the rat brain. *The European journal of neuroscience* 12(5), pp. 1669–1678.

Ryder, B. et al. 2019. A Novel Truncating FLAD1 Variant, Causing Multiple Acyl-CoA Dehydrogenase Deficiency (MADD) in an 8-Year-Old Boy. *JIMD reports* 45, pp. 37–44. doi: 10.1007/8904_2018_139.

Safdar, A. et al. 2016. The potential of endurance exercise-derived exosomes to treat metabolic diseases. *Nature reviews. Endocrinology* 12(9), pp. 504–517. doi: 10.1038/nrendo.2016.76.

Said, H.M. 2011. Intestinal absorption of water-soluble vitamins in health and disease. *The Biochemical journal* 437(3), pp. 357–372. doi: 10.1042/BJ20110326.

Said, H.M. and Ma, T.Y. 1994. Mechanism of riboflavine uptake by Caco-2 human intestinal epithelial cells. *The American journal of physiology* 266(1 Pt 1), pp. G15-21. doi: 10.1152/ajpgi.1994.266.1.G15.

Saijo, T. and Tanaka, K. 1995. Isoalloxazine ring of FAD is required for the formation of the core in the Hsp60-assisted folding of medium chain acyl-CoA dehydrogenase subunit into the assembly competent conformation in mitochondria. *The Journal of biological chemistry* 270(4), pp. 1899–1907.

Saleh, M. et al. 2004. Differential modulation of endotoxin responsiveness by human caspase-12 polymorphisms. *Nature* 429(6987), pp. 75–79. doi: 10.1038/nature02451.

Sandoval, F.J. et al. 2008. Flavin nucleotide metabolism in plants: monofunctional enzymes synthesize fad in plastids. *The Journal of biological chemistry* 283(45), pp. 30890–30900. doi: 10.1074/jbc.M803416200.

Saneto, R.P. et al. 2013. Alpers-Huttenlocher syndrome. *Pediatric neurology* 48(3), pp. 167–178. doi: 10.1016/j.pediatrneurol.2012.09.014.

Sanger, F. et al. 1977. DNA sequencing with chain-terminating inhibitors. *Proceedings of the National Academy of Sciences of the United States of America* 74(12), pp. 5463–5467.

Sassa, S. 2006. Modern diagnosis and management of the porphyrias. *British journal of haematology* 135(3), pp. 281–292. doi: 10.1111/j.1365-2141.2006.06289.x.

Scaglia, F. et al. 2004. Clinical spectrum, morbidity, and mortality in 113 pediatric patients with mitochondrial disease. *Pediatrics* 114(4), pp. 925–931. doi: 10.1542/peds.2004-0718.

Schafer, F.Q. and Buettner, G.R. 2001. Redox environment of the cell as viewed through the redox state of the glutathione disulfide/glutathione couple. *Free radical biology & medicine*

30(11), pp. 1191–1212.

Schiff, M. et al. 2015. Complex I assembly function and fatty acid oxidation enzyme activity of ACAD9 both contribute to disease severity in ACAD9 deficiency. *Human molecular genetics* 24(11), pp. 3238–3247. doi: 10.1093/hmg/ddv074.

Schiff, M. et al. 2016. SLC25A32 Mutations and Riboflavin-Responsive Exercise Intolerance. *The New England journal of medicine* 374(8), pp. 795–797. doi: 10.1056/NEJMc1513610.

Sciacco, M. et al. 1994. Distribution of wild-type and common deletion forms of mtDNA in normal and respiration-deficient muscle fibers from patients with mitochondrial myopathy. *Human molecular genetics* 3(1), pp. 13–19.

Sciacco, M. and Bonilla, E. 1996. Cytochemistry and immunocytochemistry of mitochondria in tissue sections. *Methods in enzymology* 264, pp. 509–521.

Semple, B.D. et al. 2013. Brain development in rodents and humans: Identifying benchmarks of maturation and vulnerability to injury across species. *Progress in neurobiology* 106–107, pp. 1–16. doi: 10.1016/j.pneurobio.2013.04.001.

Shatla, H.M. et al. 2014. Role of plasma amino acids and urinary organic acids in diagnosis of mitochondrial diseases in children. *Pediatric neurology* 51(6), pp. 820–825. doi: 10.1016/j.pediatrneurol.2014.08.009.

Shemesh, A. and Margolin, E. 2018. Kearns Sayre Syndrome. Treasure Island (FL)

Shepard, T.H. et al. 1998. Ultrastructural study of mitochondria and their cristae in embryonic rats and primate (N. nemistrina). *The Anatomical record* 252(3), pp. 383–392.

Shoffner, J.M. et al. 1990. Myoclonic epilepsy and ragged-red fiber disease (MERRF) is associated with a mitochondrial DNA tRNA(Lys) mutation. *Cell* 61(6), pp. 931–937.

Sibbing, D. et al. 2011. Mutations in the mitochondrial thioredoxin reductase gene TXNRD2 cause dilated cardiomyopathy. *European heart journal* 32(9), pp. 1121–1133. doi: 10.1093/eurheartj/ehq507.

Skladal, D. et al. 2003. Minimum birth prevalence of mitochondrial respiratory chain disorders in children. *Brain : a journal of neurology* 126(Pt 8), pp. 1905–1912. doi: 10.1093/brain/awg170.

Slane, B.G. et al. 2006. Mutation of succinate dehydrogenase subunit C results in increased O2.-, oxidative stress, and genomic instability. *Cancer research* 66(15), pp. 7615–7620. doi: 10.1158/0008-5472.CAN-06-0833.

Smeets, A. et al. 2005. Crystal structures of oxidized and reduced forms of human mitochondrial thioredoxin 2. *Protein science : a publication of the Protein Society* 14(10), pp. 2610–2621. doi: 10.1110/ps.051632905.

Smeitink, J.A. et al. 2006. Mitochondrial medicine: a metabolic perspective on the pathology of oxidative phosphorylation disorders. *Cell metabolism* 3(1), pp. 9–13. doi: 10.1016/j.cmet.2005.12.001.

Smeitink, J.A.M. 2003. Mitochondrial disorders: clinical presentation and diagnostic dilemmas. *Journal of inherited metabolic disease* 26(2–3), pp. 199–207.

Soerensen, J. et al. 2008. The role of thioredoxin reductases in brain development. *PloS one* 3(3), p. e1813. doi: 10.1371/journal.pone.0001813.

Solovieva, I.M. et al. 2003. Main physicochemical features of monofunctional flavokinase from Bacillus subtilis. *Biochemistry. Biokhimiia* 68(2), pp. 177–181.

Sosnay, P.R. and Cutting, G.R. 2014. Interpretation of genetic variants. *Thorax* 69(3), pp. 295–297. doi: 10.1136/thoraxjnl-2013-204903.

Sperl, W. et al. 2015. The spectrum of pyruvate oxidation defects in the diagnosis of mitochondrial disorders. *Journal of inherited metabolic disease* 38(3), pp. 391–403. doi: 10.1007/s10545-014-9787-3.

Spinazzi, M. et al. 2012. Assessment of mitochondrial respiratory chain enzymatic activities on tissues and cultured cells. *Nature protocols* 7(6), pp. 1235–1246. doi: 10.1038/nprot.2012.058.

Spyrou, G. et al. 1997. Cloning and expression of a novel mammalian thioredoxin. *The Journal of biological chemistry* 272(5), pp. 2936–2941.

Stachowicz, A. et al. 2017. Proteomic Analysis of Mitochondria-Enriched Fraction Isolated from the Frontal Cortex and Hippocampus of Apolipoprotein E Knockout Mice Treated with Alda-1, an Activator of Mitochondrial Aldehyde Dehydrogenase (ALDH2). *International journal of molecular sciences* 18(2). doi: 10.3390/ijms18020435.

Stacpoole, P.W. 1997. Lactic acidosis and other mitochondrial disorders. *Metabolism: clinical and experimental* 46(3), pp. 306–321.

Starkov, A.A. et al. 2004. Mitochondrial alpha-ketoglutarate dehydrogenase complex generates reactive oxygen species. *The Journal of neuroscience : the official journal of the Society for Neuroscience* 24(36), pp. 7779–7788. doi: 10.1523/JNEUROSCI.1899-04.2004.

Stenton, S.L. and Prokisch, H. 2018. Advancing genomic approaches to the molecular diagnosis of mitochondrial disease. *Essays in biochemistry* . doi: 10.1042/EBC20170110.

Stewart, J.B. and Chinnery, P.F. 2015. The dynamics of mitochondrial DNA heteroplasmy: implications for human health and disease. *Nature reviews. Genetics* 16(9), pp. 530–542. doi: 10.1038/nrg3966.

Subramanian, V.S. et al. 2011. Differential expression of human riboflavin transporters -1, -2, and -3 in polarized epithelia: a key role for hRFT-2 in intestinal riboflavin uptake. *Biochimica et biophysica acta* 1808(12), pp. 3016–3021. doi: 10.1016/j.bbamem.2011.08.004.

Sundaresan, M. et al. 1995. Requirement for generation of H2O2 for platelet-derived growth factor signal transduction. *Science (New York, N.Y.)* 270(5234), pp. 296–299.

Suomalainen, A. et al. 2011. FGF-21 as a biomarker for muscle-manifesting mitochondrial respiratory chain deficiencies: a diagnostic study. *The Lancet. Neurology* 10(9), pp. 806–818. doi: 10.1016/S1474-4422(11)70155-7.

Taivassalo, T. et al. 2006. Endurance training and detraining in mitochondrial myopathies due to single large-scale mtDNA deletions. *Brain : a journal of neurology* 129(Pt 12), pp. 3391–3401. doi: 10.1093/brain/awl282.

Tanaka, M. et al. 2002a. Gene therapy for mitochondrial disease by delivering restriction endonuclease SmaI into mitochondria. *Journal of biomedical science* 9(6 Pt 1), pp. 534–541. doi: 10.1159/000064726.

Tanaka, T. et al. 2002b. Thioredoxin-2 (TRX-2) is an essential gene regulating mitochondria-dependent apoptosis. *The EMBO journal* 21(7), pp. 1695–1703. doi:

10.1093/emboj/21.7.1695.

Tauskela, J.S. 2007. MitoQ--a mitochondria-targeted antioxidant. *IDrugs : the investigational drugs journal* 10(6), pp. 399–412.

Taylor, R.W. et al. 2014. Use of whole-exome sequencing to determine the genetic basis of multiple mitochondrial respiratory chain complex deficiencies. *JAMA* 312(1), pp. 68–77. doi: 10.1001/jama.2014.7184.

Taylor, R.W. and Turnbull, D.M. 2005. Mitochondrial DNA mutations in human disease. *Nature reviews. Genetics* 6(5), pp. 389–402. doi: 10.1038/nrg1606.

Tchikviladze, M. et al. 2015. A diagnostic flow chart for POLG-related diseases based on signs sensitivity and specificity. *Journal of neurology, neurosurgery, and psychiatry* 86(6), pp. 646–654. doi: 10.1136/jnnp-2013-306799.

Tello, C. et al. 2018. On the complexity of clinical and molecular bases of neurodegeneration with brain iron accumulation. *Clinical genetics* 93(4), pp. 731–740. doi: 10.1111/cge.13057.

Terlecky, S.R. et al. 2006. Peroxisomes and aging. *Biochimica et biophysica acta* 1763(12), pp. 1749–1754. doi: 10.1016/j.bbamcr.2006.08.017.

Thorburn, D.R. et al. 1993. Mitochondrial DNA-Associated Leigh Syndrome and NARP. In: Adam, M. P. et al. eds. Seattle (WA)

Thorburn, D.R. 2004. Mitochondrial disorders: prevalence, myths and advances. *Journal of inherited metabolic disease* 27(3), pp. 349–362. doi: 10.1023/B:BOLI.0000031098.41409.55.

Tietze, F. 1969. Enzymic method for quantitative determination of nanogram amounts of total and oxidized glutathione: applications to mammalian blood and other tissues. *Analytical biochemistry* 27(3), pp. 502–522.

Tonon, C. and Lodi, R. 2008. Idebenone in Friedreich's ataxia. *Expert opinion on pharmacotherapy* 9(13), pp. 2327–2337. doi: 10.1517/14656566.9.13.2327.

Torchetti, E.M. et al. 2010. Mitochondrial localization of human FAD synthetase isoform 1. *Mitochondrion* 10(3), pp. 263–273. doi: 10.1016/j.mito.2009.12.149.

Torchetti, E.M. et al. 2011. Human FAD synthase (isoform 2): a component of the machinery that delivers FAD to apo-flavoproteins. *The FEBS journal* 278(22), pp. 4434–4449. doi: 10.1111/j.1742-4658.2011.08368.x.

Treacy, E.P. et al. 1998. Mutations of the flavin-containing monooxygenase gene (FMO3) cause trimethylaminuria, a defect in detoxication. *Human molecular genetics* 7(5), pp. 839–845.

Trifunovic, A. et al. 2004. Premature ageing in mice expressing defective mitochondrial DNA polymerase. *Nature* 429(6990), pp. 417–423. doi: 10.1038/nature02517.

Trifunovic, A. and Larsson, N.-G. 2008. Mitochondrial dysfunction as a cause of ageing. *Journal of internal medicine* 263(2), pp. 167–178. doi: 10.1111/j.1365-2796.2007.01905.x.

Truong, T.H. and Carroll, K.S. 2013. Redox regulation of protein kinases. *Critical reviews in biochemistry and molecular biology* 48(4), pp. 332–356. doi: 10.3109/10409238.2013.790873.

Turrens, J.F. et al. 1985. Ubisemiquinone is the electron donor for superoxide formation by

complex III of heart mitochondria. *Archives of biochemistry and biophysics* 237(2), pp. 408–414.

Udhayabanu, T. et al. 2017. Riboflavin Responsive Mitochondrial Dysfunction in Neurodegenerative Diseases. *Journal of clinical medicine* 6(5). doi: 10.3390/jcm6050052.

Vaca Jacome, A.S. et al. 2015. N-terminome analysis of the human mitochondrial proteome. *Proteomics* 15(14), pp. 2519–2524. doi: 10.1002/pmic.201400617.

Valanne, L. et al. 1998. Neuroradiologic findings in children with mitochondrial disorders. *AJNR. American journal of neuroradiology* 19(2), pp. 369–377.

Vasquez-Vivar, J. et al. 2000. Mitochondrial aconitase is a source of hydroxyl radical. An electron spin resonance investigation. *The Journal of biological chemistry* 275(19), pp. 14064–14069.

Veltman, J.A. and Brunner, H.G. 2012. De novo mutations in human genetic disease. *Nature reviews. Genetics* 13(8), pp. 565–575. doi: 10.1038/nrg3241.

Venardos, K. et al. 2004a. Auranofin increases apoptosis and ischaemia-reperfusion injury in the rat isolated heart. *Clinical and experimental pharmacology & physiology* 31(5–6), pp. 289–294. doi: 10.1111/j.1440-1681.2004.03993.x.

Venardos, K. et al. 2004b. Effects of dietary selenium on glutathione peroxidase and thioredoxin reductase activity and recovery from cardiac ischemia-reperfusion. *Journal of trace elements in medicine and biology : organ of the Society for Minerals and Trace Elements (GMS)* 18(1), pp. 81–88. doi: 10.1016/j.jtemb.2004.01.001.

Vergani, L. et al. 1999. Riboflavin therapy. Biochemical heterogeneity in two adult lipid storage myopathies. *Brain : a journal of neurology* 122 (Pt 1, pp. 2401–2411.

Verspohl, E.J. 2006. Effect of PAO (phenylarsine oxide) on the inhibitory effect of insulin and IGF-1 on insulin release from INS-1 cells. *Endocrine journal* 53(1), pp. 21–26.

Vidali, S. et al. 2015. Mitochondria: The ketogenic diet--A metabolism-based therapy. *The international journal of biochemistry & cell biology* 63, pp. 55–59. doi: 10.1016/j.biocel.2015.01.022.

Vieira, H.L. et al. 2000. Permeabilization of the mitochondrial inner membrane during apoptosis: impact of the adenine nucleotide translocator. *Cell death and differentiation* 7(12), pp. 1146–1154. doi: 10.1038/sj.cdd.4400778.

Vlaming, M.L.H. et al. 2009. Physiological and pharmacological roles of ABCG2 (BCRP): recent findings in Abcg2 knockout mice. *Advanced drug delivery reviews* 61(1), pp. 14–25. doi: 10.1016/j.addr.2008.08.007.

Voet, D. et al. 2013. Principles of Biochemistry. In: *John Wiley & Sons, Inc.*, pp. 224–225.

Wan, X. et al. 2016. Efficacy and Safety of rAAV2-ND4 Treatment for Leber's Hereditary Optic Neuropathy. *Scientific reports* 6, p. 21587. doi: 10.1038/srep21587.

Wang, D. and Gao, G. 2014. State-of-the-art human gene therapy: part II. Gene therapy strategies and clinical applications. *Discovery medicine* 18(98), pp. 151–161.

Werner, R. et al. 2005. HepG2 cells develop signs of riboflavin deficiency within 4 days of culture in riboflavin-deficient medium. *The Journal of nutritional biochemistry* 16(10), pp. 617–624. doi: 10.1016/j.jnutbio.2005.03.006.

Witschi, A. et al. 1992. The systemic availability of oral glutathione. *European journal of clinical pharmacology* 43(6), pp. 667–669.

Wittig, I. et al. 2006a. Blue native PAGE. *Nature protocols* 1(1), pp. 418–428. doi: 10.1038/nprot.2006.62.

Wittig, I. et al. 2006b. Supercomplexes and subcomplexes of mitochondrial oxidative phosphorylation. *Biochimica et biophysica acta* 1757(9–10), pp. 1066–1072. doi: 10.1016/j.bbabio.2006.05.006.

Wittig, I. et al. 2007. High resolution clear native electrophoresis for in-gel functional assays and fluorescence studies of membrane protein complexes. *Molecular & cellular proteomics : MCP* 6(7), pp. 1215–1225. doi: 10.1074/mcp.M700076-MCP200.

Wolf, N.I. and Smeitink, J.A.M. 2002. Mitochondrial disorders: a proposal for consensus diagnostic criteria in infants and children. *Neurology* 59(9), pp. 1402–1405.

Wong, L.-J.C. 2013. Next generation molecular diagnosis of mitochondrial disorders. *Mitochondrion* 13(4), pp. 379–387. doi: 10.1016/j.mito.2013.02.001.

Wong, S.S.-N. et al. 2017. Radboud Centre for Mitochondrial Medicine Pediatric MRI score. *Mitochondrion* 32, pp. 36–41. doi: 10.1016/j.mito.2016.11.008.

Wortmann, S.B. et al. 2015. Whole exome sequencing of suspected mitochondrial patients in clinical practice. *Journal of inherited metabolic disease* 38(3), pp. 437–443. doi: 10.1007/s10545-015-9823-y.

Wortmann, S.B. et al. 2017. A Guideline for the Diagnosis of Pediatric Mitochondrial Disease: The Value of Muscle and Skin Biopsies in the Genetics Era. *Neuropediatrics* 48(4), pp. 309–314. doi: 10.1055/s-0037-1603776.

Wu, M. et al. 1995. Cloning and characterization of FAD1, the structural gene for flavin adenine dinucleotide synthetase of Saccharomyces cerevisiae. *Molecular and cellular biology* 15(1), pp. 264–271.

Wyman, M. et al. 2010. Coenzyme Q10: a therapy for hypertension and statin-induced myalgia? *Cleveland Clinic journal of medicine* 77(7), pp. 435–442. doi: 10.3949/ccjm.77a.09078.

Xanthoudakis, S. and Curran, T. 1992. Identification and characterization of Ref-1, a nuclear protein that facilitates AP-1 DNA-binding activity. *The EMBO journal* 11(2), pp. 653–665.

Xue, Y. et al. 2008. Adaptive evolution of UGT2B17 copy-number variation. *American journal of human genetics* 83(3), pp. 337–346. doi: 10.1016/j.ajhg.2008.08.004.

Yatsuga, S. et al. 2015. Growth differentiation factor 15 as a useful biomarker for mitochondrial disorders. *Annals of neurology* 78(5), pp. 814–823. doi: 10.1002/ana.24506.

Yazdanpanah, B. et al. 2009. Riboflavin kinase couples TNF receptor 1 to NADPH oxidase. *Nature* 460(7259), pp. 1159–1163. doi: 10.1038/nature08206.

Yepez, V.A. et al. 2018. OCR-Stats: Robust estimation and statistical testing of mitochondrial respiration activities using Seahorse XF Analyzer. *PloS one* 13(7), p. e0199938. doi: 10.1371/journal.pone.0199938.

Yildiz, Y. et al. 2018. Post-mortem detection of FLAD1 mutations in 2 Turkish siblings with hypotonia in early infancy. *Neuromuscular disorders : NMD* 28(9), pp. 787–790. doi:

10.1016/j.nmd.2018.05.009.

Yilmaz, K. 2009. Riboflavin treatment in a case with l-2-hydroxyglutaric aciduria. *European journal of paediatric neurology : EJPN : official journal of the European Paediatric Neurology Society* 13(1), pp. 57–60. doi: 10.1016/j.ejpn.2008.01.003.

Yonezawa, A. and Inui, K. 2013. Novel riboflavin transporter family RFVT/SLC52: identification, nomenclature, functional characterization and genetic diseases of RFVT/SLC52. *Molecular aspects of medicine* 34(2–3), pp. 693–701. doi: 10.1016/j.mam.2012.07.014.

Yoon, Y. et al. 2011. Mitochondrial dynamics in diabetes. *Antioxidants & redox signaling* 14(3), pp. 439–457. doi: 10.1089/ars.2010.3286.

Yoshioka, J. and Lee, R.T. 2014. Thioredoxin-interacting protein and myocardial mitochondrial function in ischemia-reperfusion injury. *Trends in cardiovascular medicine* 24(2), pp. 75–80. doi: 10.1016/j.tcm.2013.06.007.

Yruela, I. et al. 2010. Evolutionary divergence of chloroplast FAD synthetase proteins. *BMC evolutionary biology* 10, p. 311. doi: 10.1186/1471-2148-10-311.

Yu-Wai-Man, P. et al. 2002. Leber hereditary optic neuropathy. *Journal of medical genetics* 39(3), pp. 162–169.

Zechmann, B. et al. 2011. Subcellular distribution of glutathione and its dynamic changes under oxidative stress in the yeast Saccharomyces cerevisiae. *FEMS yeast research* 11(8), pp. 631–642. doi: 10.1111/j.1567-1364.2011.00753.x.

Zempleni, J. et al. 1996. Pharmacokinetics of orally and intravenously administered riboflavin in healthy humans. *The American journal of clinical nutrition* 63(1), pp. 54–66.

Zhang, H. et al. 2007. Mitochondrial thioredoxin-2/peroxiredoxin-3 system functions in parallel with mitochondrial GSH system in protection against oxidative stress. *Archives of biochemistry and biophysics* 465(1), pp. 119–126. doi: 10.1016/j.abb.2007.05.001.

Zhang, R. et al. 2004. Thioredoxin-2 inhibits mitochondria-located ASK1-mediated apoptosis in a JNK-independent manner. *Circulation research* 94(11), pp. 1483–1491. doi: 10.1161/01.RES.0000130525.37646.a7.

Zhao, Y. et al. 2009. Increase in thiol oxidative stress via glutathione reductase inhibition as a novel approach to enhance cancer sensitivity to X-ray irradiation. *Free radical biology & medicine* 47(2), pp. 176–183. doi: 10.1016/j.freeradbiomed.2009.04.022.

Zitka, O. et al. 2012. Redox status expressed as GSH:GSSG ratio as a marker for oxidative stress in paediatric tumour patients. *Oncology letters* 4(6), pp. 1247–1253. doi: 10.3892/ol.2012.931.

Curriculum Vitae

Persönliche Daten

Name:	Ing. Mgr. Eliška Koňaříková
Mädchenname:	Holzerová
Geburtsdatum:	3. 2. 1989
Geburtsort:	Vsetín (Tschechische Republik)
Addresse:	Měchenická 2565/28, 141 00 Prag, Tschechische Republik
Telefon	+420 608 240 241
E-Mail	eliska.konarikova@outlook.com
Nationalität	Tschechisch
Familienstand	verheiratet

Ausbildung

2013 – jetzt **Dr. rer. nat.**
Doktorat innerhalb des Marie Curie – Initial Training Networks:
MEET – Mitochondrial European Educational Training
Technische Universität München – Experimentelle Medizin
und
Institut für Humangenetik, Helmholtz Zentrum München
Dissertation: *Funktionelle Validierung von Genen für mitochondriale Erkrankungen*

2012 – 2015 **Ing**.
Tschechische Universität für Lebenswissenschaften Prag
Wirtschaftswissenschaftliche Fakultät
Studiengang: Wirtschaft und Management
Studienfach: Betriebsführung und Wirtschaft
Diplomarbeit: *Das Personal- und Sozialentwicklungsmanagement in Forschungseinrichtungen*
Abschluss im Februar 2015

2011 – 2013 **Mgr**.
Karlsuniversität in Prag
Fakultät für Naturwissenschaften
Studiengang: Biologie
Studienfach: Zell- und Entwicklungsbiologie - Zellphysiologie
Diplomarbeit: *Molekulare Mechanismen der Produktion reaktiver Sauerstoffspezies durch Flavin-Dehydrogenasen der mitochondrialen Atmungskette*
Abschluss mit *summa cum laude* im September 2013

2008 – 2011	**Bc**. Karlsuniversität in Prag Fakultät für Naturwissenschaften Studiengang: Spezielle chemische und biologische Programme Studienfach: Molekularbiologie und Biochemie von Organismen Bachelorarbeit: *Mitochondriale Produktion reaktiver Sauerstoffspezies und ihre Rolle bei physiologischen* Abschluss mit *summa cum laude* im Juni 2011
2000 – 2008	**Matura** Masaryk Gymnasium und Sprachschule Vsetín, Tschechische Republik Abschluss mit Auszeichnung im Juni 2008

Berufliche Laufbahn

08/2017 – jetzt	Administrator bei We Love Mitochondria
03/2017 – 02/2019	Elternzeit
10/2013 – 02/2017	Institut für Humangenetik, Helmholtz Zentrum München Dr. Holger Prokisch und Prof. Dr. Thomas Meitinger
3/2013 – 7/2013	Erasmus Austausch Molekulare Bioenergetik, Medizinische Fakultät, Exzellenzcluster Frankfurt Makromolekulare Komplexe Dr. Ilka Wittig und Prof. Dr. Ulrich Brandt Frankfurt, Deutschland
1/2010 – 9/2013	Institut für Physiologie, Akademie der Wissenschaften der Tschechischen Republik, Prag Abteilung für Bioenergetik Dr. Tomáš Mráček und MUDr. Josef Houštěk, DrSc.

Vorträge und Poster

Bioenergetik 2016 – Tschechisch-slowakisches Symposium
11. – 13. 11. 2016, Kokořínsko, Tschechische Republik
Vortrag: *The Story of RNA Sequencing*

<interact> 2016
3. – 4. 11. 2016, München, Deutschland
Poster: *Thioredoxin 2 deficiency causes early-onset neurodegeneration*

The American Society of Human Genetics
18. – 22. 10. 2016, Vancouver, Kanada
Poster: *NAXE mutations disrupt the cellular NAD(P)HX repair system and cause a lethal neurometabolic disorder of early childhood*

XXV. Biochemisches Treffen
13. – 16. 9. 2016, Prag, Tschechische Republik
Vortrag: *Variants in the FAD Synthase Gene as a New Cause of Combined Respiratory Chain and Multiple Acyl-CoA Dehydrogenation Deficiency Including Riboflavin-Responsive Mutants*

19. Europäische Bioenergetikkonferenz
2. – 7. 6. 2016, Riva del Garda, Italien
Poster: *Non-Loss-of-Function Frameshift Variants in the FAD Synthase Gene Cause Combined Respiratory Chain Deficiency*

Mitochondrienmedizin: Entwicklung neuer Therapien gegen Mitochondrien
4. – 6. 5. 2016, Hinxton, Großbritannien
Poster: *Variants in the FAD Synthase Gene as a New Cause of Combined Respiratory Chain and Multiple Acyl-CoA Dehydrogenation Deficiency Including Riboflavin-Responsive Mutants*

On the Tip of Omics
13. – 15. 4. 2016, Grainau, Deutschland
Vortrag: *RNA Profiling In Monogenic Disorders*

The International Congress of Human Genetics
4. – 7. 4. 2016, Kyoto, Japan
Vortrag: *Human thioredoxin-2 deficiency impairs mitochondrial redox homeostasis and causes early-onset neurodegeneration*

11th MiPconference on Mitochondrial Physiology
7. – 11. 9. 2015, Luční Bouda, Pec pod Sněžkou, Tschechische Republik
Vortrag: *Thioredoxin-2 deficiency impairs oxidative stress defense and leads to early-onset neurodegeneration with severe cerebellar atrophy*

The Society for the Study of Inborn Errors of Metabolism
1. – 4. 9. 2015, Lyon, Frankreich
Vortrag: *Thioredoxin-2 deficiency impairs oxidative stress defense and leads to early-onset neurodegeneration with severe cerebellar atrophy*

The European Society of Human Genetics
6. – 9. 6. 2015, Glasgow, Großbritannien
Poster: *Thioredoxin 2 deficiency causes early-onset neurodegeneration* – **Posterpreis**

The 2nd Course in Mitochondrial Medicine
1. – 3. 12. 2014, Bertinoro di Romagna, Italien
Vortrag: *Respiratory complexes assembly and mitochondrial lipid metabolism*

Bioenergetik 2014 – Tschechisch-slowakisches Symposium
4. – 7. 10. 2014, Lipová lázně, Tschechische Republik
Vortrag: *From Exome Sequencing to Cell Metabolism*

EUROMIT Konferenz
15. – 20. 6. 2014, Tampere, Finnland
Poster: *Sengers syndrome is caused by a broad spectrum of predicted loss-of-function acylglycerol kinase mutations, an overview of 29 patients*

Young Mitoscientists' Forum
14. – 15. 6. 2014, Tampere, Finnland
Poster: *Sengers syndrome is caused by a broad spectrum of predicted loss-of-function acylglycerol kinase mutations, an overview of 29 patients*

3. Heidelberger Forum für junge Wissenschaftler
6. – 7. 6. 2013, Heidelberg, Deutschland
Poster: *Molecular mechanism of reactive oxygen species production by flavin dehydrogenases of mitochondrial respiratory chain*

Bioenergetik 2012 – Tschechisch-slowakisches Symposium
5. – 7. 11. 2012, Milotice, Tschechische Republik
Vortrag: *Searching for the electron leak at mGPDH and SDH*

Bioenergetik 2011 – Tschechisch-slowakisches Symposium
12. – 14. 10. 2011, Jiřice, Tschechische Republik
Vortrag: *Production of reactive oxygen species by proteins mGPDH and SDH*

Publikationen

OCR-Stats: Robust estimation and statistical testing of mitochondrial respiration activities using Seahorse XF Analyzer
Yépez VA, Kremer LS, Iuso A, Gusic M, Kopajtich R, **Koňaříková E**, Nadel A, Wachutka L, Prokisch H, Gagneur J. PLoS One, 2018 Jul 11;13(7):e0199938.
doi: 10.1371/journal.pone.0199938. eCollection 2018.

NDUFB8 Mutations Cause Mitochondrial Complex I Deficiency in Individuals with Leigh-like Encephalomyopathy
Piekutowska-Abramczuk D, Assouline Z, Mataković L, Feichtinger RG, **Koňaříková E**, Jurkiewicz E, Stawiński P, Gusic M, Koller A, Pollak A, Gasperowicz P, Trubicka J, Ciara E, Iwanicka-Pronicka K, Rokicki D, Hanein S, Wortmann SB, Sperl W, Rötig A, Prokisch H, Pronicka E, Płoski R, Barcia G, Mayr JA.
American Journal of Human Genetics, 2018 Mar 1;102(3):460-467.
doi: 10.1016/j.ajhg.2018.01.008. Epub 2018 Feb 8.

Genetic diagnosis of Mendelian disorders via RNA sequencing
Laura S Kremer, Daniel M Bader, Christian Mertes, Robert Kopajtich, Garwin Pichler, Arcangela Iuso, Tobias B Haack, Elisabeth Graf, Thomas Schwarzmayr, Caterina Terrile, **Eliska Konarikova**, Birgit Repp, Gabi Kastenmüller, Jerzy Adamski, Peter Lichtner, Christoph Leonhardt, Benoit Funalot, Alice Donati, Valeria Tiranti, Anne Lombes, Claude Jardel, Dieter Gläser, Robert Taylor, Daniele Ghezzi, Johannes AMayr, Agnes Rötig, Peter Freisinger, Felix Distelmaier, Tim M Strom, Thomas Meitinger, Julien Gagneur, Holger Prokisch
Nature Communication, 2017 Jun 12;8:15824. doi: 10.1038/ncomms15824.

Riboflavin-Responsive and -Non-responsive Mutations in FAD Synthase Cause Multiple Acyl-CoA Dehydrogenase and Combined Respiratory-Chain Deficiency
Rikke K.J. Olsen*, **Eliska Konarikova***, Teresa A. Giancaspero*, Signe Mosegaard*, Veronika Boczonadi*, Lavinija Matakovic*, Alice Veauville-Merllie, Caterina Terrile, Thomas Schwarzmayr, Tobias B. Haack, Mari Auranen, Piero Leone, Michele Galluccio, Apolline Imbard, Purificacion Gutierrez-Rios, Johan Palmfeldt, Elisabeth Graf, Christine Vianey-Saban, Marcus Oppenheim, Manuel Schiff, Samia Pichard, Odile Rigal, Angela Pyle, Patrick F. Chinnery, Vassiliki Konstantopoulou, Dorothea Moslinger, Rene G. Feichtinger, Beril Talim, Haluk Topaloglu, Turgay Coskun, Safak Gucer, Annalisa Botta, Elena Pegoraro, Adriana Malena, Lodovica Vergani, Daniela Mazza, Marcella Zollino, Daniele Ghezzi, Cecile Acquaviva, Tiina Tyni, Avihu Boneh, Thomas Meitinger, Tim M. Strom, Niels Gregersen, Johannes A. Mayr*, Rita Horvath*, Maria Barile* and Holger Prokisch*
The American Journal of Human Genetics (2016),
http://dx.doi.org/10.1016/j.ajhg.2016.04.006
* These authors contributed equally to this work

Human thioredoxin-2 deficiency impairs mitochondrial redox homeostasis and causes early-onset neurodegeneration
Eliska Holzerova, Katharina Danhauser, Tobias B. Haack, Laura S. Kremer, Irina Ingold, Sho Kobayashi, Caterina Terrile, Petra Wolf, Jörg Schaper, Ertan Mayatepek, Fabian Baertling, José Pedro Friedmann Angeli, Marcus Conrad, Tim M. Strom, Thomas Meitinger, Holger Prokisch, Felix Distelmaier
Brain. 2016 Feb;139(Pt 2):346-54. doi: 10.1093/brain/awv350. Epub 2015 Dec 1.

Mitochondria: Much ado about nothing? How dangerous is reactive oxygen species production?
Holzerová E, Prokisch H.
Int J Biochem Cell Biol. 2015 Jun;63:16-20.

Sengers syndrome: six novel AGK mutations in seven new families and review of the phenotypic and mutational spectrum of 29 patients.
Haghighi A, Haack TB, Atiq M, Mottaghi H, Haghighi-Kakhki H, Bashir RA, Ahting U, Feichtinger RG, Mayr JA, Rotig A, Lebre AS, Klopstock T, Dworschak A, Pulido N, Saeed MA, Saleh-Gohari N, **Holzerova E,** Chinnery PF, Taylor RW, Prokisch H:
Orphanet J Rare Dis. 2014 Aug 20;9:119. doi: 10.1186/s13023-014-0119-3.

ROS generation and multiple forms of mammalian mitochondrial glycerol-3-phosphate dehydrogenase
Tomáš Mráček, **Eliška Holzerová**, Zdeněk Drahota, Nikola Kovářová, Marek Vrbacký, Pavel Ješina and Josef Houštěk:
BBA-Bioenergetics 2013, 1837(1):98-111. doi: 10.1016/j.bbabio.2013.08.007

High molecular weight forms of mammalian respiratory chain complex II
Nikola Kovářová, Tomáš Mráček, Hana Nůsková, **Eliška Holzerová**, Katarína Kľučková, Jakub Rohlena, Jiří Neužil, Josef Houštěk:
PLoS One. 2013, 8(8): e71869. doi:10.1371/journal.pone.0071869

Fähigkeiten und Interessen

Sprachen:	Tschechisch – Muttersprache Englisch – Fließend Deutsch – Mittelstufe (B2) Spanisch – Mittelstufe (B1)
Führerschein:	B
Computerkenntnisse:	MS Office, HTML, Adobe Photoshop, CorelDRAW Graphics Suite
Persönliche Interessen:	Lesen, Aktuelles, Sport & Fitness

Prag, 6. 2. 2019

Acknowledgements / Danksagung / Poděkování

I sincerely thank my mentor Dr. Holger Prokisch for allowing me to work with him and for his support and encouragement during my PhD. I am grateful that I could discuss with him my research progress and that he allowed me to be deeply involved in the mitochondrial community in Munich as well as worldwide. I also thank my supervisor Prof. Dr. Thomas Meitinger that I could work at his institute and that he always gave me the right inputs to improve my work and this thesis. Likewise, I thank all my colleagues not mentioned namely.

I thank all my collaborators from all parts of the world that they led me to be part of their projects and that they were always listening to my opinion. Without them this work would not have been possible.

I must thank the ITN MEET consortium to give me the opportunity to carry on my PhD project within such stimulating surroundings and for all the work burden connected.

My next thanks go to Dr. Laura Kremer for being a great colleague during night shifts and an awesome roommate.

I thank (soon to be Dr.) Robert Kopajtich also for long working hours, for his sense of humor, for his support and I am grateful for being his friend.

I thank (soon to be Dr.) Birgit Repp for teaching me new skills in the lab and also in the real world and for her friendship.

I also thank the Italian squadron Caterina Terrile, Dr. Arcangela Iuso, Dr. Elisa Mastantuono and Dr. Riccardo Berutti for their friendship and support inside and outside the lab. At this point I must also highlight my gratitude towards the Italian invention – moka coffee.

Special thanks go to Dr. Marlies Köpke for her awesomeness, great friendship and perfect English.

I openly thank Sarah Stenton and Mirjana Gušić for their great proofreading effort.

I am totally grateful Martina Kuhnert, who always helped me to fight German bureaucracy and I wanted to thank her for being always a nice and sympathetic person.

I am happy that you all became part of my life! I thank you for the wonderful atmosphere within the institute and for the fantastic time we spent together.

Last but not least I thank all my friends, my family and especially my husband and my son for allowing me to finish this work and for always being supportive.

Thanks! Danke! Díky!